Article

One Earth

Impacts of Green New Deal Energy Plans on Grid Stability, Costs, Jobs, Health, and Climate in 143 Countries

Graphical Abstract

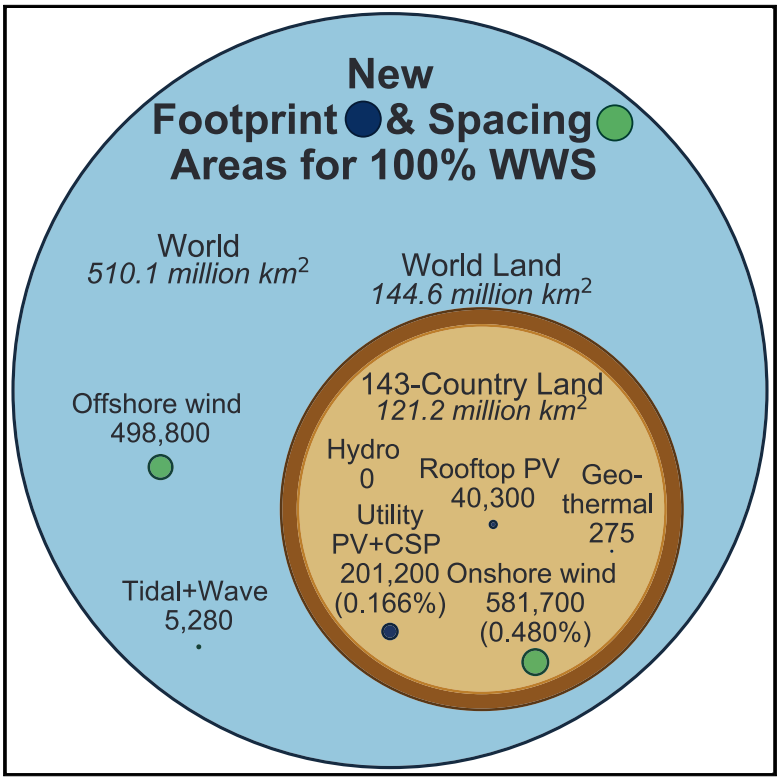

Highlights

- Green New Deal all-sector energy roadmaps are developed for 143 countries
- WWS grid stability is analyzed, and cost metrics are developed for BAU versus WWS energy
- WWS energy reduces energy needs by 57.1%, energy costs by 61%, and social costs by 91%
- WWS energy costs $73 trillion upfront and creates 28.6 million more jobs than BAU energy

Authors

Mark Z. Jacobson, Mark A. Delucchi, Mary A. Cameron, ..., Indu Priya Manogaran, Yanbo Shu, Anna-Katharina von Krauland

Correspondence

jacobson@stanford.edu

In Brief

This paper evaluates Green New Deal solutions to global warming, air pollution, and energy insecurity for 143 countries. The solutions involve transitioning all energy to 100% clean, renewable wind-water-solar (WWS) energy, efficiency, and storage. WWS reduces global energy needs by 57.1%, energy costs by 61%, and social (private plus health plus climate) costs by 91% while avoiding blackouts, creating millions more jobs than lost and requiring little land. Thus, 100% WWS needs less energy, costs less, and creates more jobs than current energy.

Jacobson et al., 2019, One Earth *1*, 449–463
December 20, 2019 © 2019 The Author(s). Published by Elsevier Inc.
https://doi.org/10.1016/j.oneear.2019.12.003

One Earth
Article

Gold Standard for the Global Goals
3 tons of CO_2 offset
CellPress

Impacts of Green New Deal Energy Plans on Grid Stability, Costs, Jobs, Health, and Climate in 143 Countries

Mark Z. Jacobson,[1,4,*] Mark A. Delucchi,[2] Mary A. Cameron,[1,3] Stephen J. Coughlin,[1] Catherine A. Hay,[1] Indu Priya Manogaran,[1] Yanbo Shu,[1] and Anna-Katharina von Krauland[1]
[1]Department of Civil and Environmental Engineering, Stanford University, Stanford, CA 94305-4020, USA
[2]Institute of Transportation Studies, University of California at Berkeley, Berkeley, CA 94804-3580, USA
[3]Hivemapper, Burlingame, CA 94010, USA
[4]Lead Contact
*Correspondence: jacobson@stanford.edu
https://doi.org/10.1016/j.oneear.2019.12.003

SCIENCE FOR SOCIETY The Earth is approaching 1.5°C global warming, air pollution kills over 7 million people yearly, and limited fossil fuel resources portend social instability. Rapid solutions are needed. We provide Green New Deal roadmaps for all three problems for 143 countries, representing 99.7% of world's CO_2 emissions. The roadmaps call for countries to move all energy to 100% clean, renewable wind-water-solar (WWS) energy, efficiency, and storage no later than 2050 with at least 80% by 2030. We find that countries and regions avoid blackouts despite WWS variability. Worldwide, WWS reduces energy needs by 57.1%, energy costs from $17.7 to $6.8 trillion/year (61%), and social (private plus health plus climate) costs from $76.1 to $6.8 trillion/year (91%) at a capital cost of ~$73 trillion. WWS creates 28.6 million more long-term, full-time jobs than are lost and needs only 0.17% and 0.48% of land for footprint and space, respectively. Thus, WWS needs less energy, costs less, and creates more jobs than current energy.

SUMMARY

Global warming, air pollution, and energy insecurity are three of the greatest problems facing humanity. To address these problems, we develop Green New Deal energy roadmaps for 143 countries. The roadmaps call for a 100% transition of all-purpose business-as-usual (BAU) energy to wind-water-solar (WWS) energy, efficiency, and storage by 2050 with at least 80% by 2030. Our studies on grid stability find that the countries, grouped into 24 regions, can match demand exactly from 2050 to 2052 with 100% WWS supply and storage. We also derive new cost metrics. Worldwide, WWS energy reduces end-use energy by 57.1%, aggregate private energy costs from $17.7 to $6.8 trillion/year (61%), and aggregate social (private plus health plus climate) costs from $76.1 to $6.8 trillion/year (91%) at a present value capital cost of ~$73 trillion. WWS energy creates 28.6 million more long-term, full-time jobs than BAU energy and needs only ~0.17% and ~0.48% of land for new footprint and spacing, respectively. Thus, WWS requires less energy, costs less, and creates more jobs than does BAU.

INTRODUCTION

The world is beginning to transition to clean, renewable energy for all energy purposes. However, to avoid 1.5°C global warming, we must stop at least 80% of all energy and non-energy fossil fuels and biofuel emissions by 2030[1] and stop 100% no later than 2050.[1,2] Air pollution from these same sources kills 4–9 million people each year (Figure 1),[3] and this damage will continue unless the sources of air pollution are eliminated. Finally, if the use of fossil fuels is not curtailed rapidly, rising demand for increasingly scarce fossil energy will lead to economic, social, and political instability, enhancing international conflict.[3,4]

In an effort to solve these problems, studies among at least 11 independent research groups have found that transitioning to 100% renewable energy in one or all energy sectors, while keeping the electricity and/or heat grids stable at a reasonable cost, is possible.[1,5–26] The reviews of Brown et al.[27] and Diesendorf and Elliston[28] further find that critiques of 100% renewable systems are misplaced. The latter study, for example, concludes, "the main critiques published in scholarly articles and books contain factual errors, questionable assumptions, important omissions, internal inconsistencies, exaggerations of limitations and irrelevant arguments."

Among the studies that find that 100% renewable energy is cost effective, many have been of limited use to policy makers because they considered only private cost and not social cost, did not compare business-as-usual (BAU) with wind-water-solar

This is an open access article under the CC BY-NC-ND license (http://creativecommons.org/licenses/by-nc-nd/4.0/).

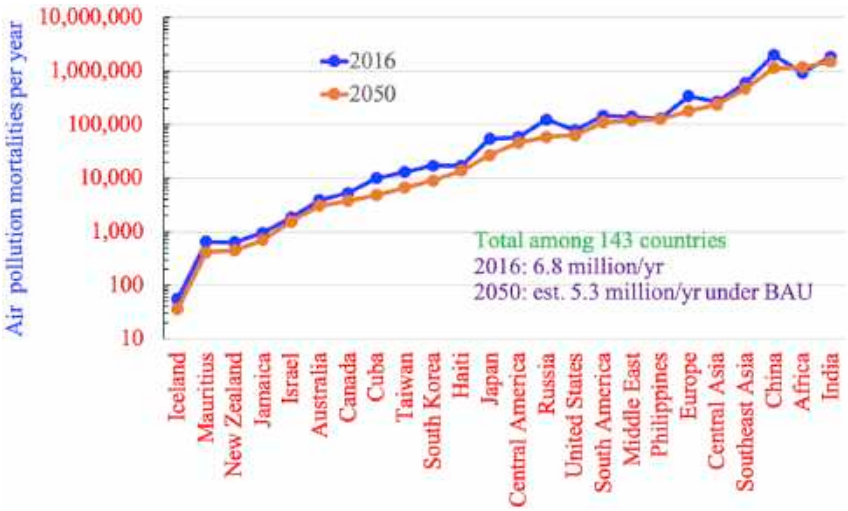

Figure 1. Estimated BAU Air-Pollution Mortalities in 2016 and 2050 by World Region

2016 and projected 2050 all-cause indoor plus outdoor air-pollution mortalities per year in 24 world regions encompassing 143 countries (see Table 1 for a list of countries in each region). We obtained 2016 data by multiplying country-specific indoor plus outdoor air-pollution deaths per 100,000 people from the World Health Organization[40] by 2016 country population. 2050 estimates were obtained with Equation S35 in Note S39. BAU energy is estimated to be responsible for 90% of the mortalities in this figure (most of the rest are from open biomass burning, wildfires, and dust). See Table S15 for a breakdown of 2016 world air-pollution deaths by cause.

(WWS) energy, and considered only cost per unit energy and not the aggregate (summed) cost over all end-use energy used.

First, social (economic) costs are private market costs plus external costs not accounted for in market costs or prices. In the present context, the most relevant external costs are those due to (1) air-pollution mortality, morbidity, and non-health damage and (2) global warming damage. A social-cost analysis is more useful to policy makers than is an analysis that considers only private costs because the former gives policy makers a more complete picture of the impacts of policies that affect climate change and air pollution than does the latter.

Second, many studies have not compared the cost of WWS energy with that of BAU energy. As such, determining the magnitude of the benefit of one over the other is difficult. Differences between WWS and BAU energy are masked even more when a private-cost analysis, which ignores health and climate costs, is performed instead of a social-cost analysis.

Third, most analyses look at the cost per unit energy rather than the aggregate energy cost per year. This problem is significant because a WWS system uses much less end-use energy than does a BAU system.

In 2009, Jacobson and Delucchi[5] calculated that transitioning the world's all-purpose energy to 100% WWS energy by 2030 could be technically and economically feasible, but for social and political reasons, a complete transition by 2030 was unlikely and could take up to a couple of decades longer. Subsequent roadmaps[1,4,15] proposed an 80% transition by 2030 and a 100% transition by no later than 2050 (e.g., Figure S1). The energy portion of the Green New Deal (GND) proposed in the US Congress[29] and earlier versions of it[30] adopted Jacobson and Delucchi's "technically and economically feasible" 2030 deadline and "100% clean, renewable, and zero-emission energy sources" goal.[30]

This paper provides GND energy roadmaps for transitioning 143 countries, representing more than 99.7% of global fossil fuel CO_2 emissions, to 100% WWS energy for all energy purposes (which include electricity, transportation, building heating and cooling, industry, agriculture, forestry, fishing, and the military; Note S28). The proposed transition timeline is no less than 80% WWS energy by 2030 and 100% by no later than 2050 (Figure S1) worldwide. The paper also provides analyses of grid stability for 24 world regions encompassing the 143 countries (Table 1). Because the 100% clean, renewable, and zero-emission energy goals of the present study are the same as those of the US GND, but with an adjusted timeline, the present study can help to evaluate the costs and feasibility of the energy component of not only the US GND but also the GNDs of 142 other countries. The US GND contains additional proposed legislation related to jobs, health care, education, and social justice.[29] The present study does not fully evaluate the costs or merits of these other components. However, because the energy transitions outlined here benefit air-pollution health, climate, and jobs, this work partly addresses some of these components. In this study, we evaluate results considering both private and social costs in terms of (1) the cost per unit end-use energy and (2) the cost aggregated over all end-use energy ("aggregate" cost). New cost metrics are provided. At the end, we discuss uncertainties and sensitivities as well as differences between the present study and two recent studies that argue that using 100% renewables for electricity is not feasible at low cost.

RESULTS AND DISCUSSION

We first projected 2016 end-use BAU energy in multiple energy sectors in 143 countries to 2050 (Note S3). 2050 BAU end-use energy loads were then electrified, the electricity for which was provided by WWS energy (Notes S4–S12). Table 2 and Figure S1 indicate that transitioning from BAU to WWS energy in 143 countries reduces 2050 annual average demand for end-use power (defined in Note S3) by 57.1% (case WWS-D in Table 2). Of this, 38.3 percentage points are due to the efficiency of using WWS electricity over combustion; 12.1 percentage points are due to eliminating energy in the mining, transporting, and refining of fossil fuels; and 6.6 percentage points are due to improvements in end-use energy efficiency and reduced energy use beyond those in the BAU case. Of the 38.3% reduction due to the efficiency advantage of WWS electricity, 21.7 percentage points are due to the efficiency advantage of WWS transportation, 3.4 percentage points are due to

Table 1. The 24 World Regions Composed of 143 Countries Treated in This Study

Region	Country or Countries within Each Region
Africa	Algeria, Angola, Benin, Botswana, Cameroon, Congo, Democratic Republic of the Congo, Egypt, Eritrea, Ethiopia, Gabon, Ghana, Ivory Coast, Kenya, Libya, Morocco, Mozambique, Namibia, Niger, Nigeria, Senegal, South Africa, South Sudan, Sudan, Tanzania, Togo, Tunisia, Zambia, Zimbabwe
Australia	Australia
Canada	Canada
Central America	Costa Rica, El Salvador, Guatemala, Honduras, Mexico, Nicaragua, Panama
Central Asia	Kazakhstan, Kyrgyz Republic, Pakistan, Tajikistan, Turkmenistan, Uzbekistan
China	China, Hong Kong, Democratic Republic of Korea, Mongolia
Cuba	Cuba
Europe	Albania, Austria, Belarus, Belgium, Bosnia-Herzegovina, Bulgaria, Croatia, Cyprus, Czech Republic, Denmark, Estonia, Finland, France, Germany, Gibraltar, Greece, Hungary, Ireland, Italy, Kosovo, Latvia, Lithuania, Luxembourg, Macedonia, Malta, Moldova Republic, Montenegro, Netherlands, Norway, Poland, Portugal, Romania, Serbia, Slovakia, Slovenia, Spain, Sweden, Switzerland, Ukraine, United Kingdom
Haiti	Haiti, Dominican Republic
Iceland	Iceland
India	India, Nepal, Sri Lanka
Israel	Israel
Jamaica	Jamaica
Japan	Japan
Mauritius	Mauritius
Mideast	Armenia, Azerbaijan, Bahrain, Iran, Iraq, Jordan, Kuwait, Lebanon, Oman, Qatar, Saudi Arabia, Syrian Arab Republic, Turkey, United Arab Emirates, Yemen
New Zealand	New Zealand
Philippines	Philippines
Russia	Georgia, Russia
South America	Argentina, Bolivia, Brazil, Chile, Colombia, Curacao, Ecuador, Paraguay, Peru, Suriname, Trinidad and Tobago, Uruguay, Venezuela
Southeast Asia	Bangladesh, Brunei Darussalam, Cambodia, Indonesia, Malaysia, Myanmar, Singapore, Thailand, Vietnam
South Korea	South Korea
Taiwan	Taiwan
United States	United States

the efficiency advantage of WWS electricity for industrial heat, and 13.2 percentage points are due to the efficiency advantage of heat pumps.

Initial estimates of nameplate capacities needed to meet annual average load were then derived for each of the 143 countries (Note S13). The 143 countries were subsequently grouped into 24 world regions (Table 1). LOADMATCH was next run from 2050 to 2052 with 30 s timesteps to match all-sector demand with supply in each region. For each region, the initial inputs were adjusted for each simulation until a zero-load-loss solution was found among all timesteps, typically within ten simulation attempts. After one successful simulation, we ran the model another 4–20 simulations, with further adjustments, to find additional lower-cost solutions. Thus, multiple zero-load loss solutions were obtained for each region, but only the lowest-cost solution is presented here. Tables S20 and S21 provide the final generator nameplate capacities and capacity factors, respectively, in each region. Table S11 provides the final storage characteristics.

Table 3 indicates that only 9% more generator nameplate capacity is needed, in the 143-country average, to meet time-dependent load than to meet annually averaged load. Storage is also needed to meet time-dependent load (Table S11).

Figure 2 shows the full 3-year time series of WWS power generation versus load plus losses plus changes in storage plus shedding for two world regions. Figure S4 shows the same but for all 24 world regions. Both figures also show a distribution of WWS power generation and of load plus losses plus changes in storage plus shedding for 100 days during each time series. The figures demonstrate no load loss at any time in any region.

The 2050–2052 WWS mean social cost per unit all-sector energy, when weighted by generation among all 24 regions, is 8.96 ¢/kWh-all-energy (USD 2013) (Figure 3A and Tables S22 and S23). However, Figure 3A shows that the individual regional averages range from 6.5 ¢/kWh-all-energy (Iceland) to 13.1 ¢/kWh-all-energy (Israel). The largest portion of cost is the cost of generation, which includes capital, operation, maintenance, and decommissioning costs (Table S14). In descending order, the next-largest costs are of transmission and distribution; electricity storage; hydrogen production, compression, and storage; and thermal energy storage.

Table 2. Reduced End-Use Demand upon a Transition from BAU to WWS Energy

		Percentage of Total						2050 Change in Demand			
Scenario	Total End-Use Demand	Residential	Commercial	Industrial	Transport	Agriculture, Forestry, and Fishing	Military and Other	Due to Higher WWS Work/Energy Ratio	Due to Eliminating Upstream Emissions with WWS	Due to Greater Efficiency with WWS Than with BAU	Total 2050 Change in Demand Due to Switching to WWS
BAU 2016	12,628 GW	21.1%	8.13%	38.4%	28.7%	2.1%	1.5%	–	–	–	–
BAU 2050	20,255 GW	19.1%	7.80%	37.4%	32.3%	1.9%	1.5%	–	–	–	–
WWS-A 2050[a]	15,932 GW	20.2%	8.50%	34.9%	32.6%	2.2%	1.6%	0%	−13.7%	−7.6%	−21.3%
WWS-B 2050[b]	11,968 GW	27.0%	11.3%	46.4%	11.8%	1.6%	1.9%	−21.7%	−12.4%	−6.8%	−40.9%
WWS-C 2050[c]	11,294 GW	28.6%	12.0%	43.2%	12.5%	1.7%	2.0%	−25.1%	−12.3%	−6.8%	−44.2%
WWS-D 2050[d]	8,693 GW	17.7%	10.5%	52.0%	16.2%	1.7%	1.8%	−38.3%	−12.1%	−6.6%	−57.1%

This table shows annually averaged end-use power demand for 2016 BAU, 2050 BAU, and 2050 100% WWS energy by sector, summed among the 143 countries in Table 1. The last column shows the total percent reduction in 2050 BAU end-use power demand due to switching from BAU to WWS energy, including the effects of reduced energy use caused by the higher work-output-to-energy-input ratio of electricity over combustion; eliminating energy used for mining, transporting, and/or refining coal, oil, natural gas, biofuels, bioenergy, and uranium; and assumed policy-driven increases in end-use energy efficiency beyond those in the BAU case. Four 2050 WWS cases are shown: WWS-A, WWS-B, WWS-C, and WWS-D. The result indicates that, of the 38.3% demand reduction due to the higher work-output-to-energy-input ratio of electricity over combustion, 21.7, 3.4, and 13.2 percentage points are due to the efficiency of WWS transportation, the efficiency of WWS electricity for industrial heat, and the efficiency of heat pumps, respectively. Table S2 shows rows "BAU 2050" and "WWS-D 2050" by country. Note S28 defines sectors.

[a]Case WWS-A eliminates the energy used for mining, transporting, and refining fossil fuels and uranium and increases energy efficiency beyond that of BAU energy (change all values for extra efficiency in Table S1 to current values from unity), but it does not change the work-output-to-energy-input ratio relative to that of BAU energy. It assumes that the efficiency of electrification is the same as that of fossil fuels (leave the electricity-to-fuel ratio = 1 for all fuels in all sectors in Table S1).

[b]Case WWS-B is the same as WWS-A, except that it includes the higher work-output-to-energy-input ratio of electric vehicles and hydrogen-fuel-cell vehicles powered by WWS energy over internal-combustion vehicles (reduce the electricity-to-fuel ratios from 1 to their current values for oil, natural gas, biofuels, and waste in the transportation sector and for oil in the agriculture, forestry, and fishing sector, military sector, and other sectors in Table S1).

[c]Case WWS-C is the same as WWS-B, except that it accounts for the higher work-output-to-energy-input ratio of high-temperature industrial processes with WWS energy (reduce the electricity-to-fuel ratios from 1 to their current values for oil, natural gas, coal, biofuels, and waste in the industrial sector in Table S1).

[d]Case WWS-D is the same as WWS-C, except that it accounts for the higher work-output-to-energy-input ratio of heat pumps over internal-combustion heating for low-temperature heat (reduce the electricity-to-fuel ratios from 1 to their current values for all remaining values below 1 in Table S1: namely, oil, natural gas, coal, biofuels, and waste in the residential and commercial sectors; heat for sale in all sectors; natural gas, coal, biofuels, and waste in the agriculture, forestry, and fishing sector, military sector, and other sectors).

Figure 3B indicates that the overall net present value of the capital cost of transitioning all energy sectors of 143 countries to 100% WWS energy while keeping the grid stable is about $72.8 trillion (USD 2013). Individual regional costs range from $2.6 billion for Iceland to $16.6 trillion for the China region. The cost for the US is about $7.8 trillion, and that for Europe is about $6.2 trillion. These capital costs pay themselves off over time by electricity and heat sales.

Figure 4 and Table 4 present results from our main cost metrics. Multiplying the private cost per unit energy in Figure 4A by the end-use energy consumed per year (or by the annual average power) in the WWS and BAU cases gives the aggregate annual private energy cost in each case, shown in Figure 4B. Among 143 countries, the aggregate annual private energy cost is $6.8 trillion/year in the WWS case and $17.7 trillion/year in the BAU case. The main (but not only) reason for this difference is the 57.1% lower end-use energy consumption in the WWS case (Tables 2 and 4).

What's more, the aggregate annual social cost across all regions worldwide is $76.1 trillion/year in the BAU case but only $6.8 trillion/year in the WWS case (Table 4 and Figure 4B). Thus, the WWS-to-BAU aggregate annual social cost ratio is 9% (Table 4). In other words, the aggregate annual social cost (energy plus health plus climate costs) of WWS energy is only 9% that of a BAU system each year. Figure 4C shows the aggregate social cost ratio and its components for all 24 world regions. The ratio varies from 3.9% for the Philippines to 24.9% for Iceland. The smallest benefit of a transition occurs in Iceland simply because Iceland has already transitioned much of its energy, so its air pollution and climate emissions are already low. Thus, it sees less remaining benefit of converting than other regions.

Table 3. Nameplate Capacities Needed by Generator Type for 100% WWS Energy

Energy Technology	(A) Nameplate Capacity of One Plant or Device	(B) 2050 All-Purpose Annual Average Demand Met by Plant or Device	(C) Initial Nameplate Capacity: Existing plus New Plants or Devices to Meet Annual Average Demand	(D) Final Nameplate Capacity: Existing plus New Plants or Devices to Meet Time-Dependent Demand	(E) Percentage of Final Nameplate Capacity Already Installed by 2018	(F) Final Numbers of New Plants or Devices Needed for 143 Countries
Annual Average Power						
Onshore wind turbine	5 MW	30.50%	8,251 GW	11,976 GW	4.76%	2,281,019
Offshore wind turbine	5 MW	14.51%	3,841 GW	3,606 GW	0.68%	716,252
Wave device	0.75 MW	0.34%	156 GW	156 GW	0.0001%	208,313
Geothermal electricity	100 MW	0.92%	97 GW	97 GW	13.67%	837
Hydropower plant[a]	1,300 MW	5.72%	1,109 GW	1,109 GW	100.0%	0
Tidal turbine	1 MW	0.08%	31 GW	31 GW	1.76%	30,075
Residential rooftop PV	0.005 MW	11.14%	5,082 GW	2,776 GW	3.44%	536,080,000
Commercial or governmental rooftop PV[b]	0.1 MW	13.84%	6,705 GW	5,121 GW	1.87%	50,250,000
Utility PV plant[b]	50 MW	19.03%	8,234 GW	13,691 GW	2.09%	268,090
Utility CSP plant[b]	100 MW	3.93%	634 GW	1,262 GW	0.43%	12,565
Total for average power	–	100.00%	34,138 GW	39,842 GW	5.53%	610,045,000
For Peaking and Storage						
Additional CSP[c]	100 MW	2.36%	381 GW	0 GW	0%	0
Solar thermal heat[c]	50 MW	–	2,573 GW	632 GW	72.6%	3,468
Geothermal heat[c]	50 MW	–	70.3 GW	70.3 GW	100.00%	0
Total peaking and storage	–	2.36%	3,024 GW	702 GW	75.31%	3,468
Total All	–	–	37,163 GW	40,544 GW	6.74%	610,049,000

This table shows the estimated (C) initial nameplate capacities (meeting the annual average all-purpose end-use power demand) and final (D) nameplate capacities (meeting time-dependent demand) of WWS generators, summed among 143 countries in 24 regions, needed to supply 100% of all-purpose energy with WWS energy. Also shown are (B) the 143-country-averaged percent end-use demand estimated to be supplied by the initial nameplate capacity of each generator (values for individual countries are given in Table S5), (E) the percentage of final 2050 nameplate capacity of each generator already installed in 2018, and (F) the final numbers of new devices of specified sizes still needed. All values are summed over 143 countries in 24 regions. "Annual average power" is annual average all-purpose energy demand divided by the number of seconds per year. The nameplate capacity of each device (A) is assumed to be the same for all countries. The percentage of annual average power demand met by each device type (B) is a demand-weighted average among the mixes given for 143 countries in Table S5 before time-dependent demand calculations are performed with LOADMATCH. The "initial" nameplate capacity (C) is equal to the total end-use demand (B) multiplied by the percentage of demand satisfied by the device and then divided by the capacity factor of the device. This initial nameplate capacity (meeting average annual demand) for each grid region is used at the start of LOADMATCH simulations. The "For Peaking and Storage" section of (C) is the initial estimate of additional CSP installations and solar thermal heat generators for the start of the LOADMATCH simulations. Column (D) shows the 143-country final nameplate capacities needed to match load after the LOADMATCH simulations for each of the 24 grid regions. Table S20 gives the final nameplate capacities for each region. Columns (D) and (E) show the fraction of final nameplate capacity already installed as of the end of 2018 and the remaining number of devices of size specified in (A) still needed, respectively.

[a]No increase in the number of dams or in the peak discharge rate of hydropower is assumed.

[b]The solar PV panels used for this calculation were SunPower E20 panels. A CSP plant is assumed to have storage with a maximum charge-discharge rate (ratio of storage size to generator size) of 2.62:1. See the footnotes in Table S7 of Jacobson et al.[4] for more details.

[c]Additional CSP is the estimated CSP plus storage beyond that for annual average power generation needed to provide peaking power to stabilize the grid. Additional solar thermal and existing geothermal heat are used for direct heat or heat storage in soil. "Geothermal heat" is existing geothermal heat, which is assumed not to change in the future (hence the same values in columns C and D).

Table 4 further indicates that the 143-country aggregate private cost ratio (Equation 9) is 39%, which means that, on average, the 100%-WWS-energy scenario cuts annual consumer energy bills by 61% worldwide. Finally, the social cost per unit energy (Equation 10) is 79% less in the WWS case than in the BAU case (Table 4).

We assumed here that the BAU cost per unit all energy equals the BAU cost per unit electricity given the lack of data on the BAU cost per unit non-electrical energy. Because the aggregate annual social and private costs in the WWS cases for all world regions are an order of magnitude lower than those in the BAU cases, we believe that assumption makes no difference to the conclusion found here, namely that WWS energy is much less expensive than BAU energy, given that the conclusion would still hold even if the assumption were off by a factor of, say, eight.

Figure 3A indicates that the 2050 cost of WWS energy per unit energy is relatively low for large regions (e.g., Canada, Russia, Africa, China, Europe, and the US) and for small countries with good WWS resources (e.g., Iceland and New Zealand). Larger land areas permit greater geographical dispersion of wind and

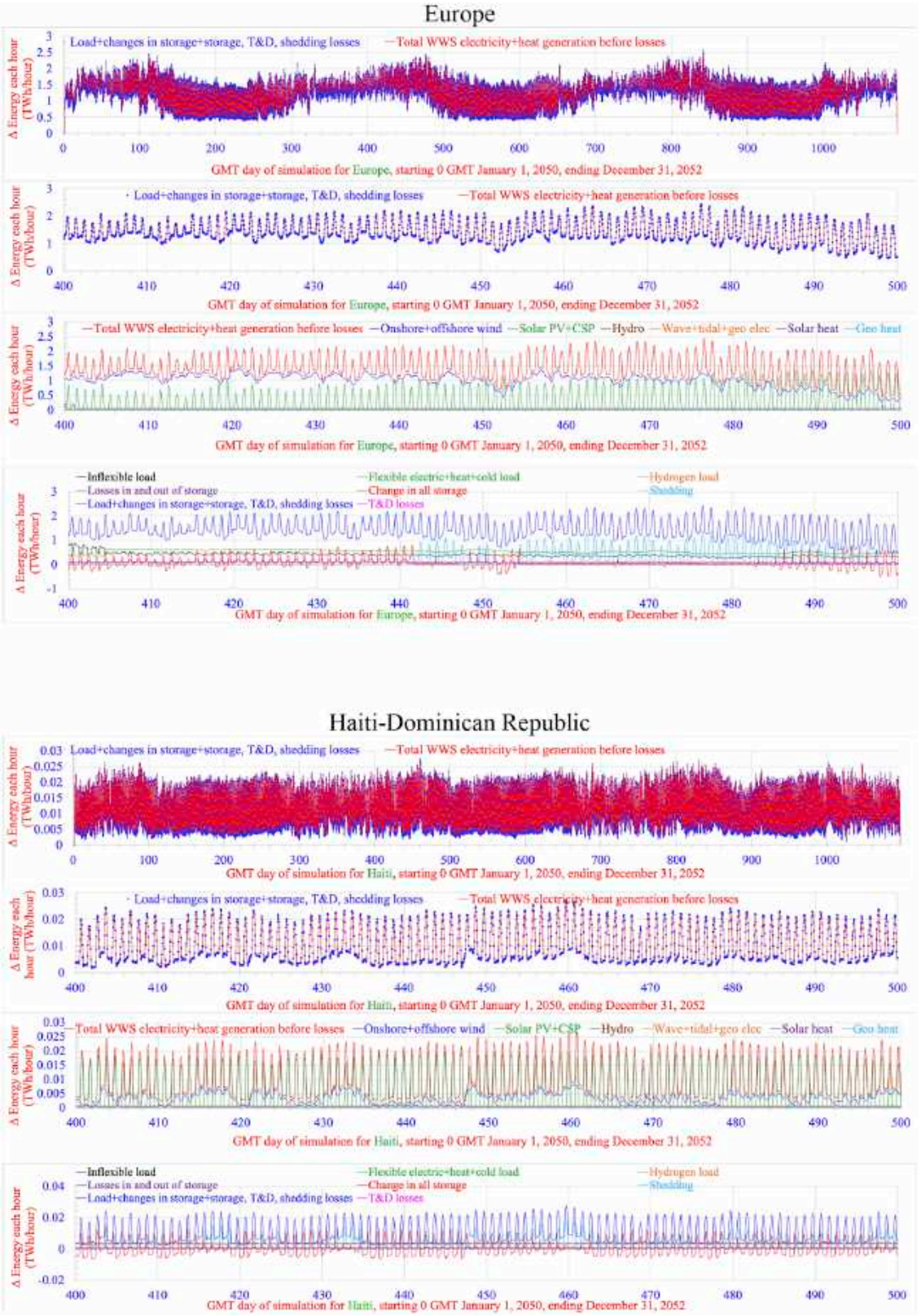

(legend on next page)

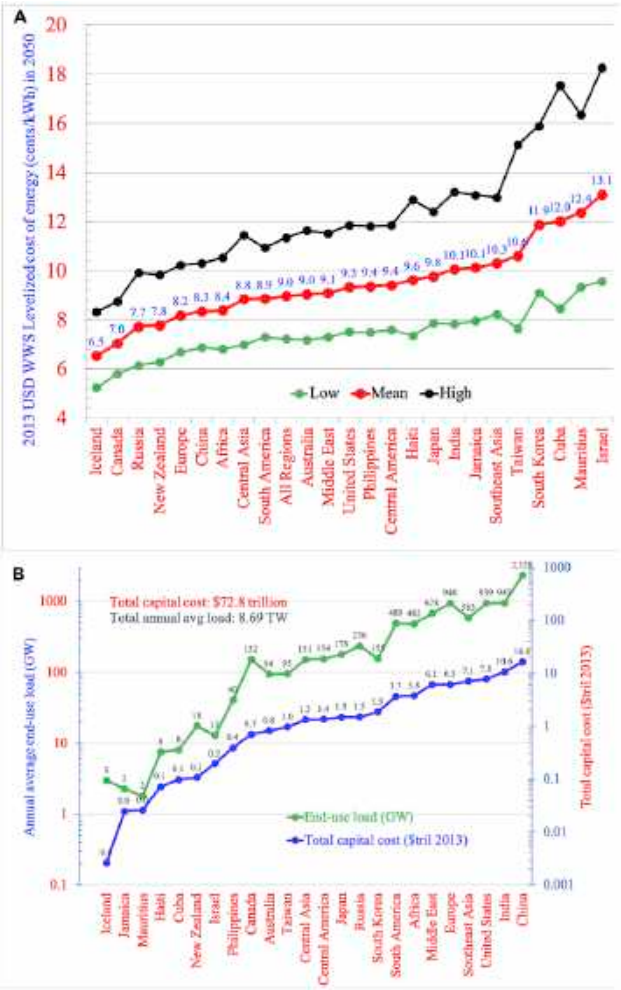

Figure 3. Energy Private Costs, Capital Costs, and Loads by World Region

(A) Low, mean, and high modeled levelized private costs (averaged between today and 2050 in 2013 USD) of converting 24 world regions encompassing 143 countries to 100% WWS energy for all energy purposes.

(B) Annual average all-purpose end-use loads and present values (2013 USD) of mean capital costs for a 100%-WWS-energy system. See Table S22 for low and high values of levelized cost.

solar energy. Connecting these dispersed resources via the regional grid reduces overall intermittency. These regions also have a good balance of solar and wind power, which are complementary in nature seasonally. Finally, the larger regions have some existing hydropower that can provide peaking power. Iceland has substantial hydropower, geothermal, and wind power.

Costs are highest in small countries with high population densities (Taiwan, Cuba, South Korea, Mauritius, and Israel). Nevertheless, the 2050 private cost of WWS energy per year in all five regions is 43%–65% that of BAU energy, indicating that a transition to WWS energy reduces costs even under the least favorable circumstances.

Land-use impacts are represented here by footprint and spacing areas required by WWS technologies. Footprint is the physical area on the top surface of soil or water needed for each energy device. New land footprint is created only for solar photovoltaic (PV) plants, concentrated solar power (CSP) plants, onshore wind turbines, geothermal plants, and solar thermal plants. Rooftop PV does not take up new land. Spacing is the area between some devices—such as wind turbines, wave devices, and tidal turbines—needed to minimize interference of the wake of one device with downstream devices. Spacing area can be used for multiple purposes, including rangeland, ranching land, industrial land (e.g., installing solar PV panels), open space, or open water. The only spacing area over land needed in a 100% WWS world is between onshore wind turbines.

The total new land areas for footprint and spacing with 100% WWS energy are about 0.17% and 0.48%, respectively, for a total of 0.65% of the 143-country land area (Note S44, Table S26, and Figure S6). This is equivalent to about 1.85 times California's land area for virtually all world energy. In comparison, about 37.4% of the world's land was agricultural land in 2016, and 2.5% was urban area in 2010.[31] The footprint needed for WWS energy is almost all for utility PV and CSP plants. Some of the utility PV can fit on the spacing area that wind occupies, illustrating the dual use of the wind land.

Finally, a transition could increase the net number of long-term, full-time jobs. Such jobs arise as a result of energy generation, transmission, and storage. Note S45 describes how changes in jobs are determined. The calculation accounts for direct jobs, indirect jobs, and induced jobs. Direct jobs are jobs for project development, onsite construction, onsite operation, and onsite maintenance of the electricity-generating facility. Indirect jobs are revenue and supply-chain jobs. They include jobs associated with construction material and component suppliers, analysts and attorneys who assess project feasibility and negotiate agreements, banks financing the project, all equipment manufacturers, and manufacturers of blades and replacement parts. The number of indirect manufacturing jobs is included in the number of construction jobs. Induced jobs result from the reinvestment and spending of earnings from direct and indirect jobs. They include jobs resulting from increased business at local restaurants, hotels, and retail stores and for childcare providers, for example. Job changes due to changes in energy prices are not included. Changes in energy pricing could trigger changes in factor allocations among capital, energy input, and labor and thus changes in job numbers.

Results here indicate that a transition could create about 28.6 million more long-term, full-time jobs than lost among the 143

Figure 2. 3-Year LOADMATCH Results for Two World Regions

Time-series comparison, from 2050 to 2052 for two world regions, of modeled (first row) total WWS power generation versus total load plus losses plus changes in storage plus shedding; (second row) same as first row but for a window of days 400–500 during the 3-year period; (third row) a breakdown of WWS power generation by source during the window; and (fourth row) a breakdown showing inflexible load; flexible electricity, heat, and cold load; flexible hydrogen load; losses in and out of storage; transmission and distribution losses; changes in storage; and shedding. The model was run at 30-s resolution. Results are shown hourly. No load loss occurred during any 30-s interval. Figure S4 shows results for all 24 world regions.

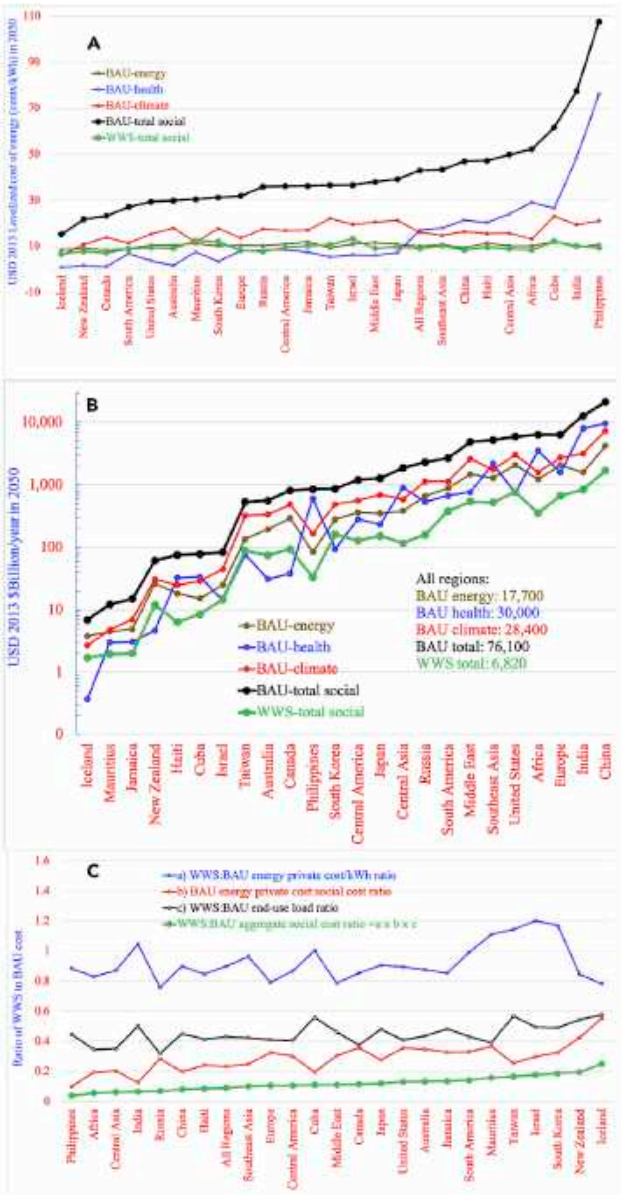

Figure 4. Summary of Private and Social Costs of WWS and BAU Energy

(A) Levelized private and social costs per kWh of energy produced by region in a BAU-energy world versus a WWS-energy world. BAU costs include energy, health, and climate costs. WWS costs include only energy costs because energy external costs are approximately zero. Energy costs are averaged between today and 2050 because the WWS-energy system will be built out during this period.

(B) Same as (A) but with the annual aggregate cost per year, obtained by multiplication of the cost per unit energy in (A) by the end-use energy consumption per year in the BAU or WWS case (from Table S2). See Table S22 for low and high annual aggregate costs of WWS energy per year.

(C) The WWS-to-BAU aggregate social cost ratio and its three component factors: the WWS-to-BAU ratio of cost per unit energy (obtained from A), the ratio of private cost of BAU energy to social cost (obtained from B), and the WWS-to-BAU ratio of end-use load (e.g., from Table S2 but for each region). 90% of all air-pollution mortalities are ascribed to BAU energy. Most of the rest are ascribed to open biomass burning, wildfires, and dust. The mean and range in aggregate health cost, summed over all regions, is $30 ($17.9–$52.7) trillion/year. That in aggregate climate costs is $28.4 ($16.0–$60.5) trillion/year. All costs are in 2013 USD.

countries (Table S28 and Note S45). Net job gains occurred in 21 out of 24 world regions. Net losses occurred in regions heavily dependent on fossil fuels, namely Canada, Russia, and parts of Africa. However, additional jobs in those and other regions could result from the need to build more electrical appliances, vehicles, and machines and to increase building energy efficiency, and these jobs were not considered here.

In the US, the estimated aggregate private and social costs of BAU energy are $2.1 and $5.9 trillion/year, respectively, whereas those of WWS energy are both $0.77 trillion/year. Thus, WWS energy decreases the aggregate private cost by 64% and aggregate social cost by 87%. The social-cost reduction arises from eliminating about 63,000 US air-pollution deaths per year (in 2050) and corresponding illnesses as well as eliminating the US energy contribution to global warming.

The US transition to 100% WWS energy is estimated to cost a mean of $7.8 trillion in net-present-value capital but create 3.1 million net long-term full-time US jobs (Table S28) and use only 0.22% of the country's land for footprint and 0.86% for spacing (Table S26). As such, a complete US transition, as also called for by the US GND,[29] will reduce aggregate energy costs each year, reduce health-care costs and mortality, reduce climate damage, and create jobs.

Uncertainties and Sensitivities

The results here contain uncertainties. Some include uncertainties arising from inconsistencies between load and resource datasets, the timing of generator and storage downtime, assuming perfect transmission, not modeling transmission congestion, not modeling frequency regulation, and projecting future energy use. Note S46 discusses these issues as well as several sensitivity tests performed here to examine uncertainties in more detail. These include cost sensitivities due to changes in the fraction of thermal loads subject to district heating and underground thermal energy storage, to changes in hydrogen storage, and to changes in demand response.

One particular concern is whether the simulations here captured the variability of energy demand and wind and solar supply, including during extreme weather events. However, GATOR-GCMOM (gas, aerosol, transport, radiation, general circulation, mesoscale, and ocean model) accounts for extreme weather events because it models the variability of weather everywhere worldwide at a 30 s time resolution on the basis of physical principles. It also accounts for competition among wind turbines for available kinetic energy and the resulting feedback of such turbines to weather. Zero-load-loss results were found here every 30 s for 3 years, thus accounting for extreme weather events, in 24 vastly different world regions, each with different WWS supplies.

Another uncertainty arises from our assumption of a perfectly interconnected transmission system. Whereas the study accounts for transmission and distribution costs and losses, it assumes that electricity can flow to where it is needed without bottlenecks. This concern applies to only about half the regions examined given that 11 regions (Iceland, Cuba, Jamaica, Haiti

Table 4. Summary of Private and Social Costs over 143 Countries

Private and Social Costs	Value
(A) Private cost per unit BAU energy[a]	9.99 ¢/kWh
(B) Health cost per unit BAU energy	16.9 ¢/kWh
(C) Climate cost per unit BAU energy	16.0 ¢/kWh
(D) Social cost per unit BAU energy (A + B + C)	42.9 ¢/kWh
(E) Private and social cost per unit WWS energy[a]	8.96 ¢/kWh
(F) End-use power demand of BAU energy[b]	20,255 GW
(G) End-use power demand of WWS energy[b]	8,693 GW
(H) Aggregate annual private cost of BAU energy in the electricity sector (A × F)	$17.7 trillion/year
(I) Health cost of BAU energy (B × F)	$30.0 trillion/year
(J) Climate cost of BAU energy (C × F)	$28.4 trillion/year
(K) Social cost of BAU energy (D × F)	$76.1 trillion/year
(L) Private and social costs of WWS energy (E × G)	$6.82 trillion/year
(M) WWS-to-BAU ratio of private cost per kWh ($R_{WWS:BAU-E}$) (E/A)	0.90
(N) Ratio of private cost of BAU energy (kWh) to social cost of BAU energy (kWh) ($R_{BAU-S:E}$) (A/D)	0.23
(O) Ratio of WWS energy used (kWh) to BAU energy used (kWh) ($R_{WWS:BAU-C}$) (G/F)	0.43
WWS-to-BAU ratio of aggregate social cost (R_{ASC}) (M × N × O)	0.09
WWS-to-BAU ratio of aggregate private cost (R_{APC}) (M × O)	0.39
WWS-to-BAU ratio of social cost per unit energy (R_{SCE}) (M × N)	0.21

This table shows the 2050 mean social costs per unit WWS versus BAU energy for 143 countries (24 world regions), as well as the WWS-to-BAU ratio of aggregate social cost and the components of its derivation (Equation 5).

[a]This is the electricity-sector cost of BAU energy per unit energy. It is assumed to equal the all-energy cost of BAU energy per unit energy. The cost per unit WWS energy is for all energy, which is almost all electricity (plus a small amount of direct heat).

[b]Multiply GW by 8,760 h/year to obtain GWh/year.

and the Dominican Republic, Israel, Japan, Mauritius, New Zealand, the Philippines, South Korea, and Taiwan) have or could have, because of their small size, well-connected transmission and distribution systems. Stable, low-cost systems were found here for all those regions. As such, there is no reason to think that the US, for example, broken up into multiple isolated or moderately interconnected regions rather than one completely interconnected region can't also maintain a low-cost, stable 100% WWS grid. In fact, many of the dozens of earlier cited papers that have examined 100% renewable grids have treated transmission spatially and have found low-cost solutions. Aghahosseini et al.,[24] for example, found stable, low-cost, time-dependent electric grid solutions when North and South America were run on 100% renewables, and transmission flows were modeled explicitly among multiple lines. Although the present paper sacrifices spatial resolution needed to treat transmission explicitly, it treats time resolution (30 s) higher than other studies.

Finally, although the impact of transmission congestion on reliability is not modeled explicitly, Jacobson et al.[15] ran sensitivity tests (see their Figure S13) to check how different fractions of wind and solar power subject to long-distance transmission might affect cost. The result was that, if congestion is an issue at the baseline level of long-distance transmission, increasing the transmission capacity will relieve congestion with only a modest increase in cost.

Many remaining uncertainties are captured by the use of low, mean, and high costs of energy, air-pollution damage, and climate damage. Table S14, for example, shows low, mean, and high estimates of capital cost, operation and maintenance cost, decommissioning cost, energy generator lifetimes, and transmission, distribution, and downtime losses assumed here. Table S22 and Figure 3 provide the resulting low, mean, and high levelized private costs of energy per unit energy and private aggregate costs of energy for each world region. Table S18 provides the low, mean, and high estimated social costs of carbon, and Table S16 provides the parameters needed for calculating low, mean, and high air-pollution costs. Table S17 provides the resulting low, mean, and high air-pollution and climate costs per unit energy by country.

Comparison with Studies Critical of 100% Renewables

Two recent studies argue that 100% renewables is not a low-cost solution. One study[32] states that 80% of current US demand can be met by solar and wind power interconnected by either a US-wide transmission grid or 12 h of electrical storage but that more than 80% requires "costly" excess storage or solar or wind nameplate capacity. The present study and numerous papers among 11 independent research groups[4–28] contradict these findings.

First, the previous study[32] did not consider electrification of transportation, building heating, or industrial heat. Electrification of such loads not only reduces end-use demand substantially, as shown here, but also reduces the daily and seasonal variability of electric loads while creating more flexible loads that are subject to demand response. For example, current US electricity demand has a summer peak due to a high summer demand for air conditioning. Winter demand for building heating is currently provided mostly by natural gas and fuel oil, so it results in less winter electricity demand. Although replacing such heat with electric heat pumps increases winter electrical load (but by much less than the energy in the fuel it replaces as a result of the high coefficient of performance of heat pumps), the electrification of winter heating evens out seasonal (between summer and winter) electrical loads substantially as a result of the high summer electrical load.

On top of that, vehicles are used daily, so electrification of transportation results in a relatively even (throughout the year) distribution of additional electric load, further reducing the summer-winter electric-load imbalance. Because electric cars are charged mostly at night (particularly with tiered electrical rates that are lowest at night), such electrification also evens out day versus night electrical loads in comparison with the present grid.

Not only did this previous study[32] assume an unrealistic load distribution, but it also did not treat demand response, district

heating, seasonal heat and cold storage, existing hydropower storage, or hydrogen production and storage for transportation. As a result, it shed excess wind and solar power instead of storing that energy in seasonal or daily thermal energy storage or hydrogen. In the present study, seasonal underground thermal energy storage is applied to the fraction of a region's thermal energy that is subject to district heating (Table S9). In addition, hydrogen is used for fuel cells for a portion of transportation, namely for long-distance heavy transport.

By not treating naturally rechargeable existing hydropower storage, the previous study[32] also limited its ability to fill in gaps in supply during key winter hours, when some of its shortfalls occurred.

The present study treats these processes and finds low-cost solutions with 100% WWS energy and storage not only in the US but also in 24 world regions.

A second study[33] used an optimization model that treats electricity from renewables, nuclear energy, natural gas with carbon capture, and biomass and battery storage in an effort to examine grid stability in two US regions. Simulations were run for 1 year with a 1-h time resolution. The model did not electrify transportation, building heating, or industrial heating; did not treat district heating or seasonal underground thermal energy storage; did not treat demand response or hydrogen production or storage; and did not treat concentrated solar power with storage, pumped hydropower storage, or hydropower storage. These processes are all treated here.

That study also did not consider the health or climate costs of the combustion sources, the delays between planning and operation of nuclear plants or plants using natural gas with carbon capture, or the resulting background-grid CO_2 and air-pollution emissions and costs due to such delays. It also assumed that carbon capture reduces 90% of CO_2 emissions, but that assumption ignores the upstream emissions from natural gas mining and transport and the fact that a natural gas plant with carbon-capture equipment requires 25%–50% more energy, and thus results in additional emissions, than the same plant without capture.[34] Thus, instead of reducing 90% of CO_2 emissions, carbon capture could result in a net emission reduction of only 10%–30% over a 20- to 100-year time frame.[35]

Moreover, that study substantially underestimated the private energy costs of nuclear power and natural gas with carbon capture. The nuclear capital cost in its mid-range case was 50% below the mean estimated nuclear capital cost from Lazard.[36] Its mid-range cost of natural gas with carbon capture was only $1,720/kW. However, the cost of the carbon-capture equipment alone for the only US power plant with carbon capture, the W.A. Thompson coal plant in Texas, was $1 billion or $4,200/kW.[35]

In sum, this previous study[33] not only biased nuclear and natural gas costs but also underestimated emissions and ignored many process that facilitate matching renewable supply with demand. Thus, its conclusion that "including nuclear power and natural gas plants that capture CO_2 consistently lower[s] the cost of decarbonizing electricity generation" was not shown. As calculated here, a transition to 100% WWS energy should reduce private and social costs substantially over those incurred by BAU energy without the need for nuclear power, fossil fuels with carbon capture, or bioenergy.

Finally, several additional studies have examined high penetrations of renewables. None of these studies examined scenarios with 100% renewables or disputed the possibility of using 100% renewables. One study[37] found that each region of the US could be powered with at least 90% renewable electricity and storage while matching power demand with supply hourly during a year. Renewable curtailment at 90% penetration was only 7%. The study did not examine 100% scenarios or scenarios in which all sectors were electrified. Two other studies similarly found that reducing US energy[38] or electricity[39] greenhouse gas emissions 80% below 1990 levels by 2050 is technically feasible and that multiple alternative pathways for achieving those reductions exist. Neither study examined 100% scenarios.

Conclusions

Here, we developed GND energy roadmaps for 143 individual countries to transition their all-purpose energy from BAU to 100% WWS, efficiency, and storage by no later than 2050 and with no less than an 80% transition by 2030. We then grouped the countries into 24 regions to study matching energy demand with 100% WWS supply plus efficiency and electricity, heat, cold, and hydrogen storage every 30 s from 2050 to 2052. Stable (no-load-loss) solutions were found in all world regions.

The cost of transitioning to 100% clean, renewable WWS, efficiency, and storage for all energy purposes while keeping the lights on can be viewed in terms of the private cost per unit energy, the aggregate private cost per year, the social cost per unit energy, and/or the aggregate social cost per year. Even more relevant is the comparative WWS versus BAU costs for these parameters. However, most studies to date have considered only private costs per unit energy, but this parameter shows only a modest difference between BAU and WWS energy. The WWS-to-BAU aggregate social cost ratio, on the other hand, indicates that the economic cost of transitioning to 100% WWS energy in 143 countries grouped into 24 regions is a mean of only 9%. In other words, 100% WWS energy reduces aggregate social costs by 91% in comparison with those incurred by BAU energy. The major reasons for this are much less end-use energy consumption, lower health and climate costs, and slightly lower private costs per unit energy with WWS energy than with BAU energy.

Further, transitioning 143 countries between today and 2050 requires only $6.8 trillion/year in annual private costs for WWS energy (accounting for electricity, heat, cold, hydrogen generation and storage, and transmission and distribution) versus $17.7 trillion/year for BAU energy. Thus, the aggregate private cost of WWS energy is 61% lower than that of BAU energy. What's more, the aggregate social cost of BAU energy is an astronomical $76.1 trillion/year.

The net present value of the capital cost of transitioning to WWS energy worldwide is ~$72.8 trillion over all years of the transition between today and 2050. That for the US alone is about $7.8 trillion. This is the estimated net present value of the capital cost of energy in the US GND.

In the US, 100% WWS energy reduces aggregate private and social energy costs by 64% and 87%, respectively, reduces human mortality and morbidity, reduces climate-relevant emissions and impacts, and creates 3.1 million more long-term, full-time jobs than BAU energy.

The capital cost of WWS is not a cost that government needs to pay. It is a cost that pays itself off with electricity sales over the life of energy, storage, and transmission and distribution equipment. However, government assistance in a transition is helpful and necessary to speed the transition and is important given the rapid pace needed for a transition.

Uncertainties in this study arise mainly from inconsistencies between load and resource datasets, the timing of generator and storage downtime, assuming perfect transmission, not modeling transmission congestion, not modeling frequency regulation, and projecting future energy use. These uncertainties were discussed in this paper and in the Supplemental Information. Sensitivity tests and papers published by others suggest that these uncertainties should not affect costs more than marginally. Nevertheless, further work would help to verify this and quantify the impact of each uncertainty on cost in different world regions.

In sum, this study indicates that transitioning to 100% WWS energy in 143 countries decreases energy requirements and aggregate private and social costs while adding about 28.6 million more long-term, full-time jobs than are lost. A 100%-WWS-energy economy uses only about 0.65% of the 143-country land area, of which 0.17% is for footprint and 0.48% is for spacing. Thus, transitioning the world entirely from BAU energy to clean, renewable energy should substantially reduce energy needs, reduce costs, create jobs, reduce air-pollution mortality, and reduce global warming.

EXPERIMENTAL PROCEDURES

Method Components

This study consisted of the following steps:

(1) Projecting the demand for BAU end-use energy to 2050 for seven fuel types in each of six energy-use sectors in each of 143 countries (Notes S2 and S3).
(2) Estimating the 2050 demand reduction due to electrifying or providing direct heat for each fuel type in each sector in each country (Notes S4–S12).
(3) Performing resource analyses and estimating a mix of WWS electricity and heat generators to meet the aggregate demand in each country in the annual average (Note S13).
(4) Using a prognostic global weather-climate-air-pollution model (GATOR-GCMOM) that accounts for competition among wind turbines for available kinetic energy to estimate wind and solar-radiation fields country by country every 30 s for several years (Notes S14–S21).
(5) Grouping the 143 countries into 24 world regions and using a model (LOADMATCH) that matches the variable supply of energy with variable demand, storage, and demand response to match demand with supply and storage every 30 s in each region from 2050 to 2052 (Notes S32–S35).
(6) Evaluating energy, health, and climate costs (Note S36–S42) with new metrics (Note S43).
(7) Calculating land-area requirements (Note S44).
(8) Calculating changes in job numbers (Note S45).
(9) Discussing and evaluating uncertainties (Note S46).

After estimating the nameplate capacities of energy generators, storage devices, and transmission lines needed for transitioning each of the 143 individual countries to 100% WWS energy in all sectors between now and 2050, we performed grid-stability analyses for the years 2050–2052 in 24 world regions encompassing the 143 countries. This process involved updating the nameplate capacities from those sufficient to meet annual average power demand to those ensuring that supply could match demand every 30 s during the 3 years in each region. We then calculated the average present value of the capital cost and the fully annualized cost of transitioning each region between today and 2050 to ensure such grid stability. We compared the resulting costs with those from a 2050 BAU scenario. We further estimated the changes in job numbers, health and climate cost savings, and land requirements of a transition.

Compared with a previous study,[1] this study uses updated energy data (2016 instead of 2012 data) for 143 (rather than 139) countries grouped into 24 (rather than 20) world regions and develops new cost metrics. It also treats each region as having a specified fraction of district heating for which seasonal and daily thermal energy storage can be used; uses new country-by-country mortality estimates[40] to project air-pollution damage costs of BAU energy; and updates estimates of country-specific population, urbanization fraction, carbon dioxide emissions, BAU fuel costs, job creation and loss, transmission and distribution efficiencies, resource potentials, rooftop areas, and land requirements, among other parameters. These updates are critical given that 61 countries have passed laws, as of the end of 2018, to transition to 100% renewable electric power and one (Denmark) has committed to transition all energy by different years between 2020 and 2050.[41] Countries that are committing to a transition could benefit from some guidance on at least one way to get there. The updated and more complete roadmaps and grid studies reported here provide such guidance for all energy sectors for 143 countries.

Cost Metrics

In this study, we present low, medium, and high estimates of external costs due to air pollution and climate change (Tables S16–S18) and then combine these external costs with estimates of private market costs to produce estimated total social costs. Social costs are evaluated in terms of both costs per unit energy and aggregate cost (Introduction).

Social-cost analyses are performed from the perspective of society rather than from the perspective of an individual or firm in the market and hence must use a social discount rate rather than a private-individual discount rate, even for the private-market-cost portion of the total social cost. To maintain consistency with the fact that our analysis is a social-cost analysis, we therefore use a social discount rate of 2% (1%–3%) for estimates of *all* our costs, both private and external, and for both WWS and BAU energy (Note S37).

The levelized private costs of BAU energy (P_{BAU}) and of WWS energy (P_{WWS}) are both defined here in units of \$/kWh-all-energy. All costs per unit energy herein for generation, storage, and transmission technologies are average values between today and 2050 but in 2013 USD. Average costs are used because the 2050 WWS energy infrastructure will be built out between today and 2050. We apply the average costs to the resulting 2050 nameplate capacities of WWS generators, storage, and transmission (determined herein) in order to estimate overall WWS costs for 143 countries grouped into 24 regions.

We estimate the average future cost of BAU electricity per unit energy in each country by weighting the cost of BAU electricity per unit energy averaged between today and 2050 for each BAU technology in each country by the current fraction of total BAU electricity consisting of each BAU technology (e.g., coal, natural gas, oil, biomass, nuclear power, and WWS).[4,42] Because we do not have data for the cost of BAU energy per unit energy outside of the electricity sector, for simplicity we assume that the cost per unit energy in other sectors (e.g., transportation, industry, etc.) equals that in the BAU electricity sector. As discussed in the Results and Discussion, this assumption makes no difference to the conclusions found here.

Additional cost-relevant parameters used here are the all-sector end-use annually averaged loads (GW or GWh-all-energy/year) of BAU energy (L_{BAU}) and WWS energy (L_{WWS}), the health cost of BAU energy per unit energy (H_{BAU}, \$/kWh-all-energy), and the climate cost of BAU energy per unit energy (C_{BAU}, \$/kWh-all-energy). The Supplemental Experimental Procedures detail how these parameters are calculated.

From these variables, social costs of BAU and WWS energy per unit energy (\$/kWh-all-energy) in 2050 are derived simply as follows:

$$S_{BAU} = P_{BAU} + H_{BAU} + C_{BAU} \quad \text{(Equation 1)}$$

$$S_{WWS} = P_{WWS} \quad \text{(Equation 2)}$$

Given that WWS energy eliminates virtually all health- and climate-relevant emissions from energy, including from the energy used for mining resources and building WWS equipment, a world powered by 100% WWS energy has little or no corresponding health or climate externality cost.

The one exception, if it is not controlled between today and 2050, is chemical CO_2 production during concrete and steel production, because building WWS equipment will require concrete and steel. Given that global chemical CO_2 emissions from concrete and steel amount to about 2% of total global CO_2 emissions and producing WWS energy equipment will consume only about 1% of the world's annually produced steel and 0.4% of the world's annually produced concrete, the net CO_2 emissions from producing WWS equipment will be only about 0.014% of current CO_2 emissions. It will go to zero if methods are developed to eliminate chemical CO_2 emissions from steel and concrete production. No air pollutants are emitted simultaneously during emissions of chemically produced CO_2 during concrete production if WWS electricity is used to provide heat and power for the production.

Nevertheless, other non-energy-related anthropogenic air pollutants and climate-affecting emissions will still occur in parallel with a 100%-WWS-energy system until they are stopped. Such emissions are due to biomass burning and human-caused wildfires; leaks of methane from landfills, feedlots, and rice paddies; halogen leaks; and nitrous oxide emissions from fertilizers. These emissions need to be mitigated simultaneously during a transition to WWS energy.

The aggregate annual social costs ($/year) for BAU and WWS energy are just the product of their social costs per unit energy and total end-use energy:

$$A_{BAU} = S_{BAU}L_{BAU} \quad \text{(Equation 3)}$$

$$A_{WWS} = S_{WWS}L_{WWS} \quad \text{(Equation 4)}$$

The ratio of these two aggregate social costs is a new metric, the WWS-to-BAU aggregate social cost ratio (R_{ASC}):

$$R_{ASC} = A_{WWS}/A_{BAU} = R_{WWS:BAU\text{-}E}\, R_{BAU\text{-}S:E}\, R_{WWS:BAU\text{-}C}, \quad \text{(Equation 5)}$$

where

$$R_{WWS:BAU\text{-}E} = P_{WWS}/P_{BAU}, \quad \text{(Equation 6)}$$

$$R_{BAU\text{-}S:E} = P_{BAU}/S_{BAU}, \quad \text{(Equation 7)}$$

and

$$R_{WWS:BAU\text{-}C} = L_{WWS}/L_{BAU} \quad \text{(Equation 8)}$$

are the WWS-to-BAU ratio of private cost of energy per kWh (dimensionless), the ratio of private cost of BAU energy per kWh to social cost of BAU energy per kWh (dimensionless), and the WWS-to-BAU ratio of end-use annual power demand (GW) (dimensionless), respectively.

A related new parameter is the WWS-to-BAU ratio of aggregate private cost:

$$R_{APC} = P_{WWS}L_{WWS}/(P_{BAU}L_{BAU}) = R_{WWS:BAU\text{-}E}R_{WWS:BAU\text{-}C}, \quad \text{(Equation 9)}$$

which gives an indication of the aggregate private energy cost per year in a region in a WWS versus BAU case. A third new metric is the WWS-to-BAU ratio of social cost per unit energy:

$$R_{SCE} = S_{WWS}/S_{BAU} = R_{WWS:BAU\text{-}E}R_{BAU\text{-}S:E}, \quad \text{(Equation 10)}$$

which gives an indication of the energy plus health plus climate cost per kWh in a WWS case versus BAU case.

Weather Model for Predicting Variable WWS Supply

This study uses a grid integration model, LOADMATCH, to simulate matching energy demand with supply and storage over time. LOADMATCH requires time-dependent intermittent WWS power generation as input. Time-dependent wind and solar generation are determined directly from a global weather-climate-air-pollution model, GATOR-GCMOM.[34,43–45] This model predicts time- and space-dependent solar thermal heat production and electricity production from onshore and offshore wind turbines, rooftop and utility-scale PV, and CSP plants. From the wind data, time-dependent fields of wave power are also derived. In general, the model simulates feedbacks among meteorology, solar and thermal-infrared radiation, gases, aerosol particles, cloud particles, oceans, sea ice, snow, soil, and vegetation. Model predictions have been compared with data in 34 peer-reviewed studies. The model has also taken part in 14 model inter-comparisons (see Note S14 for references).

GATOR-GCMOM accounts for the wind's reduced kinetic energy and speed due to the competition among wind turbines for available kinetic energy,[44] the temperature dependence of PV output,[45] and the loss of sunlight to buildings and the ground due to the conversion of radiation to electricity by solar devices. It also accounts for (1) changes in air and ground temperature due to power extraction by solar and wind devices and subsequent electricity use;[15] (2) impacts of time-dependent gas, aerosol, and cloud concentrations on solar radiation and wind fields;[34] (3) radiation to rooftop PV panels at a fixed optimal tilt at their location;[45] and (4) radiation to utility PV panels, half of which are at an optimal tilt and the other half of which track the sun with single-axis horizontal tracking.[45] Notes S14–S20 describe the model in detail.

GATOR-GCMOM was run here on the global scale for 3 years (2050–2052) at $2^\circ \times 2.5^\circ$ horizontal resolution. Modeled instantaneous power output from onshore and offshore wind turbines, solar rooftop PV, utility-scale PV, CSP plants, and solar thermal energy was written to a file every 30 s for the 3 years and aggregated over each country.

Model for Matching Supply with Demand and Storage

In general, three main types of computer models simulate the supply-demand balance, storage, and/or demand response on an electric power grid. These are power-flow (or load-flow) models, optimization models, and the trial-and-error simulation model. Notes S24–S26 describe each type of model.

LOADMATCH[1,15] is a trial-and-error simulation model (Note S26). This type of model works by running multiple simulations one at a time. Each simulation marches forward several years, one timestep at a time, just as the real world does. The main constraint during a simulation is that electricity, heat, cold, and hydrogen load, adjusted by demand response, must match energy supply and storage every timestep for an entire simulation period. If load is not met during any timestep, the simulation stops. Inputs (the nameplate capacity of one or more generators; the peak charge rate, peak discharge rate, or peak capacity of storage; or characteristics of demand response) are then adjusted one at a time on the basis of an examination of what caused the load mismatch (hence the description "trial-and-error" model). Another simulation is then run from the beginning. New simulations are run until load is met every time step of the simulation period. After load is met once, additional simulations are performed with further-adjusted inputs on the basis of user intuition and experience to generate a set of solutions that match load every timestep. The lowest-cost solution in this set is then selected. Table S19 provides the final adjustment factors of nameplate capacities used here for each world region.

Unlike with an optimization model, which solves among all timesteps simultaneously, a trial-and-error model does not know what the weather will be during the next timestep. Because a trial-and-error model is non-iterative, it requires, for example, only 55 s of computing time on a single 3.0 GHz computer processor to simulate 3.15 million 30-s timesteps (3 years). This is $1/500^{th}$ to $1/100{,}000^{th}$ of the computing time of an optimization model for the same number of timesteps. Results for the simulations shown here were calculated with a 30-s timestep. The disadvantage of a trial-and-error model compared with an optimization model is that the former does not necessarily determine the least-cost solution out of all possible solutions. Instead, it produces a set of viable solutions, from which the lowest-cost solution is selected.

Table S6 summarizes many of the processes treated in the LOADMATCH simulations. Model inputs are as follows: (1) time-dependent electricity produced from onshore and offshore wind turbines, wave devices, tidal turbines, rooftop PV, utility PV, CSP plants, and geothermal plants; (2) a hydropower-plant peak discharge rate (nameplate capacity), which was set to the present-day nameplate capacity for this study, a hydropower-plant mean recharge rate (from rainfall), and a hydropower-plant annual average electricity output; (3) time-dependent geothermal and solar thermal heat-generation rates; (4) specifications of hot-water and chilled-water sensible-heat thermal energy storage (HW-STES and CW-STES) (peak charge rate, peak discharge rate, peak storage capacity, losses into storage, and losses out of storage); (5) specifications of underground thermal energy storage (UTES), including

borehole, water pit, and aquifer storage; (6) specifications of ice storage (ICE); (7) specifications of electricity storage in pumped hydropower storage (PHS), phase-change materials coupled with CSP plants (CSP-PCM), batteries, etc.; (8) specifications of hydrogen (for use in transportation) electrolysis, compression, and storage equipment; (9) specifications of electric heat pumps for air and water heating and cooling; (10) specifications of a demand response system; (11) specifications of losses along short- and long-distance transmission and distribution lines; (12) time-dependent electricity, heat, cold, and hydrogen loads; and (13) scheduled and unscheduled maintenance downtimes for generators, storage, and transmission. Given the distributed nature of most generation and storage in this system, their downtimes are assumed to be spread evenly throughout a year (Note S46).

Note S33 describes the order of operations in LOADMATCH, including how the model treats excess generation over demand and excess demand over generation. Because the model does not permit load loss at any time, it is designed to exceed the utility industry standard of load loss once every 10 years.

Projecting BAU, WWS, Flexible, and Inflexible Loads

2050 BAU and WWS end-use loads are determined as follows. We start with 2016 BAU end-use loads from the International Energy Agency (IEA)[46] for seven fuel types in each of six sectors (residential; commercial and governmental; industrial; transport; agriculture, forestry, and fishing; and military or other) (Note S28). These end-use loads for each fuel type, sector, and country are projected to 2050 (Tables 2, S1, and S7).

The BAU projections are derived from *reference* scenario projections of the US Energy Information Administration (EIA)[47] for each fuel type in each sector in 16 world regions. The reference scenario is one of moderate economic growth and is described in detail by the EIA.[47] It accounts for policies in different countries, on population growth, on economic and energy growth, on the use of some renewable energy, on modest energy-efficiency measures, and on reduced energy use between 2016 and 2040. The EIA refers to their reference scenario as their BAU scenario. We adopt the EIA's BAU projections and extrapolate them from 2040 to 2050 by using a 10-year moving linear extrapolation for each fuel type in each sector in each world region. We then assume that the 2050 BAU end-use energy for each fuel type in each energy sector in each of 143 countries equals the corresponding 2016 end-use energy from the IEA[38] multiplied by the EIA 2050-to-2016 energy-consumption ratio, which is available after the extrapolation for each fuel type, energy sector, and EIA region.

Notes S4–S12 describe how 2050 BAU end-use energy for each fuel type in each energy sector in each country is then converted to electricity, electrolytic hydrogen for use in fuel cells for transportation, or heat, where the electricity and heat are provided by WWS energy. The notes also describe how to calculate the resulting change in end-use energy demand. They further delineate the five main reasons that demand for end-use energy decreases substantially in the WWS versus BAU scenario:

(1) Battery-electric vehicles and electrolytic hydrogen-fuel-cell vehicles are much more efficient than gasoline- and diesel-combustion vehicles for transportation.
(2) Electricity is more efficient than combustion for producing high-temperature industrial heat.
(3) Heat pumps are more efficient than combustion for providing low-temperature air and water heating.
(4) The WWS scenario eliminates the energy needed for mining, transporting, and processing fossil fuels, biofuels, bioenergy, and uranium.
(5) The WWS scenario includes slightly more energy-efficiency and demand-reduction measures than does the BAU scenario (Note S11), which is a moderate economic growth scenario that includes only moderate energy-efficiency and demand-reduction measures.[39]

Notes S28–S31 describe how annual average end-use WWS loads in each region from Table S7 for each sector are then separated into (1) electricity and heat loads needed for low-temperature heating, (2) electricity loads needed for cooling and refrigeration, (3) electricity loads needed for producing, compressing, and storing hydrogen for fuel cells used for transportation, and (4) all other electricity loads (including high-temperature industrial heat loads).

Each of these loads is further divided into flexible and inflexible loads. Flexible loads include electricity and heat loads that can be used for filling cold and low-temperature heat storage, all electricity used for producing hydrogen (given that all hydrogen can be stored), and the remaining electricity and heat loads subject to demand response. Inflexible loads are all loads that are not flexible. The flexible loads can be shifted forward in time with demand response. The inflexible loads must be met immediately. Table S10 summarizes the resulting inflexible and flexible loads in each of the 24 world regions given in Table 1. Annual loads are then distributed into time-dependent loads through the combination of contemporary electrical load profiles (hourly) with data on heating and cooling degree days for each country (Note S29).

Next, storage is sized (Tables S11 and S12), and storage, energy, and transmission and distribution cost parameters are determined (Tables S13 and S14). Model simulations are then run. In parallel, the mortality, morbidity, and non-health costs of BAU energy (Note S39, Figure 1, and Tables S15–S17) and the climate costs of BAU energy (Note S40 and Tables S17 and S18) are estimated.

DATA AND CODE AVAILABILITY

All spreadsheet derivations for the 143 country roadmaps are available online at http://web.stanford.edu/group/efmh/jacobson/Articles/I/143-countryWWS.xlsx. All data from this paper, including data going into all plots, and the LOADMATCH model are available upon request from jacobson@stanford.edu.

SUPPLEMENTAL INFORMATION

Supplemental Information can be found online at https://doi.org/10.1016/j.oneear.2019.12.003.

ACKNOWLEDGMENTS

This research did not receive any funding from any source.

AUTHOR CONTRIBUTIONS

Conceptualization, M.Z.J.; Methodology, M.Z.J. and M.A.D.; Investigation, M.Z.J., M.A.D., M.A.C., S.J.C., C.A.H., I.P.M., Y.S., and A.-K.v.K.; Software, M.Z.J.; Writing – Original Draft, M.Z.J.; Writing – Review & Editing, M.Z.J., M.A.D., M.A.C., S.J.C., C.A.H., I.P.M., Y.S., and A.-K.v.K.; Visualization, M.Z.J. and M.A.C.; Supervision, M.Z.J.

DECLARATION OF INTERESTS

The authors declare no competing interests.

Received: September 19, 2019
Revised: October 28, 2019
Accepted: December 2, 2019
Published: December 20, 2019

REFERENCES

1. Jacobson, M.Z., Delucchi, M.A., Cameron, M.A., and Mathiesen, B.V. (2018). Matching demand with supply at low cost among 139 countries within 20 world regions with 100 percent intermittent wind, water, and sunlight (WWS) for all purposes. Renew. Energy *123*, 236–248.
2. Intergovernmental Panel on Climate Change (2018). Special Report: Global Warming of 1.5°C. https://www.ipcc.ch/sr15/.
3. Olz, S., Sims, R., and Kirchner, N. (2007). Contribution of renewables to energy security (International Energy Agency). https://web.archive.org/web/20090318231652/http://www.iea.org/textbase/papers/2007/so_contribution.pdf.
4. Jacobson, M.Z., Delucchi, M.A., Bauer, Z.A.F., Goodman, S.C., Chapman, W.E., Cameron, M.A., Bozonnat, C., Chobadi, L., Clonts, H.A., Enevoldsen, P., et al. (2017). 100% clean and renewable wind, water,

and sunlight (WWS) all-sector energy roadmaps for 139 countries of the world. Joule *1*, 108–121.

5. Jacobson, M.Z., and Delucchi, M.A. (2009). A path to sustainable energy by 2030. Scientific American, November 2009 https://www.scientificamerican.com/article/a-path-to-sustainable-energy-by-2030/.
6. Lund, H., and Mathiesen, B.V. (2009). Energy system analysis of 100% renewable energy systems: the case of Denmark in years 2030 and 2050. Energy *34*, 524–531.
7. Mason, I.G., Page, S.C., and Williamson, A.G. (2010). A 100% renewable energy generation system for New Zealand utilizing hydro, wind, geothermal, and biomass resources. Energy Policy *38*, 3973–3984.
8. Hart, E.K., and Jacobson, M.Z. (2011). A Monte Carlo approach to generator portfolio planning and carbon emissions assessments of systems with large penetrations of variable renewables. Renew. Energy *23*, 2278–2286.
9. Mathiesen, B.V., Lund, H., and Karlsson, K. (2011). 100% renewable energy systems, climate mitigation, and economic growth. Appl. Energy *88*, 488–501.
10. Budischak, C., Sewell, D., Thompson, H., Mach, L., Veron, D.E., and Kempton, W. (2013). Cost-minimized combinations of wind power, solar power, and electrochemical storage, powering the grid up to 99.9% of the time. J. Power Sources *225*, 60–74.
11. Steinke, F., Wolfrum, P., and Hoffmann, C. (2013). Grid vs. storage in a 100% renewable Europe. Renew. Energy *50*, 826–832.
12. Connolly, D., and Mathiesen, B.V. (2014). Technical and economic analysis of one potential pathway to a 100% renewable energy system. Intl. J. Sustain. Energy Plann. Manage. *1*, 7–28.
13. Elliston, B., MacGill, I., and Diesendorf, M. (2014). Comparing least cost scenarios for 100% renewable electricity with low emission fossil fuel scenarios in the Australian National Electricity Market. Renew. Energy *66*, 196–204.
14. Becker, S., Frew, B.A., Andresen, G.B., Zeyer, T., Schramm, S., Greiner, M., and Jacobson, M.Z. (2014). Features of a fully renewable U.S. electricity system: optimized mixes of wind and solar PV and transmission grid extensions. Energy *72*, 443–458.
15. Jacobson, M.Z., Delucchi, M.A., Cameron, M.A., and Frew, B.A. (2015). Low-cost solution to the grid reliability problem with 100% penetration of intermittent wind, water, and solar for all purposes. Proc. Natl. Acad. Sci. USA *112*, 15060–15065.
16. Mathiesen, B.V., Lund, H., Connolly, D., Wenzel, H., Ostergaard, P.Z., Moller, B., Nielsen, S., Ridjan, I., Karnoe, P., Sperling, K., and Hvelplund, F.K. (2015). Smart energy systems for coherent 100% renewable energy and transport solutions. Appl. Energy *145*, 139–154.
17. Bogdanov, D., and Breyer, C. (2016). North-east Asian super grid for 100% renewable energy supply: optimal mix of energy technologies for electricity, gas, and heat supply options. Energy Convers. Manage. *112*, 176–190.
18. Connolly, D., Lund, H., and Mathiesen, B.V. (2016). Smart energy Europe: the technical and economic impact of one potential 100% renewable energy scenario for the European Union. Renew. Sustain. Energy Rev. *60*, 1634–1653.
19. Blakers, A., Lu, B., and Socks, M. (2017). 100% renewable electricity in Australia. Energy *133*, 417–482.
20. Zapata, S., Casteneda, M., Jiminez, M., Aristizabel, A.J., Franco, C.J., and Dyner, I. (2018). Long-term effects of 100% renewable generation on the Colombian power market. Sustain. Energy Technol. Assess. *30*, 183–191.
21. Esteban, M., Portugal-Pereira, J., Mclellan, B.C., Bricker, J., Farzaneh, H., Djalikova, N., Ishihara, K.N., Takagi, H., and Roeber, V. (2018). 100% renewable energy system in Japan: smoothening and ancillary services. Appl. Energy *224*, 698–707.
22. Sadiqa, A., Gulagi, A., and Breyer, C. (2018). Energy transition roadmap towards 100% renewable energy and role of storage technologies for Pakistan by 2050. Energy *147*, 518–533.
23. Liu, H., Andresen, G.B., and Greiner, M. (2018). Cost-optimal design of a simplified highly renewable Chinese network. Energy *147*, 534–546.
24. Aghahosseini, A., Bogdanov, D., Barbosa, L.S.N.S., and Breyer, C. (2019). Analyzing the feasibility of powering the Americas with renewable energy and inter-regional grid interconnections by 2030. Renew. Sustain. Energy Rev. *105*, 187–205.
25. Bogdanov, D., Farfan, J., Sadovskaia, K., Aghahosseini, A., Child, M., Gulagi, A., Oyewo, A.S., de Souza Noel Simas Barbosa, L., and Breyer, C. (2019). Radical transformation pathway towards sustainable electricity via evolutionary steps. Nat. Commun. *10*, 1077.
26. Hansen, K., Breyer, C., and Lund, H. (2019). Status and perspectives on 100% renewable energy systems. Energy *175*, 471–480.
27. Brown, T.W., Bischof-Niemz, T., Blok, K., Breyer, C., Lund, H., and Mathiesen, B.V. (2018). Response to 'Burden of proof: a comprehensive review of the feasibility of 100% renewable electricity systems.'. Renew. Sustain. Energy Rev. *92*, 834–847.
28. Diesendorf, M., and Elliston, B. (2018). The feasibility of 100% renewable electricity systems: a response to critics. Renew. Sustain. Energy Rev. *93*, 318–330.
29. US House of Representatives (2019). H.Res. 109 – Recognizing the duty of the federal government to create a Green New Deal. https://www.congress.gov/bill/116th-congress/house-resolution/109.
30. Green Party US (2018). Green New Deal – Full Language. https://www.gp.org/gnd_full.
31. World Bank (2017). Agricultural land. https://data.worldbank.org/indicator/AG.LND.AGRI.ZS.
32. Shaner, M.R., Davis, S.J., Lewis, N.S., and Caldeira, K. (2018). Geophysical constraints on the reliability of solar and wind power in the United States. Energy Environ. Sci. *11*, 914–925.
33. Sepulveda, N.A., Jenkins, J.D., deSisternes, F.J., and Lester, R.K. (2018). The role of firm low-carbon electricity resources in deep decarbonization of power generation. Joule *2*, 2403–2420.
34. Jacobson, M.Z., Kaufmann, Y.J., and Rudich, Y. (2007). Examining feedbacks of aerosols to urban climate with a model that treats 3-D clouds with aerosol inclusions. J. Geophys. Res. D Atmospheres *112*, D24205.
35. Jacobson, M.Z. (2019). The health and climate impacts of carbon capture and direct air capture. Energy Environ. Sci. https://doi.org/10.1039/C9EE02709B.
36. Lazard (2019). Levelized cost of energy and levelized cost of storage 2019. https://www.lazard.com/perspective/lcoe2019.
37. Hand, M.M., Baldwin, S., DeMeo, E., Reilly, J.M., Mai, T., Arent, D., Porro, G., Meshek, M., and Sandor, D. (2012). Volume 1: Exploration of High-Penetration Renewable Electricity Futures. In Renewable Electricity Futures Study (National Renewable Energy Lab), NREL/TP-6A20-52409-1.
38. Williams, J.H., Haley, B., Kahrl, F., Moore, J., Jones, A.D., Torn, M.S., and McJeon, H. (2014). Pathways to deep decarbonization in the United States. The U.S. report of the Deep Decarbonization Pathways Project of the Sustainable Development Solutions Network and the Institute for Sustainable Development and International Relations. (Energy and Environmental Economics Inc., Lawrence Berkeley National Laboratory, and Pacific Northwest National Laboratory).
39. MacDonald, A.E., Clack, C.T., Alexander, A., Dunbar, A., Wilczak, J., and Xie, Y. (2016). Future cost-competitive electricity systems and their impact on US CO_2 emissions. Nat. Clim. Chang. *6*, 526–531.
40. World Health Organization (2016). Mortality from environmental pollution. http://apps.who.int/gho/data/node.sdg.3-9-data?lang=en.
41. Renewable Energy Policy Network for the 21st Century (2019). Renewables 2019 global status report. https://www.ren21.net/gsr-2019/ https://www.ren21.net/gsr-2019/tables/table_06/table_06/.
42. Jacobson, M.Z., Delucchi, M.A., Cameron, M.A., Coughlin, S.J., Hay, C.A., Manogaran, I.P., Shu, Y., and Krauland, A.-K. (2019). Spreadsheets for 143-country, 24-world region WWS study. http://web.stanford.edu/group/efmh/jacobson/Articles/I/143-countryWWS.xlsx.

43. Jacobson, M.Z. (2001). GATOR-GCMOM: a global through urban scale air pollution and weather forecast model: 1. Model design and treatment of subgrid soil, vegetation, roads, rooftops, water, sea ice, and snow. J. Geophys. Res. Atmos. *106*, 5385–5401.

44. Jacobson, M.Z., and Archer, C.L. (2012). Saturation wind power potential and its implications for wind energy. Proc. Natl. Acad. Sci. USA *109*, 15679–15684.

45. Jacobson, M.Z., and Jadhav, V. (2018). World estimates of PV optimal tilt angles and ratios of sunlight incident upon tilted and tracked PV panels relative to horizontal panels. Sol. Energy *169*, 55–66.

46. International Energy Agency (2018). World Energy Statistics 2018 (OECD Publishing). https://doi.org/10.1787/world_energy_stats-2018-.

47. Energy Information Administration (2016). US International Energy Outlook 2016, DOE/EIA-0484(2016). http://www.eia.gov/forecasts/ieo/pdf/0484(2016).pdf.

ONEEAR, Volume *1*

Supplemental Information

Impacts of Green New Deal Energy Plans on Grid Stability, Costs, Jobs, Health, and Climate in 143 Countries

Mark Z. Jacobson, Mark A. Delucchi, Mary A. Cameron, Stephen J. Coughlin, Catherine A. Hay, Indu Priya Manogaran, Yanbo Shu, and Anna-Katharina von Krauland

Supplemental Information

This supplemental information file contains additional descriptions of the models, data, simulations, and results; additional tables; and additional figures to help explain more fully the methods and results found in this study.

Supplemental Experimental Procedure

Note S1. Major Components of the Research

This research involves several major components:

1) Projecting business-as-usual (BAU) end-use energy demand to 2050 for seven fuel types in each of six energy-use sectors, in each of 143 countries (Notes S2 and S3);

2) Estimating the 2050 reduction in demand due to electrifying or providing direct heat for each fuel type in each sector in each country (Notes S4-S12);

3) Performing resource analyses and estimating a mix of wind-water-solar (WWS) electricity and heat generators to meet the aggregate demand in each country in the annual average (Note S13).

4) Using a prognostic global weather-climate-air pollution model (GATOR-GCMOM), which accounts for competition among wind turbines for available kinetic energy, to estimate wind and solar radiation fields country-by-country every 30 s for several years (Notes S14-S21).

5) Grouping the 143 countries into 24 world regions and using a model (LOADMATCH) that matches the variable supply of energy with variable demand, storage, and demand response to match demand with supply and storage every 30 s in each region from 2050 to 2052 (Notes S32-S35).

6) Evaluating energy, health, and climate costs (Note S36-S42) with new metrics (Note S43).

7) Calculating land area requirements (Note S44).

8) Calculating changes in job numbers (Note S45).

9) Discussing and evaluating uncertainties (Note 46)

These components are discussed in detail in this document.

Note S2. Estimating 2050 End-Use Demand Upon Electrification of All Energy and a Mix of WWS Generators to Meet Demand

With a 100% clean, renewable WWS energy system, all energy sectors are electrified or powered with direct heat, where the electricity and heat are provided by WWS. Some electricity is used for hydrogen, primarily for transportation. Some electricity and heat are stored in electricity, heat, cold, and hydrogen storage. Energy efficiency and energy reduction measures are put in place to reduce demand. The next notes describe the steps in determining end-use demand.

Note S3. Projecting BAU End-Use Demand to 2050 in 143 Countries

The first step in developing a roadmap to transition the energy infrastructure of a country is to project end-use energy demand across all energy sectors forward from current demand to a future year in a BAU case. In general, a BAU case is one in which the energy infrastructure does not change drastically in the future, but demand does change due to increases in population and modest improvements in energy efficiency over time. A BAU case also includes some transition from fossil fuels to renewables, but only at recent historical rates, which are relatively slow.

End-use energy, as defined by both the International Energy Agency (IEA) and U.S. Energy Information Administration (EIA), is energy directly used by a consumer in any energy sector. It is the energy embodied in electricity, natural gas, gasoline, diesel, kerosene, and jet fuel that people use directly, including to extract and transport fuels themselves. It equals primary energy minus the energy lost in converting primary energy to end-use energy, including energy lost during transmission and distribution. Primary energy is the energy naturally embodied in chemical bonds in raw fuels, such as coal, oil, natural gas, biomass, uranium, or renewable (e.g., hydroelectric, solar, wind) electricity, before the fuel has been subjected to any conversion process.

The conversion of primary energy to end-use energy differs for different energy sectors and fuel type in each sector. The energy sectors treated here, as defined by IEA[46] and in Table S1) include residential, commercial, industrial, transportation, agriculture/forestry/fishing, and military/other. The fuel types include oil, natural gas, coal, electricity, heat, other renewables, and biofuels and waste.[46]

In the electricity sector, end-use energy is primary energy minus the energy lost during the generation, transmission, and distribution of electricity. For instance, when coal is burned to produce electricity, only about one-third of the energy embodied in the coal is converted to electricity. The rest is waste heat. Further, some of the electricity produced is lost during transmission and distribution. The end-use electricity in this case is the electricity that consumers use in the end, not the primary energy that was contained in the coal nor the energy in the electricity at the power plant itself.

In another example, solar electricity that is produced by a PV panel is primary energy. Some of that electricity is lost during transmission and distribution. In that case, the solar electricity that actually reaches a consumer after transmission and distribution losses is end-use energy. Similarly, hydroelectric power produced at a hydropower plant is primary energy. The remaining hydroelectricity after transmission and distribution losses is end-use energy.

In the transportation sector, the energy embodied in crude oil is primary energy. Converting crude oil to end-use products, including gasoline, diesel, kerosene, refinery gas, and jet fuel, involves almost no *loss* of the primary energy in crude oil, so the end-use energy available in all products is close to, but not exactly the same as, the primary energy in crude oil. Oil and its products have different chemical structures from each other.

Natural gas used for heating and cooking is very similar to the gas when it is recovered from a well, so primary energy and end-use energy are about the same. On the other hand, when natural gas is burned for electricity production (in the electricity sector), only a portion of the natural gas is converted to electricity and some of that electricity is lost during transmission and distribution, so the end-use energy in the electricity, like with coal, differs substantially from the primary energy in the natural gas creating the electricity.

Table S2 shows the projection of 2016 BAU all-purpose end-use energy demand (load) by sector to 2050 for each of 143 countries. This projection was performed starting with end-use energy consumption data by sector and fuel type for 2016 from the International Energy Agency[46]. The consumption for each fuel type in each sector and in each country was then projected forward to 2040 based on the *reference* scenario projections from the U.S. Energy Information Administration (EIA)[47] for each fuel type in each sector in 16 world regions. The reference scenario is one of moderate economic growth and is described in detail by EIA[47]. It accounts for policies in different countries, population growth, economic and energy growth, the use of some renewable energy, modest energy efficiency measures, and reduced energy use between 2016 and 2040. EIA refers to their reference scenario as their BAU scenario. We adopt EIA's BAU projections and extrapolate them from

2040 to 2050 using a 10-year moving linear extrapolation for each fuel type in each sector in each world region. We then assume that the 2050 BAU end-use energy for each fuel type in each energy sector in each of 143 countries equals the 2016 end-use energy from IEA[46] multiplied by the EIA 2050-to-2016 energy consumption ratio, available after the extrapolation, for the fuel type, energy sector, and region containing the country.

In 2016, the 143-country, annually averaged end-use demand for energy among all energy sectors was about 12.6 TW. Of this, 2.6 TW (20.7%) was electricity demand. The projection just described suggests that, in 2050, all-purpose end-use demand in the BAU case may grow to 20.3 TW (by 61%) if no large-scale transition to WWS occurs. The growth is due to a population increase and an increase in energy demand per person due to the lifting of many people out of poverty, partly mitigated by reduced energy use resulting from some modest shifts from coal to gas, biofuels, bioenergy, some WWS, and some energy efficiency.

Note S4. Determining Demand Reduction Upon Transition to WWS

The second step is to transition 2050 BAU end-use energy for each fuel type in each energy sector to electricity, electrolytic hydrogen, or heat, where the electricity and heat are provided by WWS, and to calculate the resulting change in energy demand. Most demand reduction will be due to the efficiency of electricity over combustion, eliminating energy in the mining, transporting, and refining of fossil fuels and uranium, and energy efficiency measures beyond those in the BAU case.

The main sectors to transition are electricity, transportation, building heating and cooling, industry, industry, agriculture/forestry/fishing, and the military (see Note S28). The main WWS electricity generation technologies proposed include onshore and offshore wind, concentrated solar power (CSP), geothermal power, solar PV on rooftops and in power plants, tidal power, wave power, and hydropower.

Proposed vehicles for transportation include battery-electric (BE) vehicles and BE-hydrogen fuel cell (HFC) hybrid vehicles, where the hydrogen is produced by electrolysis. BE vehicles will dominate 2- and 3-wheel transportation; short- and long-distance light-duty transportation; and most truck, construction machine, and agricultural equipment transportation. Batteries will also power most short- and moderate-distance trains, short-distance boats and ships (e.g., ferries, speedboats), short-distance military equipment, and aircraft traveling less than 1,500 km. Some short-distance trains will run on overhead-wire electricity. Among all commercial aircraft flight distances traveled worldwide, about 53.9% are short haul flights (less than 3 hours in duration, with a mean distance of 783 km)[48]. As such, approximately half the aircraft flights worldwide may be electrified with batteries.

Hydrogen fuel cell or battery-electric-HFC hybrid vehicles will likely dominate transportation by medium- and heavy-duty trucks, long-distance trains, long-distance ships, long-haul aircraft, and long-distance military equipment.

Air heating and cooling will be performed with ground-, air-, or water-source electric heat pumps. Hot water will be generated with heat pumps, in some cases with an electric resistance element for low temperatures, and with solar hot water heaters. Cook stoves will be electric induction. Clothes dryers will all be electric.

Electric arc furnaces, induction furnaces, dielectric heaters, and resistance heaters will provide high temperatures for industrial processes.

Upon electrification and providing the electricity and some direct heat with WWS, end-use energy reductions will occur for five primary reasons:

(1) The efficiency of electricity and electrolytic hydrogen over combustion for transportation;
(2) The efficiency of electricity over combustion for high-temperature industrial heat;
(3) The efficiency of moving low-temperature building air and water heat with heat pumps instead of creating heat with combustion;
(4) Eliminating the energy needed to mine, transport, and process fossil fuels, biofuels, bioenergy, and uranium; and

(5) Improving end-use energy efficiency and reducing energy use beyond what will occur under BAU.

These improvements are discussed in turn.

Note S5. Efficiency of Electricity and Electrolytic Hydrogen over Combustion for Transportation

First, replacing end-use fossil fuels (natural gas, gasoline, diesel, kerosene, jet fuel), biofuels, and bioenergy for transportation with WWS electricity eliminates waste heat of combustion because electricity and electrolytic hydrogen have higher energy-to-work conversion efficiencies than do fossil fuels, biofuels, and bioenergy. This factor is embodied in the electricity-to-fuel ratio, which is the energy required for an electric or hydrogen fuel cell machine or device to perform the same work as a BAU machine running on fossil fuels, biofuels, or bioenergy. This ratio is calculated below for battery-electric vehicles and hydrogen fuel cell vehicles versus internal combustion engine (ICE) vehicles.

Note S6. Efficiency of Battery-electric Vehicles over Fossil Fuel Vehicles

An example of the greater efficiency of electricity over combustion arises with battery-electric (BE) vehicles in comparison with ICE vehicles. Only 17 to 20% of the end-use energy embodied in a fossil fuel or liquid biofuel is used to move an ICE passenger vehicle. This is the tank-to-wheel efficiency of the vehicle. The rest of the energy (80 to 83%) is waste heat. As such, gasoline and diesel, for example, contain potential energy that is 5 to 5.9 times the end use (work) energy that is actually used to move the vehicle.

A BE vehicle, on the other hand converts 64 to 89% of electricity at the plug (before charging the car) into motion (plug-to-wheel efficiency), and the rest is waste heat. This efficiency is determined as follows and summarized in Table S3.

First, a permanent magnet electric motor has an efficiency of 89 to 96%. An induction electric motor has an efficiency of 84 to 94%[49]. Thus, the range of efficiencies of electric car motors is 84 to 96%. Whereas the Tesla Model S and Model X use an induction motor, the Tesla Model 3, for example, uses a permanent magnet motor.

In addition, efficiency losses occur due to converting electricity from the grid to chemical energy in a battery. These vehicle-charging losses can range from 4 to 20% of the electricity going into the battery, depending on the current and voltage used to charge the vehicle. Another 1 to 2% of energy is also lost during conversion of the battery's chemical energy to DC electricity. In addition, 2 to 3% is lost converting DC to AC electricity in an inverter, adjusting the voltage for use in the motor, and using power electronic controls in the vehicle. Inverter losses are only 1% of energy (thus an efficiency of up to 99%) when the inverter uses silicon carbide as the semiconductor material[50].

Accounting for all losses give the overall plug-to-wheel efficiency of a battery-electric passenger vehicle as 64 to 89%, with an average of 77% (Table S3).

The tank-to-wheel efficiency of a fossil fuel passenger vehicle divided by the plug-to wheel efficiency of an electric vehicle is the fraction of a fossil fuel vehicle's end-use energy needed for electricity to move an electric vehicle the same distance. This electricity-to-fuel ratio ranges from 0.19 (=0.17/0.89) to 0.31 (=0.2/0.64), or an average of 0.25. In other words, a fossil fuel vehicle requires 4 (3.2 to 5.3) times the energy in gasoline than an electric vehicle needs in electricity at the plug (before charging) to drive the same distance. By 2050, the average electricity-to-fuel ratio is expected to be closer to 0.19 due to improvements in vehicle charging efficiencies and battery efficiency, and the greater use of permanent magnet motors. This is the value used in Table S1 (the electricity-to-fuel ratio for WWS battery-electric vehicles replacing oil for transportation).

Note S7. Efficiency of Hydrogen Fuel Cell Vehicles over Fossil Fuel Vehicles

Whereas the efficiency of an electric passenger vehicle over an ICE vehicle results in a significant reduction in end-use energy requirements in the transportation sector, that reduction is limited by the fact that a portion of future transportation will use hydrogen fuel cells (HFCs), which are less efficient than electric vehicles (but more efficient than ICEs).

HFCs convert hydrogen to electricity, which is then used in a motor to produce rotation to move wheels or a propeller. Pure HFC or HFC-battery-electric (BE) hybrid vehicles will be used primarily for long-distance, heavy transportation.

The overall plug-to-wheel efficiency of an HFC vehicle ranges from 23 to 37%, for an average of 30%. In other words, only about 30% of the electricity used to produce and use H_2 actually moves the car. The reason is that electricity is needed to produce the hydrogen by electrolysis and compress it or liquefy it for storage in a holding tank and vehicle fuel tank. In addition, some of the hydrogen leaks between production and the fuel tank. Some energy in hydrogen's chemical bonds is then lost as heat in the fuel cell. In addition, water vapor produced by the hydrogen reaction in the fuel cell carries away latent heat. Finally, some electricity produced by the fuel cell is lost in wires between the fuel cell and electric motor, and more electricity is lost as heat in the motor. Table S3 summarizes efficiencies of different processes affecting the overall plug-to-wheel efficiency of an HFC vehicle.

The electrolyzer efficiency is the efficiency at which an electrolyzer converts electricity into energy within hydrogen. It is calculated as the higher heating value of hydrogen (141.8 MJ/kg-H_2, which equals 39.39 kWh/kg-H_2) divided by the energy per unit mass of hydrogen required to produce hydrogen by electrolysis (53.37 kWh/kg-H_2-produced)[51]. The result is an electrolyzer efficiency of 73.8%.

Electricity is needed to compress hydrogen for temporary storage and then ultimate storage in the HFC vehicle. The electricity required for compression is about 5.64 kWh/kg-H_2[51]. If this is added to the electrolyzer energy needed, the total is 59.0 kWh/kg-H_2. Dividing the higher heating value of hydrogen by this number gives an overall electrolyzer plus compressor efficiency of 66.8%. Dividing the overall efficiency by the electrolyzer efficiency of 73.8% gives a compressor efficiency of 90.4%. In other words, of the total energy needed to produce and compress a kilogram of H_2, 26.2% is lost due to electrolysis and 9.6% is lost due to compression. The remainder is stored in the bonds of a hydrogen molecule.

Once hydrogen is produced, some of it may leak. Hydrogen is a tiny molecule, much smaller than methane, so it can leak easily from pipes unless the pipes are well sealed. In a 100% WWS system, hydrogen will be produced in a controlled environment and mostly locally. Instead of hydrogen being produced far away and sent by pipeline, most will be produced locally after electricity is transmitted long distances. This will minimize pipeline loss. Leaks, however, will still occur. An estimate of hydrogen leakage provided in Table S3 is 0.3 to 1%.

Fuel cell efficiencies (electrical output of a fuel cell divided by the lower heating value of hydrogen) are between 50 and 70% (Table S3).

The latent heat loss efficiency is simply the lower heating value of hydrogen (119.96 MJ/kg-H_2) divided by the higher heating value (141.8 MJ/kg-H_2), which equals 84.6%. Of the energy in hydrogen, 15.4% is lost evaporating water produced in the fuel cell. That energy is stored as latent heat in the water vapor produced by the hydrogen reaction in the fuel cell and is released back to the air when the water vapor ultimately condenses to liquid cloud water in the atmosphere.

Inverter/wiring/power electronic losses within an HFC vehicle are estimated to be slightly less than for a BE vehicle, because such losses in a BE vehicle include converting energy in the battery to DC electricity. The analogous loss in a fuel cell is already accounted for in the fuel cell efficiency. Thus, inverter, wiring, and power electronics losses are estimated to be 1 to 3%.

The motor efficiency is the same as for a BE vehicle and includes the range between an induction motor and a permanent magnet motor.

Table S3 suggests that the efficiency of the fuel cell system inside the vehicle is 34 to 56%. However, accounting for electrolyzer, compressor, and leakage losses decreases the overall plug-to-wheel efficiency of an HFC vehicle to about 23 to 37%.

Dividing the average tank-to-wheel efficiency of a fossil fuel vehicle by the plug-to-wheel efficiency of an HFC vehicle gives the electricity-to-fuel ratio of an HFC vehicle replacing oil as 0.46 (=0.17/0.37) to 0.87 (=0.20/0.23). The lower number (0.46) is used in Table S1 in the transportation sector because this is closer to what is expected in 2050 due to efficiency improvements along the whole process of producing and using hydrogen.

A disadvantage of a BE vehicle is that the greater its range and the heavier the vehicle, the heavier the battery pack that needs to be carried around permanently. For example, most of the energy stored in batteries in a long-distance aircraft would be used just to carry the batteries. An HFC vehicle ameliorates this problem somewhat since the fuel itself (hydrogen) is extremely light, and as travel commences, the fuel weight burden decreases since H_2 is converted to oxygen and water, which are emitted from the aircraft. However, an HFC vehicle needs a large volume to store H_2, even if the H_2 is liquefied. Further, the greater the range of an HFC or HFC-BE hybrid vehicle, the greater the number of fuel cells needed, which also increases weight and volume.

All in all, though, a vehicle with HFCs is more practical than a pure BE vehicle for very long-distance aircraft, ships, trains, and some trucks. For these modes of transportation, recharging during travel is either not an option or not an attractive option. The main disadvantage of an HFC is that its plug-to-wheel efficiency for short- and moderate-distance transport is only 26 to 60% that of a BE vehicle. Conversely, the efficiency of a BE vehicle is 1.7 to 3.8 that of an HFC vehicle. In other words, an HFC vehicle needs 70 to 280% more wind turbines or solar panels to run than does a BE vehicle to go the same distance. Thus, most short and moderate distance transportation in a 100% WWS world will be BE transportation.

Note S8. Efficiency of Electricity over Combustion for High Temperature Heat

Replacing fossil fuels and bioenergy for high temperature industrial heat with WWS electricity also eliminates waste heat of combustion. For example, a natural gas furnace used for producing high temperature heat is about 80% efficient. In other words, about 80% of the energy in the chemical bonds of the natural gas is converted to useful heat. The rest of the energy is lost either as waste heat or incompletely combusted natural gas that escapes as exhaust. An electric resistance furnace for producing high temperatures, on the other hand, is about 97% efficient. Thus, about 97% of the electricity going into it gets converted to useful heat used by the industrial process. The rest is waste heat that is lost due to conduction out of the furnace without the heat being used.

As such, the ratio of the energy input of WWS electricity to energy input of BAU fuel needed to obtain the same work output in both cases is 0.82 (= 0.80 / 0.97). In other words, an electric resistance furnace needs 82% of the raw energy input as does a gas furnace to obtain the same work output. This electricity-to-fuel ratio appears in Table S1 for industrial sector WWS technologies replacing oil, natural gas, coal, and biofuels/waste.

Note S9. Reducing Load by Moving Heat with Heat Pumps Instead of Creating Heat

Air source heat pumps move low-temperature heat from one place to another rather than create new heat. As a result, they are much more efficient than fuel combustion or electric resistance heating, both of which create low-temperature heat. Air source heat pumps have a coefficient of performance (COP) of 3.2 to 4.5, whereas ground source heat pumps have a COP of 4.2 to 5.2[52]. This compares with electric resistance heaters, which have a COP = 0.97 and natural gas-powered boilers, which have a typical COP = 0.8. Since only 1 Joule (J) of electricity is needed to move 3.2 to 5.2 J of hot or cold air with a heat pump, a heat pump reduces power demand compared with electric resistance heaters or natural gas boilers substantially.

For example, in Table S1, the electricity-to-fuel ratio for WWS electric heat pumps replacing natural gas in the residential sector is given as 0.2, which is an average of 0.15 and 0.25. The range is calculated by dividing the coefficient of performance of a gas heater (0.8) by the coefficient of performance of a heat pump (3.2 to 5.2). In other words, electric heat pumps reduce end-use energy demand by 75 to 85% compared with natural gas heaters (and by 70 to 81% compared with electric resistance heaters).

The electricity to fuel ratio of 0.15 to 0.25 applies to electric heat pumps replacing natural gas, oil, coal, renewables, and biofuels, which are all used for low-temperature heating in the residential and commercial sectors.

The use of electric heat pumps for cooling does not change the electricity-to-fuel ratio for the portion of *electricity* in Table S1 used for air conditioning because electric air conditioners already act like heat pumps – they remove heat from a room and transfer it to the outside air. As such, air conditioners have a similar coefficient of performance as do heat pumps. They just don't run in reverse to produce heat. Refrigerators, like air conditioners, also act like heat pumps but only for cooling, not for heating.

Note S10. Eliminating Energy to Mine/Transport/Process BAU Fuels

Fourth, producing all energy with WWS eliminates the need to mine, transport, and process fossil fuels, biofuels, bioenergy, and uranium. Worldwide, about 12.1% of all energy is used for this purpose (Table S2). A WWS energy economy eliminates the need for this energy. Instead, wind comes right to the wind turbine and sunlight comes right to the solar panel, so no energy is needed to mine wind or sunlight.

Eliminating energy to mine, transport, and process fuels requires going into the sector-by-sector energy inventory for each country from IEA[46] and eliminating energy used for industrial and transportation sector "own-use." In the industrial sector, this includes energy for mining operations and petroleum refining. In the transportation sector, this includes energy for natural gas pipelines, oil tankers, coal trains, and gasoline trucks. About 2% of oil, 50% of coal, and 80% of natural gas in the transportation sector is used just to transport fossil fuels, biofuels, and uranium[46]. The need for this energy is eliminated upon a transition to 100% WWS.

Note S11. Increasing Energy Efficiency and Reducing Energy Use Beyond BAU

Finally, we assume that energy efficiency improvements and reduced energy use beyond those occurring in the BAU scenario reduce end-use energy demand further. The BAU projection of energy demand between today and 2050, which are based on the EIA reference case for 16 world regions[47], already accounts for moderate end-use energy efficiency improvements and reductions in energy use. However, additional policy-driven energy efficiency measures and incentives can reduce end-use energy demand further. The additional efficiencies are calculated here as the product of (a) the ratio of energy use, by fuel and energy sector, of the EIA's *high efficiency all scenarios* (HEAS) case and their *reference* (BAU) case and (b) our estimates of slight efficiency improvements beyond those in the HEAS case. Table S2 provides the resulting estimated reductions in end-use energy demand that may be achievable for each fuel in each energy category due to policy-driven improvements in efficiency beyond what is expected to occur in the BAU case.

Most of the improvements are due to increasing energy efficiency in the residential and commercial sectors. Some additional efficiency improvements arise in the industrial sector due to faster implementation of more advanced equipment than in the BAU case. In the transportation sector, improvements in vehicle design and in lightweight materials relative to BAU are assumed to occur.

Note S12. Overall Reduction in End-Use Demand

Tables 2 (main text) and S1 summarize the final estimated annually averaged end-use power demand, summed over 143 countries in 2050, after a transition from BAU to 100% WWS. Table 1 also shows the incremental benefit of the five specific improvements just discussed.

Table 2 indicates that, of the overall 57.1% reduction in end-use power demand between the 2050 BAU case and the 2050 WWS-D case, 38.3 percentage points are due to the efficiency of using WWS electricity over combustion; 12.1 percentage points are due to eliminating energy in the mining, transporting, and refining of fossil fuels; and 6.6 percentage points are due to end-use energy efficiency improvements and reduced energy use beyond those in BAU. Of the 38.3% reduction due to the efficiency of WWS electricity, 21.7 percentage points are due to the efficiency of WWS transportation, 3.4 percentage points are due to the efficiency of WWS electricity for industrial heat, and 13.2 percentage points are due to the efficiency of heat pumps (Figure S1).

In sum, transitioning from fossil fuels, biofuels, bioenergy, and uranium to 100% WWS has a large potential to reduce power demand worldwide by reducing waste heat, eliminating unnecessary energy in finding and processing fossil fuels, and improving energy efficiency.

Figure S1 also shows the transformation timeline proposed here for moving from BAU to 100% WWS in 143 countries. This timeline assumes an 80 percent conversion to WWS by 2030 and 100 percent by no later than 2050. Whereas new WWS infrastructure will be installed upon natural retirement of BAU infrastructure, policies are needed to force the remaining existing infrastructure to retire early to allow the conversion to 100% WWS at the pace necessary to eliminate air pollution mortality and avoid 1.5 ºC net global warming as much as possible.

Note S13. Selecting a Mix of WWS Energy Generators to Meet Demand

The next step in developing a 100% WWS roadmap is to estimate a mix, for each country, of the WWS electricity and heat generators that will supply the end-use all-purpose energy in the annual average. The penetration of each WWS electricity generator in each country is limited by the following constraints: 1) Each generator type cannot draw more power from its renewable resource than exists in the region of interest, 2) The land area taken up among all WWS land-based generators should be no more than a few percent of the land area of the region of interest; 3) The area of installed residential and commercial/government rooftop PV in each country should be less than the respective rooftop areas suitable for PV (Table S4); 4) No new conventional hydropower dams need to be installed, but existing ones can be improved. 5) Wind and solar, which are complementary in nature, should both be used in roughly equal proportions to the extent possible. Jacobson et al.[5] gives the methodology for determining the resources available in each country. The updated resources are provided in the spreadsheets accompanying this paper[41].

Table S5 provides the projected 2050 all-sector annual average end-use demand and an estimated percentage of the end-use demand met by each of 10 WWS electricity generators that satisfy these criteria in each of 143 countries. The mix of generators provided by country is by no means the only possible mix. It is one of many bounded by the constraints discussed. The numbers in the table assume the generators produce power sufficient to meet the annual average end use load of the country given in the table. It ignores cross-border transfers of energy that will occur in reality and doesn't account for meeting variations in power demand during the year. Additional generators needed to meet hour-by-hour variations during the year are quantified, as described in Note S41. Note S31 discusses the development of time-dependent heat, cold, electricity, and hydrogen load profiles used for this study.

Table 3 (main text) provides a weighted mean of the percentages in Table S5, summed among all 143 countries. It also provides an estimate of the nameplate capacity of existing plus new generators, summed over all countries, to meet the 2050 demand in the annual average as well as an estimated number of existing plus new generators to meet load continuously, based on results here. Finally, it provides the percentage of nameplate capacity already installed for each generator and the number of each new generator type needed among 143 countries.

The initial estimate of the number of WWS generators required for each country in Table 3 is derived starting with the end-use power demand supplied by each generator in each country, calculated from Table S5. This is divided by the annually averaged power output from one energy device (e.g., one wind turbine or one solar panel) after transmission, distribution, and maintenance losses have been accounted for. Such losses include those along lines and those from converting direct current (DC) to alternating current (AC) to high-voltage alternating current (HVAC) to high-voltage direct current (HVDC) (for extra-long-distance transmission) and back again to AC. The annual output by device after losses equals the nameplate capacity per device (same for all countries) multiplied by the country-specific annually averaged capacity factor of the device[41], diminished by transmission, distribution, and maintenance losses.

The summed nameplate capacities listed in Table 3 can match all energy needs in 143 countries *in the annual average*. However, storage and additional generators are needed to meet energy demand *hour-by-hour* during the year. In addition, solar and geothermal heat will help meet the heating portion of energy needs. Table 3 provides the level of existing solar and geothermal heat in the 143 countries along with an initial estimate of solar heat and CSP with storage needed to help meet energy demand hour-by-hour in the 143 countries. These numbers are adjusted in LOADMATCH, the model used here for matching variable demand with variable supply of energy in these countries. Table 3 shows the resulting final nameplate capacities, summed among all countries for each generator after the update.

Note S14. Predicting 2050-2052 Wind and Solar Fields with a Global Model

The grid integration model used here, LOADMATCH, requires input of time-dependent intermittent WWS power generation. Time-dependent wind and solar generation are determined directly from the global weather-climate-air-pollution model GATOR-GCMOM (Gas, Aerosol, Transport, Radiation, General Circulation, Mesoscale, and Ocean Model)[42-45, 53-82]. This model predicts output of time- and space-dependent electricity from onshore and offshore wind, rooftop and utility scale PV, and CSP; and solar-thermal heat production. From the wind data, time-dependent fields of wave power are also derived. Other time-dependent WWS fields are derived in LOADMATCH, as described shortly.

GATOR-GCMOM accounts for the reduction in the wind's kinetic energy and speed due to competition among wind turbines for available kinetic energy[44], the temperature-dependence of PV output, and the reduction in sunlight to building and the ground due to conversion of radiation to electricity by solar devices. It also accounts for changes in air and ground temperature due to power extraction by solar and wind devices and subsequent electricity use; impacts of time-dependent gas, aerosol, and cloud concentrations on solar radiation and wind fields; and radiation to solar PV panels that are either optimally tilted, single-axis tracked (horizontally or vertically), or dual axis tracked[45].

In general, the model simulates feedbacks among meteorology, solar and thermal-infrared radiation, gases, aerosol particles, cloud particles, oceans, sea ice, snow, soil, and vegetation. GATOR-GCMOM model predictions have been compared with data in 34 peer-reviewed studies[42-45,53-82]. The model has also taken part in 14 model inter-comparisons[83-96]. Below, the model is briefly described.

Note S15. Meteorological, Transport, and Surface Processes

The momentum, thermodynamic energy, and continuity equations are solved for the atmosphere with a potential-enstrophy, vorticity, energy, and mass-conserving scheme[97]. Winds and turbulence predicted by the model drive the horizontal and vertical transport of gases and size- and composition-resolved aerosol particles with a monotonic advection scheme[98]. Subgrid turbulent kinetic energy is calculated from Mellor and Yamada[99] as a function of instantaneous modeled wind shear and buoyancy due to background processes and the extraction of energy by wind turbines themselves. The model treats 17 subgrid surface classes, including several types of soil classes plus water, ice, road and rooftop classes, in each surface grid cell. It treats energy and vapor exchange between the atmosphere and each subgrid surface class in each cell. Subgrid, subsurface temperatures and moisture are tracked perpetually and independently throughout each simulation. Each subgrid soil class is divided into vegetated and bare soil. Snow can accumulate on soil and vegetation. Oceans are represented in 3-D for some calculations and 2-D for others. A 2-D time-dependent mixed-layer ocean dynamics model driven by surface wind stress is used to solve for mixed-layer ocean velocities, mixed-layer heights, and horizontal energy transport in each grid cell[100]. The scheme conserves potential enstrophy, vorticity, energy, and mass and predicted gyres and major currents. Energy diffusion to the deep ocean is treated in 3-D. Air-ocean exchange, vertical diffusion through the ocean, and 3-D ocean equilibrium chemistry and pH are solved among the Na-Cl-Mg-Ca-K-H-O-Li-Sr-C-S-N-Br-F-B-Si-P system. Sea ice in the model forms, evolves, and flows horizontally on subgrid water surfaces, and snow can accumulate on sea ice.

Note S16. Gas and Aerosol Processes

Gas processes include emissions, photochemistry, gas-to-particle conversion, gas-to-cloud conversion, gas-cloud exchange, gas-precipitation exchange, gas-ocean exchange, advection, convection, molecular diffusion, turbulent diffusion, and dry deposition. SMVGEAR II solves gas photochemistry for tropospheric and stratospheric kinetic reactions, particle surface reactions, and photolysis reactions. Aerosol processes include anthropogenic and natural emissions, binary and ternary homogeneous nucleation, condensation, dissolution, internal-particle chemical equilibrium, aerosol-aerosol coagulation, aerosol activation of clouds, aerosol-hydrometeor coagulation, sedimentation, dry deposition, and transport[101]. Chemical equilibrium calculations include the determination of the solid/liquid/ion composition, pH, and liquid water content of aerosols as a function of size. The model treats any number of discrete aerosol size distributions, each with any number of discrete size bins and chemicals per size bin. Particle number and chemical mole concentrations are tracked in each grid cell. The components within each size bin of each aerosol size distribution are internally mixed in the bin but externally mixed from other bins and other size distributions.

Note S17. Cloud and Aerosol-Cloud Processes

Cloud thermodynamics is parameterized to treat multiple subgrid cumulus clouds in each column based on an Arakawa-Schubert treatment. Aerosol particles of all composition and size and all gases are convected vertically within each subgrid cloud. Aerosol-cloud interactions and cloud and precipitation microphysics are time-dependent, explicit, and size- and composition-resolved[102]. The model simulates the size- and composition-resolved microphysical evolution of clouds and precipitation from aerosol particles, the first and second aerosol indirect effects, the semi-direct effect, and cloud absorption effects I and II (which are the heating of a cloud due to solar absorption by absorbing inclusions in cloud drops and by swollen absorbing aerosol particles interstitially between cloud drops, respectively)[77] .

Note S18. Radiative Processes

For radiative calculations, each model column is divided into clear- and cloudy-sky columns, and separate calculations are performed for each. Radiative transfer is solved simultaneously through multiple layers of air and one snow, sea ice, or ocean water layer at the bottom to calculate, rather than prescribe, spectral albedos over these surfaces. The radiative code solves for atmospheric heating rates and actinic fluxes over each of 694 wavelengths/probability intervals in the ultraviolet, visible, solar-infrared, and thermal-infrared spectra, accounting for gas and size- and composition-dependent aerosol and cloud optical properties[77].

Aerosol and cloud optical properties are calculated by integrating spectral optical properties over each size bin of each aerosol and hydrometeor particle size distribution. Aerosol spectral optical of a given size are determined by assuming that black carbon, if present, is a core surrounded by a mixed shell and that the aerosol liquid water content is a function of the ambient relative humidity and aerosol composition. Cloud spectral optical properties of a given size are determined accounting for scattering by aerosol particles between cloud particles, where aerosol particle liquid water content is determined at the relative humidity of the cloud. Cloud drop, ice crystal, and graupel optical properties are determined accounting for the time-dependent evolution of black carbon, brown carbon, and soil dust inclusions within the drops, crystals, and graupel. Ice crystal and graupel optical properties also account for the non-sphericity of these particles[77].

The radiative transfer calculation also accounts for building and vegetation shading, angle of the sun, Earth-sun distance changes over time, and Earth-space refraction.

Note S19. Treatment of Wind Turbine Energy Extraction

For this study, 1.66 million 5-MW onshore and 939,000 5-MW offshore wind turbines with hub heights of 100 m above ground level were placed in GATOR-GCMOM in countries based on a preliminary estimate of the number of turbines needed in each country. The turbines were placed in farms distributed relatively evenly throughout each country, which would likely underestimate actual wind power because many areas of countries have low wind potential. Each farm consisted of tens to hundreds of turbines. Because of the proximity of wind turbines to each other within a farm, it is necessary to account for the competitive extraction of the wind's kinetic energy by all turbines. Failing to account for such interaction results in an overestimate of available wind power.

The numerical treatment of energy extraction by each wind turbine is described in Jacobson and Archer[44]. Due to the coarse horizontal resolution used for the present simulations (2°x2.5^{o} globally), wind turbines are not resolved in the horizontal; however, because of the fine vertical resolution used, they are resolved in the vertical, with five layers per turbine. All turbines extract the precise amount of energy from the wind as their power curve dictates.

Each turbine is characterized by its rated power, rotor diameter (D), and hub height above the surface (100 m here). Each wind turbine intersects several model vertical layers. Kinetic energy is extracted from each model layer that intersects the turbine rotor each timestep. The reduction in the wind's kinetic energy reduces wind speed in each turbine's wake, creating shear that converts more kinetic energy into turbulent kinetic energy (TKE) that is modeled with the level 2.5 TKE closure of Mellor and Yamada[99]. The kinetic energy extracted by turbines is used for electric power. To conserve energy in the model, the electric power dissipates heat. Kinetic energy in the wind also dissipates, but more slowly, to heat as it encounters roughness elements on the ground. The heat produced in both cases creates buoyancy, giving rise to potential energy. Gradients in potential energy then regenerate some kinetic energy. Thus, the model conserves energy.

Note S20. Treatment of Solar Energy Extraction by PV Panels and CSP Power Plants

GATOR-GCMOM also treats extraction of energy by residential rooftop photovoltaic (PV) systems, commercial/government rooftop PV systems, utility-scale PV systems, concentrated solar power (CSP) systems, and solar thermal systems. An estimated number of each of these systems was placed in each country within GATOR-GCMOM. Utility-scale PV and/or CSP plants were placed in low latitude regions of each country and rooftop PV and solar thermal systems were placed throughout each country proportional to population.

GATOR-GCMOM predicts time-dependent direct and diffuse solar radiation as a function of wavelength, accounting for time-dependent predicted gas, aerosol particle, and cloud concentrations and optical properties in the atmosphere. It accounts for radiation to flat, fixed-tilt, single-axis tracking, and dual-axis tracking PV panels[45]. The radiative transfer calculation also accounts for surface albedo (and predicts albedo over water, snow, and ice surfaces), building and vegetation shading, angle of the sun, Earth-sun distance, Earth-space refraction, and solar intensity versus wavelength. As such, the model predicts the variable nature of solar radiation fields.

Solar PV and CSP in the model extract power, reducing solar radiation to the surface, thereby reducing panel, rooftop, and ground temperature. PV output in the model is a function of temperature, so extraction of solar radiation by the panels themselves, which affects surface temperature, also affects panel performance. The model also treats the dissipation of electrical energy to heat. Whereas panels reduce local temperatures by extracting sunlight, this energy is returned as heat upon electricity use.

Finally, since GATOR-GCMOM simulated meteorology from 2050-2052, time-dependent wind and solar fields account for higher greenhouse gas levels and a different climate than exist today. However, emission levels for the 143 countries in 2050 are much lower than today due to the fact that a 100% WWS system will replace most current emissions by 2050. This is accounted for in the model.

Note S21. Simulations Predicting Intermittent Wind and Solar Energy

GATOR-GCMOM was run on the global scale for 3 years (2050-2052) at 2 x 2.5 degree horizontal resolution. Modelled onshore and offshore wind, solar rooftop PV, utility scale PV, CSP, and solar thermal output were written every 30 seconds to a file for each country. The simulation accounted for the reduction in the wind's kinetic energy and speed due to the conversion of kinetic energy to electrical energy by wind turbines, and the conversion of electrical energy to heat. It also accounted for extraction of solar energy by rooftop PV at a fixed optimal tilt angle, determined for each region in each country that the PV existed in[45]. It further accounted for extraction by utility PV, half of which was assumed to be at fixed optimal tilt. The other half was assumed to track the sun horizontally. The simulation also accounted for extraction by CSP and solar thermal for heat. PV, CSP, and solar thermal reduced solar radiation to the surface, cooling the surface. All wind and solar electricity generated eventually dissipated as heat in the model. Jacobson et al.[1] found that the extraction of kinetic energy by wind turbines slightly cooled global temperatures.

Note S22. Matching Demand with Supply, Storage, and Demand Response

The following notes discuss matching demand with supply, storage, and demand response.

Note S23. Types of Models for Matching Demand

Three main types of computer models that simulate matching power demand with supply, storage, and/or demand response on an electric power grid have been developed. These include power flow/load flow models, optimization models, and the trial-and-error simulation model. Such models are described briefly.

Note S24. Power Flow or Load Flow Models

Power flow, or load flow, models treats thousands or more individual transmission lines connected to generators of electricity and to load centers. Inputs are the real power and voltage magnitude of each generator and the real and reactive power of each load. At one arbitrary generator (called the slack bus) the voltage phase angle is also known. Outputs are the voltage magnitude of all the loads and the voltage phase angles of both the generators (except the slack bus, where the phase angle is already known) and loads. The resulting set of nonlinear equations does not depend on time. In other words, the equations represent an equilibrium state, and the solution to the equations is an equilibrium (independent of time) solution. The solution is not an optimized

solution. Instead, it is the only real solution to a set of *N* equations and *N* unknowns. One method of solving the equations is with an iterative Newton-Raphson technique. Because power flow models are equilibrium models that represent one snapshot in time, they are not used to examine matching power demand with supply over time. Their requirement for iteration, thus heavy computational cost, also makes them difficult to use to match power demand with supply over time even if modified to do so. On the other hand, they are the only type of model currently available that can be used to simulate flows through individual transmission lines.

Note S25. Optimization Models

A second type of model is a least-cost or least-carbon optimization model. Most models used for examining grid stability are optimization models. Such models either assume perfect transmission (no representation of individual transmission lines) or include just a few main transmission lines between generators and load centers. As such, they do not treat the transmission system in nearly the same detail as a power flow model does. However, unlike power flow models, optimization models treat all time steps of a simulation period simultaneously.

With an optimization model, a problem is set up to calculate the least cost portfolio of generators or the lowest-carbon-emitting portfolio of generators to meet load[9]. Cost usually includes capital cost, fixed and variable operation and maintenance (O&M) cost, fuel cost, and decommissioning cost of each generator and storage technology. Carbon emissions include those from each generator, if any.

The minimization in each case is subject to a power balance constraint that ensures that the generation, summed over all generators, minus transmission and distribution losses plus or minuses changes from storage, equals the load on the grid each time period (usually an hour). The inputs into the calculation may include the cost (or carbon emissions) of each generator as a function of nameplate capacity; the peak charge rates, discharge rates, and capacities of storage; hourly electric power generation per unit nameplate capacity from each generator; transmission loss rates; constraints for hourly removals from or additions to storage; and hourly loads. A set of equations is derived that requires balancing load each hour over a specified time period. The equations are solved among all hours simultaneously to minimize cost or carbon. Since the cost and carbon emissions are a function of the nameplate capacity of each generator, the resulting nameplate capacities of each generator are then known.

The equations are solved with an optimization solver, of which many exist. The main problem with an optimization model is that, the more hours and variables (e.g., different types of generators and storage) that are solved for, the more difficult it is to converge the resulting set of equations in a reasonable amount of computing time, even with a large computer. As such, many optimization models have been unable to solve for a full year at an hour resolution. Instead such models have solved over a reduced number of hours per year, usually representing blocks of days in different seasons (see Table 1 of Ref. 103 for examples). Models that do solve every hour generally simplify the system by reducing the types of storage or generators or by omitting demand response, hydrogen loads, heat loads, and/or cold loads.

The problem with not treating at least every consecutive hour of a year with an optimization model is that storage becomes impossible to track correctly. The amount of electricity, heat, cold, or hydrogen in storage at a given hour can be determined only from knowing how much was in storage during the last hour and how much was added to or removed from storage during the current hour. If a model is optimizing over a few consecutive hours in one month and a few consecutive hours in a second month, the model has no knowledge at the beginning of the second month how much storage is currently available. As such, an optimization model that treats storage cannot provide accurate information about whether load can be met unless it treats all hours consecutively.

Finally, because optimization models are so time consuming, even at a 1-hour resolution, it is extremely difficult, given current computing resources, to solve over multiple years at 1 minute or less time resolution.

Note S26. Trial-and-Error Simulation Models

The trial-and-error simulation model (LOADMATCH[1,16]) was designed to overcome the main problems of the least cost or least carbon optimization model. Because of its speed, it allows for many more types of energy generation and storage than an optimization model. It takes orders of magnitude smaller timesteps than an

optimization model while taking orders of magnitude less computing time to cover the same period. For example, in the present study, a trial-and-error simulation assuming perfect transmission over 3.15 million 30-s timesteps (3 years) requires about 55 s of computing time on a single 3.0 GHz computer processor. This is 1/500th to 1/100,000th the computer time of an optimization model for the same number of timesteps.

On the other hand, the trial-and-error simulation model does not necessarily find the least cost solution. Instead, it finds multiple low-cost solutions with zero load loss. The lowest cost solution among this set is selected.

The trial-and-error simulation model works by running multiple simulations, one at a time. Each simulation marches forward for several (e.g., 2 to 50) years, one timestep at a time, just as the real world does. As such, unlike with an optimization model, which solves among all timesteps simultaneously, a trial-and-error model does not know what the weather will be during the next timestep. Timesteps can be of any size (e.g., seconds, minutes, hours). Results for the simulations shown here are calculated with a 30-s timestep.

The trial-and-error simulation model starts from some set of initial conditions (e.g., nameplate capacities of generators and storage) and marches forward in time. Its main constraint is that electricity, heat, cold, and hydrogen load, adjusted by demand response, must match energy supply and storage during every timestep for an entire simulation period. If load is not met during a single timestep, the simulation stops. A new simulation is then restarted from the beginning with an adjustment to either the nameplate capacity of one or more generators, the characteristics of storage (peak charge rate, peak discharge rate, peak storage capacity), or characteristics of demand response. New simulations are run until load is met every time step of the simulation period. After load is met once, additional simulations are run with further-adjusted inputs to generate a set of solutions that match load every timestep. The lowest cost solution in this set is then selected.

Because the model does not permit load loss at any time, it is designed to exceed the utility industry standard of load loss once every 10 years. Other aspects of planning and operating the grid, such as control details regarding frequency regulation and transient stability, are not treated here because the model is not simulating individual buses.

Model inputs are as follows: (1) time-dependent electricity produced from onshore and offshore wind turbines, wave devices, tidal turbines, rooftop PV, utility PV, CSP, and geothermal plants; (2) a hydropower plant peak discharge rate (nameplate capacity), a hydropower mean recharge rate (from rainfall), and a hydropower annual average electricity output; (3) time-dependent geothermal heat and solar-thermal heat generation rates; (4) specifications of hot-water and chilled-water sensible-heat thermal energy storage (HW-STES and CW-STES) (peak charge rate, peak discharge rate, peak storage capacity, and energy losses during charging and discharging); (5) specifications of underground thermal energy storage (UTES), including borehole, water pit, and aquifer storage; (6) specifications of ice storage (ICE); (7) specifications of electricity storage in pumped hydropower storage (PHS), phase-change materials coupled with concentrated solar power plants (CSP-PCM), and batteries (8) specifications of hydrogen electrolysis, compression, and storage equipment; (9) specifications of electric heat pumps for air and water heating and cooling; (10) specifications of a demand response system; (11) specifications of losses along short- and long-distance transmission and distribution lines; (12) time-dependent electricity, heat, cold, and hydrogen loads, and (13) scheduled and unscheduled maintenance downtimes for generators, storage, and transmission.

Cost inputs are also needed for electricity, heat, and cold generators and storage; transmission and distribution; and hydrogen water, electrolysis, compression, and storage. These costs include capital costs, technology lifetimes, fixed and variable O&M costs; decommissioning costs, and a social discount rate. WWS generators have no fuel costs, except the water cost for hydrogen production by electrolysis.

A trial-and-error model can be run assuming perfect transmission (no representation of individual lines), or it can be modified to treat some major transmission lines. In both cases, costs and power losses during transmission and distribution are calculated, but in the former case, power flows through individual transmission lines or substations are not treated. In the present study, the model is run assuming perfect transmission, but accounting for short- and long-distance transmission and distribution line losses and costs.

Note S27. Application of LOADMATCH to the Present Study

For this study, the trial-and-error model, LOADMATCH is used. In Jacobson et al.[16], it was used to model matching demand with supply, storage, and demand response among all energy sectors in the 48 contiguous U.S. states. It was updated in Jacobson et al.[1] and applied, with three different storage scenarios, to 20 world regions encompassing 139 countries. The raw energy data for the 139 countries in that study were from IEA[46] for 2012, and the contemporary nameplate capacities installed worldwide were for 2015.

Here, the model is updated further and applied to study matching demand with 100% WWS supply and storage in 24 world regions encompassing 143 countries. The IEA[46] (2019) raw energy data for these countries were available for 2016, and the contemporary nameplate capacities were available for 2018. Another difference is that this study treats each region as having a specified fraction of district heating. District heating allows community low-temperature heating and cooling loads to be subject to seasonal and daily thermal energy storage. In Jacobson et al.[1], either all low-temperature heating and cooling loads (Case A) or no heating or cooling loads (Case C) were subject to thermal energy storage. This study also accounts for the reductions in capital costs of WWS energy systems that have occurred during the last few years and the projected impacts of such changes on future cost estimates.

Further, this study uses new country-by-country mortality estimates from WHO[104] to project BAU air pollution damage costs in 2050. The study also updates estimates of country-specific population, urbanization fraction, carbon dioxide emissions, BAU fuel costs, job creation and loss, transmission and distribution efficiencies, resource potentials, rooftop areas, and land requirements, among other parameters.

Table 1 (main text) summarizes the countries included in each of the 24 world regions. Generation and load were assumed to be interconnected perfectly by transmission among all countries in a region. Winds and solar fields in each country were modeled with GATOR-GCMOM every 30 s for three years. The wind and solar fields were used to estimate the time-dependent electric power output from onshore and offshore wind turbines, wave devices, solar PV panels on rooftops, utility-scale solar PV panels, CSP plants, and solar thermal heat collectors every 30 s in each country. The wind power estimates from the climate model accounted for competition among wind turbines for available kinetic energy. Hydrogen was used only to supply some transportation loads. Table S6 summarizes the main processes treated in LOADMATCH for the present study.

Note S28. Producing Time-Dependent Low- and High-Temperature Heat/Cold Loads

Table S7 provides the 2050 annual electricity plus heat load in the WWS case by world region and sector, derived from Table S2. The sectors include residential, commercial, industrial, transport, agriculture/forestry/fishing, and military/other.

Residential and **commercial/government loads** include all electric and heat loads consumed in residential and commercial/public buildings, respectively, aside from any loads duplicated in the other sectors (e.g., transportation).

Industrial loads include energy consumed by all industries, including iron, steel, and cement; chemicals and petrochemicals; non-ferrous metals; non-metallic minerals; transport equipment; machinery; mining (excluding fuels, which are treated under transport); food and tobacco; paper, pulp, and print; wood and wood products; construction; and textile and leather.

Transportation loads include energy consumed during any type of transport by road, rail, domestic and international aviation and navigation, or by pipeline, and by agricultural and industrial use of highways. For pipelines, the energy required is for the support and operation of the pipelines. The transportation category excludes fuel used for agricultural tractors and machines, fuel for fishing vessels, and fuel delivered to international ships, since those are included under the agriculture/forestry/fishing category.

Agriculture/forestry/fishing loads include energy consumed by users classified as agriculture, hunting, forestry, or fishing. For agriculture and forestry, it includes consumption of energy for traction (excluding agricultural highway use), electricity, or heating in those industries. For fishing, it includes energy for inland,

coastal, and deep-sea fishing, including fuels delivered to ships of all flags that have refueled in the country (including international fishing) and energy used by the fishing industry.

Military/other loads include fuel used by the military for all mobile consumption (ships, aircraft, tanks, on-road, and non-road transport) and stationary consumption (forward operating bases, home bases), regardless of whether the fuel is used by the country or another country.

Note S29. Heat and Cold Loads

The annual average end-use loads in each region from Table S7 for each sector are first separated into (1) electricity and heat loads needed for low-temperature heating, (2) electric loads needed for cooling and refrigeration, (3) electricity loads needed to produce, compress, and store hydrogen for fuel cells used for transportation, and (4) all other electricity loads (including industrial heat loads). Each of these loads is then divided further into flexible and inflexible loads. Flexible loads include electricity and heat loads that can be used to fill cold and low-temperature heat storage, all electricity used to produce hydrogen (since all hydrogen can be stored), and remaining electricity and heat loads subject to demand response. Inflexible loads are all loads that are not flexible. The flexible loads may be shifted forward in time with demand response. The inflexible loads must be met immediately.

Electricity and heat needed for low temperature building air and water heat are collectively referred to as low-temperature heat loads or just heat loads. Time-dependent heat loads are approximated as follows. First, the annual average low-temperature heat load (GW) across all energy sectors in a given region is

$$L_{heat} = L_{heat,r} + L_{heat,c} + L_{heat,i} \quad \text{(S1)}$$

where

$$L_{heat,r} = (F_{ah,r}+F_{wh,r})L_r \quad \text{(S2)}$$
$$L_{heat,c} = (F_{ah,c}+F_{wh,c})L_c \quad \text{(S3)}$$
$$L_{heat,i} = F_{ah,i}L_i \quad \text{(S4)}$$

are the low-temperature heat loads in the residential, commercial, and industrial sectors, respectively. In these equations, $F_{ah,r}$ and $F_{wh,r}$ are the fractions of the residential heat load (L_r) that are for air and water heating, respectively; $F_{ah,c}$ and $F_{wh,c}$ are the fractions of the commercial heat load (L_c) that are for air and water heating, respectively; and $F_{ah,i}$ is the fraction of the industrial load (L_i) that is for low-temperature air heating. The last parameter is estimated with

$$F_{ah,i} = F_{hvac}H/(C+H) \quad \text{(S5)}$$

where F_{hvac} is the fraction of total industrial load that is for the sum of air heating, air cooling, and refrigeration in the industrial sector (approximated as 0.0624 from U.S. data[1]); and H and C are the average number of heating and cooling degree days, respectively, in a year in a region.

Heating degree days (HDDs) are the number of degrees that the outside air temperature must be raised to reach an indoor comfort-level reference temperature, summed over all days of a month or year. HDDs are more specifically calculated as the number of outdoor air temperature degrees below a reference temperature in a day, summed over all days during some period. If the air temperature is above the reference temperature for 24 hours of a day, the number of HDDs is zero for that day. The reference temperature varies depending on the country, but it is typically 18.33 ºC (65 ºF). This value is used here as the reference temperature.

Cooling degree days (CDDs) are the number of degrees that the outside air temperature must be cooled to reach the same reference temperature as for HDDs, summed over all days during a month or year. If the outdoor temperature for 24 hours of a given day is below the reference temperature, then the number of CDDs on that day is zero.

Whereas the number of heating degree days (HDDs) is a good proxy for air heating requirements, it is less accurate for water heating requirements. For example, even if the number of HDDs is zero for a day, a building

may still need hot water for dishwashing, clothes washing, showers, cooking, and cleaning. Cooling degree days (CDDs) are a proxy for the cooling requirements of a building. Whereas the number of CDDs is a good proxy for air cooling requirements, it does not help so much for refrigeration requirements in a home or building. To approximately account for each of these requirements, one heating and cooling degree days was added each day to the observed number of heating and cooling degree days. This had the effect of ensuring some heating and cooling load would occur each day of the year after daily heating and cooling loads were calculated (as discussed shortly).

Figure S2 shows the average number of HDDs and CDDs per year for the 24 world regions listed in Table 1 (prior to adding a daily minimum heating and cooling degree day). Countries or regions at higher latitudes experience more HDDs, thus heating requirements, than do tropical (low-latitude) countries. Conversely, countries or regions at lower latitudes experience more CDDs, thus cooling requirements, than do higher-latitude countries.

The fraction of total load in a sector that is low temperature heat load is

$$F_h = F_{ah} + F_{wh} \quad \text{(S6)}$$

Table S8 gives values of F_h, which apply to both the residential and commercial sectors, for several countries and world regions. The table indicates that, worldwide, about 79% of all energy consumed in residential and commercial buildings is used for air and water heating. If total residential or commercial energy demand is known in a region, it can be multiplied, as a first estimate, by F_h from Table S8 to obtain an estimate of the low-temperature (air plus water) heat load in buildings.

Based on U.S. data, the fraction of residential load needed for water heating is related to that needed for air heating by $F_{wh,r}=0.4265F_{ah,r}$. Combining this relationship with Equation S6 gives $F_{ah,r} = 0.701F_{h,r}$, and $F_{wh,r}=0.299F_{h,r}$. In the commercial sector, $F_{wh,c}=0.2118*F_{ah,c}$, giving $F_{ah,c}=0.8252*F_{h,c}$ and $F_{wh,c}=0.1748*F_{h,c}$[63], where $F_{h,r}=F_{h,c}=F_h$ (given in Table S8).

Table S8 also gives the fraction (F_{ht}) of total industrial load (L_i) that is high-temperature industrial heat load. The high-temperature heat load, $L_{temp,i}$, is thus

$$L_{htemp,i}= F_{ht}L_i \quad \text{(S7)}$$

Table S8 indicates that worldwide, about 65% of industrial energy is used for high-temperature heat. The rest is used for low-temperature air heat, air conditioning, refrigeration, transportation, and normal electricity. Table S9 provides values for F_{ah}, F_{wh}, and F_{ht} for the residential, commercial, and/or industrial sectors for 24 world regions.

Cold loads are loads in each sector for air conditioning and commercial refrigeration. The total cold load across all energy sectors is

$$L_{cold} = L_{cold,r} + L_{cold,c} + L_{cold,i} \quad \text{(S8)}$$

where

$$L_{cold,r} = F_{ac,r}L_r \quad \text{(S9)}$$
$$L_{cold,c} = (F_{ac,c}+F_{rf,c})L_c \quad \text{(S10)}$$
$$L_{cold,i} = (F_{ac,i}+F_{rf,i})L_i \quad \text{(S11)}$$

In these equations, $F_{ac,r}$, $F_{ac,c}$, and $F_{ac,i}$ are the fractions of the total residential, commercial, and industrial loads, respectively, that are for air conditioning; and $F_{rf,c}$ and $F_{rf,i}$ are the fractions of the commercial and industrial loads, respectively, that are for refrigeration.

The fractions of total load in the residential and commercial sectors that are for air conditioning are estimated to be the smaller of the air heating load multiplied by the ratio of cooling to heating degree days and a maximum allowable fraction of building electric load used for air cooling:

$$F_{ac,r} = \min(F_{ah,r}C/H,\ F_{e,r}F_{max}) \quad \text{(S12)}$$
$$F_{ac,c} = \min(F_{ah,c}C/H,\ F_{e,c}F_{max}) \quad \text{(S13)}$$
$$F_{ac,i} = \min(F_{ah,i}C/H,\ F_{e,i}F_{max}) \quad \text{(S14)}$$

respectively, where $F_{e,r}=1-F_{h,r}$, $F_{e,c}=1-F_{h,c}$, and $F_{e,i}=1-F_{ht}$ are the fractions of total load in the residential and commercial sectors, respectively, that are non-high-temperature electric loads ($F_{h,r}$ and $F_{h,c}$ are the fractions of total load in the residential and commercial sectors, respectively, that are low-temperature heat loads, and F_{ht} is the fraction of total industrial sector load that is high-temperature heat load from Table S8). Finally, F_{max} is the maximum allowable fraction of building electric load that is for air conditioning (set to 0.4)[1].

The fraction of total load in the commercial sector that is refrigeration load is then estimated as

$$F_{rf,c}=0.7383F_{ac,c.} \quad \text{(S15)}$$

Lastly, $F_{rf,i}$ is assumed to be 0.024 for all world regions based on U.S. data[1]. Table S9 provides 2050 estimates of F_{ac} and F_{rf} for the residential, commercial, and industrial sectors in 24 world regions (defined in Table 1). Refrigeration load in the residential sector is not separated from the remaining electric load.

Note S30. Inflexible Loads and Loads Subject to Storage and Demand Response

The next step is to determine the loads subject to heat, cold, hydrogen, and electricity storage; the load subject to demand response; and the inflexible load.

The load subject to heat storage, which can be charged flexibly, is

$$L_{heat,stor} = F_{dh}L_{heat} + (F_{flx,wh}-F_{dh})(F_{wh,r}L_r + F_{wh,c}L_c) \quad \text{(S16)}$$

where F_{dh} is the fraction of all low-temperature heat and cold load in each region that is provided by district heating and cooling. Table S9 gives values for 24 world regions. The district heating and cooling fraction is important, because cold and low-temperature heat energy provided by district heating and cooling is stored in water tanks, borehole fields, water pits, aquifers, or ice. Stored heat or cold is always produced hours to months before it is used, so the electricity or heat charging the storage is a flexible load. Thus, for example, an electric heat pump may produce heat or cold for storage whenever excess electricity is available on the grid. Conversely, if an electricity shortage occurs on the grid, heat pumps can be shut off, freeing electricity for the rest of the grid.

In Equation S16, $F_{flx,wh}=0.95$ is the fraction of water heating that occurs in water storage tanks and that can be charged flexibly. This term accounts for the fact that building hot water tanks that are *not* in district heating systems can be charged flexibly. Hot water tanks that are part of district heating systems are accounted for in the first term on the right side of Equation S16.

The load subject to cold storage, all of which can be charged flexibly, is

$$L_{cold,stor} = F_{dh}L_{cold} \quad \text{(S17)}$$

Thus, only cold loads subject to district cooling can be charged flexibly. Such cold loads are stored in water, ice, and aquifers, all of which can be charged flexibly.

Hydrogen is used only for transportation in this 100% WWS system. The load subject to hydrogen storage is

$$L_{H2,stor} = F_{H2}L_t \quad \text{(S18)}$$

Where F_{H2} is the fraction of the transportation load (L_t) needed to produce, compress, and store hydrogen. Table S9 provides estimates of F_{H2} for 24 world regions. Loads for producing hydrogen are all flexible because all hydrogen produced can be stored before use so long as hydrogen storage is sized correctly. As such, loads for producing hydrogen are subject to demand response. However, hydrogen is separated from other loads subject to demand response since the quantity of stored hydrogen must be tracked in the model.

Loads, aside from hydrogen loads, subject to demand response are estimated with

$$L_{DR} = L_{DR,r} + L_{DR,c} + L_{DR,i} + L_{DR,t} + L_{DR,a} + L_{DR,o} \quad \text{(S19)}$$

where

$$L_{DR,r} = F_{flx,r}[L_r-(L_{heat,r}-L_{cold,r})F_{dh}] \quad \text{(S20)}$$
$$L_{DR,c} = F_{flx,c}[L_c-(L_{heat,c}-L_{cold,c})F_{dh}] \quad \text{(S21)}$$
$$L_{DR,i} = F_{flx,hti}L_{htemp,i} + F_{flx,tri}L_{trans,i} + F_{flx,oi}[L_i-L_{htemp,i}-L_{trans,i}-(L_{heat,i}-L_{cold,i})F_{dh}] \quad \text{(S22)}$$
$$L_{DR,t} = F_{flx,t}L_t \quad \text{(S23)}$$
$$L_{DR,a} = F_{flx,a}L_a \quad \text{(S24)}$$
$$L_{DR,o} = F_{flx,o}L_o \quad \text{(S25)}$$

are the loads subject to demand response in the residential (L_r), commercial (L_i), industrial (L_i), transportation (L_t), agriculture/forestry/fishing (L_a), and military/other (L_o) sectors, respectively. In these equations, F_{flx} is the fraction of a given load that is flexible, thus subject to demand response. For example, $F_{flx,r} = F_{flx,c} = F_{flx,oi} = F_{flx,a} = 0.15$ is the fraction of the residential, commercial, and agriculture/forestry/fishing non-heating, non-cooling, non-transportation, and non-high-temperature loads that is flexible.

Further, $F_{flx,hti}= 0.70$ is the fraction of the high-temperature industrial load that is flexible. Many high-temperature industrial loads are subject to demand response, thus flexible. Some industrial loads that can be shifted include air liquefaction; induction and ladle metallurgy; water pumping with variable speed drives; and production by electrolysis of aluminum, chlor-alkali, potassium hydroxide, magnesium, sodium chlorate, and copper[105]. NRC[106] states,

"*The ability of industry to cut peak electric loads is a motivator for utilities to incentivize demand response (shifting loads to off-peak periods) in industry…In combination with peak-load pricing for electricity, energy efficiency and demand response can be a lucrative enterprise for industrial customers.*"

In addition, $F_{flx,t} = F_{flx,tri}= 0.85$ is the fraction of the transportation-sector transportation load and the industrial-sector transportation load that is flexible. $F_{flx,o}= 0.75$ is the fraction of other-sector loads that is flexible. In Equation S22,

$$L_{trans,i}= F_{tr,i}L_i \quad \text{(S26)}$$

is the industrial-sector transportation load, were $F_{tr,i} = 0.0072$ is the fraction of the industrial-sector load that is for transportation, based on U.S. data[1].

Finally, the inflexible load (F_{inflex}) is the all-sector total load ($L_{total} = L_r+L_c+L_i+L_t+L_a+L_o$) minus the loads subject to heat storage, cold storage, hydrogen storage, and demand response. Thus,

$$F_{inflex} = L_{total} - L_{heat,stor} - L_{cold,stor} - L_{H2,stor} - L_{DR} \quad \text{(S27)}$$

Inflexible loads need to be satisfied immediately in the model.

Figure S3 and Table S10 show the resulting annual average end-use 2050 WWS load by sector and separated into inflexible and flexible loads for 24 world regions.

Note S31. Time-Dependent Heating, Cooling, Electricity, and Hydrogen Loads

Next, each region's annually averaged total heating load (L_{heat}) is distributed into daily heating loads with the use of heating degree day data as follows:

$$L_{heat,day} = L_{heat}H_{day}D_y/H \quad \text{(S28)}$$

where H_{day} is the number of heating degree days on a given day of the year, D_y=365 (or 366 for leap years) is the number of days per year, and H is the number of heating degree days per year.

The total heat load is then partitioned into a daily heat load subject to storage and not subject to storage respectively, with

$$L_{heat,stor,day} = L_{heat,stor}L_{heat,day}/L_{heat} \quad \text{(S29)}$$
$$L_{heat,nostor,day} = L_{heat,day} - L_{heat,stor,day} \quad \text{(S30)}$$

The latter parameter, the heat load not subject to storage, may be treated as inflexible or partly subject to demand response. Here, 15% (= $F_{flx,r}$ = $F_{flx,c}$ = $F_{flx,oi}$ = $F_{flx,a}$) is treated as flexible and subject to demand response in all sectors. This flexible term is already included as an annual average term in the equations for loads subject to demand response (Equations 8.20 to 8.25). In Equation 8.20, for example, the term is $F_{flx,r}L_{heat,r}(1-F_{dh})$. This and similar terms must be removed and replaced with daily terms, such as $F_{flx,r}L_{heat,r}(1-F_{dh})L_{heat,day}/L_{heat}$, to obtain the daily load subject to demand response. Equations 8.20 to 8.25 are modified further for other daily or hourly terms, as discussed shortly.

Similarly, each region's annually averaged total cooling load (L_{cool}) is distributed into daily cooling loads with the use of cooling degree day data as follows,

$$L_{cool,day} = L_{cool}C_{day}D_y/C \quad \text{(S31)}$$

where C_{day} is the number of cooling degree days on a given day of the year and C is the number of cooling degree days per year. The total cold load is then partitioned into a daily cold load subject to storage and not subject to storage, respectively, with

$$L_{cold,stor,day} = L_{cold,stor}L_{cold,day}/L_{heat} \quad \text{(S32)}$$
$$L_{cold,nostor,day} = L_{cold,day} - L_{cold,stor,day} \quad \text{(S33)}$$

The cold load not subject to storage may be treated as inflexible or as partly subject to demand response. Like with the heat load not subject to storage, 15% is treated as flexible and subject to demand response in all sectors. This flexible term is already included as an annual average term in the equations for loads subject to demand response (Equations S20 to S25). In Equation S20, for example, the term is $F_{flx,r}L_{cold,r}(1-F_{dh})$. This and similar terms must be removed and replaced with daily terms, such as $F_{flx,r}L_{cold,r}(1-F_{dh})L_{cold,day}/L_{cold}$, to obtain the daily load subject to demand response.

Because hydrogen loads are flexible and hydrogen will be needed every day for long-distance, heavy transport, the annual average hydrogen load can initially be spread evenly each hour of the year. Demand response will adjust the actual timing of when the hydrogen is produced.

Once daily inflexible heat and cold loads are calculated, they are added to hourly inflexible loads, which are all remaining loads aside from those used to produce hydrogen, subject to heat or cold storage, or subject to demand response.

Hourly 2050 inflexible electricity loads are obtained from contemporary hourly BAU load data from ENTSO-E[107] for European countries and from Neocarbon Energy[108] for all other countries. The same hourly load data were used for 139 countries in Jacobson et al.[1] and shown in Figure S1 of that paper for the 20 world regions used within it. For the additional countries treated here (Mauritius, Niger, South Sudan, and Suriname), data were available for Niger and Suriname from Neocarbon Energy[108]. Data for Sudan were used as a surrogate for South Sudan. Data for Zimbabwe were used as a surrogate for Mauritius.

Contemporary electricity loads include cold loads, since air conditioning and refrigeration currently run on electricity. On the other hand, they do not include many low-temperature heat loads, because air and water today are heated mostly with natural gas, fuel oil, and wood pellets rather than electricity. The contemporary hourly electricity BAU loads are extrapolated to 2050 and converted to WWS total loads (flexible plus inflexible loads) using the annual average ratio of the total 2050 WWS load to the total contemporary BAU load. From the resulting hourly 2050 WWS load, hourly heat, cold, and hydrogen loads subject to storage are subtracted out to give the remaining electric load. The electric load is then partitioned into hourly flexible and inflexible loads. The hourly flexible loads are subject to demand response and replace the corresponding annual average flexible loads subject to demand response in Equations S20 to S25.

Figure S3 and Table S10 show the resulting breakdown of annual average inflexible and flexible loads for each region. Flexible loads are separated into loads subject to low-temperature heat storage, loads subject to low-temperature cold storage, loads subject to hydrogen storage, and remaining flexible loads, which are all subject to demand response. The hydrogen load is the load needed to produce, compress, and store hydrogen. It accounts for hydrogen leakage as well. Hydrogen is used only in fuel cells for long-distance, heavy transport in trucks, trains, ships, and aircraft in the present scenarios.

Note S32. Sizing Storage and Demand Response

Tables S11 and S12 provide specifications of electricity, heat, cold, and hydrogen storage used here. Three important characteristics of storage are its maximum charge rate, maximum discharge rate, and maximum capacity (Table S11). Other relevant storage parameters are the number of hours or days at the maximum discharge rate (Table S12), storage efficiency (Table S13), the present value of the lifecycle cost of storage (Table S13), and the lifetime of storage devices (Table S13).

The peak charge rate (kW) is the maximum amount of energy per unit time that can be added to storage. The peak discharge rate (kW) is the maximum amount of energy per unit time that can be removed from storage. The peak storage capacity (kWh) is the maximum amount of energy that can be stored. It equals the peak discharge rate multiplied by the number of hours of storage (Table S12) at the maximum discharge rate.

Whereas the peak discharge rate of a hydropower reservoir is limited by the turbine nameplate capacity and the maximum water flow rate to the turbine, the hydropower charge rate is unpredictable because it is controlled by natural rain and stream flow, which are intermittent. The energy storage capacity of a hydropower reservoir equals the peak discharge rate (kW) multiplied by the number of hours required for the reservoir to empty at the peak discharge rate.

The PHS peak charge and discharge rates (Table S11) are equal to each other and limited in each country to the present-day discharge rate plus a fraction of the present penetration, determined as the ratio of preliminary plus pending permits to existing PHS in the U.S., plus a minimum value for countries with no PHS currently installed.

Another parameter needed is the demand response (DR) time limit. This is the maximum allowable number of hours a load can be delayed by being shifted forward in time before it must be met. It is an adjustable parameter in the model but is limited to 8 hours for all regions in this study. During each LOADMATCH timestep, if a flexible load subject to demand response cannot be met, the load is shifted forward one timestep (30 s). If a portion of the load subject to demand response still cannot be met during that timestep, that portion is shifted forward again, and so forth and so on. If, after 8 hours, the remaining load still cannot be met, it immediately becomes an inflexible load and must be met; otherwise, the model stops. Each load that is shifted forward in time in this way is tracked independently of loads that are shifted forward starting at different times to ensure no load is shifted forward more than the DR time limit allows.

Note S33. Order of Operations

In LOADMATCH, instantaneous demand must match instantaneous generation plus storage every timestep. Notes S34 and S35 discuss the order of operation of such matching in two parts. The first part concerns what to do with excess current generation when it exceeds current demand. The second discusses how to meet current demand when it exceeds current supply.

Note S34. Solutions When Current WWS Electricity or Heat Supply Exceeds Demand

This note discusses the steps taken when the current (instantaneous) supply of WWS electricity or heat exceeds the current electricity or heat demand (load). The total load, whether for electricity or heat, consists of flexible and inflexible loads. Whereas flexible loads may be shifted forward in time with demand response, inflexible loads must be met immediately.

If WWS instantaneous electricity or heat supply exceeds the instantaneous inflexible electricity or heat load, then the supply is used to satisfy that load. The excess WWS is then used to satisfy as much current flexible electric or heat load as possible.

If any excess electricity exists after inflexible and current flexible loads are met, the excess electricity is sent to fill electricity, heat, cold, or hydrogen storage. Electricity storage is filled first. Excess CSP energy goes to CSP electricity storage. Remaining instantaneous CSP electricity and excess electricity from other sources are used next to charge pumped hydropower storage followed by battery storage, cold water, storage, ice storage, hot water tank storage, and underground thermal energy storage. Remaining electricity is used to produce hydrogen. Any residual after that is shed.

Heat and cold storage are filled by using the excess electricity to run a heat pump to move heat or cold from the air, water, or ground to the thermal storage medium. Hydrogen storage is filled by using electricity in an electrolyzer to produce hydrogen and in a compressor to compress the hydrogen, which is then moved to a storage tank.

If any excess direct geothermal or solar heat exists after it is used to satisfy inflexible and flexible heat loads, it is used to fill either district heat storage (water tank and underground heat storage) or an individual home's hot water tank heat storage.

Note S35. Solutions When Current Load Exceeds WWS Electricity or Heat Supply

When current inflexible plus flexible electricity load exceeds the current WWS electricity supply from the grid, the first step is to use electricity storage (CSP, pumped hydro, hydropower, and battery storage, in that order) to fill in the gap in supply. The electricity is used to supply the inflexible load first, followed by the flexible load.

If electricity storage becomes depleted and flexible load persists, demand response is used to shift the flexible load to a future hour.

If the inflexible plus flexible heat load subject to storage exceeds WWS direct heat supply, then stored district heat (in water tanks and underground storage) is used to satisfy district heat loads subject to storage, and stored building heat (in hot water tanks) is used to satisfy building water heat loads. If stored heat becomes exhausted, then any remaining low-temperature air or water heat load becomes either an inflexible load (85%) that must be met immediately with electricity or a flexible load (15%) that can be met with electricity but can be shifted forward in time with demand response.

Similarly, if the inflexible plus flexible cold load subject to storage exceeds cold storage (in ice or water), excess cold load becomes either an inflexible load (85%) that must be met immediately with electricity or a flexible load (15%) that can be met with electricity but can be shifted forward in time with demand response.

Finally, if current hydrogen load depletes hydrogen storage, the remaining hydrogen load becomes an inflexible electrical load that must be met immediately with current electricity.

In any of the cases above, if electricity is not available to meet the remaining load, the simulation stops and must be restarted after increasing generation or storage.

Note S36. Energy Generation, Storage, and Transmission/Distribution Costs

The model calculates the cost of generating electricity and heat in each region based on capital costs, technology lifetimes, fixed and variable O&M costs; decommissioning costs, and a social discount rate (Table

S14). It also calculates the cost of short- and long-distance transmission and distribution (footnote of Table S14) and of storage (Table S13).

WWS generators have no fuel costs, except the water cost for hydrogen production by electrolysis. Whereas the study accounts for the cost of electricity used to run equipment such as heat pumps and electric arc furnaces, it does not account for the costs of the equipment or associated ducts (if any) or wires, to be consistent with the fact that it doesn't account for the cost of analogous equipment in the BAU case (e.g., gas heaters or fossil-fuel furnaces or their required ducts or pipelines).

Next, the reasons for using a social discount rate and some details of the hydrogen cost analysis are provided.

Note S37. Using the Social Discount Rate Rather than the Private Discount Rate

The social discount rate (SDR) is the discount rate used in a social-cost analysis. The social cost of an investment is the investment's direct cost plus its externality costs (e.g., health and climate costs). A social discount rate is used primarily when the costs and benefits of a project occur at different times and over more than one generation. Such projects are called intergenerational projects.

By contrast, the private discount rate (PDR) is the interest rate that banks will charge builders and consumers for taking out loans. Such loans may be used to pay for the construction of a power plant or to build a house. The PDR is also the opportunity cost of capital. In other words, it is the rate of return that can be obtained by investing capital in a market. Private discount rates are appropriate only for relatively short-term public projects that dollar-for-dollar crowd out private investment[109,110]. The private discount rate in 2019 in the United States was between 3 and 6%.

Social discount rates are smaller than private discount rates, because society, as a whole, cares more about the welfare of distant future generations than does the average consumer or investor, who is generally concerned with near-term impacts during his or her lifetime. As a result, social discount rates appropriately weigh the present value of future impacts higher than do private discount rates. The (incorrect) use of a relatively high private discount rate in the evaluation of long-term climate-change mitigation would undervalue future social benefits and thus bias present-day investments away from efforts that provide long-term benefits to society. In order to properly evaluate long-term costs and benefits from the perspective of society, the social discount rate must be used.

Moore et al.[110] reviewed accepted methods of estimating social discount rates and concluded,

> *…no matter which method one chooses, the estimates for the social discount rate vary…between 0 and 3.5 percent for projects with intergenerational impacts* (p. 809).

Drupp et al.[111] surveyed 197 experts and similarly found that 92% of them believe the social discount rate should be between 1% and 3%. OMB[112] also recommended 1% to 3%, which is the range adopted by Jacobson et al.[5] and here.

An analysis of the investment and environmental costs of transitioning the energy infrastructures of countries to 100% WWS between today and 2050 is a social-cost analysis. As such, it requires the use of a social discount rate of 2 (1-3)% (Table S14). Not only does such an analysis cover multiple generations of infrastructure, but it also accounts for the health and climate cost avoidance of such a transition. Note that the social discount rate applies to *all* components of the social-cost analysis, including the direct investment costs, because all costs are treated from the perspective of society.

Note S38. The Cost of Hydrogen Production, Compression, and Storage

Hydrogen is stored as a compressed gas to power on-board fuel cells for long-distance road, rail, and water transportation, and as a liquid for fuel cells to power aircraft for long-distance flights. Hydrogen is not used as part of this study for fuel cells to produce grid electricity due to the inefficiency of this process. Hydrogen is also not used here for any industrial combustion process because electrical arc furnaces, dielectric heaters, and induction furnaces are available for this task. When too much WWS electricity is available, some is used to

produce hydrogen by electrolysis and to compress and store the hydrogen. Hydrogen is then either stored or used immediately for transportation.

The costs of hydrogen production via electrolysis (including water cost), compression, and storage are derived as follows. First, Table S10 provides the average power (energy per year) required for hydrogen production from electrolysis and hydrogen compression in each region. This energy per year is converted into hydrogen produced per year assuming 53.37 kWh/kg-H_2 for electrolysis and 5.639 kWh/kg-H_2 for compression[52], for a total of 59.01 kWh/kg-H_2. Although these are older estimates for conversion efficiency, we use them to ensure we do not overestimate hydrogen production due to other uncertainties in the analysis. The resulting annual average power demand for hydrogen and hydrogen production rates, for all 143 countries, are 523 GW and 77.6 Tg-H_2/yr, respectively (Table S10).

Next, we size storage tanks equal to the resulting kg-H_2/year produced in each region (Table S10) multiplied by the ratio of the maximum number of days of hydrogen storage (Table S12) to the average number of days per year of simulation.

Electrolyzer costs are then calculated assuming a \$300-\$450/kW capital cost[113], a 10-15 year lifetime, a 50%-95% use factor, an annual operation and maintenance cost of 1.5% of capital cost[51], and an installation factor multiplied by capital cost of 1.2-1.3[114]. A social discount rate is used. The resulting electrolyzer cost is \$0.557 (0.195-0.918)/kg-H_2. Water costs for electrolysis are another \$0.00472-0.00944)/kg-H_2[52].

Compressor costs are calculated assuming a capital cost of \$400,000-\$515,000 for a compression rate of 33 kg-H_2/hour from 20 to 350 bars followed by dry running piston compressing up to 950 bars[114], compressor lifetime of 10-15 years, a use factor of 50%-95%, annual operation and maintenance cost of 1.5% of capital cost, and an installation factor multiplied by capital cost of 1.2-1.3[114]. The resulting compressor cost is \$0.372 (0.148-0.596)/kg-H_2.

Storage costs are calculated assuming a capital cost of \$450-550/kg-H_2[115], storage tank lifetimes of 30-50 years, annual operation and maintenance cost of 1.5% of capital cost, and an installation factor multiplied by capital cost of 1.2-1.3[114]. The resulting overall hydrogen storage cost varies by region, depending on the maximum storage required. For example, for the United States, it was \$1,11 (0.46-1.77)/kg-H_2-used (rather than stored), whereas for Africa, it was \$1.02 (0.40-1.65)/kg-H_2.

Note S39. Calculating Health Costs

Transitioning countries to WWS immediately reduces air pollution health problems. Fewer health problems result in cost savings due to lower hospitalization rates, fewer emergency room visits, fewer lost workdays, fewer lost school days, lower insurance rates, lower taxes, lower workman's compensation rates, and reduced loss of companionship and quality of life.

Air pollution causes premature mortality in several ways. It contributes to death from heart disease, stroke, chronic obstruction pulmonary disease (COPD), lower respiratory tract infection, lung cancer, and asthma. Common types of COPD are chronic bronchitis and emphysema. Common types of lower respiratory tract infections are the flu, bronchitis, and pneumonia.

In 2016, 56.9 million people died from all causes worldwide[116]. Table S15 shows that air pollution caused between 24% and 45% of the deaths for each of five out of the six leading causes of death. About 4.5 million people died prematurely from outdoor air pollution and 7.1 million, from indoor plus outdoor pollution in 2016[104]. Thus, about 12.5% of all deaths worldwide in 2016 were due to indoor plus outdoor air pollution, making it the second leading cause of death after heart disease. 20% of premature air pollution deaths are of children age five and younger. Figure 1 (main text) shows a distribution of most of the mortalities among 24 world regions encompassing 143 countries. These countries are home to about 96 percent of the mortalities. The China and India regions absorbed the brunt of the mortalities.

The Global Burden of Disease study[117] similarly estimated that about 5.5 (5.1 to 5.9) million deaths worldwide in 2013 were caused by outdoor plus indoor air pollution. Of these, 2.8 to 3.1 million were from outdoor $PM_{2.5}$,

0.16 to 0.27 million were from outdoor ozone, and 2.5 to 3.3 million were from indoor air pollution from solid fuel burning.

Burnett et al.[118] further calculated 8.9 (7.5 to 10.3) million deaths per year worldwide in 2015 due to outdoor plus indoor air pollution. They hypothesized that the additional deaths from air pollution they found may have been due to the fact that previous studies considered only a limited number of categories of death that air pollution contributes to.

The air pollution deaths in Table S15 are due almost entirely to combustion products of fossil fuels, biofuels, bioenergy, open biomass burning, and human-caused wildfires. The indoor mortalities are additionally due to the indoor burning of bioenergy (e.g., wood, dung, waste), coal, and gas for home heating and cooking, primarily in developing countries. A 100% WWS replacing BAU energy world will eliminate an estimated 90% of the indoor and outdoor air pollution deaths. Remaining deaths are still likely to arise due to pollution from open biomass burning, wildfires, and dust.

Because premature mortalities arising from a BAU energy infrastructure result in a social health cost to society, it is important to quantify the avoided cost of reducing such mortalities, related morbidities, and non-health costs due to air pollution. This is done next.

The total annual damage cost ($/y USD) of air pollution due to conventional fuels (fossil fuel and biofuel combustion and evaporative emissions) in a country is estimated as[5]

$$AP_{C,Y} = D_{C,Y} VOSL_{C,Y} F_1 F_2 \tag{S34}$$

where $D_{C,Y}$ is the air pollution premature mortality rate (deaths/y) in country C in target year Y, $VOSL_{C,Y}$ is the value of statistical life ($/death) in the country and for the target year, F_1 is the ratio of mortality plus morbidity (illness) costs to mortality costs alone, and F_2 is the ratio of health cost (mortality plus morbidity costs) plus non-health costs to health costs alone. Non-health costs include costs due to animal health impacts; lost visibility; reduced agricultural output; and corrosion to building materials and works of art. Table S16 gives low, medium, and high estimates of F_1 and F_2. These are held constant for all countries and years.

The premature mortality rate in a country in target year Y is projected from a base year (BYD) during which death rates from air pollution are available, with

$$D_{C,Y} = D_{C,BYD}\left(e^{\Delta A_C[Y-BYD]}\right)\left(\frac{P_{C,Y}}{P_{C,BYD}}\right)^{\kappa} \tag{S35}$$

where ΔA_C (Table S16) is the fractional rate of change per year in the air pollution death rate in country C due to emission controls, P is population, and κ is the change in exposed population per unit change in population (Table S16). Figure 1 shows the application of Equation S35 to 24 world regions encompassing 143 countries. It indicates that BAU mortalities may be less in 2050 than in 2016 in almost all regions despite higher populations in 2050. The reason is that improvements in BAU emission-reduction technologies between 2016 and 2050 outpace population growth. The only exception is in Africa, where population growth outpaces technology improvements, resulting in higher air pollution mortality in 2050 than in 2016.

The value of statistical life is a widely used metric determined by economists to assign the cost of reducing mortality risk. It is the value of reducing 1 statistical mortality in a population. For example, if the average person in a city of 100,000 is willing to pay $75 to reduce her or his mortality risk by 1/100,000th, the statistical value of reducing one mortality is $7.5 million. The value of statistical life is also determined from how much more employers pay their workers who have a higher risk of dying on the job.

The VOSL varies with time and in each country. An estimate of the variation of VOSL (USD $million per death in 2013 USD) in country C during year Y is[5]

$$VOSL_{C,Y} = VOSL_{US,Y}\left(T + \left[1-T\right]\left[\frac{G_{C,Y}}{G_{US,Y}}\right]^{\gamma_{GDP,US,BYV}\left(\frac{G_{C,Y}}{G_{US,BYV}}\right)^{\gamma_{GDP}}}\right) \quad \text{(S36)}$$

where

$VOSL_{US,Y}$ = VOSL in the U.S. in year Y (given in Table S16 for Y=2050);
T = fraction of the country's VOSL held constant at the U.S. VOSL for that year;
$G_{C,Y}$ = gross domestic product (GDP) per capita in the country in year Y;
$G_{US,Y}$ = U.S. GDP per capita in year Y (estimated in Table S16 for Y=2050);
$G_{US,BYV}$ = U.S. GDP/cap base year BYV for calculating VOSL (Table S16 for BYV=2006);
$\gamma_{GDP,US,BYV}$=elasticity of GDP per capita in base year BYV (Table S16 for BYV=2006);
γ_{GDP} = elasticity of the GDP per capita for all years (Table S16).

Low, mid, and high values of VOSL are derived from Equation S36 since Table S16 provides low, mid, and high values for each parameter in the equation.

The GDP per capita in Equation S36 is the GDP at purchasing power parity (PPP). Equation S36 and the corresponding values of T in Table S16 indicate that a small portion of the VOSL is assumed to be constant across all countries. This constant portion is the fraction of the VOSL that is independent of relative wealth, productivity or consumption. The equation also indicates that the VOSL is a function of change in income. In addition, the elasticity of the GDP per capita is itself a function of the GDP per capita ratio between the country and the U.S.

Equation S35 requires a premature mortality rate from indoor plus outdoor air pollution in a base year in each country. Here, we estimate such mortalities for the base year 2016 by multiplying country-specific total air pollution mortalities per 100,000 population from WHO[104] by population. Table S17 estimates the mortalities in the same countries in 2050 under the BAU scenario using the methodology just described. The table further quantifies the health cost of such mortalities in 2050 based on the application of Equation S34. The table indicates that, in 2050, an estimated 5.3 million people per year may die in the 143 countries examined in the BAU case. The resulting cost, averaged over all energy, is $0.169 (0.101-0.297)/kWh (USD 2013). The aggregate air pollution mortality, morbidity, and non-health cost in 2050 among the 143 countries is about $30 (17.9-52.7) trillion/yr (Figure 4 of the main text). This is calculated as the product of the cost per unit energy and the annual average end-use power demand in 2050 in the BAU case from Table S1, all multiplied by the number of hours per year.

Note S40. Calculating Climate Costs

The damage that carbon dioxide equivalent (CO_2e) emissions cause to the global economy through their impacts on climate is the social cost of carbon (SCC). Units of the SCC are U.S. dollars per metric tonne-CO_2e emissions. Climate change damage costs include costs arising from higher sea levels (coastal infrastructure losses), reduced crop yields for certain crops, more intense hurricanes, more droughts and floods, more wildfires and air pollution, more migration due to crop losses and famine, more heat stress and heat stroke, more disease of certain types, fishery and coral reef losses, and greater air cooling requirements, among other impacts. Only a portion of these costs are offset by lower heating requirements and higher yields for some crops.

The SCC of emissions is likely to increase over time as CO_2 and other warming agents accumulate in the atmosphere and temperatures continue to rise. The accumulation will accelerate as more people rise out of poverty in developing countries and consume energy faster than their predecessors. As such, the SCC is tied to the gross domestic product (GDP) of a country.

Van den Bergh and Botzen[119] argue that the lower bound of the SCC (in 2014) should be at least $125 per tonne-$CO_2$e. Moore and Diaz[120] found that incorporating the effect of climate change on the rate of economic growth can increase the SCC to between $200 and $1,000 per tonne-$CO_2$e. Burke et al.[121] similarly found that accounting for the long-term effects of temperature rise on economic productivity results in climate change damage estimates that are 2.5 to 100 times higher than those from earlier studies. Table S18 provides low, mid, and high estimates of the SCC in 2050 derived from these studies plus the estimated growth rates of the SCC. The mid value from the range, $500 per metric tonne-$CO_2$e in 2013 USD[5], is used to derive the BAU climate change cost in Table S17 from 2050 estimate of fossil-fuel CO_2 emissions by country. Averaged over all countries, this cost is 16.0 (9-34.1) $0.16 (0.09-0.341)/kWh (USD 2013). The aggregate climate damage in 2050 among the 143 countries is then $28.4 (16.0-60.5) trillion/yr (Figure 4 of the main text). This is calculated as the product of the cost per unit energy and the annual average end-use power demand in 2050 in the BAU case from Table S1, all multiplied by the number of hours per year.

This resulting BAU climate change cost may be low because it is calculated with the fossil-fuel CO_2 rather than CO_2e emissions. As such, it ignores the large impacts of black carbon, methane, nitrous oxide, halogens, and tropospheric ozone on climate, which together roughly equal the CO_2 effect. It also ignores biofuel and anthropogenic biomass burning CO_2 and CO_2e. Although some of the burned CO_2 returns to regrow plants and trees, it doesn't when permanent deforestation occurs, and none of the non-CO_2 chemicals regrow. Further, the CO_2 that does regrow stays in the atmosphere for 1-80 years before regrowth so causes warming during this period. As such, even if the SCC were too high, the BAU climate change cost would still likely be in the range of that estimated here.

Note S41. Results and Metrics

For each case in each of the 24 world regions, the model was run forward in time. Simulations were run for three years (3.15 million 30-s timesteps) from 2050 to 2052. For each region, the initial inputs were adjusted until a zero-load-loss solution was found among all timesteps, typically within 10 simulations. The model was then run another 4 to 20 times, with further adjustments, to find lower-cost solutions. Thus, multiple zero-load-loss solutions were obtained for each region, but only the lowest-cost solution is presented. Table S19 provides the ratio of the final nameplate capacities to the first-guess nameplate capacities, for each generator in each region. Table S20 provides the final nameplate capacities in each region. Table S21 provides the simulation-averaged capacity factors for each generator in each region. Figure S4 shows the full 3-year time series of WWS power generation versus load plus losses plus changes in storage plus shedding. For a portion of the time series, it also shows the breakdown of WWS power generation and a breakdown of load plus losses plus changes in storage plus shedding. The figure confirms no load loss at any time in any region.

Note S42. Costs of Energy Per Unit Energy and Capital Costs

Supply matched total load (end-use load plus changes in storage plus losses plus shedding) every 30 s for three years in all 24 regions encompassing the 143 countries. Table S22 and Figure 3 (main text) summarize energy private costs among all world regions.

The WWS cost per unit energy in each case includes the costs of new electricity and heat generation, short-distance transmission, long-distance transmission, distribution, heat storage, cold storage, electricity storage, and hydrogen production/compression/storage (Table S23).

In a 2050 WWS world, WWS energy private costs (costs of energy alone) are assumed to equal WWS energy social costs (energy private costs plus health and climate damage costs due to energy). The reason is that, in 2050, WWS generators, storage, and transmission will result in zero emissions while in use. Further, their production and decommissioning will also be free of energy-related emissions. The health and climate costs of zero emissions are zero.

The 2050 to 2052 all-energy WWS mean social cost per unit energy, when weighted by generation among all 24 regions is 8.96 ¢/kWh-all-energy (USD 2013) (Table S23). However, Figure 3 shows that the individual regional averages range from 6.3 ¢/kWh-all-energy (Iceland) to 13.1 ¢/kWh-all-energy (Israel). The largest portion of cost is generation, followed by transmission and distribution, electricity storage, hydrogen production, and thermal energy storage, respectively.

Figure 3 also indicates that the overall upfront capital cost of transitioning 143 countries while keeping the grid stable may be about $72.8 trillion (USD 2013). Individual regional ranges are $2.6 billion for Iceland to $16.6 trillion for China. The U.S. cost is about $7.8 trillion, and the Europe cost, about $6.2 trillion.

However, the upfront capital cost is not necessarily the relevant metric. A more useful metric is the aggregate annual energy cost in comparison with business-as-usual (BAU). An even more relevant metric is the WWS-to-BAU aggregate social cost ratio. Figure 4 (main text) illustrates these parameters.

The top left panel in Figure 4 provides the 2050 cost per unit energy for each region in the 100% WWS cases. It also shows, for comparison, the estimated cost (per unit energy) of energy, air pollution, and climate damage from the BAU case. The figure indicates that, whereas the private costs per unit energy of WWS and BAU energy alone are similar, the WWS social cost (energy plus health plus climate cost) per unit energy is only about 21% that of BAU.

Note S43. New Metrics

Multiplying the private cost per unit energy in the top left panel of Figure 4 by the end-use energy consumed per year (or by the annual average power) in the WWS and BAU cases, respectively, gives the aggregate annual private energy cost in each case. The result is shown in the top right panel of Figure 4. The figure indicates that, among 143 countries, the aggregate annual private energy cost in the WWS case is $6.83 trillion/yr and in the BAU case is $17.7 trillion/yr. The main difference is the 57.1% lower end-use energy consumption in the WWS case (Table 4, main text).

In comparison, the BAU aggregate annual social cost (A_{BAU}) (energy plus health plus climate cost) is $76.1 trillion/yr. The WWS aggregate annual social cost (A_{WWS}) is the same as the WWS aggregate annual private energy cost because WWS has no health or climate impact.

This leads to the **WWS-to-BAU aggregate social cost ratio** (**R_{ASC}**), which is the ratio of the WWS aggregate annual social cost to the BAU aggregate annual social cost. Mathematically, it is

$$R_{ASC} = A_{WWS}/A_{BAU} = R_{WWS:BAU-E} R_{BAU-S:E} R_{WWS:BAU-C} \quad \text{(S37)}$$

where $R_{WWS:BAU-E}$ is the WWS-to-BAU levelized cost of energy (cost per kWh) ratio, $R_{BAU-S:E}$ is the BAU energy-cost-per-kWh-to-social-cost-per-kWh ratio, and $R_{WWS:BAU-C}$ is the WWS-to-BAU end-use energy consumption (kWh/y or annual average kW) ratio. Based on the aggregate annual social costs in Figure 4, R_{ASC} is 9%. Thus, in terms of aggregate social costs (private plus health plus climate costs of energy), a WWS system costs only 9% of a BAU system each year.

Table 4 (main text) illustrates how to calculate the WWS-to-BAU aggregate social cost ratio using the second definition in Equation S37. The result is the same. The annual energy plus health plus climate cost in a 100% WWS region is 91% less than when the region is under BAU.

A related parameter is the **WWS-to-BAU aggregate private cost ratio**,

$$R_{APC} = R_{WWS:BAU-E} R_{WWS:BAU-C} \quad \text{(S38)}$$

which gives an indication of the aggregate private energy cost per year in a region in a WWS versus a BAU case. The 143-country aggregate private cost ratio from Table 4 is 39%. In other words, people in a region with 100% WWS pay 61% less for energy per year than when BAU energy is used.

A third parameter is the **WWS-to-BAU social cost per unit energy ratio,**

$$R_{SCE} = R_{WWS:BAU-E} R_{BAU-S:E} \quad \text{(S39)}$$

which gives an indication of the energy plus health plus climate cost per unit energy in a WWS case versus a BAU case. In the present example for 143 countries, the social cost per unit energy is 79% less in the WWS case than in the BAU case.

In island countries, such as in the Caribbean, the actual direct price paid for BAU electricity is a mean of about 33 ¢/kWh[122]. This price reflects, among other factors, the cost of transporting fuels to the islands and price hikes due to frequent supply shortages. Such high costs should not occur when WWS electricity, which is produced locally, is combined with storage.

The current 33 ¢/kWh BAU cost of energy per unit energy is 2.6 to 3.3 times the modeled cost of WWS energy replacing BAU energy for Haiti-Dominican Republic (9.62 ¢/kWh), Cuba (~12 ¢/kWh), and Jamaica (10.1 ¢/kWh) (Figure 3). In addition, the WWS-to-BAU energy consumption ratios in those three regions are 0.41, 0.56, and 0.48, respectively (Figure 4), so the aggregate private cost people will pay in a 100% WWS world will be 12 to 20 percent what they pay currently.

Table S23 also gives the overall cost of hydrogen in ¢/all-kWh-delivered electricity. The overall cost of H_2 in ¢/all-kWh-delivered is equal to the cost in ¢/kWh-to-H_2 multiplied by the fraction of delivered power used for hydrogen, derived from Table S10. The ¢/kWh-to-H_2 equals the \$/kg-H_2 divided by 59.009 kWh/ kg-H_2. These costs exclude electricity costs, which are included elsewhere in Table S23.

Table S24 summarizes the energy budget (total end use load, supply, changes in storage, and losses) for all 24 world regions. Statistics among all 24 world regions suggest the following. 72.2% of all energy produced or supplied from storage was used for end-use load; 6.7% was lost during short and long-distance transmission, distribution, and downtime; 2.7% was lost during transfer in and out of storage; and 18.4% was shed. Most storage losses occurred with UTES storage.

Of all end-use load, 9.65% was electricity or direct heat used for low-temperature heat subject to storage, 1.13% was electricity used for cold subject to storage, 6.01% was electricity used for hydrogen that was either stored or used immediately, and the rest (83.21%) was remaining electricity used to meet immediate inflexible demand or subject to demand response

Of all energy generated (for end-use load plus losses plus shedding plus changes in storage), among the 24 regions, 49.5% was generated by onshore plus offshore wind, 44.1% was generated by utility plus rooftop PV

plus CSP, 5.02% was generated by hydropower, 0.71% was generated by geothermal electricity, 0.26% was generated by wave electricity, 0.06% was generated by tidal electricity, 0.14% was generated by solar heat, and 0.14% was generated by geothermal heat.

Note S44. Land Requirements

Footprint is the physical area on the top surface of soil or water needed for each energy device. It does not include areas of underground structures. Spacing is the area between some devices, such as wind turbines, wave devices, and tidal turbines, needed to minimize interference of the wake of one turbine with downwind turbines. Spacing area can be used for multiple purposes, including rangeland, ranching land, industrial land (e.g., installing solar panels), open space, or open water. Table S25 provides estimated footprint and spacing areas per MW of nameplate capacity of WWS energy generation technologies considered here.

Applying the installed power densities in Table S25 to the nameplate capacity needed to provide grid stability from Table S20 gives the total land footprint and spacing areas required in each of the 24 regions encompassing 143 countries, as shown in Table S26 and Figure S5.

New land footprint arises only for solar PV plants, CSP plants, onshore wind turbines, geothermal plants, and solar thermal plants. Offshore wind, wave, and tidal generators are in water, so they don't take up new land, and rooftop PV does not take up new land. The footprint area of a wind turbine is relatively trivial (primarily the area of the tower and of exposed cement above the ground surface). Table S26 provides the footprint area required for each region.

The total new land area for footprint (before removing the fossil fuel infrastructure) required with 100% WWS is about 0.17% of the 143-country land area (Figure S6), almost all for utility PV and CSP. WWS has no footprint associated with mining fuels to run the equipment, but both WWS and BAU energy infrastructures require one-time mining for raw materials for new plus repaired equipment construction.

The only spacing area over land needed in a 100% WWS world is between onshore wind turbines. Figure S6 indicates that the spacing area for onshore wind to power 143 countries is about 0.48% of the 143-country land area.

Together, the new land footprint and spacing areas for 100% WWS across all energy sectors are 0.65% of the 143-country land area (Figure S6), and most of this land area is multi-purpose spacing land.

Note S45. Long-Term, Full-Time Jobs Created Versus Lost

A final metric discussed relevant to policy decision-making is net job creation and loss. A transition to WWS reduces fossil fuel, biofuel, bioenergy, and nuclear jobs. Such jobs include jobs in the mining, transporting, and processing of fuels as well as in the generation of electric power. Transitioning also reduces jobs in the building of internal combustion engines, gas water and air heaters, gas stoves, gas turbines, coal plants, pipelines, gas stations, gas storage facilities, and refineries.

However, a transition also creates jobs in building and installing solar PV panels, CSP plants, wind turbines, geothermal plants, tidal devices, and wave devices. It also creates jobs in the electricity, heat, cold, and hydrogen storage industries. More transmission lines will be needed in a WWS world, so jobs increase in that sector as well. Jobs are also needed installing battery charging stations and building electric vehicles, electric heat pumps, electric induction cooktops, electric lawn mowers, electric arc furnaces, electric induction furnaces, etc. Electric vehicles that need to be built include onroad passenger vehicles, non-road vehicles, trucks, buses, trains, ships, aircraft, agricultural machines, construction machines, and military vehicles.

Common tools for estimating the number jobs produced due to new electric power generation or transmission are the Jobs and Economic Development Impact (JEDI) models[123]. These models estimate the number of construction and operation jobs plus earnings due to building an electric power generator or transmission line. The models treat direct jobs, indirect jobs, and induced jobs.

Direct jobs are jobs for project development, onsite construction, onsite operation, and onsite maintenance of the electricity generating facility. Indirect jobs are revenue and supply chain jobs. They include jobs associated with construction material and component suppliers; analysts and attorneys who assess project feasibility and negotiate agreements; banks financing the project; all equipment manufacturers; and manufacturers of blades and replacement parts. The number of indirect manufacturing jobs is included in the number of construction jobs. Induced jobs result from the reinvestment and spending of earnings from direct and indirect jobs. They include jobs resulting from increased business at local restaurants, hotels, and retail stores and for childcare providers, for example. Changes in jobs due to changes in energy prices are not included. Energy price changes may trigger changes in factor allocations among capital, energy input, and labor that result in changes in the number of jobs.

Specific output from the JEDI models for each new electric power generator includes temporary construction jobs, permanent operation jobs, and earnings, all per unit nameplate capacity. A temporary construction job is defined as a full-time equivalent job required for building infrastructure for one year. A full-time equivalent (FTE) job is a job that provides 2,080 hours per year of work. Permanent operation jobs are full-time jobs that last as long as the energy facility lasts and that are needed to manage, operate, and maintain an energy generation facility. In a 100% WWS system, permanent jobs are effectively indefinite because, once a plant is decommissioned, another one must be built to replace it. The new plant requires additional construction and operation jobs.

The number of temporary construction jobs is converted to a number of permanent construction jobs as follows. One permanent construction job is defined as the number of consecutive 1-year construction jobs for L years to replace $1/L$ of the total nameplate capacity of an energy device every year, all divided by L years, where L is the average facility life. In other words, suppose 40 GW of nameplate capacity of an energy technology must be installed over 40 years, which is also the lifetime of the technology. Also, suppose the installation of 1 MW creates 40 1-year construction jobs (direct, indirect, and induced jobs). In that case, 1 GW of wind is installed each year and 40,000 1-year construction jobs are required each year. Thus, over 40 years, 1.6 million 1-year jobs are required. This is equivalent to 40,000 40-year jobs. After the technology life of 40 years, 40,000 more 1-year jobs are needed continuously each year in the future. As such, the 40,000 construction jobs are permanent jobs.

Table S27 provides an estimated number of permanent, full-time construction and operation jobs per MW of nameplate capacity for several electricity-generating and storage technologies and for transmission and distribution expansion. The total number of jobs produced in a region is nominally the new nameplate capacity of each electricity generator or storage device multiplied by the number of construction-plus-operation jobs per MW from the table.

The jobs per unit nameplate capacity in Table S27 are for the United States. Equivalent numbers can be derived for other countries as a function of energy output and GDP per capita in the other country versus the U.S. as described in Jacobson et al.[5]. As energy output increases, the number of jobs per MW of nameplate capacity decreases slightly because of economies of scale and efficiencies in the use of labor. Similarly, as GDP per capita increases, the number of jobs per MW of nameplate capacity decreases slightly because of a substitution of capital for labor.

Jobs losses due to a transition to WWS will include losses in the mining, transport, processing, and use of fossil fuels, biofuels, bioenergy, and uranium. Jobs will also be lost in the BAU electricity generation industry and in the manufacturing of appliances that use combustion fuels. In addition, when comparing the number of jobs in a BAU versus WWS system, jobs are lost due to *not* constructing BAU electricity generation plants, petroleum refineries, and oil and gas pipelines.

Table S28 estimates the number of permanent, full-time jobs created and lost due to a transition in 143 countries to 100% WWS by 2050. The table accounts for jobs in the electricity generation, storage, and transmission (including HVDC transmission for long distances) industries. However, it does not account for job creation in the manufacturing electric appliances or machines.

In terms of job losses, the table accounts for losses due to eliminating mining, transporting, processing, and consuming fossil fuels, biofuels, and uranium. However, it does not account for jobs lost in the manufacture of combustion appliances or machines. It does account for the retention of non-energy petroleum industry jobs (e.g., for lubricants, asphalt, petrochemical feedstock, and petroleum coke) and for jobs lost due to not building BAU infrastructure.

The table indicates that, whereas a transition may reduce the world workforce by almost 1% due to jobs losses in the fossil fuel, biofuel, and nuclear industries, it will more than make up for these losses with job increases in WWS electricity generation and transmission. In fact, a transition may increase the net number of long-term, full-time jobs created over lost by about 28.6 million among the 143 countries. As such, a transition to 100% WWS is expected not only to save consumers money by reducing energy, health, and climate costs, but also to create many more long-term, full-time jobs than lost in aggregate, worldwide.

Note S46. Uncertainties in Assumptions and Sensitivity Tests

One uncertainty, applicable to any grid integration model investigating the future, arises due to the inconsistency between load and resource data sets. The wind and solar data are derived from GATOR-GCMOM for the years 2050-2052, but the load data are based on 2010-2014 or 2030 data extrapolated to 2050-2052. Because both load and WWS supply data are country-specific, they are roughly consistent with each other on both diurnal and seasonal scales. For example, high heat loads occur during winter due to low temperatures. The climate model also predicts low temperatures during winter, and the resulting winds and solar fields are consistent with these low temperatures and the other meteorological conditions causing them. Thus, the same physical processes affecting wind and solar fields in the climate model affect loads on seasonal and diurnal scales.

Another type of uncertainty arises due to how LOADMATCH treats the potential mismatch between supply and demand that arises due to (a) scheduled or unscheduled maintenance of energy generators, (b) variability of load and WWS resources, (c) assuming perfect transmission, (d) not modeling transmission congestion, and (e) not modeling frequency regulation.

LOADMATCH treats these cases as follows.

First, because the WWS energy systems determined here for each world region contain thousands to hundreds of thousands of distributed wind turbines, solar arrays, and battery storage banks, their forced and unforced outages are assumed to be spread evenly over a year. Low, mean, and high estimates of this continuous loss are calculated as are transmission and distribution losses (Table S14).

However, by assuming that energy loss from a single down wind turbine equals the loss of energy available to consumers, we likely overestimate energy loss in the model. The reason is that, when a single wind turbine is down, all the other turbines in a wind farm receive and extract more kinetic energy because of lesser competition among turbines for the limited kinetic energy available, so the aggregate power loss among all

turbines is slightly less than the power lost to the down turbine. The impact of this is that our assumption that energy loss to consumers is proportional to down time of wind turbines slightly underestimates energy available to the system.

Second, uncertainties in load and WWS resources are accounted for substantially in the variable nature of the load data by country and over time and by modeling wind and solar resources over multiple years at high time resolution (30 seconds). In addition, different sets of loads and renewable resources are modeled here for 24 world regions, each for three years. Results are consistently stable despite very different climate and load conditions in each region. Results are also stable despite the fact that LOADMATCH has no knowledge of the load or generation data even one timestep ahead of time and is required to meet load 100% of the time, thus exceed the electric utility industry standard of a loss-of-load expectation (LOLE) of 1 day in 10 years. This indicates the risk to grid operators of the supply not matching demand with the simulated system in place may be relatively minor.

A third uncertainty arises due our assumption of a perfectly interconnected transmission system. Whereas, we account for transmission and distribution costs and losses, we assume that electricity can flow to where it is needed without bottlenecks. However, this concern is alleviated by the fact that almost half of the regions examined (Iceland, Cuba, Jamaica, Haiti/Dominican Republic, Israel, Japan, Mauritius, New Zealand, Philippines, South Korea, and Taiwan) have or could have, due to their small sizes, well-connected transmission and distribution systems. Stable, low-cost systems were found here for all those regions. As such, there is no reason to think that the United States, for example, broken up into multiple isolated or moderately-interconnected regions versus one completely-interconnected region can't also maintain a low-cost, stable 100% WWS grid.

In fact, many of the dozens of papers that have examined 100% renewable grids have treated transmission spatially and have found low-cost solutions. For example, Aghahosseini et al.[25] found stable, low-cost, time-dependent electric grid solutions when each North and South America were run on 100% renewables, and transmission flows were modeled explicitly among multiple lines.

Finally, while the present paper sacrifices spatial resolution to treat transmission explicitly, it treats time resolution (30 s) higher than other studies, aside from those using LOADMATCH, to date.

On a related note, although the impact of transmission congestion on reliability is not modeled explicitly, sensitivity tests were run in Figure S13 of Jacobson et al.[16] to check the impact on cost of different fractions of wind and solar power produced subject to long-distance transmission. The result was that, if congestion is an issue at the baseline level of long-distance transmission, increasing the transmission capacity will relieve congestion with only a modest increase in cost.

Another uncertainty arises due to the lack of modeling of frequency regulation. Traditionally, grid operators have increased frequency by increasing generation from gas, coal, oil, nuclear, or hydroelectric plants. In a WWS world, operators will increase frequency by increasing hydroelectric, geothermal, wind, and solar PV output as well as output from CSP storage, batteries, and pumped hydropower storage. Conversely, grid operators will reduce frequencies that are too high by reducing generation and storage or turning on artificial loads. In the case of wind turbines, an operator can increase generation by running some turbines in partial load mode such that, when a decrease in grid frequency occurs, the operator increases turbine output by varying blade pitch. Alternatively, the operator may control short releases of electricity from wind turbines to the grid[124]. Similarly, some solar PV plants can be run in slightly curtailed mode such that, when a decrease in grid frequency occurs, output is increased. Inverters can also be optimized to provide frequency control to the grid[125]. As such, we believe frequency regulation will be adjusted to work well with future WWS grids.

A further uncertainty relates to our projections of 2050 BAU and WWS energy demand. Whereas, we transitioned to WWS based on the EIA's reference (BAU) scenario of moderate economic growth, it is possible that growth will occur faster than EIA projects, resulting in the need for more WWS infrastructure

than in the reference WWS case. Whereas, additional WWS generators will result in more land use and higher aggregate costs, it will result in a greater aggregate private and social cost benefit and more jobs created relative to BAU than in the reference WWS scenario. The reason is that, with more economic growth than in the BAU reference case, more BAU fuels will be needed, resulting in more air pollution health and climate damage. Because BAU fuels are more expensive than is WWS energy, moving from BAU to WWS energy in the high-energy scenario will reduce energy, health, and climate costs more than in the reference scenario.

Other uncertainties arise due to uncertainties in energy, health, and climate costs. We attempt to capture these uncertainties by modeling low, mean, and high values of all such costs. Table S14, for example, shows low, mean, and high estimates of capital costs, operation and maintenance costs, decommissioning costs, lifetimes, and transmission/distribution/ downtime losses assumed here. Table S22 and Figure 3 provide the resulting low, mean, and high levelized private costs of energy per unit energy and private aggregate costs of energy for each world region. Table S18 provides the low, mean, and high estimated social costs of carbon, and Table S16 provides the parameters needed to calculate low, mean, and high air pollution costs. Table S17 provides the resulting low, mean, and high air pollution and climate costs per unit energy by country.

Another way to estimate uncertainty is to run sensitivity tests. Previously, Jacobson et al.[16] (in their Figure S7 to S19) showed the sensitivity of U.S. electricity cost using LOADMATCH to the maximum number of hours load can be shifted with demand response, the maximum number of hours of UTES and non-UTES storage, the maximum number of hours of hydrogen storage, the maximum charge rate of UTES and non-UTES storage, the percent of generated wind and solar that is subject to long-distance transmission, the maximum nameplate capacity of underground thermal energy storage, the roundtrip efficiency of ice storage, the roundtrip efficiency of pumped hydropower storage, the roundtrip efficiency of underground thermal energy storage, the round-trip efficiency of CSP with storage, and the percent of transportation load that is flexible.

For the present study, several additional sensitivity tests were run. First, a sensitivity test was run to examine the impact of the fraction of district heating/cooling in the U.S. on overall energy costs. Baseline fractions for all regions are given in Table S9. In LOADMATCH, only loads subject to district heating/cooling can be stored seasonally in underground thermal energy storage (for heat loads), water tank storage (for heat or cold loads), or ice storage (for cold loads). Thus, varying the fraction of thermal loads subject to district heating also varies the upper limit of these types of storage.

Increasing the U.S. fraction of all heating and cooling subject to district heating/cooling from the baseline of 0.2 to 0.9 reduced the levelized energy cost by about 3.4% compared with the baseline case. The reason was that, although more district heating increased heat and cold thermal energy storage costs, it reduced electricity storage costs (since with more district heating, less heat and cold were produced by heat pumps in individual buildings that were run on stored electricity). Further, more district heating allowed more excess electricity to be used to produce heat and cold, avoiding shedding of some excess electricity.

Another test was to eliminate U.S. underground thermal energy storage altogether without affecting any other type of thermal energy storage. This increased the levelized energy cost by 1.6% while keeping the grid stable. This result is consistent with the finding above that increasing the fraction of heating and cooling subject to district heating/cooling (thus increasing underground storage) reduces costs.

An addition sensitivity test was to eliminate stationary U.S. hydrogen storage by setting the number of days of hydrogen storage in Table S12 to zero. Hydrogen in the model was used only for fuel cells in some transportation. With no stationary storage, hydrogen was produced only on demand. Although that reduced hydrogen storage costs, it increased the need for more WWS generators, increasing the overall levelized cost of energy by 1.5%.

A final test was to eliminate demand response for high-temperature industrial processes (set $F_{flx,hti}$= 0). The default assumption was that 70% of such load was subject to demand response ($F_{flx,hti}$= 0.70). Eliminating the ability of industry to use demand response for high-temperature processes increased overall levelized energy costs by only 0.75% due to the need to install more WWS generators.

Supplemental Tables

Table S1. Factors to multiply BAU end-use energy consumption by in different IEA[46] (2019) energy categories to obtain equivalent WWS end-use energy consumption. They are the ratio of BAU work-output/energy-input to WWS work-output/energy-input, by fuel and sector.

	Residential		Comm./Govt.		Industrial		Transportation		Ag/For/Fishing		Military/other	
Fuel	Elec: fuel ratio	Extra effic-iency	Elec: fuel ratio	Extra effic-iency	Elec: fuel ratio	Extra effic-iency	Elec: fuel ratio	Extra Effic-iency	Elec: fuel ratio	Extra effic-iency	Elec: fuel ratio	Extra effic-iency
Oil	0.2[a]	0.84	0.2[a]	0.95	0.82[e]	0.98	.19/.46[f]	0.96	.19/.46[f]	0.96	.19/.46[f]	0.96
Natural gas	0.2[a]	0.81	0.2[a]	1	0.82[e]	0.98	.19/.46[g]	0.88	0.2[a]	0.91	0.2[a]	0.91
Coal	0.2[a]	1	0.2[a]	1	0.82[e]	0.97	.19[h]	0.96	0.2[a]	1	0.2[a]	1
Electricity	1[b]	0.77	1[b]	0.78	1[b]	0.92	1[b]	1	1[b]	0.78	1[b]	0.78
Heat for sale	0.25[c]	1.0	0.25[c]	1	0.25[c]	1	--	--	0.25[c]	1	0.25[c]	1
WWS heat	1[d]	1	1[d]	1	1.0[d]	1	--	--	1[d]	1	1[d]	1
Biofuels/waste	0.2[a]	0.87	0.2[a]	1	0.82[e]	1	.19[h]	0.96	0.2[a]	0.93	0.2[a]	0.93

Residential loads include electricity and heat consumed by households, excluding transportation.

Comm./Govt. loads include electricity and heat consumed by commercial and public buildings, excluding transportation.

Industrial includes energy consumed by all industries, including iron, steel, and cement; chemicals and petrochemicals; non-ferrous metals; non-metallic minerals; transport equipment; machinery; mining (excluding fuels, which are treated under transport); food and tobacco; paper, pulp, and print; wood and wood products; construction; and textile and leather.

Transportation loads include energy consumed during any type of transport by road, rail, domestic and international aviation and navigation, or by pipeline, and by agricultural and industrial use of highways. For pipelines, the energy required is for the support and operation of the pipelines. The transportation category excludes fuel used for agricultural traction, fuel for fishing vessels, and fuel delivered to international ships, since those are included under the agriculture/forestry/fishing category.

Agriculture/forestry/fishing loads include energy consumed by users classified as agriculture, hunting, forestry, or fishing. For agriculture and forestry, it includes consumption of energy for traction (excluding agricultural highway use), electricity, or heating in those industries. For fishing, it includes energy for inland, coastal, and deep-sea fishing, including fuels delivered to ships of all flags that have refueled in the country (including international fishing) and energy used by the fishing industry.

Military/other loads include fuel used by the military for all mobile consumption (ships, aircraft, tanks, on-road, and non-road transport) and stationary consumption (forward operating bases, home bases), regardless of whether the fuel is used by the country or another country.

Elec:fuel ratio (electricity-to-fuel ratio) is the ratio of the energy input of end-use WWS electricity to energy input of BAU fuel needed for the same work output. For example, a value of 0.5 means that the WWS device consumed half the end-use energy as did the BAU device to perform the same work.

Extra efficiency is the effect of the additional efficiency and energy reduction measures that we assume are used in WWS system beyond what are used in a BAU system, which is based on a moderate economic growth assumption by EIA[47]. For example, in the case of natural gas, oil, and biofuels for residential air and water heating, it is additional efficiency due to better insulation of pipes and weatherizing homes. For residential electricity, it is due to more efficient light bulbs and appliances. In the industrial sector, it is due to faster implementation of more energy efficient technologies than in the BAU case. The improvements are calculated as the product of (a) the ratio of energy use, by fuel and energy sector, of the EIA's *high efficiency all scenarios* (HEAS) case and their *reference* (BAU) case and (b) our estimates of slight efficiency improvements beyond those in the HEAS case.

Oil includes end-use energy embodied in oil products, including refinery gas, ethane, liquefied petroleum gas, motor gasoline (excluding biofuels), aviation gasoline, gasoline-type jet fuel, kerosene-type jet fuel, other kerosene, gas oil, diesel oil, fuel oil, naphtha, white spirit, lubricants, bitumen, paraffin waxes, petroleum coke, and other oil products. Does not include oil used to generate electricity.

Natural gas includes end-use energy embodied in natural gas. Does not include natural gas used to generate electricity.

Coal includes end-use energy embodied in hard coal, brown coal, anthracite, coking coal, other bituminous coal, sub-bituminous coal, lignite, patent fuel, coke oven coke, gas coke, coal tar, brown coal briquettes, gas works gas, coke oven gas, blast furnace gas, other recovered gases, peat, and peat products. Does not include coal used to generate electricity.

Electricity includes end-use energy embodied in electricity produced by any source.

Heat for sale is end use energy embodied in any heat produced for sale. This includes mostly waste heat from the combustion of fossil fuels, but it also includes some heat produced by electric heat pumps and boilers.

WWS heat is end use energy in the heat produced from geothermal heat reservoirs and solar hot water heaters.

Biofuels and waste include end use energy for heat and transportation from solid biomass, liquid biofuels, biogas, biogasoline, biodiesel, bio jet kerosene, charcoal, industrial waste, and municipal waste.

[a]The ratio 0.2 assumes electric heat pumps (coefficient of performance, COP = 3.2 to 5.2) replace oil, gas, coal, biofuel, and waste combustion heaters (COP = 0.80) for low temperature air and water heating in buildings. The ratio is calculated by dividing the COP of BAU heaters by that of heat pumps to give 0.15 to 0.25, where the low number is closer to ground-source heat pumps and the high number is closer to air-source heat pumps. The final ratio is just an average of the two.

[b]Since *electricity* is already end-use energy, there is no reduction in end-use energy (only in primary energy) from using WWS technologies to produce electricity.

[c]Since *heat for sale* is low-temperature heat, it will be replaced by heat from electric heat pumps (COP = 3.2 to 5.2) giving an electricity-to-fuel ratio of 0.19 (=1/5.2) to 0.31 (=1/3.2), or an average of 0.25. Heat for sale is also low-temperature heat in the industrial sector, so it is replaced in that sector with heat pumps as well.

[d]Since *WWS heat* is already from WWS resources, there is no reduction in end-use or primary energy upon a transition to 100% WWS for this source.

[e]The ratio 0.82 for industrial heat processes assumes electric resistance heaters, arc furnaces, induction furnaces, and dielectric heaters replace oil, gas, coal, biofuel, and waste combustion heaters. The industrial sector electricity-to-fuel ratio and extra efficiency measure factors are applied only after industrial sector BAU energy used for mining and processing fossil fuels, biofuels, bioenergy, and uranium (industry "own use") has been removed from each fuel sector. The amount of industry own use is determined in IEA[46] for each country and fuel sector.

[f]The electricity-to-fuel ratio for a battery-electric (BE) vehicle is 0.19; that for a hydrogen fuel cell (HFC) vehicle is 0.46. 2% of BAU energy in the form of *oil* in the *transportation* sector is used to transport fossil fuels, biofuels, bioenergy, and uranium. That BAU energy is eliminated in a 100% WWS world (no elimination is needed in the *agriculture/forestry/fishing* or *military/other* sectors). Of the remaining transportation, 76% is electrified. Thus, 76% is multiplied by the electricity-to-fuel ratio for BE vehicles to determine the WWS electricity used for BE transportation replacing oil and 24% is multiplied by the electricity-to-fuel ratio for an HFC.

[g]About 80% of *natural gas* energy in the transportation sector is used to transport fossil fuels, biofuels, bioenergy, and uranium (e.g., through pipelines or other means). That BAU energy is eliminated in a 100% WWS world. Of the remainder, 95% is electrified with BE vehicles and 5% is electrified with HFC vehicles.

[h]*Coal* is still used in the transportation sector in some industrial locomotives in China (where over 90% of all coal transportation occurs) and in a few other countries. About 50% of coal in the transportation sector is used to transport fossil fuels, biofuels, bioenergy, and uranium. That BAU energy is eliminated in a 100% WWS world. Of the remainder, which is used to transport other industrial goods, 100% will be electrified. Similarly, 100% of the *biofuels and waste* currently used in transportation will be electrified in 2050.

Table S2. 1st row of each country: estimated 2050 total annually-averaged end-use load (GW) and percentage of the total load by sector if conventional fossil-fuel, nuclear, and biofuel use continues from today to 2050 under a BAU trajectory. 2nd row of each country: estimated 2050 total end-use load (GW) and percent of total load by sector if 100% of BAU end-use all-purpose delivered load in 2050 is instead provided by WWS. The last column shows the percent reductions in total 2050 BAU load due to switching from BAU to WWS, including the effects of (a) energy use reduction due to the higher work to energy ratio of electricity over combustion, (b) eliminating energy use for the upstream mining, transporting, and/or refining of coal, oil, gas, biofuels, bioenergy, and uranium, and (c) policy-driven increases in end-use efficiency beyond those in the BAU case. This table is summarized in Table 2 of the main text. Note S28 defines the sectors.

Country	Scen-ario	2050 Total end-use load (GW)	Resid-ential percent of total end-use load	Com-mercial per-cent of total end-use load	Indus-trial per-cent of total end-use load	Trans-port per-cent of total end-use load	Ag/For/Fish-ing per-cent of total end-use load	Mil-itary/ other per-cent of total end-use load	(a) Percent change end-use load w/WWS due to higher work: energy ratio	(b) Percent change end-use load w/WWS due to eliminat-ing upstream	(c) Percent change end-use load w/WWS due to effic-iency beyond BAU	Overall percent change in end-use load with WWS
Albania	BAU	4.3	29	10.3	16.8	40.2	3.7	0				
	WWS	1.8	40	15.1	21.1	21.8	1.9	0	-42.07	-5.87	-9.03	-56.96
Algeria	BAU	143.6	17.2	0	20.8	57.4	0.4	4.2				
	WWS	39.6	21.6	0	37.8	32.9	0.8	6.9	-44.17	-21.27	-7.01	-72.45
Angola	BAU	29.6	44.7	5.9	14.3	35.1	0.1	0				
	WWS	9.6	37.6	3.4	33	25.9	0	0	-57.78	-1.84	-8	-67.62
Argentina	BAU	163.1	20.5	6.4	31.6	37.2	4.2	0				
	WWS	57.1	20.5	11.4	49.2	16.6	2.4	0	-39.1	-18.54	-7.32	-64.95
Armenia	BAU	4.9	36.3	9.8	12.2	36	1.3	4.3				
	WWS	1.6	38.3	14.9	27.7	11.8	1.3	6.1	-40.21	-16.62	-10.24	-67.07
Australia	BAU	214.5	10.5	11.8	43.2	32.5	2	0				
	WWS	93.6	12.8	19.5	48.3	18.4	1.1	0	-33.98	-16.1	-6.3	-56.38
Austria	BAU	49.1	21.4	9.8	30.5	36.9	1.4	0				
	WWS	21	18.8	13.1	44.7	22.3	1	0	-38.38	-12.1	-6.77	-57.25
Azerbaijan	BAU	20.2	39.9	8.1	24.5	24.2	3.2	0				
	WWS	7.3	37.7	14.6	28.1	16.8	2.7	0	-44.01	-10.48	-9.54	-64.03
Bahrain	BAU	17.5	14.3	9	53.2	23.3	0.1	0				
	WWS	9.2	20.2	13.3	55.9	10.6	0.1	0	-23.8	-16.3	-7.14	-47.24
Bangladesh	BAU	75.3	38.4	2.1	30.4	25.2	3.7	0.2				
	WWS	30.9	26.2	3.2	59.8	8.2	2.3	0.3	-40.35	-9.92	-8.66	-58.92
Belarus	BAU	37	29.3	12.9	31.3	22.3	4.3	0				
	WWS	12.4	27.1	18.8	35.8	14.8	3.5	0	-47.4	-13.37	-5.8	-66.58
Belgium	BAU	69.7	18.1	11.5	32.4	36.3	1.6	0.1				
	WWS	29.2	14.1	14.3	48	22.4	1.1	0	-43.39	-7.91	-6.81	-58.11
Benin	BAU	9.5	30.1	10.3	5.8	53.8	0	0				
	WWS	2.5	23.1	11.2	17.7	48	0	0	-65.84	-1	-6.4	-73.24
Bolivia	BAU	18.1	10.7	3	24.2	53.1	7	2				
	WWS	5.6	13.5	6.6	47.9	25.2	5.7	1.2	-42.66	-20.06	-6.07	-68.8
Bosnia and Herzegovina	BAU	8.2	33.2	11.6	26	28.8	0.3	0				
	WWS	3.5	37.7	15.4	29.9	16.7	0.3	0	-39.78	-10	-8.26	-58.05
Botswana	BAU	5.4	24.3	6	18.2	49.4	1.5	0.6				
	WWS	2.2	20.4	10.5	36.2	29.7	2.1	1.2	-50.74	-1.86	-7.62	-60.23
Brazil	BAU	593.2	8.6	5.1	42.7	39.2	4	0.3				
	WWS	279.1	10.6	8.1	59.4	18.2	3.1	0.6	-36.97	-10.53	-5.45	-52.95
Brunei Darussalam	BAU	5.3	8.9	10.7	45.3	34.6	0	0.5				
	WWS	1.5	21.1	28.5	21.8	28.3	0	0.3	-36.9	-28.62	-5.29	-70.81
Bulgaria	BAU	23	23.7	13	30	32	1.2	0.1				
	WWS	10	28.6	20.5	33.8	16.4	0.7	0	-37.1	-11.71	-7.69	-56.5

Cambodia	BAU	15.6	35	7.1	21.2	35.9	0.7	0				
	WWS	6.1	21.1	11.9	44.6	22	0.3	0	-52.71	-0.87	-7.44	-61.02
Cameroon	BAU	16.3	49.8	17.9	7.3	22.9	0.1	1.9				
	WWS	4.5	38.5	15.3	21.7	20	0.2	4.3	-63.55	-1.02	-8.04	-72.62
Canada	BAU	404.5	13.4	11.5	46.3	25.5	2.8	0.4				
	WWS	151.5	17.3	18.2	44	17.7	2	0.8	-33.31	-23.18	-6.05	-62.53
Chile	BAU	69.6	14.5	10.3	37.9	36.5	0.8	0.1				
	WWS	35	13.2	12.3	58.9	15	0.3	0.2	-33.89	-8.61	-7.19	-49.7
China	BAU	5,060.40	16.6	4	47.5	28	1.4	2.6				
	WWS	2,284.60	15.8	5	64.5	10.4	1.1	3.1	-32.65	-16.03	-6.17	-54.85
Taiwan	BAU	167.3	10.1	7.4	45.6	33.1	0.9	2.9				
	WWS	94.9	12	8.6	60.2	14.8	0.7	3.7	-30.51	-5.61	-7.16	-43.28
Colombia	BAU	79.9	14.7	4.6	34.6	38.4	1	6.7				
	WWS	29.3	17.5	8.4	46	22.4	0.7	5	-42.07	-15.32	-5.98	-63.37
Congo	BAU	4.8	48	0.9	4.1	46.9	0	0				
	WWS	1.2	41.9	0.7	11.8	45.5	0	0	-65.82	-1.56	-7.98	-75.36
Congo, Dem. Republic of	BAU	44.1	70.3	0.6	23.7	5.4	0	0				
	WWS	15.3	39	1.2	56	3.8	0	0	-56.12	-0.36	-8.9	-65.38
Costa Rica	BAU	8.7	12.4	10.7	19.8	54.8	1.7	0.7				
	WWS	4	17.6	16.8	35	28.6	1.5	0.4	-45.49	-1.5	-7.31	-54.3
Cote d'Ivoire	BAU	17.4	44.4	13.4	13.7	26.7	1.8	0				
	WWS	5.7	31.7	16.3	31.5	19.4	1	0	-57.37	-1.67	-8.2	-67.24
Croatia	BAU	14.9	34.3	13.7	20.9	28.7	2.4	0				
	WWS	5.8	33.6	21.9	25.2	18	1.3	0	-44.24	-7.86	-8.71	-60.81
Cuba	BAU	14.4	18.3	5	44	20	2.6	10.1				
	WWS	8.1	20.7	6.8	58.4	9.6	1.3	3.3	-33.14	-4.08	-6.88	-44.1
Cyprus	BAU	4.2	16.9	15.3	8.9	56.6	1.6	0.6				
	WWS	1.8	26.3	25.6	15	31	1.4	0.7	-46.18	-1.92	-8.36	-56.47
Czech Republic	BAU	43.5	26.4	12.6	34.1	24.7	2.1	0.1				
	WWS	17.5	21	16.8	43.5	17.3	1.3	0.1	-41.48	-11.55	-6.66	-59.69
Denmark	BAU	25.9	28.9	13.7	21.3	32	4.1	0				
	WWS	9.6	26.9	20.5	26.8	22.3	3.5	0	-47.76	-8.44	-6.64	-62.84
Dominican Republic	BAU	13.2	18.6	7.5	27.1	44.9	1.9	0				
	WWS	6.2	18.9	11	45.2	22.6	2.4	0	-42.15	-3.09	-7.6	-52.84
Ecuador	BAU	25.7	11.2	6.7	20	54.8	0.8	6.5				
	WWS	9.7	15.1	10.1	34.7	34.5	0.4	5.2	-50.74	-5	-6.31	-62.05
Egypt	BAU	186.9	20.7	7.2	26.8	41.4	2.3	1.5				
	WWS	83.7	27.7	12.5	38.7	18.3	2.2	0.6	-35.58	-11.38	-8.25	-55.21
El Salvador	BAU	5.5	17.1	8.3	17.7	55.6	0	1.3				
	WWS	2.3	18.5	13.3	33.8	32	0	2.4	-49.11	-1.96	-7.47	-58.55
Eritrea	BAU	1.2	70.6	8.4	3.6	17.4	0	0				
	WWS	0.3	58.8	13.5	11.2	16.4	0	0	-64.05	-0.64	-10.04	-74.73
Estonia	BAU	5.5	28.7	17.1	23.7	27.4	3.1	0				
	WWS	2	25	27.6	27.2	17.8	2.4	0	-46.04	-9.97	-7.25	-63.26
Ethiopia	BAU	79.3	83.1	2.4	4.6	8.9	0.5	0.5				
	WWS	17.9	68.4	4.8	16.5	9.4	0.4	0.4	-66.81	-0.23	-10.43	-77.47
Finland	BAU	42.2	22	12.8	43.2	18.4	2.4	1.3				
	WWS	21.7	19.2	14.9	54.3	9.6	1.4	0.5	-35.15	-6.97	-6.57	-48.68
France	BAU	251.6	26.9	17.5	22.1	30.6	2.5	0.4				
	WWS	112.4	25.3	23.3	29.7	19.8	1.7	0.2	-40.57	-5.86	-8.92	-55.34
Gabon	BAU	13.6	18.4	1.3	67.5	12.2	0.3	0.2				
	WWS	8.7	7.7	1.1	86.3	4.6	0.1	0.2	-32.04	-0.73	-3.59	-36.36
Georgia	BAU	8.6	31.7	13.2	13.7	37.8	0.5	3.1				
	WWS	3.4	25.8	20.4	27.9	19.6	0.4	6	-43.79	-6.59	-9.91	-60.29
Germany	BAU	366.4	24.3	16	30.5	29.2	0	0				
	WWS	155.2	19.2	19.2	43.2	18.4	0	0	-41.69	-8.39	-7.56	-57.64
Ghana	BAU	18.3	27.5	5.4	21.2	44.8	1.1	0				
	WWS	7.4	23.4	7.1	42.6	26.3	0.5	0	-50.82	-1.35	-7.21	-59.38
Gibraltar	BAU	5.4	0	0	0.1	99.4	0	0.5				
	WWS	1.3	0	0.1	0.2	98	0	1.7	-69.72	-1.88	-4.17	-75.78

Greece	BAU	33.4	21.5	13.4	26.1	36.8	1.2	1				
	WWS	13.9	26	23.2	27.2	21.3	1.9	0.4	-38.74	-11.74	-8.03	-58.51
Guatemala	BAU	19.2	48.6	4.4	10.1	36.9	0	0				
	WWS	5.7	36.5	9	25	29.6	0	0	-59.88	-1.84	-8.53	-70.25
Haiti	BAU	5	65.9	1.5	10.2	22.4	0	0				
	WWS	1.3	46.1	1.5	31.8	20.6	0	0	-64.6	-0.45	-8.91	-73.95
Honduras	BAU	9	36.9	7.8	18.3	36.2	0	0.7				
	WWS	3.6	26.8	12.7	38.3	21.8	0	0.3	-51.45	-0.69	-8.21	-60.35
Hong Kong, China	BAU	78.8	5.6	12.6	8.1	73.7	0	0				
	WWS	28.9	9.9	25.4	16.5	48.1	0	0.1	-54.63	-1.96	-6.79	-63.38
Hungary	BAU	30.9	33.2	11.9	27.4	24.3	3	0.2				
	WWS	12	24.7	14.5	41	17.4	2.3	0.2	-45.19	-8.36	-7.82	-61.36
Iceland	BAU	5.2	14.9	14.2	43.1	19.9	7.4	0.6				
	WWS	3	9.4	12.6	64.3	9.7	3.8	0.2	-34.2	-2.31	-5.83	-42.34
India	BAU	1,831.30	21.6	4.1	39.7	27.5	4.5	2.6				
	WWS	926.3	16.7	4.2	59.5	12.1	4.9	2.5	-36.59	-5.84	-6.99	-49.42
Indonesia	BAU	428.6	27.6	4.7	30	36.3	1.2	0.1				
	WWS	174.8	21	8.2	49	21	0.8	0	-46.72	-5.68	-6.81	-59.21
Iran, Islamic Republic of	BAU	436.2	22.5	4.9	37.6	30.6	4.2	0.2				
	WWS	178.2	17.3	5.9	57.3	14.6	4.5	0.5	-39.5	-12.48	-7.18	-59.15
Iraq	BAU	53.1	18.4	1.2	33.9	41.5	0	5				
	WWS	20.3	25.9	2.4	35.7	25.9	0	10.1	-40.5	-14.73	-6.47	-61.7
Ireland	BAU	17.7	22.1	13.2	23.1	39.7	1.9	0				
	WWS	7.6	19.9	17.1	39.6	22	1.4	0	-45.94	-3.38	-7.76	-57.08
Israel	BAU	25.9	15.5	14.4	27.4	37.8	1.3	3.6				
	WWS	12.8	24.5	21.9	30.1	18.3	2	3.2	-33.2	-9.1	-8.26	-50.56
Italy	BAU	217.4	24.4	13.2	24.3	36.1	1.9	0.1				
	WWS	83.2	19.2	20.3	35.6	23.5	1.5	0	-42.19	-11.58	-7.97	-61.74
Jamaica	BAU	4.7	6.9	4.4	36	50.6	2.1	0.1				
	WWS	2.3	8.7	2.3	61.1	24.9	2.9	0.1	-45.8	-1.01	-5.06	-51.87
Japan	BAU	372.4	16	20	35.1	27.4	1.2	0.3				
	WWS	178	17.3	23.2	42.6	16.1	0.6	0.1	-34.46	-10.13	-7.62	-52.21
Jordan	BAU	15.8	20.4	6.7	20.1	46.5	3.5	2.8				
	WWS	7.3	29.2	9.5	30.3	24	5.9	1.1	-41.82	-3.83	-8.07	-53.72
Kazakhstan	BAU	120.8	7.9	6.8	73	9.7	0.9	1.7				
	WWS	35.5	11.1	7.6	70.1	9	0.8	1.4	-32.58	-35.12	-2.96	-70.66
Kenya	BAU	36.9	56.2	1.1	10.6	31.5	0.2	0.3				
	WWS	10.5	39.9	3	30.3	26.4	0.1	0.2	-61.96	-0.79	-8.7	-71.45
Korea, Dem. People's Rep.	BAU	19.7	1.3	0	58.5	7.8	0	32.4				
	WWS	11.6	0.4	0	78.5	3.2	0	18	-34.76	-1.76	-4.56	-41.07
Korea, Republic of	BAU	316.7	10.9	15.6	42.6	28.8	1.5	0.5				
	WWS	155.2	8.6	21.5	55	13	1.6	0.2	-32.97	-10.74	-7.29	-51
Kosovo	BAU	2.9	42.4	11.5	18	26.6	1.5	0				
	WWS	1.3	44.1	12.4	28.1	14.1	1.3	0	-42.2	-3.07	-9.79	-55.06
Kuwait	BAU	66.2	15.3	5.9	54.8	24	0	0				
	WWS	30.5	24.6	9.9	53	12.4	0	0	-27.61	-20.3	-5.92	-53.83
Kyrgyzstan	BAU	7.3	44.4	7.9	11	33.5	2.5	0.7				
	WWS	3.3	56	7.5	16.5	17.9	1.6	0.6	-43.19	-2.21	-9.56	-54.95
Latvia	BAU	8.3	28.1	16.6	17.1	35	3.1	0				
	WWS	3.2	23.7	22.2	30.1	22.1	1.8	0	-51.95	-2.8	-6.7	-61.45
Lebanon	BAU	12	29.5	6.3	14.8	43.4	0	6.1				
	WWS	5.8	32.4	10.2	26.5	21.5	0	9.5	-40.85	-0.79	-10.2	-51.85
Libya	BAU	30.3	9.8	1.7	7.8	76.3	1	3.4				
	WWS	10.3	17.6	3.9	14.6	53.8	2.3	7.7	-56.76	-3.02	-6.35	-66.13
Lithuania	BAU	12.2	24.7	12.1	27.1	34.7	1.4	0.1				
	WWS	4.2	25.2	19.5	30.8	23.3	1.1	0.1	-47.46	-11.61	-6.04	-65.1
Luxembourg	BAU	6	12.5	11.8	18.1	57.2	0.5	0				
	WWS	2.3	9.7	15.9	36.5	37.6	0.2	0	-52.72	-2.65	-6.61	-61.98
Macedonia, Republic of	BAU	4	32	13.8	19.5	33.8	0.9	0				
	WWS	2	37.3	17.3	28.6	16.2	0.7	0	-37.28	-2.66	-9.84	-49.78

Malaysia	BAU	170.4	6.7	9.6	36.5	46.6	0.6	0				
	WWS	77.1	9.7	15.2	50.5	24.3	0.3	0	-39.21	-9.53	-5.99	-54.73
Malta	BAU	4.8	4.6	7	1.7	86.3	0.3	0.1				
	WWS	1.4	11	15.6	4.4	68.5	0.2	0.3	-62.36	-1.77	-5.8	-69.93
Mauritius	BAU	4.6	8.6	7.8	12.8	70.3	0.2	0.2				
	WWS	1.8	14.4	14.3	27.4	43	0.3	0.5	-52.86	-1.48	-6.66	-60.99
Mexico	BAU	315.7	12.6	4.9	38.6	39.2	2.8	1.9				
	WWS	131.3	14.9	6.9	50.3	22	2.3	3.6	-38.94	-13.48	-6.01	-58.42
Moldova, Republic of	BAU	5.5	45	10.9	15.5	26.2	2.2	0.2				
	WWS	2	37.6	14.9	29.5	16.6	1.3	0.1	-51.63	-2.68	-8.8	-63.11
Mongolia	BAU	8.5	22.7	7	32.6	22.6	1.9	13.2				
	WWS	3.3	19.5	4.5	51.4	13.7	1.2	9.7	-53.62	-3.54	-3.7	-60.86
Montenegro	BAU	1.5	40.9	14.5	13.7	30.4	0.5	0				
	WWS	0.8	42.6	20.7	21.3	15.1	0.3	0	-37.51	-1.81	-11.24	-50.56
Morocco	BAU	43.4	18.1	8.7	18.7	47.1	7.4	0				
	WWS	18.3	19.9	9.6	37	27.1	6.4	0	-49.45	-0.92	-7.35	-57.72
Mozambique	BAU	24	48.6	5.2	23.5	18.1	3.8	0.8				
	WWS	8.8	27.2	4.1	54.1	11.5	1.9	1.2	-54.5	-0.75	-7.88	-63.14
Myanmar	BAU	36.2	49.9	2.8	15.8	16.9	6.2	8.4				
	WWS	11.3	33.2	4	33.7	10.4	3.6	15.1	-54.62	-5.42	-8.67	-68.72
Namibia	BAU	5.3	4.7	0.1	9.9	47.3	18.6	19.4				
	WWS	1.9	2.2	0	22.5	30.8	9.2	35.2	-55.61	-0.88	-6.78	-63.28
Nepal	BAU	25.6	68.1	2.4	9.4	17.9	2.2	0.1				
	WWS	6.9	50.1	3.4	28.4	16	1.7	0.4	-63.29	-0.35	-9.48	-73.13
Netherlands	BAU	105.6	15.5	11.7	31.1	36.4	5.3	0				
	WWS	40.1	12.8	17.1	41.3	24.4	4.4	0	-45.37	-10.08	-6.6	-62.04
Curacao	BAU	6.4	0.9	0	27.6	70.6	0	0.8				
	WWS	1.4	0.7	0	17.7	78.7	0	2.9	-55.87	-19.41	-3.27	-78.55
New Zealand	BAU	32.4	10.5	11.5	39.8	33.7	4.4	0.1				
	WWS	17.6	12.6	15.2	53.7	14.9	3.5	0.1	-33.55	-5.19	-6.98	-45.72
Nicaragua	BAU	4.7	31.7	11.4	16.1	38.6	2.2	0				
	WWS	1.7	24.5	14.5	32.8	26.3	1.9	0	-54.39	-2.79	-7.71	-64.89
Niger	BAU	5.8	69.3	1.9	4.5	24.2	0	0				
	WWS	1.4	58.7	3.2	14.2	23.7	0.2	0	-65.25	-0.78	-9.62	-75.64
Nigeria	BAU	276.1	63.4	3.4	12.1	20.9	0	0.2				
	WWS	68	49.7	4.7	25.2	20.2	0	0.2	-62.66	-4.32	-8.41	-75.38
Norway	BAU	47	17.5	13.2	45.8	22.2	1.1	0.2				
	WWS	20.2	27.2	21.6	38.6	11.3	1.3	0.1	-24.03	-25.15	-7.78	-56.96
Oman	BAU	60.8	7.6	4.7	59.8	24.2	0.1	3.5				
	WWS	33.1	10.3	6.7	70.9	10.7	0.2	1.2	-29.97	-10.98	-4.67	-45.62
Pakistan	BAU	202.6	38.1	3.5	27.1	30	1	0.2				
	WWS	82.1	25.9	4.7	52.6	14.7	2	0.1	-45.85	-5.53	-8.08	-59.46
Panama	BAU	17.8	6.2	6.9	8.2	78.5	0.2	0				
	WWS	6	9.6	15.1	19.2	55.9	0.1	0	-58.91	-1.66	-5.87	-66.45
Paraguay	BAU	10.7	22.1	8.6	23.2	46.1	0	0				
	WWS	4.9	21.7	14.4	40.4	23.5	0	0	-44.78	-1.64	-7.54	-53.96
Peru	BAU	46.6	12.8	5.1	29.7	50.7	1.7	0				
	WWS	17.5	13.4	9.1	49.3	26.7	1.6	0	-42.29	-13.94	-6.28	-62.51
Philippines	BAU	90.8	17	11.8	24.6	45.4	1.3	0				
	WWS	40.5	17.8	15.4	41.1	24.3	1.4	0	-44.9	-3.18	-7.38	-55.45
Poland	BAU	119.2	24.9	13	29.5	28.5	4.1	0				
	WWS	44.6	19.9	19.9	39.7	18.3	2.4	0	-43.44	-13.09	-6.04	-62.56
Portugal	BAU	30.3	15.2	13.6	33.7	35.5	1.9	0.1				
	WWS	13.1	17.1	22.1	39.4	20	1.3	0.1	-37.81	-12.06	-6.97	-56.84
Qatar	BAU	70.4	7.2	2.4	68.9	20.5	0	1				
	WWS	24.4	15.4	5.4	62.8	14.1	0	2.2	-28.23	-33.28	-3.82	-65.33
Romania	BAU	47.9	31.9	9.1	31.7	25	1.5	0.8				
	WWS	18.3	26.3	12.4	43.6	16.2	1	0.4	-44.73	-9.87	-7.27	-61.87
Russian Federation	BAU	733.9	23.8	8.1	39.3	27.5	1.3	0				
	WWS	233	25.2	12.8	45.1	15.6	1.3	0	-41.26	-21.09	-5.89	-68.25

Saudi Arabia	BAU	334.7	14.1	7.9	41.8	36.2	0	0				
	WWS	174.7	20	11.7	51.7	16.5	0	0	-32.91	-8.13	-6.76	-47.8
Senegal	BAU	8.9	27.4	3.8	18.8	48.1	0.3	1.6				
	WWS	3.4	19.9	7.6	38.8	30.3	0.6	2.9	-53.11	-1.59	-7.3	-62.0
Serbia	BAU	19.1	37	10.8	28.3	22.3	1.5	0				
	WWS	8.9	41.2	13.6	32.5	11.8	0.9	0	-36.48	-7.85	-8.78	-53.11
Singapore	BAU	216.5	1.1	3.1	10.5	85.3	0	0				
	WWS	67.1	2.6	7.4	21.8	68.1	0	0.1	-60.72	-3.71	-4.56	-68.99
Slovak Republic	BAU	19.8	17	11.9	41.1	29	1	0				
	WWS	7.7	15	17	52.4	14.9	0.7	0	-34.52	-20.29	-6.39	-61.2
Slovenia	BAU	8	24.2	12	26	36.1	1.2	0.4				
	WWS	3.6	20.4	16.8	42	20.2	0.5	0.1	-43.33	-3.36	-7.78	-54.47
South Africa	BAU	231.2	13.8	6.2	44.3	32.1	2.3	1.3				
	WWS	104.6	13.5	8	58	17.7	1.7	1	-37.21	-11.86	-5.68	-54.75
South Sudan	BAU	1.9	17.1	4	9.5	65.2	4.1	0.1				
	WWS	0.5	19.9	9.9	3.5	61.8	4.8	0.1	-60.7	-8.39	-5.71	-74.79
Spain	BAU	165.3	15.6	12.4	29.4	40.1	2.3	0.2				
	WWS	65.7	18.3	19.4	34.8	25.5	1.7	0.3	-39.77	-13.6	-6.89	-60.26
Sri Lanka	BAU	28.7	22.7	4.8	23.8	47.5	0	1.2				
	WWS	11.8	17.3	7.8	46.9	27.5	0	0.5	-51	-1.39	-6.4	-58.79
Sudan	BAU	31.9	33.8	16.5	12.4	34.7	0.9	1.6				
	WWS	11.1	30.2	15.4	28.4	23.8	1.4	0.8	-56.82	-1.03	-7.31	-65.15
Suriname	BAU	1.2	15	7.1	16.9	47	13.9	0				
	WWS	0.5	22.4	11.8	32.8	26.9	6.1	0	-48.52	-2.33	-7.53	-58.38
Sweden	BAU	58.5	23.4	14.2	32.8	28.9	0.8	0				
	WWS	30.5	24.1	16.9	42.3	16.1	0.6	0	-34.02	-6.45	-7.43	-47.9
Switzerland	BAU	33.6	27.1	18	18	35.6	0.5	0.8				
	WWS	16	25.4	20.8	27.4	25.5	0.6	0.3	-40.56	-3.25	-8.6	-52.41
Syrian Arab Republic	BAU	14.7	19.3	4.3	32	36.7	4	3.7				
	WWS	6.8	23.7	4.9	46.8	19	1.6	4.1	-40.71	-5.95	-7.25	-53.91
Tajikistan	BAU	5.1	29	6.2	12.6	18	7.8	26.3				
	WWS	2.7	40.9	9.1	20.4	8.3	11.6	9.7	-35.79	-1.1	-10.58	-47.47
Tanzania, United	BAU	50.8	53.8	0.8	20.3	15.9	5.5	3.7				
	WWS	17	31.4	1.9	49.9	11.4	3.2	2.2	-58.31	-0.3	-8.03	-66.64
Republic of Thailand	BAU	266.1	7.9	7.3	39.6	41.9	2.8	0.6				
	WWS	123	9.3	11.5	58.9	18.2	1.1	1	-36.29	-11.58	-5.91	-53.78
Togo	BAU	5.5	47.6	11.2	4.7	36.2	0	0.3				
	WWS	1.4	40.8	10.7	14.9	32.7	0	0.9	-64.92	-0.7	-7.94	-73.56
Trinidad and Tobago	BAU	19.3	4.8	1.4	68.7	25.2	0	0				
	WWS	7.4	7.5	2.7	74.1	15.7	0	0	-30.91	-27.57	-3.28	-61.77
Tunisia	BAU	33.2	13.3	5.9	19.8	57.1	3.9	0				
	WWS	10.7	17.3	11.7	46.1	21.1	3.8	0	-37.85	-22.7	-7.36	-67.91
Turkey	BAU	163	21	13.1	32.9	29.7	3.3	0				
	WWS	71.5	19.4	16.6	45.8	15.3	2.9	0	-39.14	-9.9	-7.12	-56.16
Turkmenistan	BAU	41.1	2.3	33.5	19.2	27.6	1.3	16.1				
	WWS	8.7	7	31.6	21.8	19.6	4.8	15.1	-56.3	-19.02	-3.46	-78.79
Ukraine	BAU	109.4	35.7	10.5	32.5	18.2	3	0				
	WWS	43.1	30.8	13.6	42.5	10.9	2.1	0	-41.65	-11.05	-7.95	-60.65
United Arab Emirates	BAU	194.9	6.8	5.4	41.9	43.7	0	2.2				
	WWS	104.7	9.5	7.9	60.1	19.4	0	3.1	-38.02	-2.59	-5.66	-46.28
United Kingdom	BAU	233.7	26.9	13	25.1	33.6	0.7	0.7				
	WWS	88.8	24.6	19.6	31.7	23.1	0.7	0.3	-44.32	-9.46	-8.22	-62
United States of America	BAU	2,303.20	14.3	15	30.8	37.3	1.5	1.2				
	WWS	939.5	18.1	20	38	20.6	1	2.2	-40.09	-12.19	-6.93	-59.21
Uruguay	BAU	10.1	16.1	7.5	38.3	34.1	3.9	0				
	WWS	5.2	17.1	10.3	55.1	15.6	2	0	-37.46	-4.37	-6.5	-48.34
Uzbekistan	BAU	53.5	40.3	8.6	25.6	10.1	5.4	10				
	WWS	18.8	26.4	7.9	44.5	4.9	9.4	6.9	-46.33	-9.18	-9.27	-64.78
Venezuela	BAU	92.5	8.7	5.2	49.4	36.6	0.1	0				
	WWS	36.2	12.1	8.7	56.6	22.5	0.2	0	-37.17	-18.95	-4.7	-60.82

Vietnam	BAU	165.4	24.3	4.5	43.1	27.1	1.1	0				
	WWS	91.3	18.5	4.8	64.3	11.7	0.7	0	-36.62	-0.99	-7.2	-44.81
Yemen	BAU	5.6	31.7	4.2	17.4	41.7	1.6	3.4				
	WWS	2.3	40	4.8	26.6	24.6	0.7	3.3	-46.61	-4.21	-8.67	-59.48
Zambia	BAU	19.9	51.4	1.5	38.9	7.1	0.7	0.5				
	WWS	9.6	26.5	2	67	3.6	0.6	0.3	-43.39	-0.53	-8.08	-52
Zimbabwe	BAU	20.2	66.4	2.4	9.7	12.4	7.8	1.3				
	WWS	5.9	49.9	6.2	26.6	10.1	6.2	1	-60.15	-0.69	-9.99	-70.83
All countries	**BAU**	**20,255**	**19.1**	**7.8**	**37.4**	**32.3**	**1.9**	**1.5**				
	WWS	**8,693**	**17.7**	**10.5**	**52**	**16.2**	**1.7**	**1.8**	**-38.34**	**-12.1**	**-6.64**	**-57.08**

BAU values are extrapolated from IEA[46] data for 2016 to 2050 as calculated in Jacobson et al.[41]. Briefly, EIA's International Energy Outlook (IEO) projects energy use by end-use sector, fuel, and 16 world regions out to 2040 (EIA[47]) in a reference, or BAU, scenario that represents modest economic growth. This is extended to 2075 using a ten-year moving linear extrapolation. The EIA projections account for policies, population growth, economic and energy growth, some modest renewable energy additions, and modest energy efficiency measures and reduced energy use in each sector. EIA sectors and fuels are then mapped to IEA sectors and fuels, and each country's 2016 energy consumption by sector and fuel from IEA[46] is scaled by the ratio of EIA's 2050/2016 energy consumption by sector and fuel for each region. The transportation load includes, among other loads, energy produced in each country for international transportation and shipping. 2050 WWS values are estimated from 2050 BAU values assuming electrification of end-uses and effects of additional energy-efficiency measures beyond those in the BAU case.

Table S3. Efficiencies of individual factors affecting the overall plug-to-wheel efficiency of a battery-electric passenger vehicle and a hydrogen fuel cell vehicle. Low and high estimates of efficiency are given. See text for a discussion of the numbers.

	Battery-electric (BE) vehicle		Hydrogen fuel cell (HFC) vehicle	
Type of efficiency	Low efficiency	High efficiency	Low efficiency	High efficiency
Battery charging	0.80	0.96		
Battery discharging (to DC)	0.98	0.99		
Electrolyzer			0.738	0.738
Compressor			0.904	0.904
Leakage			0.99	0.997
Fuel cell producing DC electricity			0.5	0.7
Fuel cell latent heat loss			0.846	0.846
DC to AC inverter/wiring/power electronics	0.97	0.98	0.97	0.98
Electric AC motor	0.84	0.96	0.84	0.96
Overall plug-to-wheel	**0.64**	**0.89**	**0.23**	**0.37**

Table S4. Residential and commercial/government rooftop areas suitable for solar PV panels and potential nameplate capacity of suitable rooftop areas, for 143 countries. About 19.0% and 60.1% of potential residential and commercial, respectively, rooftop areas are proposed to be installed by 2050 in the roadmaps discussed in this paper.

Country	Residential roof-top area suitable for PVs in 2012 (km^2)	Potential nameplate capacity of suitable area in 2050 ($MW_{dc-peak}$)	Commercial/ govt. roof-top area suitable for PVs in 2012 (km^2)	Potential nameplate capacity of suitable area in 2050 ($MW_{dc-peak}$)	Country	Residential rooftop area suitable for PVs in 2012 (km^2)	Potential nameplate capacity of suitable area in 2050 ($MW_{dc-peak}$)	Commercial/ govt. rooftop area suitable for PVs in 2012 (km^2)	Potential nameplate capacity of suitable area in 2050 ($MW_{dc-peak}$)
Albania	25	6,004	17	4,179	Kyrgyzstan	77	18,454	31	7,318
Algeria	686	164,115	386	92,286	Latvia	12	2,906	22	5,176
Angola	758	181,328	278	66,594	Lebanon	22	5,220	11	2,713
Argentina	603	144,204	419	100,166	Libya	203	48,533	113	27,115
Armenia	28	6,640	16	3,817	Lithuania	23	5,477	43	10,303
Australia	907	216,896	544	130,210	Luxembourg	2	392	2	388
Austria	82	19,598	66	15,878	Macedonia, Rep. of	23	5,428	15	3,471
Azerbaijan	139	33,206	85	20,343	Malaysia	910	217,740	348	83,310
Bahrain	10	2,465	4	971	Malta	2	444	1	192
Bangladesh	1,359	325,065	195	46,667	Mauritius	22	5,313	6	1,512
Belarus	35	8,376	59	14,194	Mexico	1,940	464,094	972	232,424
Belgium	22	5,276	19	4,613	Moldova, Republic of	16	3,882	9	2,178
Benin	272	65,116	42	10,071	Mongolia	50	11,986	47	11,168
Bolivia	269	64,265	105	25,120	Montenegro	7	1,564	5	1,204
Bosnia & Herzegovina	39	9,383	25	5,912	Morocco	445	106,332	193	46,191
Botswana	62	14,850	34	8,013	Mozambique	717	171,550	100	24,026
Brazil	3,689	882,214	1,625	388,671	Myanmar	1,006	240,657	225	53,888
Brunei Darussalam	20	4,736	8	1,808	Namibia	43	10,359	21	4,955
Bulgaria	54	12,815	53	12,597	Nepal	430	102,939	55	13,112
Cambodia	350	83,804	59	14,005	Netherlands	32	7,542	53	12,676
Cameroon	503	120,274	114	27,250	Curacao	2	519	1	213
Canada	386	92,379	738	176,590	New Zealand	81	19,433	62	14,730
Chile	240	57,502	158	37,756	Nicaragua	109	26,107	33	7,785
China	15,139	3,620,836	9,211	2,203,033	Niger	841	201,125	68	16,210
Taiwan	292	69,728	127	30,384	Nigeria	5,005	1,196,999	1,326	317,102
Colombia	961	229,862	360	86,165	Norway	42	10,128	78	18,624
Congo	202	48,304	65	15,662	Oman	103	24,586	57	13,665
Congo, Dem. Republic	2,153	514,979	261	62,451	Pakistan	2,660	636,177	704	168,272
Costa Rica	67	15,973	28	6,625	Panama	110	26,395	44	10,419
Cote d'Ivoire	538	128,697	112	26,803	Paraguay	137	32,751	59	14,048
Croatia	44	10,603	35	8,327	Peru	687	164,421	271	64,899
Cuba	141	33,796	67	16,017	Philippines	2,131	509,569	532	127,334
Cyprus	30	7,294	10	2,420	Poland	203	48,538	357	85,291
Czech Republic	58	13,864	59	14,227	Portugal	139	33,348	70	16,851
Denmark	24	5,713	42	9,951	Qatar	17	4,112	8	1,994
Dominican Republic	92	22,071	42	10,061	Romania	180	43,053	88	21,156
Ecuador	436	104,181	140	33,473	Russian Federation	884	211,440	1,630	389,873
Egypt	1,963	469,527	692	165,527	Saudi Arabia	1,093	261,444	609	145,638
El Salvador	56	13,462	20	4,794	Senegal	325	77,673	60	14,378
Eritrea	152	36,406	15	3,667	Serbia	61	14,543	61	14,628
Estonia	6	1,392	11	2,654	Singapore	28	6,744	6	1,518
Ethiopia	3,839	918,272	272	64,989	Slovak Republic	42	10,094	39	9,436
Finland	30	7,088	75	17,831	Slovenia	17	4,035	19	4,503

France	542	129,641	475	113,722	South Africa	669	160,101	344	82,199
Gabon	92	22,051	39	9,254	South Sudan	492	117,663	54	12,995
Georgia	38	9,057	25	5,913	Spain	558	133,572	254	60,651
Germany	460	110,015	502	120,097	Sri Lanka	555	132,778	111	26,630
Ghana	521	124,622	124	29,632	Sudan	1,554	371,671	347	83,063
Gibraltar	0	13	0	6	Suriname	23	5,502	9	2,263
Greece	84	20,172	73	17,492	Sweden	48	11,472	88	21,123
Guatemala	298	71,360	87	20,878	Switzerland	80	19,031	68	16,159
Haiti	93	22,271	14	3,411	Syrian Arab Republic	316	75,661	138	33,124
Honduras	158	37,825	46	11,007	Tajikistan	114	27,290	32	7,742
Hong Kong, China	14	3,231	5	1,153	Tanzania, United Rep.	1,067	255,127	177	42,431
Hungary	72	17,150	72	17,284	Thailand	1,337	319,888	485	115,995
Iceland	3	742	6	1,422	Togo	193	46,188	20	4,792
India	19,163	4,583,398	5,075	1,213,892	Trinidad and Tobago	26	6,210	8	1,981
Indonesia	5,958	1,424,942	1,885	450,757	Tunisia	128	30,667	69	16,467
Iran, Islamic Republic	1,214	290,449	729	174,348	Turkey	895	214,161	616	147,450
Iraq	648	154,991	362	86,531	Turkmenistan	123	29,417	80	19,118
Ireland	48	11,564	55	13,271	Ukraine	222	53,207	192	45,818
Israel	79	18,813	36	8,685	United Arab Emirates	124	29,582	63	15,021
Italy	708	169,446	256	61,262	United Kingdom	194	46,350	330	78,966
Jamaica	41	9,916	13	3,068	United States	8,259	1,975,467	5,680	1,358,464
Japan	716	171,213	402	96,084	Uruguay	38	9,162	23	5,573
Jordan	64	15,194	35	8,343	Uzbekistan	326	77,918	164	39,322
Kazakhstan	398	95,246	364	87,141	Venezuela	665	158,993	258	61,755
Kenya	1,234	295,198	194	46,374	Vietnam	1,345	321,671	327	78,159
Korea, DPR	146	34,863	43	10,279	Yemen	658	157,446	158	37,786
Korea, Republic of	458	109,429	253	60,420	Zambia	590	141,177	144	34,452
Kosovo	12	2,840	7	1,732	Zimbabwe	344	82,380	47	11,123
Kuwait	28	6,769	15	3,492					
					World total	**112,000**	**26,759,000**	**46,600**	**11,152,000**

Table S5. Projected 2050 WWS annually averaged all-sector end-use power demand for 143 countries and initial estimates, for the start of the LOADMATCH simulations, of one mix of power generators that can meet that annually averaged demand. Annual average power is annual energy (GWh/yr) divided by the number of hours per year. The percentages for each country add to 100%. Multiply each percentage by the end-use demand to get the end-use demand met by each device. Divide the end-use demand for each device by its capacity factor to obtain nameplate capacity of each device needed to meet annually averaged demand. These numbers are adjusted in LOADMATCH in order to meet time-dependent demand. Table 3 compares the initial and final nameplate capacities, summed over all countries. Table S20 shows the final nameplate capacities by world region.

Country	2050 end-use demand (GW)	Onshore wind (%)	Offshore wind (%)	Wave (%)	Geo-thermal (%)	Hydro-electric (%)	Tidal (%)	Res PV (%)	Com/ gov PV (%)	Utility PV (%)	CSP (%)
Albania	1.840	21.01	6.83	0	0	43.54	0.11	5.85	13.01	6.83	2.82
Algeria	39.558	42.58	2.18	0.1	0	0.29	0.01	9.37	20.82	19.68	4.98
Angola	9.589	37.54	9.64	0.89	0	11.23	0.06	8.26	18.36	9.64	4.39
Argentina	57.149	38.77	9.95	0	1.4	7.9	0.02	8.53	18.95	9.95	4.53
Armenia	1.601	27.37	0	0	1.25	34.72	0	6.02	13.38	14.05	3.2
Australia	93.588	26.95	15.09	0.96	0.36	3.99	0.12	9.43	15.72	22.64	4.73
Austria	21.000	36.18	0	0	0	19.59	0	10.55	9.05	24.62	0
Azerbaijan	7.253	22.57	0	0	0	6.77	0	12.55	27.89	29.29	0.93
Bahrain	9.228	0.38	17	0	0	0	0.02	3.49	1.66	72.46	5
Bangladesh	30.916	7.08	7.12	0.62	0	0.32	0.1	23.18	9.68	46.96	4.95
Belarus	12.364	44.81	0	0	0.07	0.36	0	7.99	7.15	39.63	0
Belgium	29.194	7.96	22.64	0	0	0.19	0	1.82	1.61	65.78	0
Benin	2.532	33.97	13.74	1	0	0.46	0.03	11.78	20.36	13.74	4.93
Bolivia	5.640	32.66	0	0	18.65	4.96	0	7.18	15.97	16.76	3.82
Bosnia & Herzegovina	3.457	22.32	4.79	0	0	27.91	0.01	8.83	19.61	15.8	0.72
Botswana	2.155	42.75	0	0	0	0	0	9.41	20.9	21.95	5
Brazil	279.105	35.53	9.12	0.84	0	16.04	0.02	7.82	17.37	9.12	4.16
Brunei Darussalam	1.540	2.34	25.43	1	0	0	0.09	21.8	18.96	25.43	4.95
Bulgaria	9.987	40.28	11.05	0	0	10.46	0.02	9.47	17.68	11.05	0
Cambodia	6.069	25.56	12.91	0	0	8.34	0.04	11.07	24.59	12.91	4.58
Cameroon	4.470	39.08	3.56	0.92	0	7.61	0.05	8.6	19.11	16.5	4.57
Canada	151.542	32.74	8.87	0.73	2.63	23.6	0.29	7.6	14.67	8.87	0
Chile	35.034	36.71	10.06	0.87	3.8	9.41	0.06	8.62	16.13	10.06	4.29
China	2284.621	34.84	14.29	0.05	0.07	6.3	0.02	12.25	13.22	14.29	4.68
Taiwan	29.285	2.21	23.92	0.15	30.38	1.05	0.01	10.01	4.94	23.92	3.42
Colombia	1.191	34.42	8.83	0.81	0	18.3	0.38	7.57	16.83	8.83	4.03
Congo	15.252	41.43	10.63	0.93	0	6.91	0.09	9.11	20.25	10.63	0
Congo, Dem. Republic	3.965	39.8	0.86	0.07	0	6.82	0	9.5	17	21.3	4.66
Costa Rica	5.685	21.46	5.51	0.51	24.74	24.43	0.13	4.72	10.49	5.51	2.51
Cote d'Ivoire	5.822	35.38	10.99	0.93	0	6.67	0.05	9.42	20.94	10.99	4.62
Croatia	8.063	13.31	0	0	0	13.96	0.24	16.25	16.6	37.92	1.72
Cuba	1.366	42.12	10.81	1	0	0.35	0.13	9.27	20.59	10.81	4.93
Cyprus	1.828	8.39	22.11	1	0	0	0.19	18.95	22.3	22.11	4.94
Czech Republic	17.522	43.73	0	0	0	2.83	0	9.59	9.39	34.47	0
Denmark	9.614	44.46	22.1	1	0	0.04	0.17	6.66	3.47	22.1	0
Dominican Republic	6.233	22.1	12.74	0	8.85	3.92	0.08	10.92	24.28	12.74	4.36
Ecuador	9.744	33.38	3.09	0.79	0.33	20.23	0.56	7.34	16.32	14.05	3.9
Egypt	83.693	42.1	10.8	0	0	1.52	0.01	9.26	20.58	10.8	4.92
El Salvador	2.283	22.93	5.89	0.54	36.35	9.39	0.09	5.04	11.21	5.89	2.68
Eritrea	0.303	41.72	10.71	0	0	0	2.4	9.18	20.4	10.71	4.88
Estonia	2.013	44.68	19.88	0	0	0.18	0.53	8.53	6.33	19.88	0
Ethiopia	17.872	35.94	0	0	7.11	8.83	0	7.91	17.57	18.45	4.2
Finland	21.667	41.84	22.73	0	0	6.99	0.02	3.92	1.76	22.73	0
France	112.365	40.28	13.15	0.92	0.03	7.51	0.2	11.27	11.65	13.15	1.83
Gabon	8.666	15.66	23.34	0.99	0	1.44	0.04	20	15.2	23.34	0
Georgia	3.429	25.28	6.49	0	0	43.75	0.06	5.56	12.36	6.49	0
Germany	155.226	41.05	20.42	0.1	0.02	1.35	0.01	8.18	8.46	20.42	0
Ghana	7.445	22.97	13.25	0.92	0	8.44	0.04	11.36	25.24	13.25	4.53

Gibraltar	1.315	1.15	96.52	0.18	0	0	0.02	0.1	0.06	1.97	0
Greece	13.865	37.48	9.62	0.89	2.6	8.66	0.17	8.25	18.33	9.62	4.38
Guatemala	5.712	24.4	6.26	0.58	32.95	9.36	0.04	5.37	11.93	6.26	2.85
Haiti	1.309	20.57	17.47	0	0	1.73	0.4	14.97	22.48	17.47	4.89
Honduras	3.563	35.09	9.01	0.83	11.14	5.85	0.09	7.72	17.16	9.01	4.1
Hong Kong, China	28.850	0.07	97.2	0.14	0	0	0.01	1.09	0.5	0.98	0
Hungary	11.954	15.6	0	0	2.42	0.2	0	17.38	14.74	49.65	0
Iceland	2.983	40.69	1.22	0.42	25.54	31.65	0.44	0	0	0.04	0
India	926.295	36.92	6.23	0.06	0.02	2.12	0.02	12.03	15.86	21.85	4.89
Indonesia	174.839	15.79	15.28	0.94	4.45	1.34	0.03	13.1	29.11	15.28	4.66
Iran, Islamic Republic	178.193	28.92	12.56	0	0	2.68	0	14.67	14.63	21.67	4.87
Iraq	20.320	40.83	0.91	0	0	4.49	0	8.98	19.96	20.04	4.78
Ireland	7.591	43.9	17.45	0.99	0	1.4	0.07	14.96	3.78	17.45	0
Israel	12.820	8.21	15.61	0	0	0.03	0.02	21.26	11.01	38.87	5
Italy	83.169	37.31	13.97	0.35	0.98	7.79	0.02	11.97	9.1	13.97	4.54
Jamaica	2.268	5.4	24.03	0	0	0.4	0.17	20.6	20.4	24.03	4.97
Japan	177.969	10.24	31.55	0.93	0.69	5.84	0.28	11.78	7.14	31.55	0
Jordan	7.330	42.72	1.42	0	0	0.07	0.01	9.77	19.63	21.39	5
Kazakhstan	35.452	43.48	0	0	0	3.39	0	9.56	21.25	22.32	0
Kenya	10.530	35.46	9.1	0.84	12.92	3.27	0.03	7.8	17.34	9.1	4.15
Korea, DPR	11.620	36.13	13.74	0	0	17.55	1.73	11.78	4.91	13.74	0.43
Korea, Republic of	155.187	4.44	37.18	0	0	1.98	0.15	8.9	5.27	37.18	4.89
Kosovo	1.317	22.55	0	0	47.16	2.23	0	4.96	11.02	11.57	0.51
Kuwait	30.545	0.71	14.03	0	0	0	0.01	2.97	1.74	75.53	5
Kyrgyzstan	3.308	26.91	0	0	0	37.04	0	5.92	13.16	13.82	3.15
Latvia	3.202	34.8	12.52	0	0	22.58	0.09	10.73	6.77	12.52	0
Lebanon	5.762	2.62	27.44	0	0	1.74	0.03	14.87	7.95	40.43	4.91
Libya	10.270	42.73	10.97	0	0	0	0.05	9.4	20.89	10.97	5
Lithuania	4.249	44.5	14.28	0	0	1.1	0.02	12.24	13.58	14.28	0
Luxembourg	2.296	7.63	0	0	0	0.68	0	1.66	1.74	88.3	0
Macedonia, Rep. of	2.024	17.5	0	0	0	13.69	0	14.24	21.36	33.22	0
Malaysia	77.139	2.7	25.24	0.19	0	3.64	0.02	21.7	16.3	25.39	4.81
Malta	1.429	1.07	43.52	0.59	0	0	0.13	4.2	2.01	43.52	4.96
Mauritius	1.790	1.68	26.76	0.98	0	1.58	0.08	22.94	14.35	26.76	4.87
Mexico	131.278	39.44	10.12	0.93	2.96	3.84	0.02	8.68	19.28	10.12	4.61
Moldova, Republic of	2.035	44.32	0	0	0	1.51	0	13.45	9.32	31.39	0
Mongolia	3.340	44.87	0	0	0	0.28	0	9.87	21.94	23.03	0
Montenegro	0.765	24.55	8.06	0	0	36.18	0.24	6.91	15.36	8.06	0.64
Morocco	18.336	41.01	10.53	0.97	0	3.06	0.03	9.02	20.05	10.53	4.8
Mozambique	8.843	36.8	9.45	0.87	0	10.65	2.39	8.1	17.99	9.45	4.3
Myanmar	11.333	37.67	9.67	0.89	0	10.65	0.33	8.29	18.42	9.67	4.41
Namibia	1.939	39.59	10.16	0.94	0	6.22	0.24	8.71	19.35	10.16	4.63
Nepal	6.888	25.98	0	0	0	4.63	0	17.29	6.98	40.34	4.77
Netherlands	40.098	10.45	43.09	0	0	0.04	0.01	1.86	1.47	43.09	0
Curacao	17.566	1.31	42.9	0	0	0	0.16	5.38	2.36	42.9	4.99
New Zealand	1.667	32.42	10.38	0.77	9.32	13.83	0.25	8.89	9.97	10.38	3.79
Nicaragua	1.409	32.3	8.29	0.76	20.38	3.07	0.23	7.11	15.79	8.29	3.78
Niger	67.956	42.75	0	0	0	0	0	9.41	20.9	21.95	5
Nigeria	20.216	13.63	0	0.3	0	1.29	0.01	14.37	31.94	33.54	4.92
Norway	33.053	13.71	5.56	0.31	0	68.83	0.39	4.77	0.87	5.56	0
Oman	82.144	12.96	14.48	0.66	0	0	0.02	11.11	6.94	48.87	4.97
Pakistan	5.969	23.99	10.55	0.24	0	3.65	0	15.23	16.55	24.98	4.81
Panama	4.926	36.46	9.36	0.86	0	13.13	0.73	8.02	17.82	9.36	4.26
Paraguay	17.482	6.38	0	0	0	85.07	0	1.4	3.12	3.28	0.75
Peru	40.458	33.56	0.02	0.79	6.62	14.04	0.05	7.38	16.41	17.21	3.93
Philippines	44.642	7.68	15.13	0.6	11.24	3.95	0.27	12.97	28.82	15.13	4.2
Poland	13.064	44.64	11.46	0	0.2	0.58	0.01	9.82	21.83	11.46	0
Portugal	24.422	35.05	9	0.83	0.6	15.77	0.82	7.71	17.13	9	4.1
Qatar	18.269	0.56	21.02	0	0	0	0.01	2.31	1.32	69.77	5
Romania	233.033	37.45	12.02	0	0.44	16.32	0.01	10.31	11.42	12.02	0
Russian Federation	174.704	40.25	13.06	0.5	0.17	8.96	0.03	11.19	11.88	13.06	0.9
Saudi Arabia	3.366	42.75	3.84	0	0	0	0	11.28	14.65	22.48	5

Senegal	8.934	41.46	10.64	0.98	0	1.95	0.08	9.12	20.27	10.64	4.85
Serbia	67.141	13.71	0	0	0	11.01	0	16.5	20.29	38.5	0
Singapore	7.684	0.02	92.66	0	4.94	0	0	1.11	0.32	0.94	0
Slovak Republic	3.631	40.52	0	0	0	9.97	0	11.6	10.86	27.06	0
Slovenia	104.603	36.48	9.8	0	2.3	16.61	0.02	9.06	14.38	11.35	0
South Africa	0.476	42.19	13.7	1	0	0.3	0.01	11.74	12.43	13.7	4.93
South Sudan	65.686	42.75	0	0	0	0	0	9.41	20.9	21.95	5
Spain	11.835	37.36	11.92	0.88	0.06	11.34	0.33	10.21	11.61	11.92	4.37
Sri Lanka	11.108	39.66	10.18	0.94	0	6.25	0.04	8.73	19.39	10.18	4.64
Sudan	0.505	39.54	10.15	0	0	7.48	0.03	8.7	19.33	10.15	4.62
Suriname	30.479	34.89	8.96	0.82	0	17.08	0.48	7.68	17.06	8.96	4.08
Sweden	16.000	33.75	17.39	0	0	24.93	0.07	4.45	2.03	17.39	0
Switzerland	6.797	26.91	0	0	0	39.31	0	6.56	11.9	15.32	0
Syrian Arab Republic	94.907	38.67	9.93	0	0	9.51	0.02	8.51	18.91	9.93	4.52
Tajikistan	2.680	7.75	0	0	0	81.88	0	1.7	3.79	3.98	0.91
Tanzania, United Rep.	16.956	41.47	10.64	0.98	0	1.41	0.61	9.12	20.27	10.64	4.85
Thailand	122.975	3.75	18.81	0	0.08	1.31	0.01	22.28	15.65	33.18	4.93
Togo	1.442	26.62	18.51	0.89	0	1.2	0.04	15.86	13.48	18.51	4.89
Trinidad and Tobago	7.375	0.45	37.95	0.5	0	0	0.03	13.66	4.49	37.95	4.97
Tunisia	10.655	42.62	10.94	0	0	0.27	0.04	9.38	20.84	10.94	4.98
Turkey	71.476	35.48	2.08	0	1.33	15.65	0.02	7.81	17.35	16.13	4.15
Turkmenistan	8.725	42.75	0	0	0	0.01	0	9.4	20.9	21.94	5
Ukraine	43.052	42.41	15.21	0	0	5.73	0.02	13.04	8.39	15.21	0
United Arab Emirates	104.716	7.1	12.26	0	0	0	0.01	4.3	2.45	68.88	5
United Kingdom	88.812	20.29	32.66	0.96	0	0.93	2.81	5.41	4.27	32.66	0
United States	939.460	31.44	16.42	0.96	0.57	3.9	0.01	10.95	14.6	16.42	4.73
Uruguay	5.233	36.55	9.38	0.86	0	13.57	0.07	8.04	17.87	9.38	4.27
Uzbekistan	18.840	40.94	0	0	0	4.23	0	9.01	20.02	21.02	4.79
Venezuela	36.234	35.91	9.22	0.18	0	15.8	0.02	7.9	17.56	9.22	4.2
Vietnam	91.272	0.72	25.19	0.57	0	8.07	0.01	21.59	14.08	25.19	4.57
Yemen	2.263	13.21	16.31	0.97	3.12	0	0.26	13.98	31.06	16.31	4.78
Zambia	9.572	37.85	0	0	0.73	10.74	0	8.33	18.5	19.43	4.43
Zimbabwe	5.881	39.86	0	0	0	6.76	0	9.58	16.8	22.34	4.66
World total/average	**8,693**	**30.5**	**14.51**	**0.34**	**0.92**	**5.72**	**0.08**	**11.14**	**13.84**	**19.03**	**3.93**

Table S6. Several of the parameters treated in the LOADMATCH model simulations discussed here for matching supply with demand in 24 different world regions among 143 countries.

Parameter	Is the parameter treated?
Onshore and offshore wind electricity	Yes
Residential, Comm/Govt. PV electricity	Yes
Utility PV electricity	Yes
CSP electricity	Yes
Geothermal electricity	Yes
Tidal and wave electricity	Yes
Direct solar and geothermal heat	Yes
Battery storage	Yes
CSP storage	Yes
Pumped hydropower storage	Yes
Existing hydropower dam storage	Yes
Added hydropower turbines	No
Heat storage (water, underground)	Yes
Cold storage (water, ice)	Yes
Hydrogen storage	Yes
Hydrogen fuel cells for transportation	Yes
Battery-electric vehicles	Yes
District heating	Some
Electric heat pumps	Yes
Electrified industry	Yes
Losses from T&D, storage, downtime	Yes
Wind array losses	Yes
Perfect transmission interconnections	Yes
Costs of generation, T&D, storage,	Yes
Avoided cost of air pollution damage	Yes
Avoided cost of climate damage	Yes
Land requirements	Yes
Changes in job numbers	Yes

Table S7. 2050 annual average end-use electric plus heat load (GW) by sector and region after energy in all sectors has been converted to WWS. Instantaneous loads can be higher or lower than annual average loads.

Region	Total	Resi-dential	Com-mercial	Trans-port	Industrial	Agriculture/forest/fishing	Military/ other
Africa	482	139	33.4	96.9	198	7.57	6.98
Australia	93.6	12.0	18.2	17.2	45.2	1.00	0.00
Canada	151	26.2	27.6	26.9	66.7	3.04	1.25
Central America	154	24.7	12.1	36.9	72.7	3.15	4.85
Central Asia	151	33.78	11.3	18.7	79.4	4.45	3.49
China	2,328	364	122	252	1,489	25.9	74.3
Cuba	8.06	1.67	0.55	0.78	4.71	0.10	0.27
Europe	940	207	178	187	354	12.6	1.19
Haiti	7.54	1.78	0.70	1.68	3.23	0.15	0.00
Iceland	2.98	0.28	0.38	0.29	1.92	0.11	0.01
India	945	160	40.5	117	559	45.9	23.0
Israel	12.8	3.14	2.81	2.34	3.86	0.26	0.41
Jamaica	2.27	0.20	0.05	0.57	1.39	0.07	0.00
Japan	178	30.8	41.4	28.7	75.8	1.08	0.22
Mauritius	1.79	0.26	0.26	0.77	0.49	0.01	0.01
Mideast	678	121	62.2	109	366	11.0	8.18
New Zealand	17.6	2.21	2.68	2.63	9.43	0.61	0.02
Philippines	40.5	7.20	6.25	9.83	16.6	0.56	0.00
Russia	236	59.7	30.6	37.0	106	3.04	0.21
South America	489	62.5	43.5	94.0	274	11.2	3.79
Southeast Asia	583	87.6	52.1	140	296	4.80	3.18
South Korea	155	13.4	33.4	20.2	85.4	2.54	0.28
Taiwan	94.9	11.4	8.15	14.0	57.1	0.68	3.52
United States	939	170	188	194	357	9.62	20.9
Total 2050	8,693	1,542	917	1,408	4,521	149	156

Table S8. Fraction of 2010 annual average residential or commercial total energy (electricity plus heat) load that is heat load (the rest is electricity load) and fraction of annual average industry sector total energy load that is high-temperature heat load (the rest is electricity plus low-temperature heat load), by country or region. Heat load includes load for both air and water heating. From Jacobson et al.[1], derived from data in De Stercke[126].

Country or region	Fraction of total load in the residential or commercial sector that is low-temperature heat load (F_h)	Fraction of total load in the industrial sector that is high-temperature heat load (F_{ht})
Asia other	0.816	0.643
Australia	0.649	0.623
Brazil	0.660	0.658
Canada	0.723	0.640
China	0.857	0.637
Russia	0.881	0.721
France	0.757	0.578
Germany	0.804	0.588
India	0.856	0.705
Italy	0.816	0.581
Japan	0.665	0.594
LAM other	0.756	0.623
MEA other	0.743	0.709
Nigeria	0.963	0.836
OECD other	0.748	0.590
Poland	0.865	0.666
RE other	0.811	0.634
South Africa	0.746	0.503
United Kingdom	0.805	0.588
United States	0.689	0.643
World average	0.787	0.647

Asia other = Asia other than China and India; LAM other = Latin America other than Brazil; MEA other = Middle East and Africa other than South Africa and Nigeria; OECD other = countries in the Organization for Economic Cooperation and Development other than Australia, France, Germany, Japan, Italy, United Kingdom, United States; RE other = reforming economies in Eastern Europe and the former Soviet Union other than Poland and Russia.

Table S9. Parameters for modeling thermal energy use in different regions. F_{dh} is the fraction of total 2050 air heating, water heating, air conditioning, plus refrigeration load that is subject to district heating, thus thermal energy storage. F_{H2} is the fraction of total 2050 all-sector load (from Table S7) needed to produce, compress, and store hydrogen for transportation. The average across all regions is 6.01%, which represents 37.1% of the transportation load. The remaining values are the fractions of either residential, commercial, or industrial 2050 load (from Table S7) that are required for either air heating (F_{ah}), water heating (F_{wh}), air cooling (F_{ac}), refrigeration (F_{rf}), or high-temperature industrial processes (F_{ht}) in each region.

			Residential			Commercial				Industrial			
Region	F_{dh}	F_{H2}	F_{ah}	F_{wh}	F_{ac}	F_{ah}	F_{wh}	F_{ac}	F_{rf}	F_{ht}	F_{ah}	F_{ac}	F_{rf}
Africa	0.1	0.084	0.56	0.24	0.08	0.63	0.13	0.09	0.07	0.66	0.014	0.049	0.024
Australia	0.1	0.073	0.46	0.19	0.14	0.54	0.11	0.14	0.10	0.62	0.026	0.037	0.024
Canada	0.2	0.056	0.51	0.22	0.05	0.60	0.13	0.06	0.04	0.64	0.057	0.005	0.024
Central America	0.1	0.102	0.53	0.23	0.10	0.62	0.13	0.10	0.07	0.62	0.031	0.031	0.024
Central Asia	0.01	0.050	0.57	0.24	0.07	0.67	0.14	0.07	0.05	0.64	0.030	0.033	0.024
China	0.3	0.031	0.60	0.26	0.06	0.71	0.15	0.06	0.04	0.64	0.047	0.016	0.024
Cuba	0.15	0.035	0.53	0.23	0.10	0.62	0.13	0.10	0.07	0.62	0.000	0.062	0.024
Europe	0.5	0.067	0.54	0.23	0.07	0.64	0.14	0.08	0.06	0.59	0.055	0.007	0.024
Haiti	0.05	0.095	0.53	0.23	0.10	0.62	0.13	0.10	0.07	0.62	0.000	0.062	0.024
Iceland	0.92	0.033	0.52	0.22	0.00	0.62	0.13	0.00	0.00	0.59	0.062	0.000	0.024
India	0.1	0.049	0.60	0.26	0.06	0.71	0.15	0.06	0.04	0.71	0.009	0.053	0.024
Israel	0.2	0.079	0.46	0.19	0.14	0.54	0.11	0.14	0.10	0.62	0.015	0.048	0.024
Jamaica	0	0.105	0.53	0.23	0.10	0.62	0.13	0.10	0.07	0.62	0.000	0.062	0.024
Japan	0.1	0.054	0.47	0.20	0.13	0.55	0.12	0.13	0.10	0.59	0.039	0.024	0.024
Mauritius	0.05	0.187	0.52	0.22	0.10	0.61	0.13	0.10	0.08	0.71	0.000	0.062	0.024
Middle East	0.05	0.069	0.52	0.22	0.10	0.61	0.13	0.10	0.08	0.71	0.015	0.048	0.024
New Zealand	0.05	0.064	0.46	0.19	0.02	0.54	0.11	0.02	0.02	0.62	0.060	0.003	0.024
Philippines	0.05	0.102	0.57	0.24	0.07	0.67	0.14	0.07	0.05	0.64	0.000	0.062	0.024
Russia	0.5	0.051	0.62	0.26	0.04	0.73	0.15	0.04	0.03	0.72	0.059	0.003	0.024
South America	0.1	0.073	0.50	0.21	0.12	0.58	0.12	0.12	0.09	0.64	0.022	0.040	0.024
Southeast Asia	0.1	0.099	0.57	0.24	0.07	0.67	0.14	0.07	0.05	0.64	0.001	0.062	0.024
South Korea	0.15	0.054	0.52	0.22	0.10	0.62	0.13	0.10	0.07	0.59	0.049	0.013	0.024
Taiwan	0.15	0.059	0.57	0.24	0.07	0.67	0.14	0.07	0.05	0.64	0.007	0.055	0.024
United States	0.2	0.083	0.48	0.21	0.12	0.57	0.12	0.12	0.09	0.64	0.049	0.013	0.024

Table S10. Annual average WWS all-sector inflexible and flexible loads (GW) for 2050 by world region. "Total load" is the sum of "inflexible load" and "flexible load." "Flexible load" is the sum of "cold load subject to storage," "low-temperature heat load subject to storage," "load subject to demand response (DR)", and "load for H_2" production, compression, and storage (accounting for leaks as well). Annual average loads are distributed in time as described in the text. Thus, instantaneous loads, either flexible or inflexible, can be much higher or lower than annual average loads. Derivation of the loads is described in Notes S29-S31. Also shown is the annual hydrogen mass needed in each region, estimated as the load multiplied by 8,760 hr/yr and divided by 59.01 kWh/kg-H_2.

Region	Total end-use load (GW)	Inflex-ible load (GW)	Flex-ible load (GW)	Cold load subject to storage (GW)	Low-temp-erature heat load subject to storage (GW)	Load sub-ject to DR	Load for H_2 (GW)	H_2 needed (Tg-H_2/yr)
Africa	482	223.4	258.3	3.12	45.9	168.7	40.6	6.02
Australia	93.6	46.1	47.5	0.89	5.8	34.0	6.8	1.01
Canada	152	71.4	80.2	1.17	15.4	55.1	8.5	1.27
Central America	154	68.8	85.7	0.85	9.1	60.0	15.7	2.33
Central Asia	151	76.5	74.6	0.08	9.7	57.4	7.5	1.11
China	2,328	1,019	1,309	27.6	218.7	990.3	72.4	10.74
Cuba	8.06	3.91	4.15	0.10	0.61	3.16	0.29	0.04
Europe	939.7	365.9	573.8	25.3	191.3	293.8	63.3	9.40
Haiti	7.54	3.63	3.91	0.03	0.54	2.63	0.71	0.11
Iceland	2.98	1.18	1.80	0.04	0.56	1.10	0.10	0.01
India	945.0	434.5	510.5	5.63	57.8	401.0	46.1	6.84
Israel	12.8	6.17	6.65	0.28	1.48	3.87	1.01	0.15
Jamaica	2.27	1.01	1.26	0.00	0.05	0.97	0.24	0.04
Japan	178.0	92.2	85.8	1.74	14.4	60.0	9.6	1.43
Mauritius	1.79	0.69	1.10	0.01	0.10	0.66	0.33	0.05
Mideast	677.7	315.2	362.5	2.49	38.6	274.8	46.6	6.92
New Zealand	17.6	9.07	8.50	0.02	0.85	6.51	1.13	0.17
Philippines	40.5	18.9	21.5	0.14	2.9	14.3	4.1	0.61
Russia	236.5	85.1	151.4	3.60	52.1	83.7	12.0	1.78
South America	489	226	263	3.37	24.0	200.2	35.6	5.28
Southeast Asia	583	256	327	3.84	35.9	229.4	58.0	8.61
South Korea	155	78.1	77.0	1.56	11.8	55.3	8.4	1.25
Taiwan	94.9	42.7	52.2	0.96	5.6	40.1	5.6	0.83
United States	939	428	512	15	96	322	78	11.58
Total	**8,693**	**3,874**	**4,819**	**98**	**839**	**3,359**	**522**	**77.6**

37.1% of the transportation electric load is used to produce, compress, and store H_2. Annual-average H_2 loads are derived in Jacobson et al.[41]

Table S11. Aggregate (among all storage devices in a country or region) maximum instantaneous charge rates, maximum instantaneous discharge rates, and maximum energy storage capacities of the different types of electricity storage (PHS, CSP-PCM, batteries, hydropower), cold storage (CW-STES, ICE), and heat storage (HW-STES, UTES) technologies treated here, by region. Table S12 gives the maximum number of hours of storage at the maximum discharge rate. The product of the maximum discharge rate and hours of storage gives the maximum energy storage capacity.

	Africa			Australia			Canada			Central America		
Storage technology	Max charge rate GW	Max dis-charge rate GW	Max stor-age capac-ity TWh	Max charge rate GW	Max dis-charge rate GW	Max stor-age capac-ity TWh	Max charge rate GW	Max dis-charge rate GW	Max stor-age capac-ity TWh	Max charge rate GW	Max dis-charge rate GW	Max stor-age capac-ity TWh
PHS	27.8	27.8	0.389	10.7	10.7	0.150	16.6	16.6	0.233	6.0	6.0	0.084
CSP-elec.	45.9	45.9	--	13.0	13.0	--	0	0	--	21.1	21.1	--
CSP-PCM	74.1	--	1.037	21.0	--	0.294	0	--	0	34.0	--	0.476
Batteries	1,300	1,300	2.52	500	500	0.970	100	100	0.194	300.0	300.0	0.582
Hydropower	12.4	29.3	109	3.7	8.1	32.7	35.8	80.8	313	7.8	18.3	68.4
CW-STES	1.2	1.2	0.018	0.4	0.4	0.005	0.469	0.469	0.0066	0.3	0.3	0.005
ICE	1.9	1.9	0.026	0.5	0.5	0.007	0.703	0.703	0.0098	0.5	0.5	0.007
HW-STES	90.8	90.8	0.727	23.2	23.2	0.186	54.6	54.6	0.7646	27.1	27.1	0.216
UTES-heat	2.0	90.8	21.8	6.6	23.2	2.78	8.42	54.6	13.1	2.7	27.1	5.20
UTES-elec.	272.5	--	--	69.6	--	--	109	--	--	81.2	--	--
	Central Asia			China			Cuba			Europe		
PHS	12.0	12.0	0.168	116	116	1.62	3.0	3.0	0.042	197	197	2.76
CSP-elec.	11.6	11.6	--	296	296	--	1.7	1.7	--	21.1	21.1	--
CSP-PCM	18.7	--	0.262	478	--	6.69	2.8	--	0.039	34.0	--	0.475
Batteries	800	800	1.55	2,600	2,600	5.04	230	230	0.446	1,200	1,200	2.33
Hydropower	8.4	20.0	73.7	146	318	1,279	0.0	0.1	0.245	75.8	167.4	664
CW-STES	0.0	0.0	0.001	11.0	11.0	0.154	0.0	0.0	0.001	10.1	10.1	0.142
ICE	0.1	0.1	0.001	16.5	16.5	0.232	0.1	0.1	0.001	15.2	15.2	0.213
HW-STES	29.6	29.6	0.236	712	712	3.56	0.8	0.8	0.007	507	507	3.04
UTES-heat	0.0	29.6	24.8	351	712	137	0.0	0.8	0.138	168	507	122
UTES-elec.	29.6	--	--	1,425	--	--	2.5	--	--	760	--	--
	Haiti			Iceland			India			Israel		
PHS	2.0	2.0	0.028	0	0	0	28.8	28.8	0.403	10.0	10.0	0.140
CSP-elec.	0.9	0.9	--	0	0	--	233	233	--	2.1	2.1	--
CSP-PCM	1.5	--	0.021	0	--	0	375	--	5.26	3.4	--	0.047
Batteries	85.0	85.0	0.165	0	0	0	7,000	7,00	13.6	250	250	0.485
Hydropower	0.3	0.6	2.34	0.944	1.97	8.27	20.7	47.3	181	0.0	0.0	0.029
CW-STES	0.0	0.0	0.000	0.017	0.017	0	2.3	2.3	0.032	0.1	0.1	0.002
ICE	0.0	0.0	0.000	0.025	0.025	0	3.4	3.4	0.047	0.2	0.2	0.002
HW-STES	0.8	0.8	0.006	1.19	1.19	0.010	410	410	3.28	6.5	6.5	0.052
UTES-heat	0.0	0.8	0.018	0	1.185	0.000	7.8	410	88.6	3.5	6.5	2.343
UTES-elec.	1.5	--	--	0	--	--	1,230	--	--	19.5	--	--
	Jamaica			Japan			Mauritius			Mideast		
PHS	3.00	3.00	0.042	177	177	2.47	40.0	40.0	0.560	14.5	14.5	0.203
CSP-elec.	0.28	0.28	--	0	0	--	0.23	0.23	--	117	117	--
CSP-PCM	0.45	--	0.006	0	--	0	0.38	--	0.005	189	--	2.65
Batteries	15.0	15.0	0.029	590	590	1.15	5.00	5.00	0.010	2,400	2,400	4.66
Hydropower	0.01	0.02	0.080	10.4	22.3	91.1	0.03	0.06	0.247	18.7	44.7	164
CW-STES	0	0	0	0.7	0.7	0.010	0	0	0	1.0	1.0	0.014
ICE	0	0	0	1.0	1.0	0.015	0	0	0	1.5	1.5	0.021
HW-STES	0.44	0.44	0.004	53.0	53.0	0.424	0.21	0.21	0.002	153.4	153.4	1.23

UTES-heat	0.00	0.44	0.011	2.5	53.0	6.36	0.00	0.21	0.015	16.2	153	36.8
UTES-elec.	0.13	--	--	159	--	--	0.42	--	--	460	--	--
	New Zealand			**Philippines**			**Russia**			**South America**		
PHS	6.00	6.00	0.084	22.4	22.4	0.314	20.8	20.8	0.292	19.5	19.5	0.273
CSP-elec.	1.16	1.16	--	2.9	2.9	--	3.2	3.2	--	39.2	39.2	--
CSP-PCM	1.87	--	0.026	4.7	--	0.066	5.2	--	0.073	63.2	--	0.884
Batteries	50.0	50.0	0.097	80.0	80.0	0.155	40.0	40.0	0.078	10.0	10.0	0.019
Hydropower	2.43	5.35	21.3	1.6	3.6	14.0	22.4	50.2	196	73.3	166	643
CW-STES	0.01	0.01	0	0.1	0.1	0.001	1.4	1.4	0.020	1.3	1.3	0.019
ICE	0.01	0.01	0	0.1	0.1	0.001	2.2	2.2	0.030	2.0	2.0	0.028
HW-STES	2.15	2.15	0.017	2.9	2.9	0.024	160	160	1.60	98.8	98.8	0.790
UTES-heat	0	2.15	1.29	14.4	2.9	2.53	19.3	160	154	10.5	98.8	16.6
UTES-elec.	4.30	--	--	8.8	--	--	160	--	--	198	--	--
	Southeast Asia			**South Korea**			**Taiwan**			**United States**		
PHS	53.5	53.5	0.749	96.5	96.5	1.35	49.1	49.1	0.688	95.8	95.8	1.342
CSP-elec.	340	340	--	17.7	17.7	--	0.0	0.0	--	92.9	92.9	--
CSP-PCM	549	--	7.68	28.5	--	0.399	0.0	--	0.000	149.8	--	2.098
Batteries	950	950	1.84	1,900	1,900	3.69	1,900	1,900	3.69	3,300	3,300	6.402
Hydropower	15.9	36.3	140	3.1	6.5	26.9	1.0	2.1	8.712	36.7	80.1	321
CW-STES	1.5	1.5	0.022	0.6	0.6	0.009	0.4	0.4	0.005	6.0	6.0	0.084
ICE	2.3	2.3	0.032	0.9	0.9	0.013	0.6	0.6	0.008	9.0	9.0	0.126
HW-STES	104	104	0.829	38.0	38.0	0.304	41.1	41.1	0.329	324	324	2.59
UTES-heat	0.0	104	7.47	0.0	38.0	5.478	1.3	41.1	7.90	18.3	324	15.5
UTES-elec.	311	--	--	114	--	--	123	--	--	972	--	--

PHS = pumped hydropower storage; PCM = Phase-change materials; CSP=concentrated solar power; CW-STES = Chilled-water sensible heat thermal energy storage; HW-STES = Hot water sensible heat thermal energy storage; and UTES = Underground thermal energy storage (either boreholes, water pits, or aquifers). The peak energy storage capacity equals the maximum discharge rate multiplied by the maximum number of hours of storage at the maximum discharge rate. Table S12 gives maximum storage times at the maximum discharge rate.

Heat captured by CSP solar collectors can either be used immediately to produce electricity, put in storage, or both. The maximum direct CSP electricity production rate (CSP-elec) equals the maximum electricity discharge rate, which equals the nameplate capacity of the generator. The maximum charge rate of CSP phase-change material storage (CSP-PCM) is set to 1.612 multiplied by the maximum electricity discharge rate, which allows more energy to be collected than discharged directly. Thus, the maximum overall simultaneous direct electricity plus storage CSP production rate is 2.612 multiplied by the discharge rate. The maximum energy storage capacity equals the maximum electricity discharge rate multiplied by the maximum number of hours of storage at full discharge, set to 22.6 hours, or 1.612 multiplied by the 14 hours required for CSP storage to charge when charging at its maximum rate.

Hydropower can be charged only naturally, but its annual-average charge rate must equal at least its annual energy output divided by the number of hours per year. It is assumed simplistically here that hydro is recharged at that rate, where its annual energy output in 2050 is close to its current value. Hydropower's maximum discharge rate in 2050 is its 2018 nameplate capacity. The maximum storage capacity is set equal to the 2050 annual energy output of hydro.

The CW-STES charge/discharge rate is set equal to 40% of the maximum daily averaged cold load subject to storage, which itself is calculated as the maximum of Equation S32 during the period of simulation. The ICE storage charge/discharge rate is set to 60% of the same peak cold load subject to storage.

The HW-STES charge and discharge rates are set equal to the maximum daily-averaged heat load subject to storage, calculated as the maximum value during the period of simulation from Equation S29.

UTES heat stored in underground soil can be charged by either solar or geothermal heat or excess electricity. The maximum charge rate of heat to UTES storage (UTES-heat) is set to the nameplate capacity of the solar thermal collectors. In several regions, no solar thermal collectors are used. Instead, UTES is charged only with excess grid electricity. The maximum charge rate of excess grid electricity converted to heat stored in UTES (UTES-elec.) is set by trial and error for each country. The maximum UTES heat discharge rate is set to that of HW-STES storage, which is limited by the warm storage load.

Table S12. Number of hours or days of storage at the maximum discharge rate of each storage type (given in Table S11 for each region). The maximum discharge rate multiplied by the number of hours of storage equals the peak storage capacity in Table S11.

Region	(a) CSP (hr)	(b) PHS (hr)	(c) ICE (hr)	(d) HW-, CW-STES (hr)	(e) Batteries (hr)	(f) UTES (day)	(g) H_2 (day)
Africa	22.6	14	14	8	1.94	10	1
Australia	22.6	14	14	8	1.94	5	3
Canada	22.6	14	14	14	1.94	10	0
Central America	22.6	14	14	8	1.94	8	3
Central Asia	22.6	14	14	8	1.94	35	3
China	22.6	14	14	5	1.94	8	7
Cuba	22.6	14	14	8	1.94	7	8
Europe	22.6	14	14	6	1.94	10	5
Haiti	22.6	14	14	8	1.94	1	5
Iceland	22.6	14	14	8	1.94	0	1
India	22.6	14	14	8	1.94	9	6
Israel	22.6	14	14	8	1.94	15	9
Jamaica	22.6	14	14	8	1.94	1	5
Japan	22.6	14	14	8	1.94	5	5
Mauritius	22.6	14	14	8	1.94	3	8
Mideast	22.6	14	14	8	1.94	10	10
New Zealand	22.6	14	14	8	1.94	25	3
Philippines	22.6	14	14	8	1.94	36	10
Russia	22.6	14	14	10	1.94	40	28
South America	22.6	14	14	8	1.94	2	1
Southeast Asia	22.6	14	14	8	1.94	3	3
South Korea	22.6	14	14	8	1.94	6	8
Taiwan	22.6	14	14	8	1.94	6	5
United States	22.6	14	14	8	1.94	2	2

Table S13. Present value of mean 2019 to 2050 lifecycle costs of new storage capacity and round-trip efficiencies of the storage technologies treated here.

Storage technology	Present-value of lifecycle cost of new storage ($/kWh-max energy storage capacity)			Round-trip charge/store/ discharge efficiency (percent)
	Middle	Low	High	
Electricity				
PHS	14	12	16	80
CSP-PCM	20	15	23	99
LI Batteries	60	30	90	85
Cold				
CW-STES	6.5	0.13	12.9	84.7
ICE	36.7	12.9	64.5	82.5
Heat				
HW-STES	6.5	0.13	12.9	83
UTES	0.90	0.071	1.71	56

From Jacobson et al.[1], except with 2019 to 2050 mean battery costs updated[127].

PHS = pumped hydropower storage; CSP-PCM = concentrated solar power with phase change material for storage; LI Batteries = lithium ion batteries; CW-STES = cold water sensible-heat thermal energy storage; ICE = ice storage; HW-STES = hot water sensible-heat thermal energy storage; UTES = underground thermal energy storage (modeled as borehole). PHS efficiency is the ratio of electricity delivered to the sum of electricity delivered and electricity used to pump the water.

Storage costs per unit energy generated in the overall system of each storage technology are calculated as the product of the maximum energy storage capacity (Table S11) and the lifecycle-averaged capital cost of storage per unit maximum energy storage capacity (this table), annualized with the same discount rate as for power generators (Table S14), but with 2050 storage lifetimes of 17 (12 to 22) years for batteries and 32.5 (25 to 40) years all other storage, all divided by the annual average end-use load met.

The CSP-PCM cost is for the PCM material and storage tanks. The CSP-PCM efficiency is the ratio of the heat available for the steam turbine after storage to the heat from the solar collector that goes into storage. The additional energy losses due to reflection and absorption by the CSP mirrors (45% of incident solar energy is lost to reflection) and due to converting CSP heat to electricity (71.3% of heat is wasted and only 28.7% is converted to electricity) are accounted for in the CSP efficiency without storage. Battery efficiency is the ratio of electricity delivered to electricity put into the battery. CW-STES and HW-STES efficiencies are the ratios of the energy returned as cooling and heating, respectively, after storage, to the electricity input into storage. The UTES efficiency is the fraction of heated fluid entering underground storage that is ultimately returned during the year (either short or long term) as air or water heat for a building.

Table S14. Parameters for determining costs of energy from electricity and heat generators.

	Capital cost new installations ($Million/MW)	O&M Cost ($/kW/yr)	Decom-missioning cost (% of capital cost)	Lifetime (years)	TDM losses (% of energy generated)
Onshore wind	1.27 (1.07-1.47)	37.5 (35-40)	1.25 (1.2-1.3)	30 (25-35)	7.5 (5-10)
Offshore wind	1.86 (1.49-2.24)	80 (60-100)	2 (2-2)	30 (25-35)	7.5 (5-10)
Residential PV	2.97 (2.65-3.28)	27.5 (25-30)	0.75 (0.5-1)	44 (41-47)	1.5 (1-2)
Commercial/government PV	2.06 (1.80-2.31)	16.5 (13-20)	0.75 (0.5-1)	46 (43-49)	1.5 (1-2)
Utility-scale PV	1.32 (1.16-1.49)	19.5 (16.5-22.5)	0.75 (0.5-1)	48.5 (45-52)	7.5 (5-10)
CSP with storage[a]	4.84 (4.42-5.26)	50 (40-60)	1.25 (1-1.5)	45 (40-50)	7.5 (5-10)
Geothermal for electricity	3.83 (2.47-5.18)	45 (36-54)	2.5 (2-3)	45 (40-50)	7.5 (5-10)
Hydropower	2.81 (2.38-3.25)	15.5 (15-16)	2.5 (2-3)	85 (70-100)	7.5 (5-10)
Wave	4.01 (2.74-5.28)	175 (100-250)	2 (2-2)	45 (40-50)	7.5 (5-10)
Tidal	3.57 (2.85-4.29)	125 (50-200)	2.5 (2-3)	45 (40-50)	7.5 (5-10)
Solar thermal for heat	1.22 (1.12-1.33)	50 (40-60)	1.25 (1-1.5)	35 (30-40)	3 (2-4)
Geothermal for heat	3.83 (2.47-5.18)	45 (36-54)	2 (1-3)	45 (40-50)	7.5 (5-10)

Capital costs (per MW of nameplate capacity) are an average of 2019 and 2050. 2050 costs are derived in Jacobson et al.[41], which uses the same methodology as in Jacobson et al.[5]. Remaining values are the same as in Jacobson et al.[1]. O&M=Operation and maintenance. TDM = transmission/distribution/maintenance. TDM losses are a percentage of all energy produced by the generator and are an average over short and long-distance (high-voltage direct current) lines.

Short-distance transmission costs are $0.0105 (0.01-0.011)/kWh. Distribution costs are $0.02375 (0.023-0.0245)/kWh. Long-distance transmission costs are $0.00406 (0.00152-0.00903)/kWh (in USD 2013) (Table S28 of Jacobson et al.[3]), which assumes 1,200 to 2,000 km lines. It is assumed that 30% of all annually-averaged electricity generated is subject to long-distance transmission in all regions except Cuba, Haiti, Iceland, Israel, Jamaica, Mauritius, South Korea, and Taiwan (0%); New Zealand (15%); and Central America, Japan, and the Philippines (20%).

The discount rate used for generation, storage, transmission/distribution, and social costs is a social discount rate of 2 (1-3)%.

[a]The capital cost of CSP with storage includes the cost of extra mirrors and land but excludes costs of phase-change material and storage tanks, which are given in Table S13. The cost of CSP with storage depends on the ratio of the CSP storage maximum charge rate plus direct electricity use rate (which equals the maximum discharge rate) to the CSP maximum discharge rate. For this table, for the purpose of benchmarking the "CSP with storage" cost, we use a ratio of 3.2:1. (In other words, if 3.2 units of sunlight come in, a maximum of 2.2 units can go to storage and a maximum of 1 unit can be discharged directly as electricity at the same time.) The ratio for "CSP no storage" is 1:1. In our actual simulations and cost calculations, we assume a ratio of 2.61:1 for CSP with storage[1] and find the cost for this assumed ratio by interpolating between the "CSP with storage" benchmark value and the "CSP no storage" value in this table.

Table S15. Leading causes of death worldwide in 2016. Also shown are the percentage and number of deaths in each category due to outdoor plus indoor air pollution and, separately, outdoor air pollution alone. See Figure 1 of the main text for a graphical version of total air pollution mortalities by world regions.

Cause of death	Total all-cause [a]	Indoor plus outdoor air pollution		Outdoor air pollution only	
	Number of deaths/y (millions)	Percent of all-cause deaths[b]	Number of deaths/y (millions)	Percent of all-cause deaths[c]	Number of deaths/y (millions)
1. Ischemic heart disease (coronary artery disease)	9.43	25	2.36	17	1.60
2. Stroke	5.78	24	1.39	16	0.81
3. COPD (chronic bronchitis, emphysema)[d]	3.04	43	1.31	25	0.76
4. Lower respiratory infection (flu, bronchitis, pneumonia)	2.96	45	1.32	26	0.77
5. Alzheimer's disease/dementia	2.00	0	0	0	0
6. Trachea, bronchus, lung cancers	1.71	29	0.50	16	0.27
7. Diabetes	1.60	0	0	0	0
8. Road accidents	1.40	0	0	0	0
9. Diarrheal disease (cholera, dysentery)	1.38	0	0	0	0
10. Tuberculosis	1.29	0	0	0	0
Asthma	0.42	43	0.18	25	0.10
Total number of deaths worldwide	**56.9**	**12.5**	**7.1**	**7.9**	**4.5**

[a]WHO[116]

[b]WHO[104], except that the percentage of lower respiratory infection deaths that are due to indoor plus outdoor air pollution is estimated as the percentage of respiratory deaths that are from outdoor air pollution from WHO[104] multiplied by the ratio of the percentage of deaths from outdoor-plus-indoor to outdoor air pollution for COPD. The asthma percentage is assumed to be the same as the COPD percentage.

[c]WHO[104], except that the percentage of stroke deaths that are due to outdoor air pollution is estimated as the percentage of stroke deaths that are from indoor plus outdoor air pollution from WHO[104] multiplied by the ratio of the percentage of outdoor to indoor-plus-outdoor air pollution for ischemic heart disease. The asthma percentage is assumed to be the same as the COPD percentage.

[d]Chronic obstructive pulmonary disease (COPD) deaths are due to smoking and air pollution. They exclude asthma deaths, which are added separately.

Table S16. Parameters in the calculation of the value of statistical life over time and by country.

Parameter	LCHB	Middle	HCLB
U.S. VOSL in base year 2006 ($VOSL_{US,BYV}$) ($mil/death USD 2006)	9.00	7.00	5.00
U.S. VOSL in target year 2050 ($VOSL_{US,Y}$) ($mil/death USD 2013)	15.37	10.40	6.47
2006 global average VOSL ($mil/death USD 2006)	4.00	3.48	3.43
2050 global average VOSL ($mil/death USD 2013)	8.15	7.09	6.99
U.S. GDP per capita in 2006 ($G_{US,BYV}$) (USD $/person 2006)	52,275	52,275	52,275
U.S. GDP per capita target year 2050 ($G_{US,Y}$) (USD $/person 2013)	96,093	96,093	96,093
Multiplier for morbidity impacts (F_1)	1.25	1.15	1.05
Multiplier for non-health impacts (F_2)	1.10	1.10	1.05
Fractional reduction in mortalities per year (ΔA_c)	-0.014	-0.015	-0.016
Exponent giving change in mortality with population change (κ)	1.14	1.11	1.08
Fraction of country's VOSL fixed at U.S. TY value (T)	0.10	0.00	0.00
GDP/capita elasticity ($\gamma_{GDP,US,BYV}$) of VOSL, U.S. base year 2006	0.75	0.50	0.25
GDP/capita elasticity (γ_{GDP}) of VOSL, all years	-0.15	-0.15	-0.15

LCHB = low cost, high benefit. HCLB = high cost, low benefit. VOSL = value of statistical life. GDP = gross domestic product at purchasing power parity (PPP). From Jacobson et al.[5], except that the low and high fraction reduction in mortalities per year are updated here. Multiply LCHB VOSL by the high estimate of air pollution premature deaths to obtain the high estimate of air pollution cost in the BAU case (or greatest avoided air pollution benefit in the WWS case).

Table S17. (a) Mean values of the private levelized cost of energy (LCOE) for conventional fuels (BAU) in 2050 in the electricity sector in 143 countries. The LCOE estimates do not include externality costs. (b) Mean estimates by country of 2050 $PM_{2.5}$ plus ozone related premature mortalities from air pollution in the BAU case (10% of these, which are from non-energy emissions such as open biomass burning, wildfires, and desert dust, are estimated to remain even with the elimination of fossil fuels). (c) Low, mean, and high BAU costs per unit energy due to mortalities, morbidities, and non-air-pollution effects (accounting for the fact that 90% of mortalities are due to BAU) upon a conversion to WWS. (d) Percentage of world CO_2 emissions by country in 2017. (e) Low, mean, and high BAU climate-change costs per unit energy in 2050. All costs are in 2013 USD.

Country	(a) 2050 BAU mean LCOE (¢/kWh-elec-tricity)	(b) 2050 BAU mean air pollution mortalities /y	(c) 2050 BAU low health cost ($2013) ¢/kWh-BAU-all-energy	(c) 2050 BAU mean health cost ($2013) ¢/kWh-BAU-all-energy	(c) 2050 BAU high health cost ($2013) ¢/kWh-BAU-all-energy	(d) 2017 % of world CO_2 emissions	(e) 2050 BAU low climate cost ¢/kWh-BAU-all-energy	(e) 2050 BAU mean climate cost ¢/kWh-BAU-all-energy	(e) 2050 BAU high climate cost ¢/kWh-BAU-all-energy
Albania	6.37	1,766	15.3	34.1	68.6	0.014	5.8	10.4	22.1
Algeria	11.88	10,815	3	5.3	13.1	0.446	8.5	15.1	32.1
Angola	8.95	20,206	24.3	32.8	51.8	0.086	8	14.1	30.1
Argentina	10.31	12,153	3.1	6.2	11.8	0.586	7.7	13.7	29.1
Armenia	9.4	1,429	12	21.1	37.3	0.013	4.9	8.8	18.7
Australia	10.34	3,039	0.7	1.6	3.7	1.122	10.1	17.9	38
Austria	8.67	1,744	1.7	4.2	8.8	0.202	6.3	11.1	23.6
Azerbaijan	11.53	3,755	8.9	19.1	38.7	0.091	8	14.2	30.3
Bahrain	11.89	172	0.6	1.2	2.2	0.1	14.4	25.6	54.5
Bangladesh	11.8	161,254	67.7	70.8	110.4	0.236	8.8	15.6	33.2
Belarus	11.88	5,004	6.6	13.9	26.5	0.174	8.4	14.9	31.7
Belgium	11.12	2,300	1.7	3.8	7.9	0.291	6.4	11.3	24
Benin	11.69	17,112	43.5	36.4	68.3	0.02	5.7	10.2	21.6
Bolivia	10.34	5,510	10	12.8	21	0.057	6.8	12	25.5
Bosnia & Herzegovina	8.49	3,647	18	35.9	65.7	0.071	15.5	27.4	58.4
Botswana	9.72	940	7.1	12.8	21.9	0.022	11.1	19.8	42.1
Brazil	8.53	49,584	3.3	6.1	11.3	1.375	5.2	9.2	19.7
Brunei Darussalam	11.89	36	0.3	1	2.2	0.019	10	17.7	37.6
Bulgaria	9.51	3,776	7.5	17	41.8	0.138	10.7	19.1	40.6
Cambodia	8.31	12,111	25.2	26.5	41.2	0.029	5.3	9.4	20.1
Cameroon	7.77	26,050	43.5	43.2	73	0.027	4.6	8.1	17.2
Canada	8.24	3,768	0.4	1.1	2.4	1.722	7.8	13.8	29.4
Chile	9.53	4,119	2.6	5.7	11.4	0.252	8.3	14.6	31.2
China	9.27	1,090,410	10	21.4	39.3	30.342	9.2	16.4	34.8
Taiwan	9.27	6,670	0.8	5.3	15.9	0.738	12.4	22	46.8
Colombia	8.1	11,703	5.6	9.3	16.3	0.209	5.6	9.9	21.2
Congo	8.95	4,532	33	41.1	62.7	0.015	8.7	15.4	32.9
Congo, Dem. Republic	6.38	93,575	32.9	17.9	60.3	0.01	0.6	1.1	2.3
Costa Rica	8.24	1,008	4.5	7.8	13.8	0.023	5.6	9.9	21.2
Cote d'Ivoire	11.05	33,708	55.8	57.1	94	0.035	5.5	9.8	20.8
Croatia	8.48	1,964	6.2	14.8	33.7	0.049	5.9	10.4	22.1
Cuba	11.98	4,852	10.2	26.5	72.8	0.087	13	23	48.9
Cyprus	12.06	280	3.6	8.7	17.5	0.02	8.3	14.8	31.5
Czech Republic	9.9	3,222	3.5	7.5	15.6	0.306	10.7	19.1	40.6
Denmark	12.61	1,004	1.9	4.6	9.8	0.094	5.5	9.8	20.9
Dominican Republic	11.35	3,213	9.3	15.7	27	0.064	10.4	18.5	39.5
Ecuador	9.13	2,873	3.7	6.4	12.4	0.11	9.2	16.3	34.7
Egypt	11.49	63,338	13.9	20.4	35.3	0.722	10.6	18.7	39.9
El Salvador	11.32	1,560	9.4	13.7	23.5	0.022	8.5	15.1	32.2
Eritrea	11.9	6,885	120.3	91.9	198.1	0.002	4.7	8.3	17.7
Estonia	12.52	298	1.9	5.3	13.4	0.05	13.9	24.6	52.5

Ethiopia	6.91	152,284	41.9	31.3	66.3	0.042	1.4	2.5	5.4
Finland	9.74	545	0.5	1.5	3.5	0.131	4.7	8.4	17.8
France	9.39	10,528	2	4.7	9.6	0.943	5.7	10.1	21.6
Gabon	9.51	1,059	3.2	6.4	12.8	0.018	3.7	6.5	13.9
Georgia	7.58	4,102	18.5	36.7	68.3	0.032	6.7	11.8	25.1
Germany	10.85	19,077	2.6	6.2	12.9	2.222	9.3	16.4	34.9
Ghana	8.76	25,500	43.6	46.5	73.8	0.052	7.8	13.8	29.3
Gibraltar	10.84	20	0.1	0.5	1.4	0.002	0.5	0.9	1.9
Greece	10.6	4,605	5.6	12.8	39.2	0.201	9.2	16.3	34.7
Guatemala	9.96	7,226	13.1	17	26.3	0.05	5.5	9.8	20.9
Haiti	11.44	10,487	46.1	32.3	68.7	0.01	4.2	7.4	15.8
Honduras	10.74	3,161	10.5	12.2	20.4	0.029	7	12.5	26.5
Hong Kong, China	10.42	3,972	1	7.1	21.1	0.125	4.4	7.9	16.8
Hungary	10.23	4,162	6.1	12.5	22.6	0.142	7	12.4	26.4
Iceland	8.36	36	0.3	0.8	1.9	0.011	3.4	6	12.7
India	9.68	1,444,634	32.2	48.8	75.8	6.847	11.1	19.7	41.9
Indonesia	10.4	155,519	14.6	24.7	41.4	1.426	9.3	16.6	35.3
Iran, Islamic Republic	11.57	21,470	2.3	4	6.8	1.873	10.9	19.3	41
Iraq	11.51	12,511	10.8	17.5	29.3	0.556	26.5	47	100.1
Ireland	11.81	782	2.1	5.6	12.5	0.109	9.4	16.6	35.4
Israel	10.9	1,545	3	6.2	12.1	0.187	11	19.5	41.5
Italy	11.06	18,054	3.9	8.9	17.8	1.007	7.1	12.5	26.7
Jamaica	11.85	697	4.5	7.4	13.2	0.021	9.6	17	36.1
Japan	10.78	27,181	3.2	7.2	14.7	3.684	11.9	21.2	45
Jordan	11.88	1,857	4.9	7.3	12.2	0.069	10.9	19.4	41.3
Kazakhstan	9.8	7,774	3.1	7.7	18.1	0.743	11	19.4	41.4
Kenya	10.65	17,789	13.1	12.9	21.7	0.052	3.8	6.8	14.5
Korea, DPR	7.39	37,704	46.6	42.3	76.4	0.105	15	26.6	56.7
Korea, Republic of	10.14	8,990	1.5	3.4	7.6	1.878	10	17.7	37.6
Kosovo	9.57	266	3.1	5.8	9.3	0.024	14.4	25.5	54.3
Kuwait	11.89	888	0.9	1.9	3.7	0.271	10.4	18.4	39.1
Kyrgyzstan	6.89	3,791	14.6	22.3	41.5	0.031	7.6	13.4	28.6
Latvia	10.35	877	5	12.3	26.9	0.022	4.8	8.6	18.2
Lebanon	11.74	1,297	4.6	7.8	12.5	0.064	13.6	24.2	51.4
Libya	11.89	2,935	4.3	6.7	10.8	0.161	14.5	25.7	54.7
Lithuania	12.05	1,340	5.5	13.6	29.1	0.043	6.3	11.1	23.6
Luxembourg	11.96	103	1	2.7	6.2	0.027	6.7	11.9	25.4
Macedonia, Rep. of	8.81	1,486	17	33.5	59.5	0.022	9.9	17.6	37.5
Malaysia	10.44	9,353	2.6	5.7	14.7	0.722	11.9	21.1	44.9
Malta	12.03	104	1.2	2.8	5.8	0.005	2	3.5	7.4
Mauritius	11.13	418	3.5	7.4	18.1	0.011	6.6	11.8	25.1
Mexico	11.1	29,995	4.5	7.9	13.6	1.415	10.2	18.1	38.6
Moldova, Republic of	11.61	1,384	8.3	13.6	26.7	0.023	7.5	13.2	28.1
Mongolia	9.86	2,600	13.5	21.9	35.1	0.072	23.6	41.9	89.3
Montenegro	8.01	480	13.3	30.4	59.1	0.012	13.9	24.6	52.4
Morocco	10.4	10,344	8.4	11.9	20.3	0.172	10.8	19.2	40.9
Mozambique	7.12	24,816	19.6	12.8	32.6	0.022	2.5	4.4	9.3
Myanmar	8.6	50,419	47.7	55.6	84.9	0.079	6.2	10.9	23.2
Namibia	6.49	965	7.2	10.7	17	0.012	6.2	11	23.5
Nepal	6.38	38,210	42.1	39.7	65.9	0.023	2.5	4.5	9.5
Netherlands	11.15	3,352	1.6	3.9	8	0.488	7	12.5	26.6
Curacao	11.15	10	0	0.1	0.4	0.013	4.4	7.9	16.7
New Zealand	9.2	444	0.6	1.6	3.7	0.103	6.1	10.8	23.1
Nicaragua	12.37	1,908	13.9	17.7	27.7	0.017	7.5	13.2	28.1
Niger	10.97	52,062	166.8	111.3	282.7	0.007	3.3	5.8	12.4
Nigeria	10.88	417,695	55.5	73	111	0.265	2.6	4.7	9.9
Norway	6.61	569	0.5	1.7	4	0.131	4.3	7.5	16.1
Oman	11.89	752	0.6	1.4	3.5	0.219	9.1	16.2	34.4
Pakistan	10.07	205,431	33.7	40.2	62.8	0.55	7.6	13.5	28.8
Panama	8.47	782	1.8	3.6	6.7	0.034	4.1	7.3	15.5
Paraguay	6.37	2,511	8.3	11.8	18.6	0.018	3.7	6.5	13.8
Peru	9.23	13,130	10.9	16.9	27.6	0.156	7.2	12.7	27.1

Philippines	10.59	126,709	50.3	76	120	0.383	11.8	21	44.7
Poland	10.25	14,363	5.7	11.3	20.1	0.89	11.4	20.2	43
Portugal	10.89	1,654	2.2	5.3	12.1	0.158	8	14.2	30.1
Qatar	11.89	203	0.2	0.5	1.1	0.273	9.8	17.4	37
Romania	9.69	13,080	11.6	30.2	77.5	0.226	8.4	14.9	31.8
Russian Federation	10.21	55,075	3.7	8	15.4	4.923	9.9	17.5	37.3
Saudi Arabia	11.89	9,804	1.8	3.8	8.9	1.782	13.5	23.9	50.9
Senegal	11.44	12,993	35.9	33	62.1	0.027	8.3	14.8	31.5
Serbia	8.78	4,208	8.8	20.2	40.2	0.162	15.2	26.9	57.4
Singapore	11.89	2,107	0.6	1.6	3.7	0.153	2	3.5	7.5
Slovak Republic	9.47	1,731	4.1	8.5	18	0.106	8.1	14.4	30.7
Slovenia	8.88	534	3	6.7	13.8	0.042	8.1	14.4	30.6
South Africa	9.69	18,139	3.3	5.2	8.7	1.305	15.4	27.4	58.3
South Sudan	11.9	19,104	230.4	183.2	365.9	0.003	4.9	8.6	18.3
Spain	10.84	8,585	2.3	5.5	11.6	0.786	7.3	12.9	27.4
Sri Lanka	8.69	13,636	20.4	33.4	53.8	0.067	6.5	11.6	24.7
Sudan	7.8	65,754	62.3	68.6	109.5	0.059	5	8.9	19
Suriname	8.57	225	7.8	13.1	21.7	0.006	10.9	19.3	41.1
Sweden	8.7	981	0.7	2	5	0.142	3.7	6.6	14
Switzerland	7.79	1,089	1.6	4.2	9.4	0.111	5	8.9	19
Syrian Arab Republic	11.76	9,262	23.6	32.7	51.1	0.079	13.6	24.1	51.3
Tajikistan	6.42	5,315	30.2	39.2	69.9	0.016	5.6	9.9	21
Tanzania, United Rep.	10.05	31,301	16.5	14.8	25.6	0.041	2.2	3.9	8.3
Thailand	11.41	35,599	5.6	11.1	20.2	0.779	8.2	14.6	31.1
Togo	8.19	12,450	47.4	33.9	75.7	0.008	4	7.1	15
Trinidad and Tobago	11.89	271	0.7	1.4	2.4	0.105	11.7	20.7	44.2
Tunisia	11.91	4,211	5.3	7.8	12.5	0.088	7.3	12.9	27.5
Turkey	9.94	28,480	8.3	14.4	24	1.198	11.2	19.9	42.3
Turkmenistan	11.89	2,073	2.6	5	9	0.202	8.8	15.5	33.1
Ukraine	9.55	26,830	9.6	17.1	29.9	0.574	9.4	16.6	35.3
United Arab Emirates	11.89	797	0.3	0.6	1.2	0.566	7.3	13	27.7
United Kingdom	11.16	13,823	2.9	6.7	14.1	1.058	6.9	12.2	26.1
United States	10.43	62,676	1.4	3.7	8.2	14.247	8.6	15.2	32.3
Uruguay	9.11	675	2.6	5.3	10.6	0.019	4.1	7.3	15.4
Uzbekistan	10.65	11,609	8.1	13	22.9	0.266	8.9	15.7	33.5
Venezuela	8.37	7,249	3.3	5.5	9.6	0.407	9.4	16.7	35.6
Vietnam	9.2	44,139	9.5	12.9	20.6	0.61	10.4	18.4	39.1
Yemen	11.89	26,192	143.3	162.2	262.4	0.035	15.8	28	59.7
Zambia	6.54	15,969	24.1	25.2	41.3	0.014	1.9	3.4	7.2
Zimbabwe	8.02	10,769	11.8	9.4	19.2	0.034	4.6	8.1	17.3
World total/average	**9.99**	**5,285,036**	**10.1**	**16.9**	**29.7**	**99.74**	**9**	**16.0**	**34.1**

a) The 2050 LCOE cost of retail electricity for BAU fuels in each country combines the percentage mix of BAU electricity generators in 2050 with 2050 mean LCOEs for each generator, derived herein. Such costs include all-distance transmission, pipelines, and distribution, but they exclude health and climate externality costs. The 2050 BAU mix includes some existing WWS (mostly hydropower) plus future increases in WWS electricity in the BAU case and energy efficiency.

b) Premature mortalities in each country in 2050 are estimated by projecting country-specific indoor plus outdoor air pollution mortality estimates for 2016 from WHO[104] to 2050 using the equations derived in Note S39. Table S15 indicates that the mean number of such deaths worldwide in 2016 was about 7.1 million. The number in the 143 countries examined was 6.8 million (Figure 1). The present table suggests that the number of deaths may drop to 5.3 million per year by 2050 in a BAU economy because lower emissions due to improvements in emission controls will have a greater impact than the higher population exposed to air pollution.

c) The total damage cost of air pollution due to conventional fuels (fossil fuel and biofuel combustion and evaporative emissions) in a country is the sum of mortality costs, morbidity costs, and non-health costs (e.g., lost visibility and agricultural output) in the country. It is calculated with Equation S34. The resulting damage cost per kWh-BAU-all-energy is determined by dividing the total air pollution damage cost per year in 2050 per country by the kWh from all energy in the BAU case per year produced by the country.

d) Percentage of 2017 world anthropogenic fossil-fuel CO_2 emissions by country[128]. The total worldwide (218 countries) was 35,849 gigatonnes (GT)-CO_2 and in the 143 countries treated here was 35,756 GT-CO_2. These numbers are estimated to rise by 2050 in the BAU scenario to 57,103 GT-CO_2 for 218 countries and 56,955 GT-CO_2 for 143 countries.

e) Product of the fossil-fuel CO_2 emissions rate per country in 2050 and the mid-value of the social cost of carbon (SCC) from Table S18 ($500/tonne-$CO_2$e), divided by the kWh from all energy in the BAU case per year produced by the country.

Table S18. Low, mid, and high estimates of the social cost of carbon (SCC).

Parameter	Low estimate	Mid estimate	High estimate
2010 Global SCC (2007 USD)	125	250	600
Annual percentage increase in SCC	1.8	1.5	1.2
2050 Global SCC (2013 USD)	282	500	1,063

Units of the SCC are USD per metric tonne-CO_2e. From Jacobson et al.[5].

Table S19. LOADMATCH capacity adjustment factors (CAFs), which show the ratio of the final nameplate capacity of several generators used for this study to meet load continuously, after running LOADMATCH, to the pre-LOADMATCH initial nameplate capacity estimated herein (e.g., Table 3, main text) to meet load in the annual average. Thus, a CAF less than 1.0 means that the LOADMATCH-stabilized grid meeting hourly demand requires less than the nameplate capacity needed to meet annual average load (which is our initial, pre-LOADMATCH nameplate-capacity assumption). Column (f) is the ratio of CSP turbine nameplate capacity (CSP storage discharge rate) needed to keep the grid stable relative to the CSP turbine nameplate capacity needed for annual average power in each region. Jacobson et al.[16] estimated this factor as 1.6 for determining CSP nameplate capacities, so a number less than 1.6 here indicates fewer CSP turbines are needed to meet load continuously than to meet it in the annual average. Tables 3 and S20 provides the final CSP nameplate capacity, accounting for this factor. All generators not on this list have a CAF = 1.

Region	(a) Onshore wind CAF	(b) Off-shore wind CAF	(c) Res. Roof PV CAF	(d) Com./Gov Roof PV CAF	(e) Utility PV CAF	(f) CSP turbine factor	(g) Solar Thermal CAF
Africa	1.29	0.8	0.7	0.7	1	1	0.01
Australia	1.18	0.7	0.75	0.75	1.95	1.6	0.181
Canada	1.4	0.9	0.2	0.7	0.5	0	0.2
Central America	1.35	1	0.88	0.88	0.98	1.6	0.06
Central Asia	1.41	0.9	0.85	0.85	1	1	0
China	1.82	0.7	0.55	0.55	1.7	1.4	0.464
Cuba	1.18	1.1	1.2	1.2	1.5	2.4	0
Europe	1.38	1	0.68	0.9	0.8	1	0.5
Haiti	1	1	1.05	1.1	1.1	1.5	0
Iceland	0.4	0.04	0	0	0	0	0
India	1.05	0.6	0.1	1.3	3	2.59	0.019
Israel	1	0.88	0.1	2.5	3.68	2	0.571
Jamaica	1	1	1	1	1.09	1.2	0
Japan	1.7	2	0.2	0.2	1.75	0	0.036
Mauritius	0.85	1	1	1	1.5	1.5	0
Mideast	2.1	0.8	0.75	0.75	1.38	2	0.057
New Zealand	1.49	0.4	0.6	0.6	1.65	0.8	0
Philippines	1.35	0.85	0.9	0.9	1.75	0.9	0.8
Russia	1.4	0.6	0.45	0.45	0.85	0.7	0.24
South America	1.25	0.75	0.6	0.6	1.28	1	0.077
Southeast Asia	0.2	0.65	0.88	0.88	1.92	7	0
South Korea	0.5	1.75	0.25	2.6	1.63	1.18	0
Taiwan	0.6	1.69	0.7	2.5	1.21	0	0.046
United States	1.56	1.5	0.45	0.45	2.17	1.75	0.064

Table S20. Final (from LOADMATCH) 2050 total (existing plus new) nameplate capacity (GW) of WWS generators by world region needed to match power demand with supply and storage continuously over time. Also provided are 143-country totals for 2050 and installed as of 2018 end, the nameplate capacity (MW) per device, and the 143-country total number of existing plus new devices needed at that nameplate capacity. The nameplate capacity equals the maximum possible instantaneous discharge rate.

Region	Onshore wind	Off-shore wind	Resi-dential roof-top PV	Comm /govt rooftop PV	Utility PV	CSP with storage	Geothermal - electricity	Hydro power	Wave	Tidal	Solar thermal	Geothermal heat
Africa	767	98.4	196	372	435.2	45.9	3.61	29.3	12.0	1.90	2.04	0.14
Australia	95	23.5	34.9	59.8	202.7	13.0	0.40	8.1	2.91	0.50	6.57	0.02
Canada	183	29.8	11.7	98	34.3	0.0	5.00	80.8	4.05	2.00	8.42	1.47
Central America	350	55.3	57.1	129	73.2	21.1	10.7	18.3	11.8	0.38	2.67	0.16
Central Asia	181	21.2	94.2	145	181	11.6	0.00	20.0	1.79	0.02	0	0.003
China	3,708	735	803	928	2,809	296	1.86	318	8.71	3.02	351	17.9
Cuba	12.24	3.00	4.21	9.43	6.04	1.71	0.00	0.1	0.23	0.05	0	0
Europe	1,196	395	317	507	885	21.1	3.17	167	15.5	15.0	168	22.3
Haiti	6.21	2.92	4.55	9.71	5.47	0.94	0.68	0.60	0.00	0.05	0.00	0.00
Iceland	1.19	0.00	0.00	0.00	0.0	0.0	0.89	1.99	0.04	0.06	0.00	2.04
India	978	100	67	1,159	3,159	233	0.28	47.3	5.06	0.72	7.76	0.99
Israel	2.60	5.42	1.16	15.9	77.3	2.09	0.00	0.01	0.00	0.01	3.50	0.08
Jamaica	0.48	1.88	2.52	2.49	3.15	0.28	0.00	0.02	0.00	0.02	0	0
Japan	92.5	282.3	21.8	14.2	467	0.00	1.46	22.3	12.7	2.20	2.54	2.19
Mauritius	0.09	1.28	1.96	1.23	3.38	0.23	0.00	0.1	0.06	0.01	0	0
Mideast	1,004	140	245	315	1,467	117.3	1.41	44.7	1.92	0.28	16.2	3.17
New Zealand	21.8	1.75	5.32	6.62	16.9	1.16	2.00	5.3	0.41	0.20	0	0.49
Philippines	17.0	18.3	23.7	52.0	52.7	2.94	5.73	3.6	1.95	0.50	14.4	0.003
Russia	349	45.2	67.9	89.8	138	3.24	0.50	50.2	4.92	0.36	19.3	0.38
South America	1,304	106	118	256	316	39.2	5.35	166	23.2	1.23	10.5	0.58
Southeast Asia	53.8	458	441	468	1,262	340.3	13.8	36.3	14.8	0.79	0	0.16
South Korea	10.8	319	17.8	119	479	17.7	0.00	6.5	0.00	1.00	0	0.84
Taiwan	4.48	107	32.1	57.5	130	0.0	33.6	2.1	1.05	0.03	1.27	0
United States	1,638	657	207	307	1,487	92.9	6.52	80.1	33.0	0.35	18.3	17.4
Total 2050	**11,976**	**3,606**	**2,776**	**5,121**	**13,691**	**1262**	**97.0**	**1,109**	**156.2**	**30.6**	**632**	**70.3**
Total 2018	571	24.6	95.6	95.6	287	5.5	13.3	1,109	0.0	0.54	459	70.3
Device MW	5.00	5.00	0.01	0.10	50.0	100	100	1,300	0.8	1.00	50.0	50.0
Device number	2,395,132	721,173	555,195,984	51,205,592	273,825	12,620	970	853	208,314	30,614	12,640	1,407

Device MW = the nameplate capacity of one device in megawatts. Device number is the number in 2050 of all devices among 139 countries of the given nameplate capacity per device.

Table S21. Average 2050-2052 capacity factors (percent of nameplate capacity produced as electricity before transmission, distribution or maintenance losses) by region in this study.

Region	Onshore wind	Off-shore wind	Rooftop PV	Utility PV	CSP with storage	Geo-thermal elec-tricity	Hydr opow er	Wave	Tidal	Solar therm al	Geo-thermal heat
Africa	0.372	0.431	0.203	0.204	0.584	0.809	0.539	0.201	0.226	0.111	0.974
Australia	0.389	0.504	0.202	0.243	0.616	0.904	0.659	0.332	0.247	0.111	0.974
Canada	0.490	0.563	0.191	0.197	0.000	0.862	0.514	0.297	0.236	0.105	0.973
Central America	0.262	0.322	0.220	0.251	0.628	0.840	0.556	0.126	0.230	0.123	0.973
Central Asia	0.517	0.474	0.200	0.222	0.531	0.000	0.550	0.121	0.216	0.000	0.966
China	0.432	0.399	0.200	0.226	0.554	0.896	0.524	0.139	0.236	0.110	0.973
Cuba	0.296	0.360	0.229	0.257	0.657	0.000	0.619	0.379	0.232	0.000	0.000
Europe	0.419	0.520	0.189	0.197	0.508	0.861	0.548	0.237	0.237	0.100	0.973
Haiti	0.331	0.473	0.232	0.256	0.670	0.877	0.638	0.000	0.216	0.000	0.000
Iceland	0.473	0.544	0.000	0.000	0.000	0.925	0.683	0.317	0.252	0.000	0.973
India	0.316	0.374	0.196	0.231	0.619	0.857	0.631	0.133	0.234	0.110	0.973
Israel	0.370	0.333	0.236	0.258	0.625	0.000	0.546	0.000	0.252	0.131	0.974
Jamaica	0.297	0.488	0.240	0.270	0.695	0.000	0.409	0.000	0.208	0.000	0.000
Japan	0.383	0.478	0.174	0.195	0.000	0.909	0.482	0.141	0.249	0.095	0.973
Mauritius	0.278	0.363	0.208	0.229	0.599	0.000	0.483	0.318	0.251	0.000	0.000
Mideast	0.461	0.383	0.219	0.228	0.597	0.798	0.528	0.135	0.233	0.120	0.973
New Zealand	0.465	0.550	0.191	0.207	0.492	0.885	0.523	0.353	0.242	0.000	0.973
Philippines	0.284	0.385	0.224	0.251	0.664	0.858	0.524	0.133	0.235	0.126	0.983
Russia	0.468	0.578	0.178	0.199	0.435	0.863	0.505	0.256	0.237	0.098	0.973
South America	0.178	0.455	0.211	0.231	0.596	0.883	0.570	0.151	0.239	0.118	0.973
Southeast Asia	0.100	0.211	0.189	0.206	0.552	0.879	0.633	0.192	0.227	0.000	0.974
South Korea	0.311	0.441	0.177	0.176	0.439	0.000	0.520	0.000	0.251	0.000	0.973
Taiwan	0.282	0.373	0.195	0.213	0.000	0.927	0.587	0.144	0.255	0.108	1.081
United States	0.374	0.348	0.213	0.223	0.567	0.892	0.556	0.294	0.244	0.115	0.973
Average	**0.368**	**0.406**	**0.200**	**0.219**	**0.552**	**0.870**	**0.554**	**0.182**	**0.236**	**0.111**	**0.974**

Capacity factors of offshore and onshore wind turbines account for array losses (extraction of kinetic energy by turbines). In all cases, capacity factors are before transmission, distribution, and maintenance losses, which are given in Table S14. The average is weighted by nameplate capacity (Table S20). The symbol "--" indicates no installation of the technology. Rooftop PV panels are fixed-tilt at the optimal tilt angle of the country they reside in; utility PV panels are half fixed optimal tilt and half single-axis horizontal tracking[45].

Table S22. 2050 regional annual-average end-use WWS loads; present values of the mean total capital cost for new electricity heat, cold, and hydrogen generation and storage and long-distance transmission; low, mean, and high levelized private costs of all energy (¢/kWh-all-energy-sectors, averaged between today and 2050, in USD 2013); and low, mean, and high aggregate private energy costs per year (2013 USD $billion/yr). See Figures 3 and 4 of the main text for graphical versions of some of these data.

Region	Annual average end-use load (GW)	Mean total capital cost ($tril 2013)	Low (¢/kWh-all energy)	Mean (¢/kWh-all energy)	High (¢/kWh-all energy)	Low annual all-energy cost ($bil/yr)	Mean annual all-energy cost ($bil/yr)	High annual all-energy cost ($bil/yr)
Africa	482	3.77	6.80	8.38	10.53	287	354	444
Australia	94	0.82	7.18	9.04	11.63	58.9	74.1	95.3
Canada	152	0.70	5.80	7.04	8.73	76.9	93.4	116
Central America	154	1.36	7.60	9.41	11.84	103	127	160
Central Asia	151	1.34	6.98	8.83	11.45	92.3	117	152
China	2,328	16.6	6.87	8.33	10.30	1,401	1,699	2,100
Cuba	8.06	0.10	8.45	12.01	17.53	5.97	8.49	12.4
Europe	940	6.15	6.68	8.18	10.22	550	674	842
Haiti	7.54	0.07	7.35	9.62	12.88	4.85	6.36	8.51
Iceland	2.98	0.0026	5.23	6.54	8.32	1.37	1.71	2.18
India	945	10.6	7.82	10.06	13.20	647	832	1,093
Israel	12.8	0.20	9.57	13.10	18.26	10.7	14.7	20.5
Jamaica	2.27	0.025	7.94	10.12	13.08	1.58	2.01	2.60
Japan	178	1.49	7.85	9.76	12.39	122	152	193
Mauritius	1.79	0.026	9.33	12.36	16.35	1.46	1.94	2.56
Mideast	678	6.14	7.29	9.08	11.52	433	539	684
New Zealand	17.6	0.11	6.28	7.77	9.82	9.7	12.0	15.1
Philippines	40.5	0.40	7.49	9.35	11.81	26.5	33.2	41.8
Russia	236	1.49	6.15	7.72	9.92	127	160	206
South America	489	3.68	7.29	8.86	10.93	312	379	468
Southeast Asia	583	7.06	8.23	10.30	12.98	421	526	663
South Korea	155	1.88	9.08	11.87	15.89	123	161	216
Taiwan	94.9	0.97	7.64	10.60	15.13	63.5	88.1	126
United States	939	7.82	7.50	9.33	11.85	617	768	975
Total/average	**8,693**	**72.82**	**7.22**	**8.96**	**11.34**	**5,498**	**6,825**	**8,638**

The annual energy cost equals the end-use load multiplied by the number of hours per year multiplied by the levelized cost of energy. Table S23 contains details of the cost breakdown in each region.

Table S23. Summary of 2050 WWS mean capital costs of new electricity plus heat generators and storage ($ trillion in 2013 USD) and mean levelized private costs of energy (LCOE) (USD ¢/kWh-all-energy or ¢/kWh-electricity-replacing-BAU-electricity) averaged over the 3-year simulations for 24 world regions (defined in Table 1). Also shown are the energy consumed per year in each case and the resulting aggregate annual energy cost to the region.

	Africa	Australia	Canada	Central America	Central Asia	China	Cuba
Capital cost new generators only ($trillion)	3.33	0.71	0.59	1.24	1.14	14.83	0.069
Cap cost new generators + storage ($trillion)	3.77	0.82	0.70	1.36	1.34	16.58	0.098
Components of total LCOE (¢/kWh-all-energy)							
Short-dist. transmission	1.05	1.05	1.05	1.05	1.05	1.05	1.05
Long-distance transmission	0.122	0.122	0.121	0.081	0.122	0.121	0.000
Distribution	2.375	2.375	2.375	2.375	2.375	2.375	2.375
Electricity generators	4.307	4.590	3.164	5.388	4.452	4.324	5.141
Additional hydro turbines	0	0	0	0	0	0	0
Solar thermal collectors	0.005	0.072	0.075	0.020	0.000	0.169	0.000
CSP-PCM+PHS+battery storage	0.339	0.657	0.088	0.265	0.630	0.168	3.330
CW-STES+ICE storage	0.001	0.002	0.002	0.001	0.000	0.003	0.003
HW-STES storage	0.006	0.008	0.021	0.006	0.007	0.007	0.004
UTES storage	0.027	0.018	0.051	0.020	0.096	0.035	0.010
H_2 production/compression/storage	0.146	0.149	0.089	0.207	0.101	0.082	0.099
Total LCOE (¢/kWh-all-energy)	**8.38**	**9.04**	**7.04**	**9.41**	**8.83**	**8.33**	**12.01**
LCOE (¢/kWh-replacing BAU electricity)	8.19	8.86	6.87	9.17	8.62	8.21	11.90
GW annual avg. end-use demand (Table S10)	481.7	93.6	152	154.4	151.1	2,328.4	8.1
TWh/y end-use demand (GW x 8,760 h/y)	4,220	820	1,327	1,353	1,324	20,397	71
Annual energy cost ($billion/yr)	**353.6**	**74.1**	**93.4**	**127.3**	**116.9**	**1,699.5**	**8.5**
	Europe	Haiti	Iceland	India	Israel	Jamaica	Japan
Capital cost new generators only ($trillion)	5.16	0.06	0.002	9.13	0.16	0.022	1.31
Cap cost new generators + storage ($trillion)	6.15	0.073	0.0026	10.65	0.20	0.025	1.49
Components of total LCOE (¢/kWh-all-energy)							
Short-dist. transmission	1.05	1.05	1.05	1.05	1.05	1.05	1.05
Long-distance transmission	0.121	0.000	0.000	0.122	0.000	0.000	0.081
Distribution	2.375	2.375	2.375	2.375	2.375	2.375	2.375
Electricity generators	3.984	4.628	1.728	5.398	6.671	5.484	5.574
Additional hydro turbines	0	0	0	0	0	0	0
Solar thermal collectors	0.229	0.000	1.314	0.010	0.292	0.000	0.038
CSP-PCM+PHS+battery storage	0.171	1.343	0.000	0.911	2.350	0.952	0.482
CW-STES+ICE storage	0.006	0.001	0.003	0.001	0.005	0.000	0.002
HW-STES storage	0.014	0.003	0.014	0.015	0.017	0.007	0.010
UTES storage	0.076	0.001	0.000	0.055	0.107	0.003	0.021
H_2 production/compression/storage	0.158	0.222	0.057	0.122	0.233	0.247	0.127
Total LCOE (¢/kWh-all-energy)	**8.18**	**9.62**	**6.54**	**10.06**	**13.10**	**10.12**	**9.76**
LCOE (¢/kWh-replacing BAU electricity)	7.93	9.40	6.47	9.86	12.74	9.86	9.60
GW annual avg. end-use demand (Table S10)	939.7	7.5	3.0	945.0	12.8	2.3	178.0
TWh/y end-use demand (GW x 8,760 h/y)	8,232	66	26	8,278	112	20	1,559
Annual energy cost ($billion/yr)	**673.5**	**6.4**	**1.7**	**832.5**	**14.7**	**2.0**	**152.1**
	Mauritius	Mideast	New Zealand	Philippines	Russia	South America	Southeast Asia
Capital cost new generators only ($trillion)	0.017	5.34	0.093	0.34	1.13	3.40	6.43
Cap cost new generators + storage ($trillion)	0.026	6.14	0.107	0.40	1.49	3.68	7.06
Components of total LCOE (¢/kWh-all-energy)							
Short-dist. transmission (¢/kWh-all-energy)	1.05	1.05	1.05	1.05	1.05	1.05	1.05
Long-distance transmission	0.000	0.122	0.061	0.081	0.122	0.122	0.122
Distribution	2.375	2.375	2.375	2.375	2.375	2.375	2.375
Electricity generators	5.187	4.794	3.673	4.817	3.348	5.115	6.164
Additional hydro turbines	0	0	0	0	0	0	0

Solar thermal collectors	0.000	0.034	0.053	0.364	0.087	0.024	0.001
CSP-PCM+PHS+battery storage	3.213	0.453	0.384	0.313	0.034	0.031	0.367
CW-STES+ICE storage	0.001	0.001	0.000	0.001	0.003	0.002	0.002
HW-STES storage	0.004	0.008	0.004	0.003	0.029	0.007	0.006
UTES storage	0.005	0.032	0.043	0.037	0.381	0.006	0.008
H_2 production/compression/storage	0.522	0.213	0.131	0.315	0.296	0.126	0.203
Total LCOE (¢/kWh-all-energy)	**12.36**	**9.08**	**7.77**	**9.35**	**7.72**	**8.86**	**10.30**
LCOE (¢/kWh-replacing BAU electricity)	11.83	8.82	7.59	8.99	7.01	8.71	10.07
GW annual avg. end-use demand (Table S10)	1.8	677.7	17.6	40.5	236.5	489.1	583.2
TWh/y end-use demand (GW x 8,760 h/y)	16	5,936	154	354	2,071	4,284	5,109
Annual energy cost ($billion/yr)	**1.9**	**539.0**	**12.0**	**33.2**	**160.0**	**379.5**	**526.0**

	South Korea	Taiwan	United States	24 world regions
Capital cost new generators only ($trillion)	1.60	0.72	6.85	**63.7**
Cap cost new generators + storage ($trillion)	1.88	0.97	7.819	**72.8**
Components of total LCOE (¢/kWh-all-energy)				
Short-dist. transmission (¢/kWh-all-energy)	1.05	1.05	1.05	**1.05**
Long-distance transmission	0.000	0.000	0.121	**0.116**
Distribution	2.375	2.375	2.375	**2.375**
Electricity generators	6.761	4.648	5.109	**4.747**
Additional hydro turbines	0	0	0	**0**
Solar thermal collectors	0.010	0.014	0.056	**0.09**
CSP-PCM+PHS+battery storage	1.492	2.324	0.436	**0.388**
CW-STES+ICE storage	0.002	0.002	0.004	**0.003**
HW-STES storage	0.008	0.015	0.012	**0.01**
UTES storage	0.021	0.037	0.010	**0.044**
H_2 production/compression/storage	0.151	0.139	0.157	**0.141**
Total LCOE (¢/kWh-all-energy)	**11.87**	**10.60**	**9.33**	**8.96**
LCOE (¢/kWh-replacing BAU electricity)	11.69	10.41	9.14	**8.76**
GW annual avg. end-use demand (Table S10)	155.2	94.9	939.5	**8,693**
TWh/y end-use demand (GW x 8,760 h/y)	1,359	831	8,230	**76,151**
Annual energy cost ($billion/yr)	**161.4**	**88.1**	**767.6**	**6,825**

The LCOEs are derived from capital costs assuming a social discount rate for an intergenerational project of 2.0 (1 to 3) percent and lifetimes, annual O&M, and end-of-life decommissioning costs that vary by technology, all divided by the total annualized end-use demand met, given in the present table. Capital costs are an estimated average of those between 2015 and 2050 and are a mean (in USD $1 million/MW) of 1.27 for onshore wind, 3.06 for offshore wind, 2.97 for residential rooftop PV, 2.06 for commercial/government PV, 1.32 for utility PV, 4.33 for CSP with storage, 3.83 for geothermal electricity and heat, 2.81 for hydropower, 3.57 for tidal, 4.01 for wave, and 1.22 for solar thermal for heat.

Since the total end-use load includes heat, cold, hydrogen, and electricity loads (all energy), the "electricity generator" cost, for example, is a cost per unit all energy rather than per unit electricity alone. The 'Total LCOE' gives the overall cost of energy, and the 'Electricity LCOE' gives the cost of energy for the electricity portion of load replacing BAU electricity end use. It is the total LCOE less the costs for UTES and HW-STES storage, H_2, and less the portion of long-distance transmission associated with H_2.

Long-distance transmission costs are provided in the footnote to Table S14.

Storage costs are derived as described in Table S13.

H_2 costs are derived as in Note S38 and Note S43. These costs exclude electricity costs, which are included separately in the present table.

Table S24. Summary of WWS energy requirements met, energy losses, energy supplies, and changes in storage, during the 3-year (26,291.5 hour) simulations for 24 world regions. All units are TWh over the 3-year simulation. Table 1 identifies the countries within each region.

	Africa	Australia	Canada	Central America	Central Asia
A1. Total end use demand	**12,665**	**2,461**	**3,984**	**4,060**	**3,973**
Electricity for electricity inflexible demand	5,926	1,227	1,930	1,820	2,031
Electricity for electricity, heat, cold storage + DR	5,673	1,054	1,829	1,828	1,745
Electricity for H_2 direct use + H_2 storage	1,066	180	225	413	197
A2. Total end use demand	**12,665**	**2,461**	**3,984**	**4,060**	**3,973**
Electricity for direct use, electricity storage, + H_2	11,438	2,302	3,612	3,812	3,740
Low-T heat load met by heat storage	1196.0	150.9	361	237.9	232.4
Cold load met by cold storage	32	8	10.9	10	1
A3. Total end use demand	**12,665**	**2,461**	**3,984**	**4,060**	**3,973**
Electricity for direct use, electricity storage, DR	10,310	2,105	3,324	3,386	3,520
Electricity for H_2 direct use + H_2 storage	1,066	180	225	413	197
Electricity + heat for heat subject to storage	1,207	153	404	240	254
Electricity for cold load subject to storage	82	23	30.8	22	2
B. Total losses	**2,596**	**1,010**	**824**	**1,272**	**1,530**
Transmission, distribution, downtime losses	962	230	326	335	337
Losses CSP storage	4.00	1.49	0.00	1.56	0.90
Losses PHS storage	38.6	20.1	12.6	6.9	18.1
Losses battery storage	35.6	11.6	0.0	13.7	19.8
Losses CW-STES + ICE storage	5.73	1.39	1.97	1.82	0.15
Losses HW-STES storage	158.7	20.7	60.1	41.0	28.4
Losses UTES storage	328	36	39	27	72
Losses from shedding	1,063	689	383.6	844	1,055
Net end-use demand plus losses (A1 + B)	***15,261***	***3,470***	***4,807***	***5,332***	***5,503***
C. Total WWS supply before T&D losses	**15,256**	**3,471**	**4,797**	**5,333**	**5,496**
Onshore + offshore wind electricity	8,613	1,281	2,802	2,877	2,723
Rooftop + utility PV+ CSP electricity	6,073	2,008	729	1,907	2,477
Hydropower electricity	415	139.5	1,092	268.1	290
Wave electricity	63.6	25.41	31.65	39.29	5.69
Geothermal electricity	76.8	9.51	113.27	236.2	0.00
Tidal electricity	11.7	3.25	12.39	2.30	0.12
Solar heat	1.49	4.81	5.80	2.15	0.00
Geothermal heat	0.88	0.10	9.38	1.05	0.02
D. Net taken from (+) or added to (-) storage	**5.58**	**-1.04**	**10.56**	**-0.65**	**7.81**
CSP storage	0.34	0.02	0.00	-0.05	0.20
PHS storage	0.21	-0.04	0.17	-0.01	0.13
Battery storage	0.21	-0.24	-0.03	-0.06	0.55
CW-STES+ICE storage	0	0	0.012	0	0
HW-STES storage	0.654	-0.046	0.57	0.086	0.177
UTES storage	3.253	-0.696	9.83	-0.519	6.276
H_2 storage	0.876	-0.049	0.00	-0.11	0.486
Energy supplied plus taken from storage (C+D)	***15,261***	***3,470***	***4807***	***5,332***	***5,503***

	China	Cuba	Europe	Haiti	Iceland
A1. Total end use demand	**61,207**	**212**	**24,705**	**198**	**78**
Electricity for electricity inflexible demand	27,306	106	10,186	97	35
Electricity for electricity, heat, cold storage + DR	31,998	98	12,854	82	41
Electricity for H_2 direct use + H_2 storage	1,903	8	1,664	19	3

A2. Total end use demand	**61,207**	**212**	**24,705**	**198**	**78**
Electricity for direct use, electricity storage, + H_2	55,335	197	19,675	186	67
Low-T heat load met by heat storage	5,607.6	13.7	4,757	12.3	11.7
Cold load met by cold storage	264	1	272	0	0
A3. Total end use demand	**61,207**	**212**	**24,705**	**198**	**78**
Electricity for direct use, electricity storage, DR	52,834	186	17,346	165	60
Electricity for H_2 direct use + H_2 storage	1,903	8	1,664	19	3
Electricity + heat for heat subject to storage	5,746	16	5,029	14	15
Electricity for cold load subject to storage	725	3	666	1	1
B. Total losses	**23,521.57**	**67.64**	**5,710.23**	**58.57**	**7.53**
Transmission, distribution, downtime losses	5,798.30	16.06	2,031.65	14.05	6.45
Losses CSP storage	14.28	0.17	1.09	0.11	0.00
Losses PHS storage	69.7	3.9	172.8	3.1	0.0
Losses battery storage	17.5	1.4	9.5	1.0	0.0
Losses CW-STES + ICE storage	47.69	0.15	49.21	0.05	0.02
Losses HW-STES storage	813.8	1.4	818.1	1.3	0.1
Losses UTES storage	1,043	6	415	5	0
Losses from shedding	15,717.6	39.1	2,212.9	34.4	0.9
Net end-use demand plus losses (A1 + B)	***84,728***	***280***	***30,415***	***257***	***86***
C. Total WWS supply before T&D losses	**84,741**	**280**	**30,427**	**257**	**86**
Onshore + offshore wind electricity	49,831.8	123.8	18,554	90.4	14.9
Rooftop + utility PV+ CSP electricity	30,071.5	152.3	8,949	140.4	0.0
Hydropower electricity	4,375.88	1.04	2,409	10.13	35.65
Wave electricity	31.78	2.28	96.68	0.00	0.36
Geothermal electricity	43.83	0.00	71.71	15.67	21.65
Tidal electricity	18.69	0.29	93.15	0.30	0.38
Solar heat	253.41	0.00	110.61	0.00	0.00
Geothermal heat	114.41	0.00	142.77	0.00	13.05
D. Net taken from (+) or added to (-) storage	**-12.80**	**-0.05**	**-12.52**	**0.02**	**0.01**
CSP storage	-0.27	0.01	-0.05	0.01	0.00
PHS storage	-0.16	0.00	-0.28	0.02	0.00
Battery storage	-0.50	-0.05	-0.23	-0.02	0.00
CW-STES+ICE storage	0	0	0	0	0
HW-STES storage	2.076	0.006	0.311	0.005	0.005
UTES storage	-13.678	-0.01	-12.164	0.011	0
H_2 storage	-0.23	-0.005	-0.077	-0.003	0.002
Energy supplied plus taken from storage (C+D)	***84,728***	***280***	***30,415***	***257***	***86***

	India	Israel	Jamaica	Japan	Mauritius
A1. Total end use demand	**24,838**	**337**	**60**	**4,678**	**47**
Electricity for electricity inflexible demand	11,528	168	26	2,454	20
Electricity for electricity, heat, cold storage + DR	12,099	142	27	1,971	18
Electricity for H_2 direct use + H_2 storage	1,211	27	6	253	9
A2. Total end use demand	**24,838**	**337**	**60**	**4,678**	**47**
Electricity for direct use, electricity storage, + H_2	23,301	297	58	4,290	46
Low-T heat load met by heat storage	1499.3	37.1	1.3	372.1	0.9
Cold load met by cold storage	38	3	0	16	0
A3. Total end use demand	**24,838**	**337**	**60**	**4,678**	**47**
Electricity for direct use, electricity storage, DR	21,963	264	52	4,002	35
Electricity for H_2 direct use + H_2 storage	1,211	27	6	253	9
Electricity + heat for heat subject to storage	1,516	39	1	378	3
Electricity for cold load subject to storage	148	7	0	46	0

B. Total losses	**14,398**	**404**	**27.6**	**2,760**	**8.77**
Transmission, distribution, downtime losses	2562.78	49.12	4.65	547.97	3.13
Losses CSP storage	31.48	0.23	0.04	0.00	0.03
Losses PHS storage	64.6	15.8	2.3	33.7	3.0
Losses battery storage	450.2	2.1	0.0	0.4	0.0
Losses CW-STES + ICE storage	6.82	0.45	0.00	2.86	0.00
Losses HW-STES storage	212.3	4.5	0.3	61.0	0.1
Losses UTES storage	355	9	0	47	0
Losses from shedding	10714.9	322.9	20.4	2067.1	2.1
Net end-use demand plus losses (A1 + B)	***39,236***	***741***	***87***	***7,438***	***56***
C. Total WWS supply before T&D losses	**39,229**	**741**	**87**	**7,439**	**56**
Onshore + offshore wind electricity	9109.7	72.7	27.8	4479.7	12.9
Rooftop + utility PV+ CSP electricity	29294.7	664.7	59.1	2565.2	41.5
Hydropower electricity	784.43	0.10	0.25	281.88	0.76
Wave electricity	17.75	0.00	0.00	47.14	0.50
Geothermal electricity	6.31	0.00	0.00	34.89	0.00
Tidal electricity	4.46	0.06	0.11	14.37	0.04
Solar heat	5.62	3.01	0.00	1.59	0.00
Geothermal heat	6.33	0.53	0.00	13.98	0.00
D. Net taken from (+) or added to (-) storage	**6.67**	**0.12**	**-0.01**	**-0.54**	**0.13**
CSP storage	4.65	0.04	0.00	0.00	0.00
PHS storage	0.38	0.13	0.00	-0.25	0.05
Battery storage	2.17	-0.03	0.00	-0.11	0.00
CW-STES+ICE storage	0	0	0	0	0
HW-STES storage	3.117	0.047	0	0.373	0.002
UTES storage	-3.552	-0.136	-0.001	-0.58	0.014
H_2 storage	-0.096	0.068	-0.002	0.034	0.058
Energy supplied plus taken from storage (C+D)	***39,236***	***741***	***87***	***7,438***	***56***

	Mideast	New Zealand	Philip-pines	Russia	South America
A1. Total end use demand	**17,814**	**462**	**1,064**	**6,216**	**12,858**
Electricity for electricity inflexible demand	8,330	239	501	2,346	6,001
Electricity for electricity, heat, cold storage + DR	8,259	193	455	3,554	5,922
Electricity for H_2 direct use + H_2 storage	1,225	30	108	316	935
A2. Total end use demand	**17,814**	**462**	**1,064**	**6,216**	**12,858**
Electricity for direct use, electricity storage, + H_2	16,788	440	986	4,881	12,211
Low-T heat load met by heat storage	997.7	22.0	76.2	1290.1	617.5
Cold load met by cold storage	28	0	1	45	30
A3. Total end use demand	**17,814**	**462**	**1,064**	**6,216**	**12,858**
Electricity for direct use, electricity storage, DR	15,510	410	875	4,437	11,204
Electricity for H_2 direct use + H_2 storage	1,225	30	108	316	935
Electricity + heat for heat subject to storage	1,014	22	77	1,369	631
Electricity for cold load subject to storage	65	1	4	95	89
B. Total losses	10,331	125.41	296.67	1,045	1,821
Transmission, distribution, downtime losses	1,916	40.45	74.64	495	976
Losses CSP storage	7.14	0.07	0.39	0.10	4.28
Losses PHS storage	12.2	4.7	35.6	12.0	35.0
Losses battery storage	38.8	0.3	2.8	0.2	1.6
Losses CW-STES + ICE storage	5.13	0.04	0.20	8.11	5.45
Losses HW-STES storage	144.9	2.7	4.6	185.7	107.2

Losses UTES storage	201	5	33	273	65
Losses from shedding	8,006	72.6	145.8	70.0	626.8
Net end-use demand plus losses (A1 + B)	28,146	587	1,360	7,261	14,680
C. Total WWS supply before T&D losses	**28,133**	**587**	**1,359**	**7,203**	**14,678**
Onshore + offshore wind electricity	13,581	292	312	4,979	7,349
Rooftop + utility PV+ CSP electricity	13,860	167	846	1,496	4,609
Hydropower electricity	620	73.5	50.0	666	2,483
Wave electricity	6.81	3.82	6.85	33.11	92.39
Geothermal electricity	29.6	46.5	129	114	124
Tidal electricity	1.74	1.27	3.08	2.23	7.72
Solar heat	12.8	0.00	11.9	12.4	8.13
Geothermal heat	20.3	3.12	0.02	2.44	3.74
D. Net taken from (+) or added to (-) storage	**13.01**	**-0.16**	**1.00**	**58.14**	**2.00**
CSP storage	2.21	0.00	0.02	-0.02	0.75
PHS storage	-0.01	-0.01	-0.03	-0.07	0.25
Battery storage	-0.47	-0.01	-0.02	-0.02	0.02
CW-STES+ICE storage	0	0	0	0	0
HW-STES storage	1.104	-0.002	0.021	0.854	0.654
UTES storage	6.28	-0.129	1.035	50.133	-0.474
H_2 storage	3.88	-0.008	-0.037	7.272	0.768
Energy supplied plus taken from storage (C+D)	***28,146***	***587***	***1,360***	***7,261***	***14,680***

	Southeast Asia	South Korea	Taiwan	United States	All Regions
A1. Total end use demand	**15,333**	**4,080**	**2,495**	**24,696**	**228,521**
Electricity for electricity inflexible demand	6,796	2,074	1,145	11,465	**103,757**
Electricity for electricity, heat, cold storage + DR	7,011	1,785	1,202	11,180	**111,022**
Electricity for H_2 direct use + H_2 storage	1,525	221	148	2,051	**13,742**
A2. Total end use demand	**15,333**	**4,080**	**2,495**	**24,696**	**228,521**
Electricity for direct use, electricity storage, + H_2	14,362	3,753	2,351	22,027	**206,157**
Low-T heat load met by heat storage	940.5	307.0	138.0	2,514	**21,394**
Cold load met by cold storage	30	20	6	155	**970**
A3. Total end use demand	15,333	4,080	2,495	24,696	**228,521**
Electricity for direct use, electricity storage, DR	12,763	3,509	2,175	19,720	**190,152**
Electricity for H_2 direct use + H_2 storage	1,525	221	148	2,051	**13,742**
Electricity + heat for heat subject to storage	943	309	147	2,529	**22,055**
Electricity for cold load subject to storage	101	41	25	395	**2,573**
B. Total losses	4,667	2,856	637	12,111	**88,085**
Transmission, distribution, downtime losses	1,227	482	207	2,587	**21,231**
Losses CSP storage	40.80	1.09	0	4.00	**113**
Losses PHS storage	77.8	63.9	59.3	69.4	**835**
Losses battery storage	51.6	7.7	11.0	27.1	**704**
Losses CW-STES + ICE storage	5.38	3.59	1.08	28.0	**175**
Losses HW-STES storage	148.9	47.0	18.7	464	**3,346**
Losses UTES storage	167	57	34	102	**3,318**
Losses from shedding	2948.6	2193.0	305.8	8,828	**58,364**
Net end-use demand plus losses (A1 + B)	***20,000***	***6,936***	***3,132***	***36,807***	***316,606***
C. Total WWS supply before T&D losses	**19,989**	**6,937**	**3,125**	**36,807**	**316,514**
Onshore + offshore wind electricity	2,683	3,781	1,083	22,124	**156,798**
Rooftop + utility PV+ CSP electricity	16,304	3,056	1,186	12,978	**139,634**
Hydropower electricity	604	88.7	32.2	1,170	**15,893**

Wave electricity	74.5	0	3.99	255	**839**
Geothermal electricity	318	0	820	153	**2,261**
Tidal electricity	4.68	6.61	0.18	2.24	**191**
Solar heat	0.00	0	0.90	13.85	**449**
Geothermal heat	1.04	5.35	0	111	**450**
D. Net taken from (+) or added to (-) storage	**10.30**	**-1.29**	**6.10**	**-0.26**	**92**
CSP storage	7.30	-0.04	0	-0.21	**15**
PHS storage	0.56	-0.14	0.44	-0.13	**1**
Battery storage	0.19	-0.37	-0.18	-0.64	**0**
CW-STES+ICE storage	0	0	0	-0.021	**0**
HW-STES storage	0.788	-0.03	0.213	2.331	**13**
UTES storage	0.999	-0.548	5.019	-1.344	**49**
H_2 storage	0.404	-0.161	0.606	-0.244	**13**
Energy supplied plus taken from storage (C+D)	***20,000***	***6,936***	***3,132***	***36,807***	***316,606***

End-use demands in A1, A2, A3 should be identical. Transmission/distribution/maintenance losses are given in Table S14. Round-trip storage efficiencies are given in Table S13. Generated electricity is shed when it exceeds the sum of electricity demand, cold storage capacity, heat storage capacity, and H_2 storage capacity. Onshore and offshore wind turbines in the climate model are assumed to be Senvion (formerly Repower) 5 MW turbines with 126-m diameter rotors, 100 m hub heights, a cut-in wind speed of 3.5 m/s, and a cut-out wind speed of 30 m/s. Rooftop PV panels in GATOR-GCMOM were modeled as fixed-tilt panels at the optimal tilt angle of the country they resided in; utility PV panels were modeled as half fixed optimal tilt and half single-axis horizontal tracking[45]. All panels were assumed to have a nameplate capacity of 390 W and a panel area of 1.629668 m^2, which gives a 2050 panel efficiency (Watts of power output per Watt of solar radiation incident on the panel) of 23.9%, which is an increase from the 2015 value of 20.1%. Each CSP plant before storage is assumed to have the mirror and land characteristics of the Ivanpah solar plant, which has 646,457 m^2 of mirrors and 2.17 km^2 of land per 100 MW nameplate capacity and a CSP efficiency (fraction of incident solar radiation that is converted to electricity) of 15.796%, calculated as the product of the reflection efficiency of 55% and the steam plant efficiency of 28.72%. The efficiency of the solar thermal for heat hot fluid collection (energy in fluid divided by incident radiation) is 34%.

Table S25. Footprint and spacing areas per MW of nameplate capacity and installed power densities for WWS electricity or heat generation technologies.

WWS technology	Footprint (m^2/MW)	Spacing (km^2/MW)	Installed power density (MW/km^2)
Onshore wind	3.22	0.051	19.8
Offshore wind	3.22	0.139	7.2
Wave device	700	0.033	30.3
Geothermal plant	3,290	0	304
Hydropower plant	502,380	0	2.0
Tidal turbine	290	0.004	250
Residential roof PV	5,230	0	191
Commercial/govt. roof PV	5,230	0	191
Solar PV plant	12,220	0	81.8
Utility CSP plant	29,350	0	34.1
Solar thermal for heat	1,430	0	700

From Jacobson et al.[5], except that spacing areas for onshore and offshore wind are calculated assuming 20 MW/km^2 for onshore wind and 7.2 MW/km^2 for offshore wind, based on data for Europe and outside of Europe[129], and the footprint area for solar thermal for heat is from Jacobson et al.[16]. The installed power density is the inverse of either the spacing or, if spacing is zero, the footprint of the technology.

Table S26. Spacing areas for new onshore wind turbines, and footprint areas for new utility PV, CSP, solar thermal for heat, geothermal for electricity and heat, and hydropower in each grid region. Spacing areas are areas between wind turbines needed to avoid interference of the wake of one turbine with the next. Such spacing area can be used for multiple purposes, including farmland, rangeland, open space, or utility PV. Footprint areas are land areas on the ground that cannot be used for multiple purposes. Rooftop PV is not included because it does not take up new land. Conventional hydro new footprint is zero because no new dams are proposed as part of these roadmaps. Offshore wind, wave, and tidal are not included because they don't take up new land. Table S25 gives the installed power densities assumed. Areas are given both as an absolute area and as a percentage of the region land area, which excludes inland or coastal water bodies. For comparison, the total area and land area of Earth are 510.1 and 144.6 million km^2, respectively.

Region	Region land area (km^2)	Footprint Area (km^2)	Spacing area (km^2)	Footprint area as percentage of region land area (%)	Spacing area as a percentage of region land area (%)
Africa	22,988,130	6,614	38,826	0.029	0.169
Australia	7,682,300	2,788	4,535	0.036	0.059
Canada	9,093,510	425	8,697	0.005	0.096
Central America	2,429,460	1,516	17,560	0.062	0.723
Central Asia	4,697,670	2,539	9,163	0.054	0.195
China	11,063,254	41,747	178,549	0.377	1.614
Cuba	106,440	123	624	0.116	0.586
Europe	5,671,860	10,692	52,594	0.189	0.927
Haiti	75,880	96	307	0.126	0.405
Iceland	100,250	0	61	0.000	0.061
India	3,179,250	45,238	48,057	1.423	1.512
Israel	21,640	998	131	4.612	0.604
Jamaica	10,830	46	19	0.428	0.178
Japan	364,560	5,307	4,535	1.456	1.244
Mauritius	2,040	48	4	2.354	0.185
Mideast	6,327,218	21,307	50,798	0.337	0.803
New Zealand	263,310	243	1,077	0.092	0.409
Philippines	298,170	757	845	0.254	0.284
Russia	16,446,360	1,804	17,789	0.011	0.108
South America	17,176,021	4,991	65,518	0.029	0.382
Southeast Asia	3,927,017	25,423	2,677	0.647	0.068
South Korea	97,350	6,320	485	6.492	0.498
Taiwan	36,193	1,682	193	4.646	0.533
United States	9,147,420	20,501	78,616	0.224	0.859
All regions	**121,206,133**	**201,205**	**581,660**	**0.166**	**0.480**

Table S27. Estimated mean number of long-term, full-time construction and operation jobs per MW nameplate capacity of different electric power sources and storage types in the United States. A full-time job is a job that requires 2,080 hours per year of work. The job numbers include direct, indirect, and induced jobs.

Electric power generator	Construction Jobs/MW or Jobs/km	Operation Jobs/MW or Jobs/km
Onshore wind electricity	0.24	0.37
Offshore wind electricity	0.31	0.63
Wave electricity	0.15	0.57
Geothermal electricity	0.71	0.46
Hydropower electricity	0.14	0.30
Tidal electricity	0.16	0.61
Residential rooftop PV	0.88	0.32
Commercial/government rooftop PV	0.65	0.16
Utility PV electricity	0.24	0.85
CSP electricity	0.31	0.86
Solar thermal for heat	0.71	0.85
Geothermal heat	0.14	0.46
Pumped hydro storage (PHS)	0.77	0.3
CSP storage (CSP-PCM)	0.62	0.3
Battery storage	0.092	0.2
Chilled-water storage (CW-STES)	0.15	0.3
Ice storage (ICE)	0.15	0.3
Hot water storage (HW-STES)	0.15	0.3
Underground heat storage (UTES)	0.15	0.3
Hydrogen production and storage	0.32	0.3
AC transmission (jobs/km)	0.073	0.062
AC distribution (jobs/km)	0.033	0.028
HVDC transmission (jobs/km)	0.088	0.082

From Jacobson et al.[5], except storage values are estimated here. Values for onshore wind, offshore wind, wave, geothermal, hydropower, tidal, PV, and CSP were derived from NREL[123] JEDI models output. Values for solar thermal for heat and geothermal heat were taken from values for utility PV and geothermal electricity, respectively. Values for transmission were derived in Jacobson et al.[5]. The number of full-time construction jobs in Table S28 is the number of 1-year jobs divided by the lifetime (in years) of the device (Table S14). For transmission, the lifetime was assumed to be 70 y. Jobs for battery construction and operation were estimated low to account for economies of scale and automation of battery manufacturing.

Table S28. Estimated 143-country jobs created and lost due to transitioning from BAU energy to WWS across all energy sectors. The job creation accounts for new jobs in the electricity, heat, cold, and hydrogen generation, storage, and transmission (including HVDC transmission) industries. However, it does not account for changes in the numbers of jobs due to the production of electric appliances and machines or due to increasing building energy efficiency. Construction jobs are for new WWS devices only. Operation jobs are for new and existing devices. Jobs for electricity generation technologies are the number of long-term, full-time jobs per MW in each region multiplied by the "Total 2050" minus "Total 2018" nameplate capacities for each device from Table S20 for construction jobs and the "Total 2050" nameplate capacities alone for operation jobs. The jobs per MW for each device in each country is calculated with the methodology in Jacobson et al.[5] to scale U.S. jobs from Table S27 by year and country. For storage, the number of jobs per MW from Table S27 is multiplied by the maximum discharge rate of the storage technology for each region from Table S11. The transmission/distribution jobs are calculated in Jacobson et al.[41]. The losses are due to eliminating jobs for mining, transporting, processing, and using fossil fuels, biofuels, and uranium. Also shown is the percentage of total jobs in each sector that is lost. Fossil-fuel jobs due to non-energy uses of petroleum, such as lubricants, asphalt, petrochemical feedstock, and petroleum coke, are retained. For transportation sectors, the jobs lost are those due to transporting fossil fuels (e.g., through truck, train, barge, ship, or pipeline); the jobs not lost are those for transporting other goods. The table does not account for jobs lost in the manufacture of combustion appliances, including automobiles, ships, or industrial machines.

Energy sector	Number of jobs produced or lost	Percent of jobs in sector that are lost
WWS jobs created		
Construction jobs	**24,389,000**	
Generation	15,285,000	
Storage	8,159,000	
Transmission	945,000	
Operation jobs	**30,151,000**	
Generation	21,709,000	
Storage	7,697,000	
Transmission	745,000	
Total jobs produced	**54,540,000**	
BAU jobs lost		
Oil and gas extraction	2,217,000	89
Coal mining	1,257,000	96
Uranium mining	85,100	100
Support for oil and gas	3,329,000	89
Oil and gas pipeline construction	1,506,000	89
Mining & oil/gas machinery	1,074,000	89
Petroleum refining	651,000	94
Asphalt paving and roofing materials	0	0
Gas stations with stores	1,775,000	30
Other gas stations	420,000	50
Fossil electric power generation utilities	992,000	100
Fossil electric power generation non-utilities	302,000	100
Nuclear and other power generation	1,150,000	100
Natural gas distribution	1,169,000	100
Auto oil change shops/other repair	59,100	10
Rail transportation of fossil fuels	584,100	52
Water transportation of fossil fuels	279,000	23
Truck transportation of fossil fuels	863,000	8
Biofuel except electricity	6,682,000	100
Jobs lost from not increasing fossil fuel use[a]	1,488,000	
Total jobs lost	**25,892,000**	**0.70[b]**

Net jobs produced minus jobs lost	**28,648,000**	

[a]Jobs lost from not expanding fossil fuel production are additional refinery and electric power construction and operation jobs that would have accrued by 2050 if BAU instead of WWS continued.

[b]The total world labor force in 2015 was 3.47 billion.

Supplemental Figures

Figure S1. Timeline for 143 countries, representing more than 99.7 percent of world fossil-fuel CO_2 emissions, to transition from conventional fuels (BAU) to 100% wind-water-solar (WWS) in all energy sectors. Also shown are the annually averaged end-use power demand reductions that occur along the way. The energy sectors transitioned include the electricity, transportation, building heating/cooling, industrial, agriculture/forestry/fishing, and military sectors. The percentages next to each WWS energy source are the 2050 estimated percent supply of end-use power by the source. The 100 percent demarcation in 2050 indicates that 100 percent of end-use power in the annual average will be provided by WWS among all energy sectors by no later than 2050, but ideally sooner. An 80 percent transition is proposed to occur by no later than 2030. End-use power demand reductions occur for five reasons: (1) the efficiency of moving low-temperature building heat with heat pumps instead of creating heat with combustion; (2) the efficiency of electricity over combustion for high-temperature industrial heat; (3) the efficiency of electricity in battery-electric (BE) vehicles and in electrolytic hydrogen fuel cell (HFC) vehicles over combustion vehicles for transportation; (4) eliminating the energy to mine, transport, and process fossil fuels, biofuels, bioenergy, and uranium; and (5) improving end-use energy efficiency and reducing energy use beyond in the BAU case. The total demand reduction due to these factors is 57.1 percent.

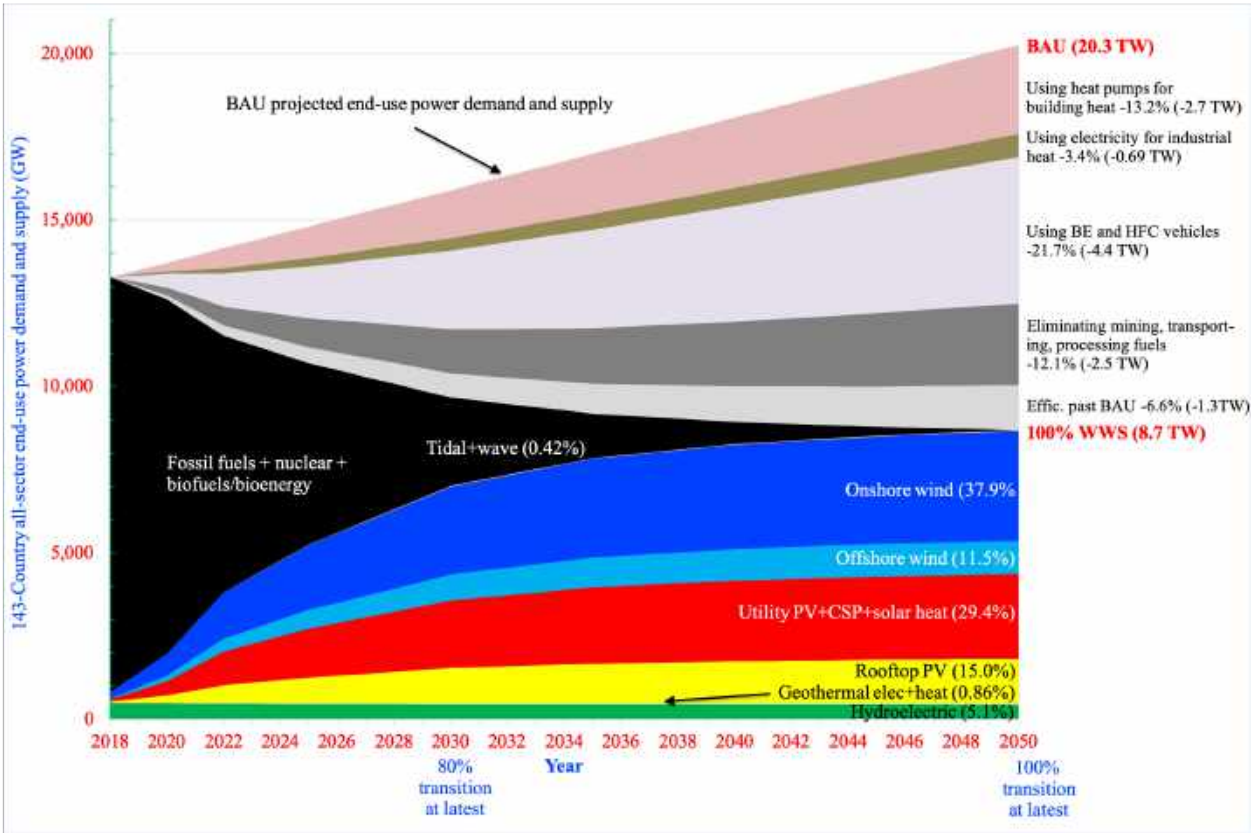

Figure S2. Number of cooling degree days (CDD) and heating degree days (HDD), in °C, averaged over two years (either 2013 and 2014 or 2017 and 2018) for 24 world regions, defined in Table 1. The reference temperature was 18.33 °C (65 °F). From Bizee[130]. For individual countries, the values are from one location in the country. For grid regions, they are a weighted average of all countries in the region, where the weighting is based on the end-use power demand in the country (Table S2).

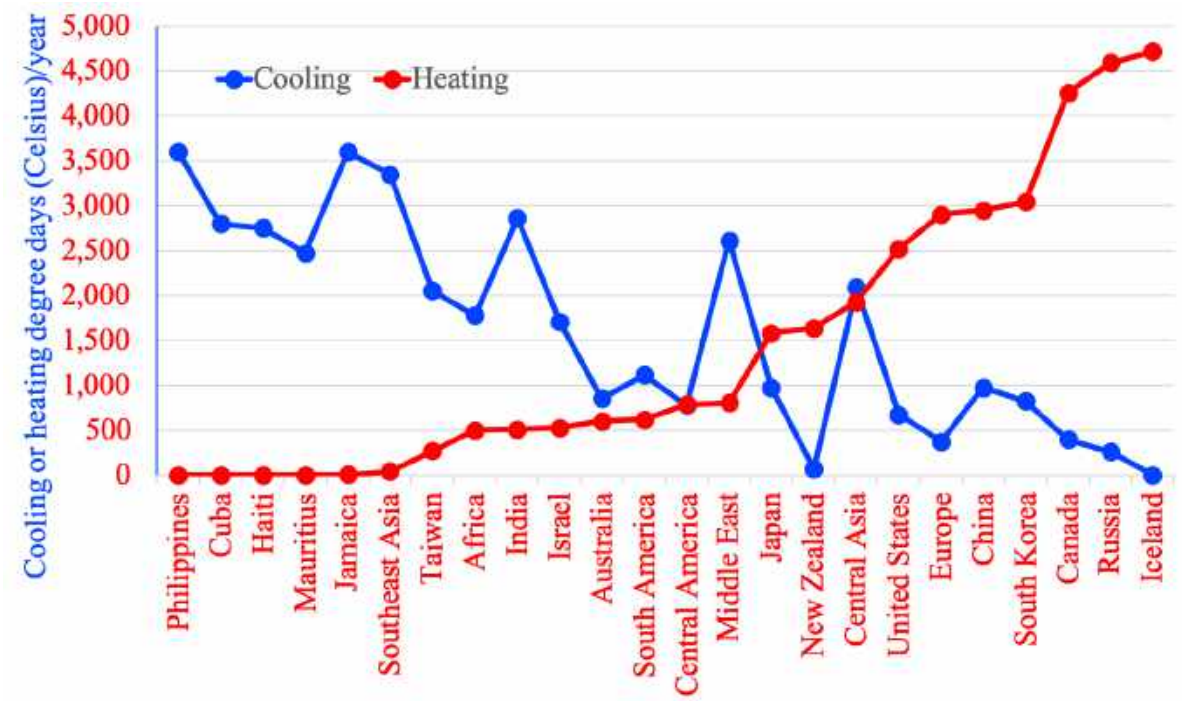

Figure S3. Top: Annual average end-use 2050 WWS total load (GW) in 24 world regions, broken down by energy-use sector. Bottom: Annual average end-use 2050 WWS total load broken into inflexible and flexible load, with flexible load broken into low-temperature heat load subject to storage (warm storage), cold load subject to storage (cold load), hydrogen load, and load subject to demand response.

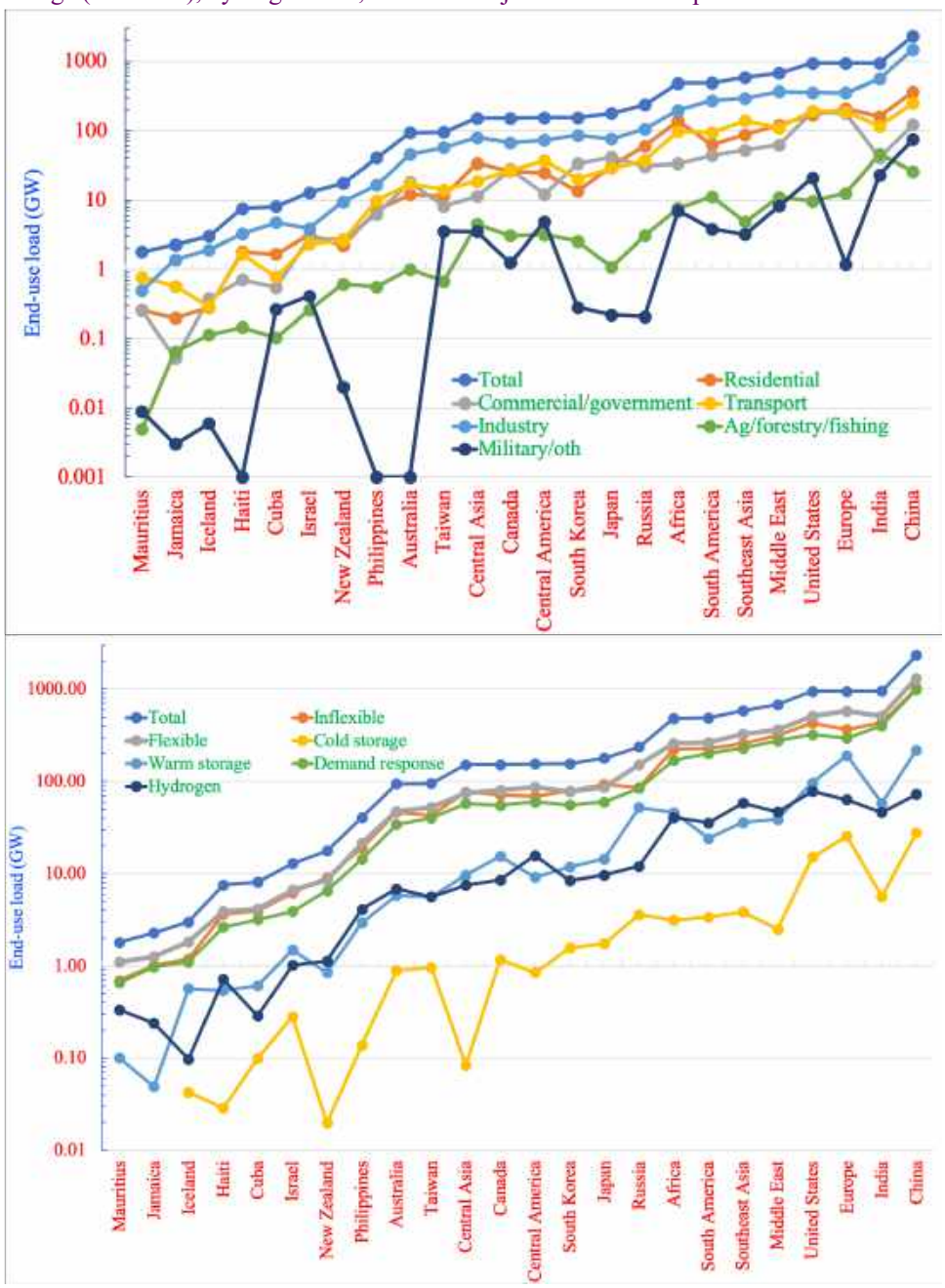

Figure S4. Time-series comparison, from 2050 to 2052, for 24 world regions defined in Table 1. First row: modeled time-dependent total WWS power generation versus load plus losses plus changes in storage plus shedding. Second row: same as first row, but for a window of days 400 to 500 during the three-year period. Third row: a breakdown of WWS power generation by source during the window. Fourth row: a breakdown of inflexible load; flexible electric, heat, and cold load; flexible hydrogen load; losses in and out of storage; transmission and distribution losses; changes in storage; and shedding. The model was run at 30-s resolution. Results are shown hourly. No load loss occurred during any 30-s interval. This figure expands upon Figure 2 of the main text.

Africa

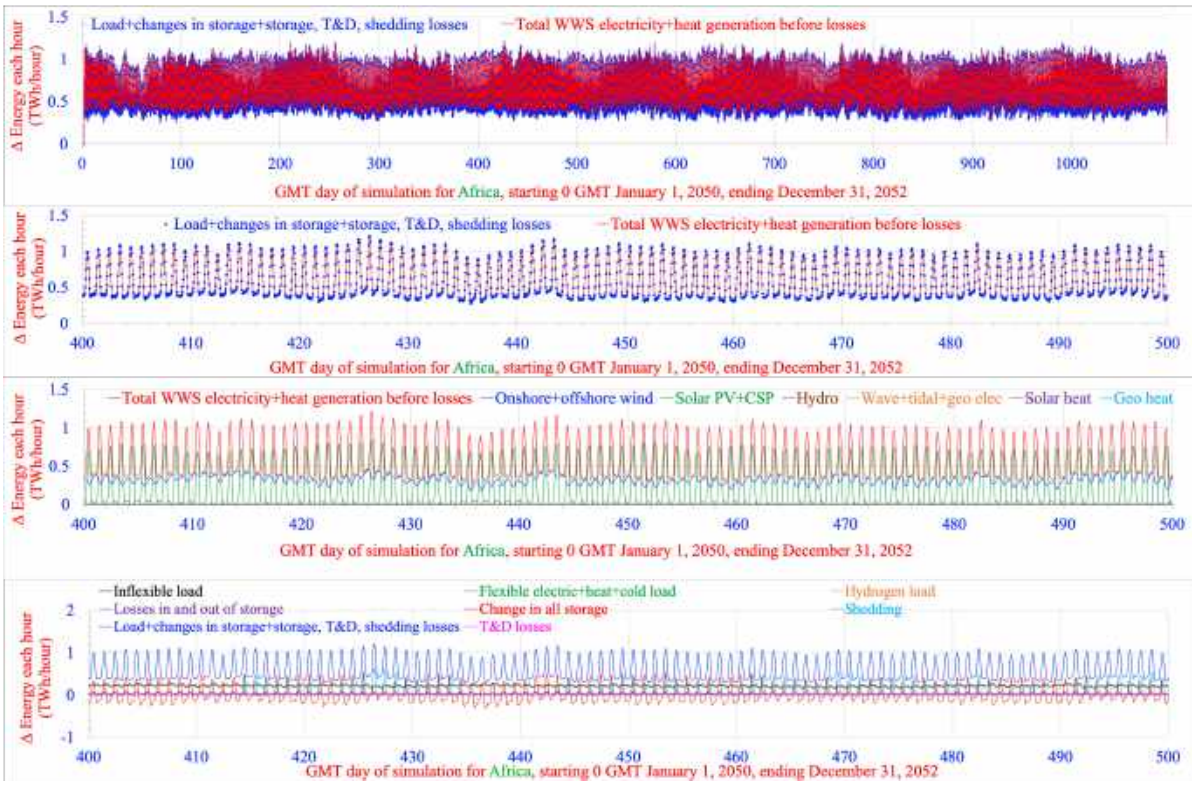

Australia

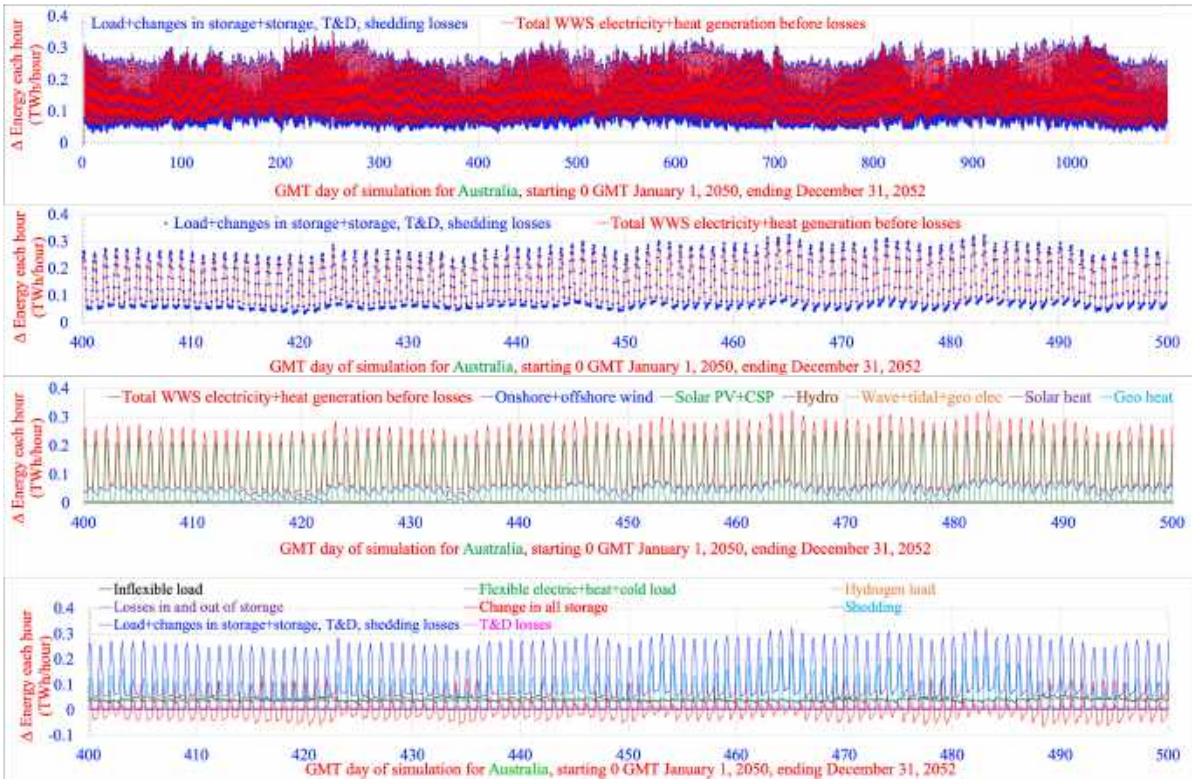
Δ Energy each hour (TWh/hour)
Load+changes in storage+storage, T&D, shedding losses
Total WWS electricity+heat generation before losses
GMT day of simulation for Australia, starting 0 GMT January 1, 2050, ending December 31, 2052
Load+changes in storage+storage, T&D, shedding losses
Total WWS electricity+heat generation before losses
GMT day of simulation for Australia, starting 0 GMT January 1, 2050, ending December 31, 2052
Total WWS electricity+heat generation before losses
Onshore+offshore wind
Solar PV+CSP
Hydro
Wave+tidal+geo elec
Solar heat
Geo heat
GMT day of simulation for Australia, starting 0 GMT January 1, 2050, ending December 31, 2052
Inflexible load
Losses in and out of storage
Load+changes in storage+storage, T&D, shedding losses
Flexible electric+heat+cold load
Change in all storage
T&D losses
Hydrogen load
Shedding
GMT day of simulation for Australia, starting 0 GMT January 1, 2050, ending December 31, 2052

Canada

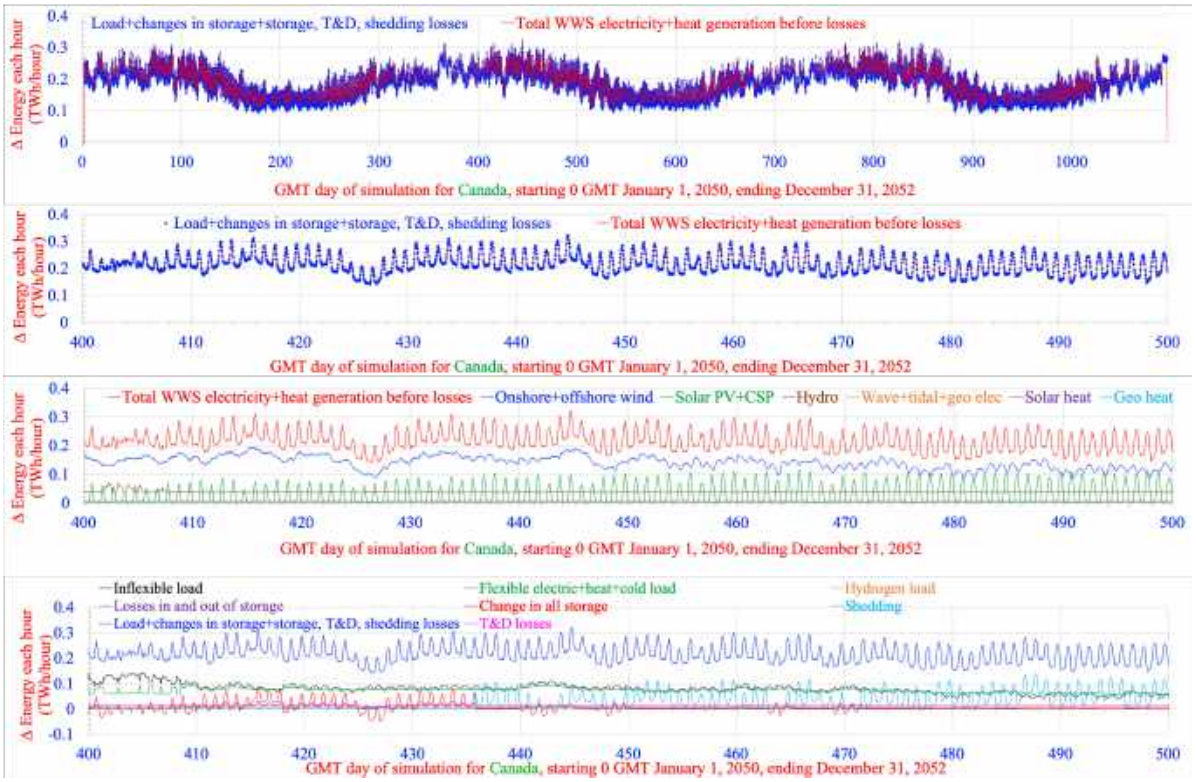
Load+changes in storage+storage, T&D, shedding losses
Total WWS electricity+heat generation before losses
Δ Energy each hour (TWh/hour)
GMT day of simulation for Canada, starting 0 GMT January 1, 2050, ending December 31, 2052
Total WWS electricity+heat generation before losses
Onshore+offshore wind
Solar PV+CSP
Hydro
Wave+tidal+geo elec
Solar heat
Geo heat
Inflexible load
Losses in and out of storage
Load+changes in storage+storage, T&D, shedding losses
Flexible electric+heat+cold load
Change in all storage
T&D losses
Hydrogen load
Shedding

Central America

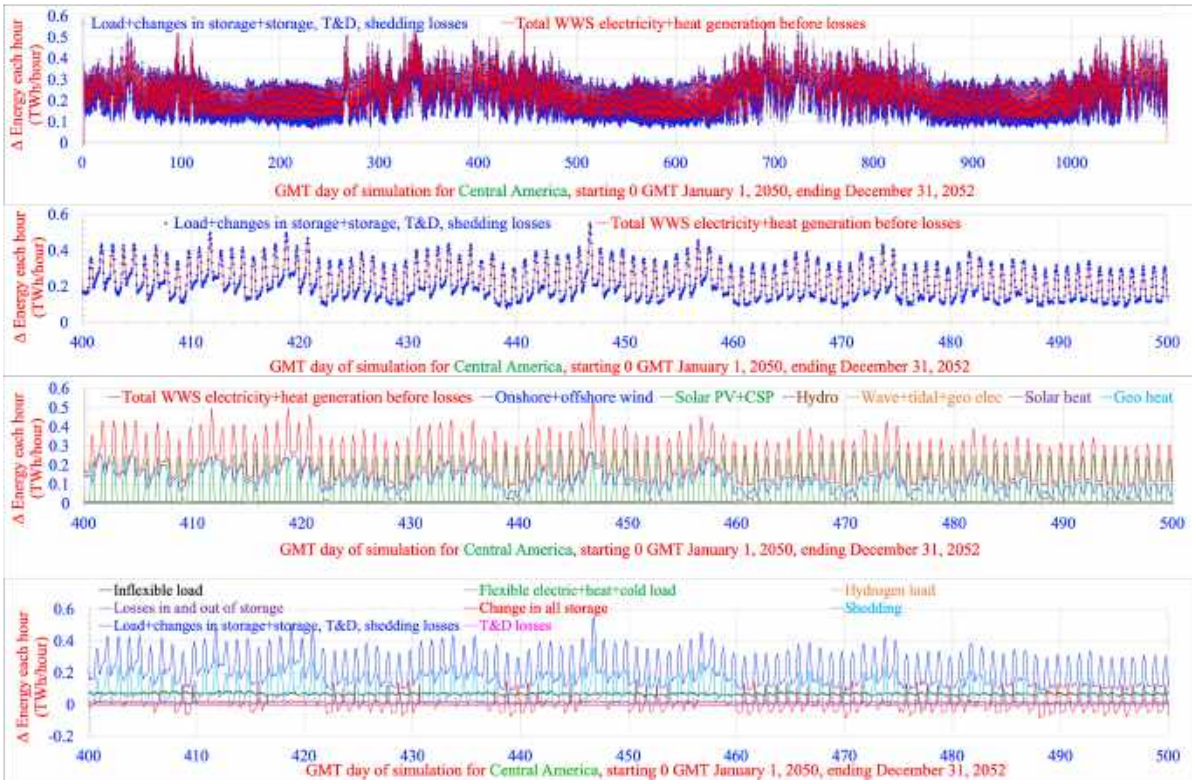

Central Asia

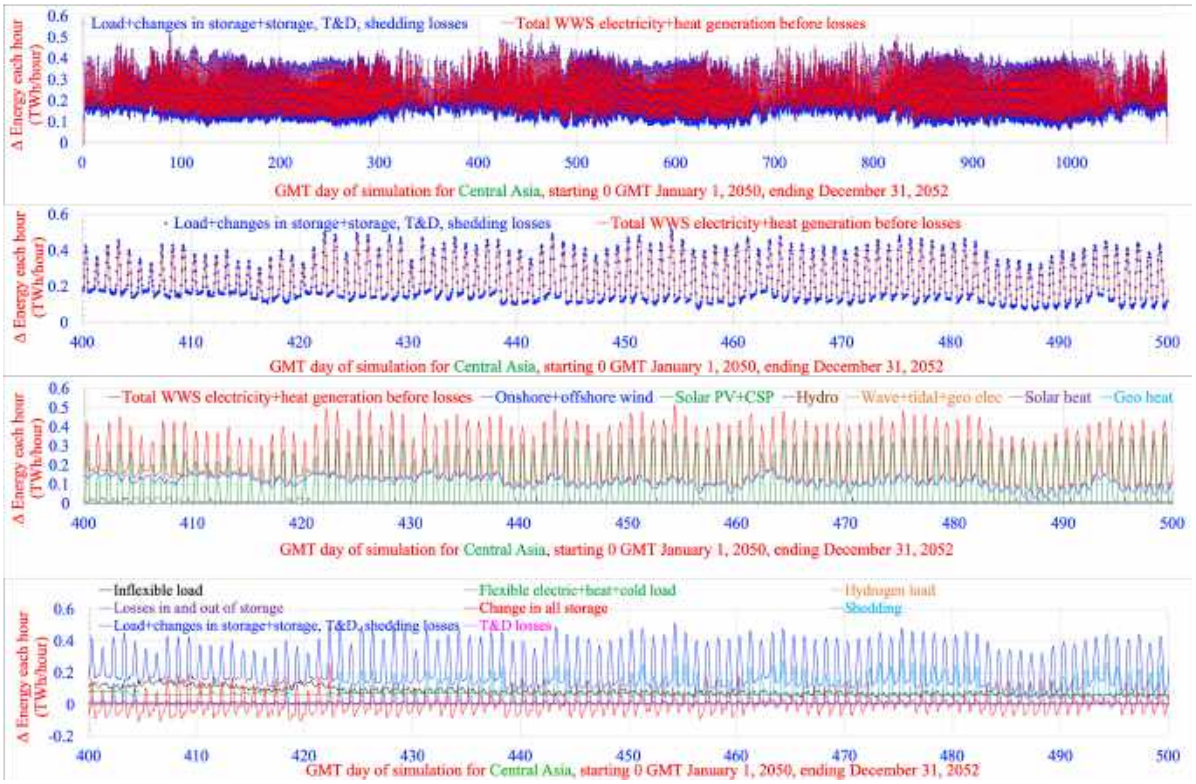

China Region

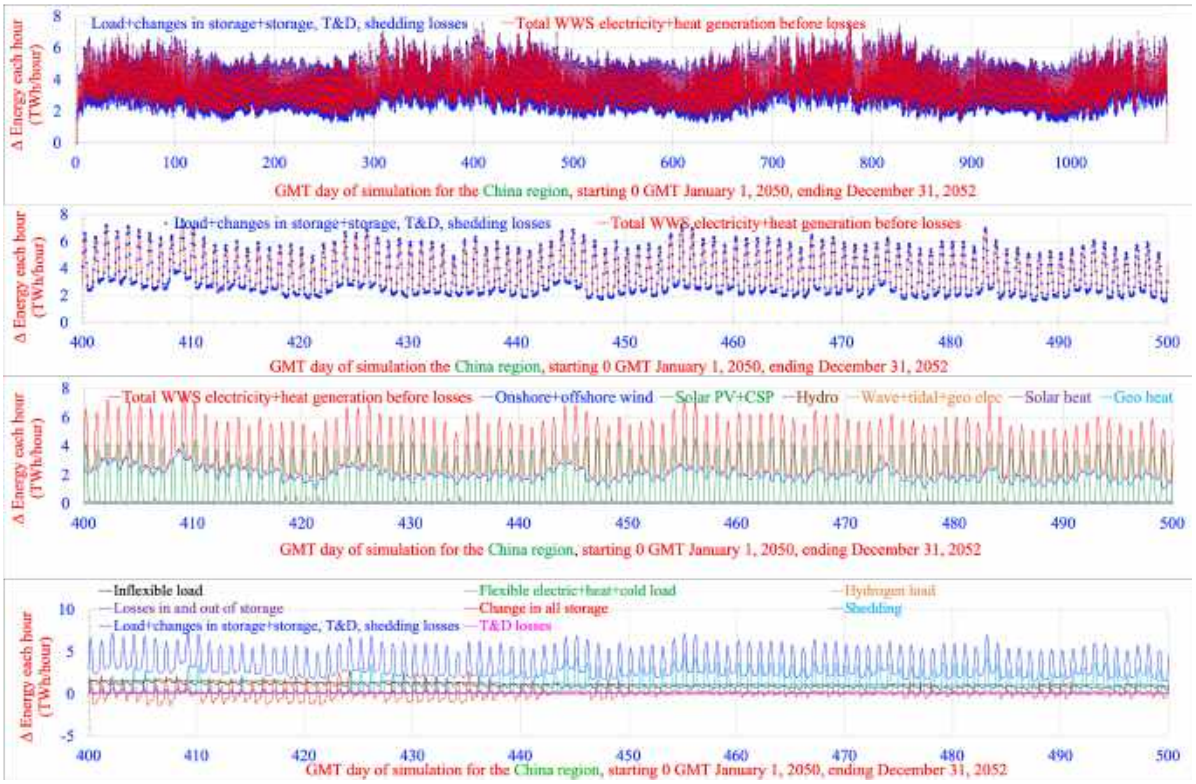

Cuba

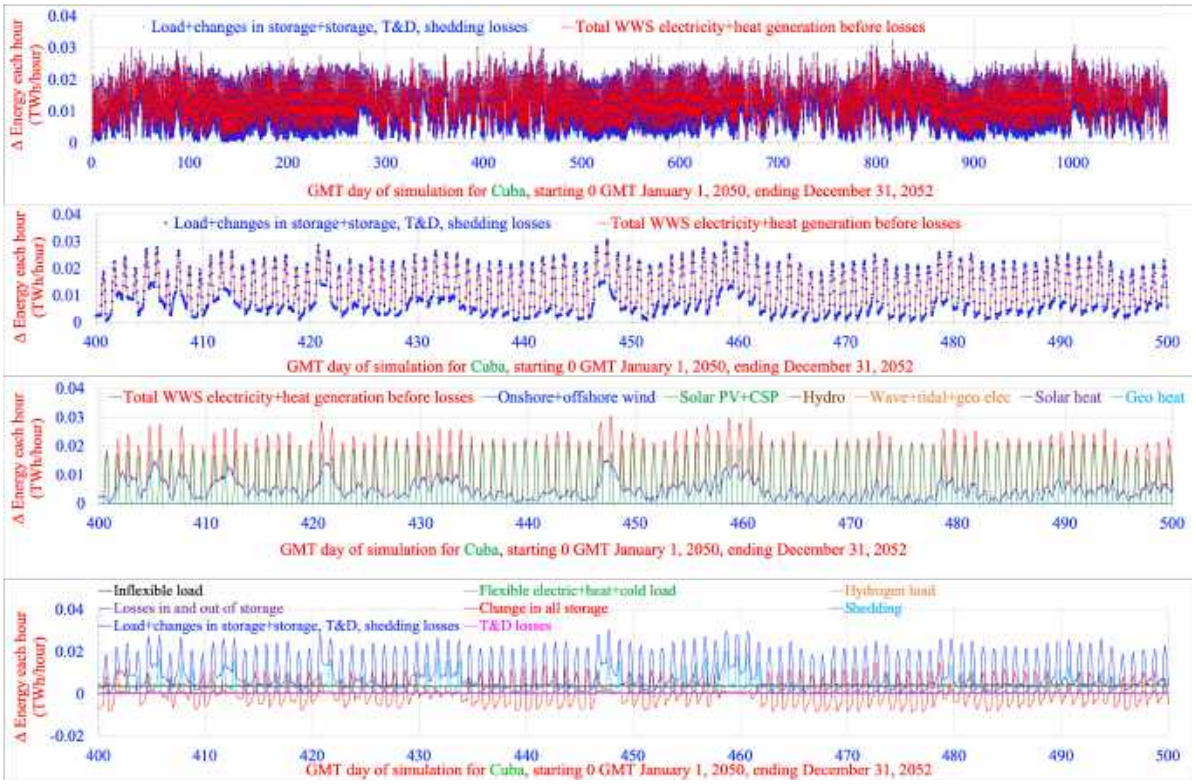
Load+changes in storage+storage, T&D, shedding losses
Total WWS electricity+heat generation before losses
Δ Energy each hour (TWh/hour)
GMT day of simulation for Cuba, starting 0 GMT January 1, 2050, ending December 31, 2052
Total WWS electricity+heat generation before losses
Onshore+offshore wind
Solar PV+CSP
Hydro
Wave+tidal+geo elec
Solar heat
Geo heat
Inflexible load
Flexible electric+heat+cold load
Hydrogen load
Losses in and out of storage
Change in all storage
Shedding
Load+changes in storage+storage, T&D, shedding losses
T&D losses

Europe

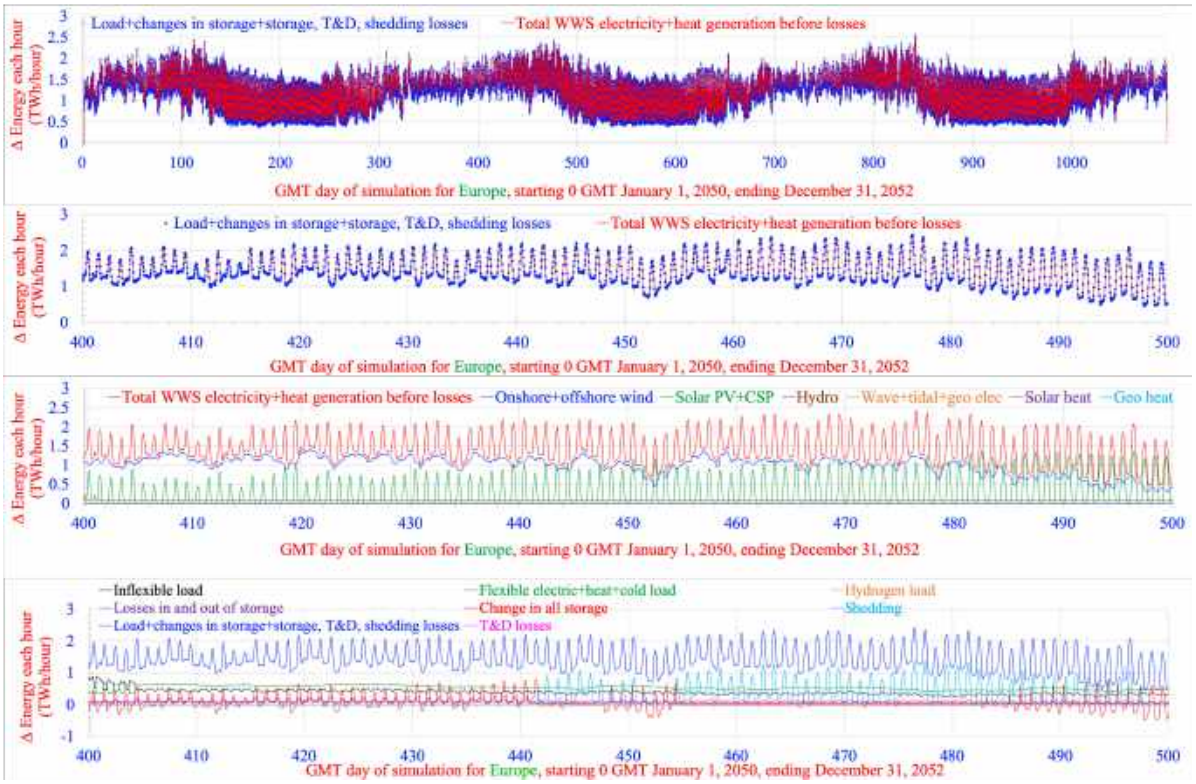
Load+changes in storage+storage, T&D, shedding losses
Total WWS electricity+heat generation before losses
Δ Energy each hour (TWh/hour)
GMT day of simulation for Europe, starting 0 GMT January 1, 2050, ending December 31, 2052
Load+changes in storage+storage, T&D, shedding losses
Total WWS electricity+heat generation before losses
Δ Energy each hour (TWh/hour)
GMT day of simulation for Europe, starting 0 GMT January 1, 2050, ending December 31, 2052
Total WWS electricity+heat generation before losses
Onshore+offshore wind
Solar PV+CSP
Hydro
Wave+tidal+geo elec
Solar heat
Geo heat
Δ Energy each hour (TWh/hour)
GMT day of simulation for Europe, starting 0 GMT January 1, 2050, ending December 31, 2052
Inflexible load
Flexible electric+heat+cold load
Hydrogen load
Losses in and out of storage
Change in all storage
Shedding
Load+changes in storage+storage, T&D, shedding losses
T&D losses
Δ Energy each hour (TWh/hour)
GMT day of simulation for Europe, starting 0 GMT January 1, 2050, ending December 31, 2052

Haiti-Dominican Republic

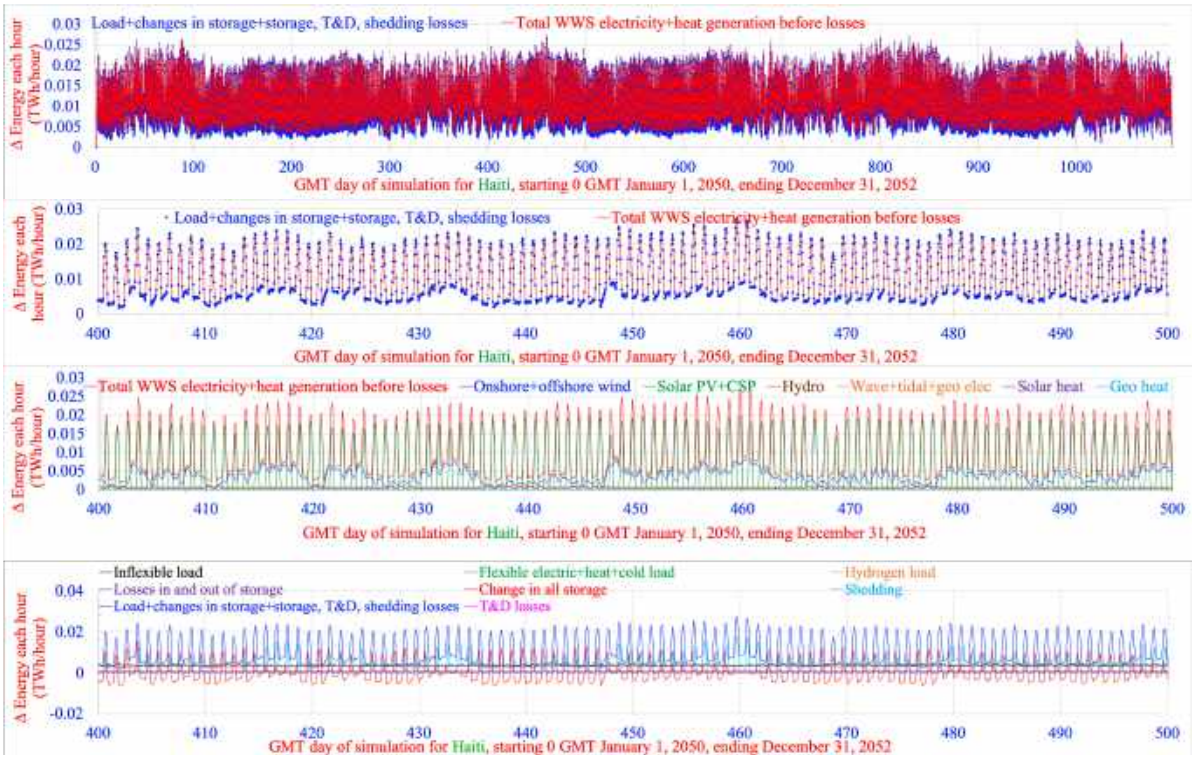

Iceland

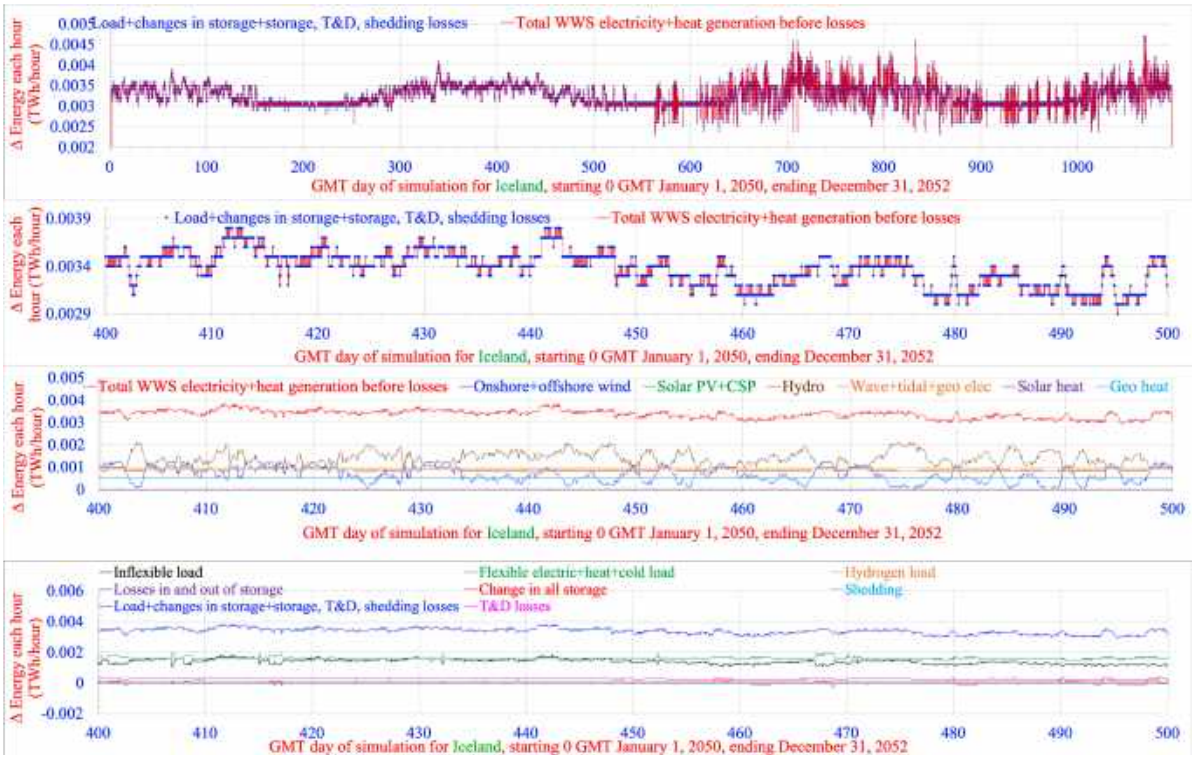
Load+changes in storage+storage, T&D, shedding losses
Total WWS electricity+heat generation before losses
Δ Energy each hour (TWh/hour)
GMT day of simulation for Iceland, starting 0 GMT January 1, 2050, ending December 31, 2052
Load+changes in storage+storage, T&D, shedding losses
Total WWS electricity+heat generation before losses
Δ Energy each hour (TWh/hour)
GMT day of simulation for Iceland, starting 0 GMT January 1, 2050, ending December 31, 2052
Total WWS electricity+heat generation before losses
Onshore+offshore wind
Solar PV+CSP
Hydro
Wave+tidal+geo elec
Solar heat
Geo heat
Δ Energy each hour (TWh/hour)
GMT day of simulation for Iceland, starting 0 GMT January 1, 2050, ending December 31, 2052
Inflexible load
Losses in and out of storage
Load+changes in storage+storage, T&D, shedding losses
Flexible electric+heat+cold load
Change in all storage
T&D losses
Hydrogen load
Shedding
Δ Energy each hour (TWh/hour)
GMT day of simulation for Iceland, starting 0 GMT January 1, 2050, ending December 31, 2052

India Region

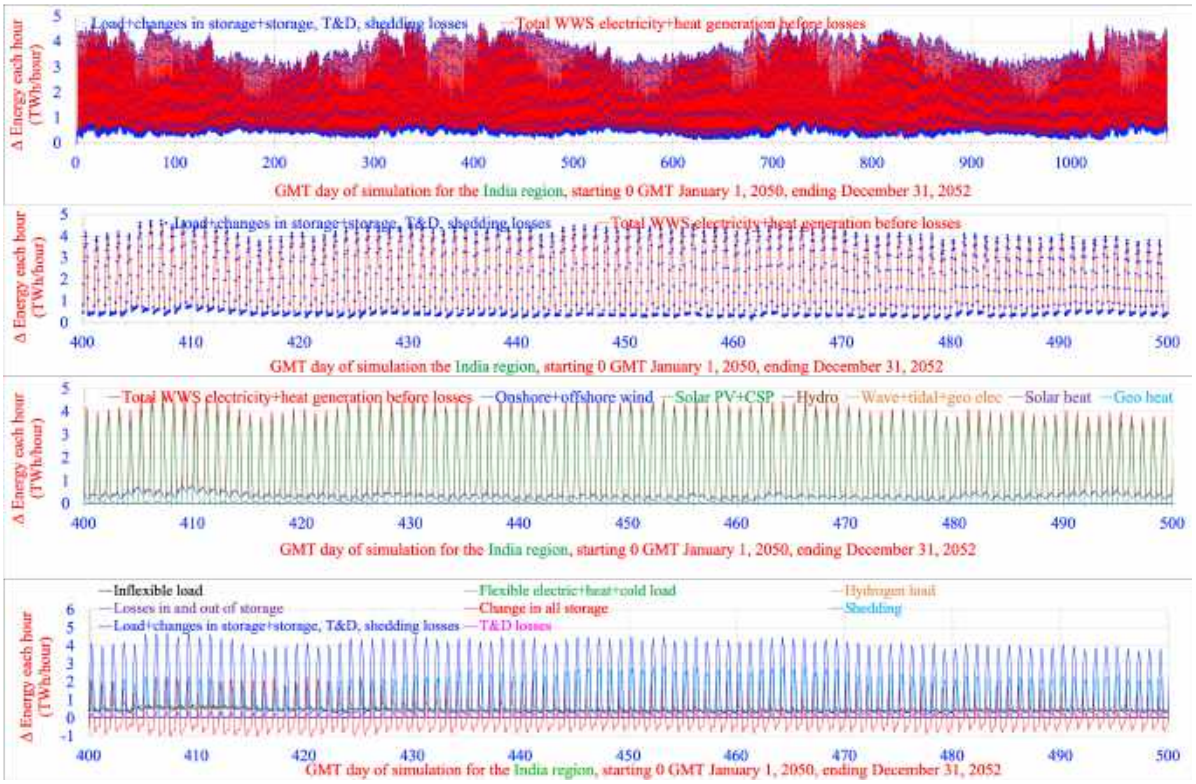

Israel

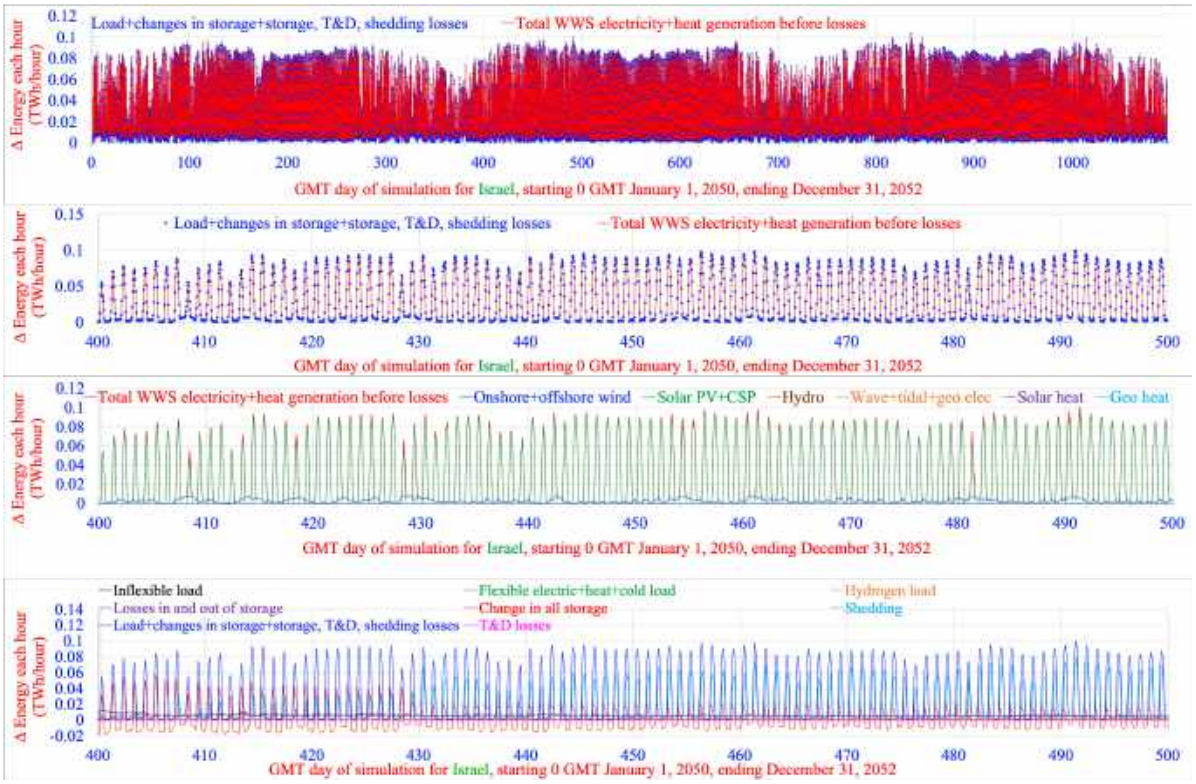
Load+changes in storage+storage, T&D, shedding losses
Total WWS electricity+heat generation before losses
Δ Energy each hour (TWh/hour)
GMT day of simulation for Israel, starting 0 GMT January 1, 2050, ending December 31, 2052
Load+changes in storage+storage, T&D, shedding losses
Total WWS electricity+heat generation before losses
Δ Energy each hour (TWh/hour)
GMT day of simulation for Israel, starting 0 GMT January 1, 2050, ending December 31, 2052
Total WWS electricity+heat generation before losses
Onshore+offshore wind
Solar PV+CSP
Hydro
Wave+tidal+geo elec
Solar heat
Geo heat
Δ Energy each hour (TWh/hour)
GMT day of simulation for Israel, starting 0 GMT January 1, 2050, ending December 31, 2052
Inflexible load
Losses in and out of storage
Load+changes in storage+storage, T&D, shedding losses
Flexible electric+heat+cold load
Change in all storage
T&D losses
Hydrogen load
Shedding
Δ Energy each hour (TWh/hour)
GMT day of simulation for Israel, starting 0 GMT January 1, 2050, ending December 31, 2052

Jamaica

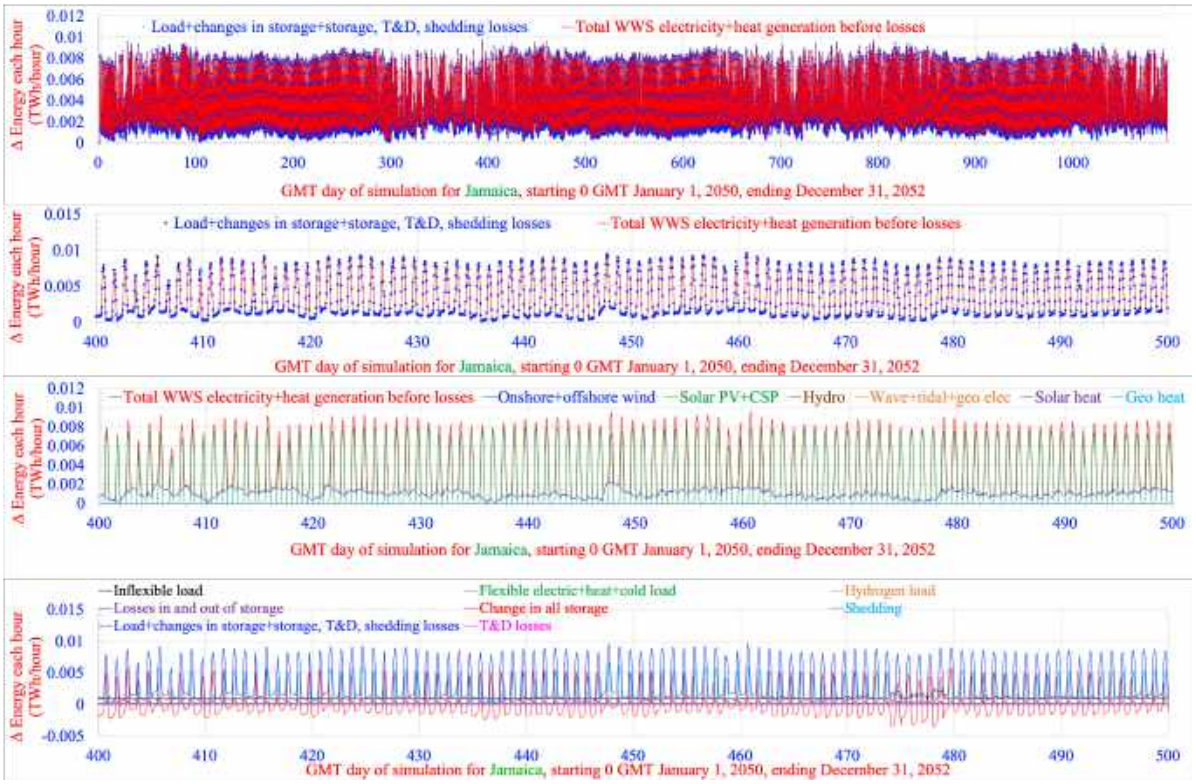
Δ Energy each hour (TWh/hour)
Load+changes in storage+storage, T&D, shedding losses
Total WWS electricity+heat generation before losses
GMT day of simulation for Jamaica, starting 0 GMT January 1, 2050, ending December 31, 2052
Onshore+offshore wind
Solar PV+CSP
Hydro
Wave+tidal+geo elec
Solar heat
Geo heat
Inflexible load
Losses in and out of storage
Flexible electric+heat+cold load
Change in all storage
Hydrogen load
Shedding
T&D losses

Japan

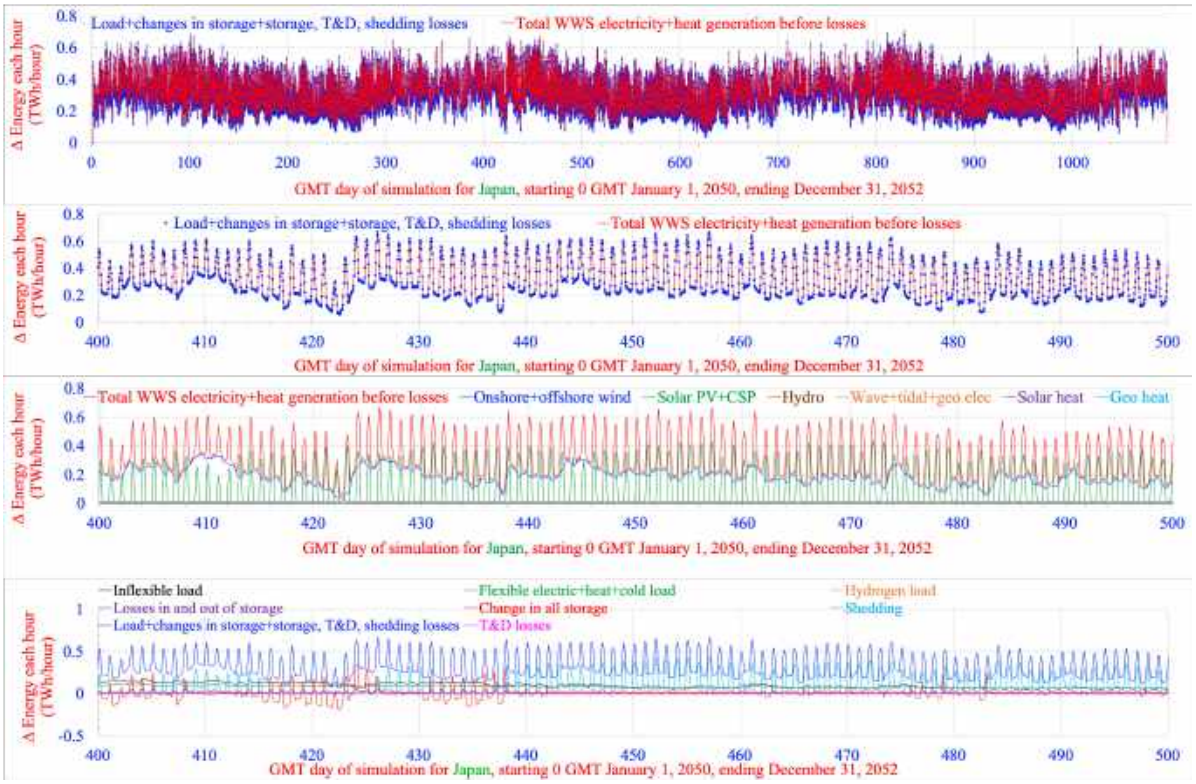
Δ Energy each hour (TWh/hour)
Load+changes in storage+storage, T&D, shedding losses
Total WWS electricity+heat generation before losses
GMT day of simulation for Japan, starting 0 GMT January 1, 2050, ending December 31, 2052
Total WWS electricity+heat generation before losses
Onshore+offshore wind
Solar PV+CSP
Hydro
Wave+tidal+geo elec
Solar heat
Geo heat
Inflexible load
Losses in and out of storage
Load+changes in storage+storage, T&D, shedding losses
Flexible electric+heat+cold load
Change in all storage
T&D losses
Hydrogen load
Shedding

Mauritius

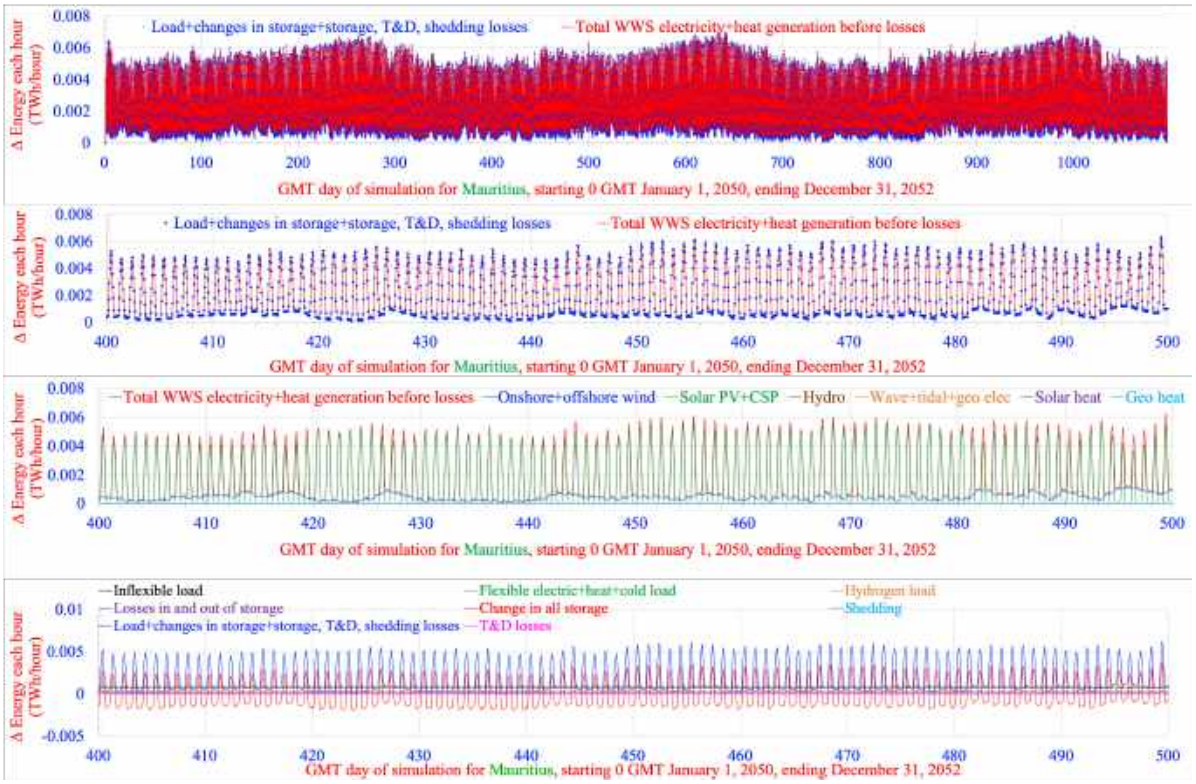
Δ Energy each hour (TWh/hour)
Load+changes in storage+storage, T&D, shedding losses
Total WWS electricity+heat generation before losses
GMT day of simulation for Mauritius, starting 0 GMT January 1, 2050, ending December 31, 2052
Total WWS electricity+heat generation before losses
Onshore+offshore wind
Solar PV+CSP
Hydro
Wave+tidal+geo elec
Solar heat
Geo heat
Inflexible load
Losses in and out of storage
Load+changes in storage+storage, T&D, shedding losses
Flexible electric+heat+cold load
Change in all storage
T&D losses
Hydrogen load
Shedding

Mideast

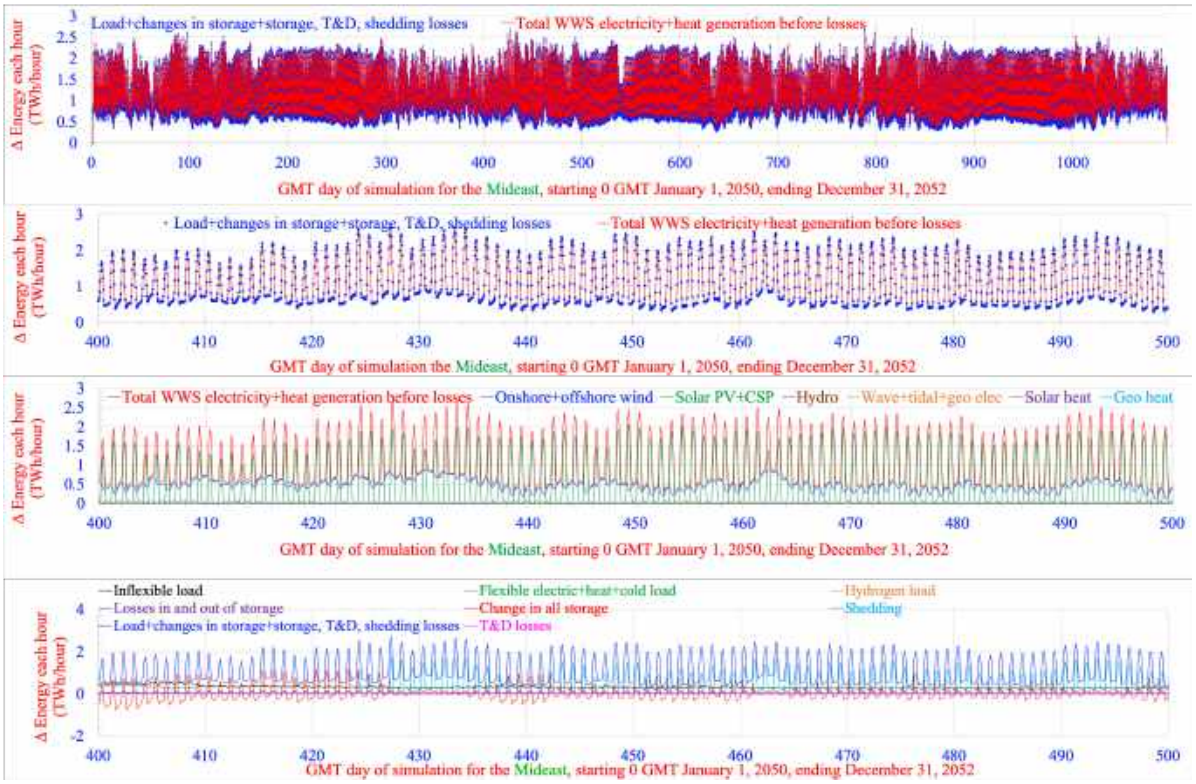
Δ Energy each hour (TWh/hour)
Load+changes in storage+storage, T&D, shedding losses
Total WWS electricity+heat generation before losses
GMT day of simulation for the Mideast, starting 0 GMT January 1, 2050, ending December 31, 2052
Total WWS electricity+heat generation before losses
Onshore+offshore wind
Solar PV+CSP
Hydro
Wave+tidal+geo elec
Solar heat
Geo heat
Inflexible load
Losses in and out of storage
Load+changes in storage+storage, T&D, shedding losses
Flexible electric+heat+cold load
Change in all storage
T&D losses
Hydrogen load
Shedding

New Zealand

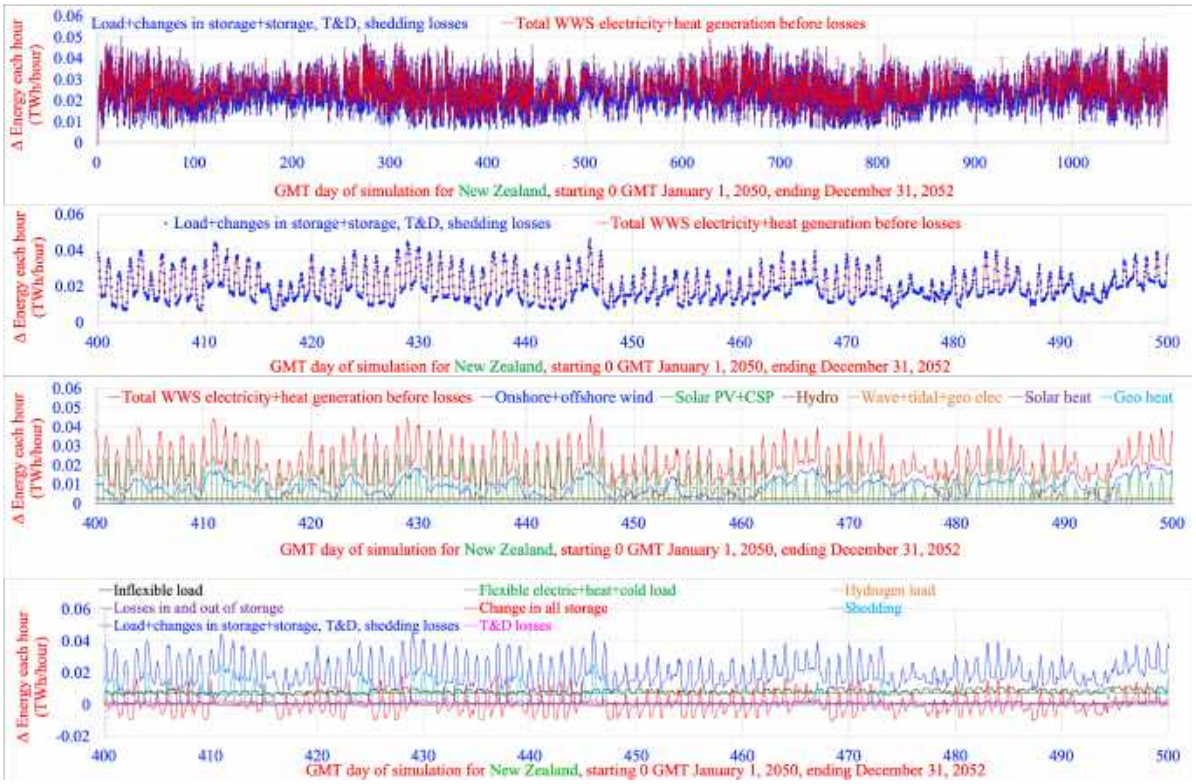
Δ Energy each hour (TWh/hour)
Load+changes in storage+storage, T&D, shedding losses
Total WWS electricity+heat generation before losses
GMT day of simulation for New Zealand, starting 0 GMT January 1, 2050, ending December 31, 2052
Total WWS electricity+heat generation before losses
Onshore+offshore wind
Solar PV+CSP
Hydro
Wave+tidal+geo elec
Solar heat
Geo heat
Inflexible load
Losses in and out of storage
Load+changes in storage+storage, T&D, shedding losses
Flexible electric+heat+cold load
Change in all storage
T&D losses
Hydrogen load
Shedding

Philippines

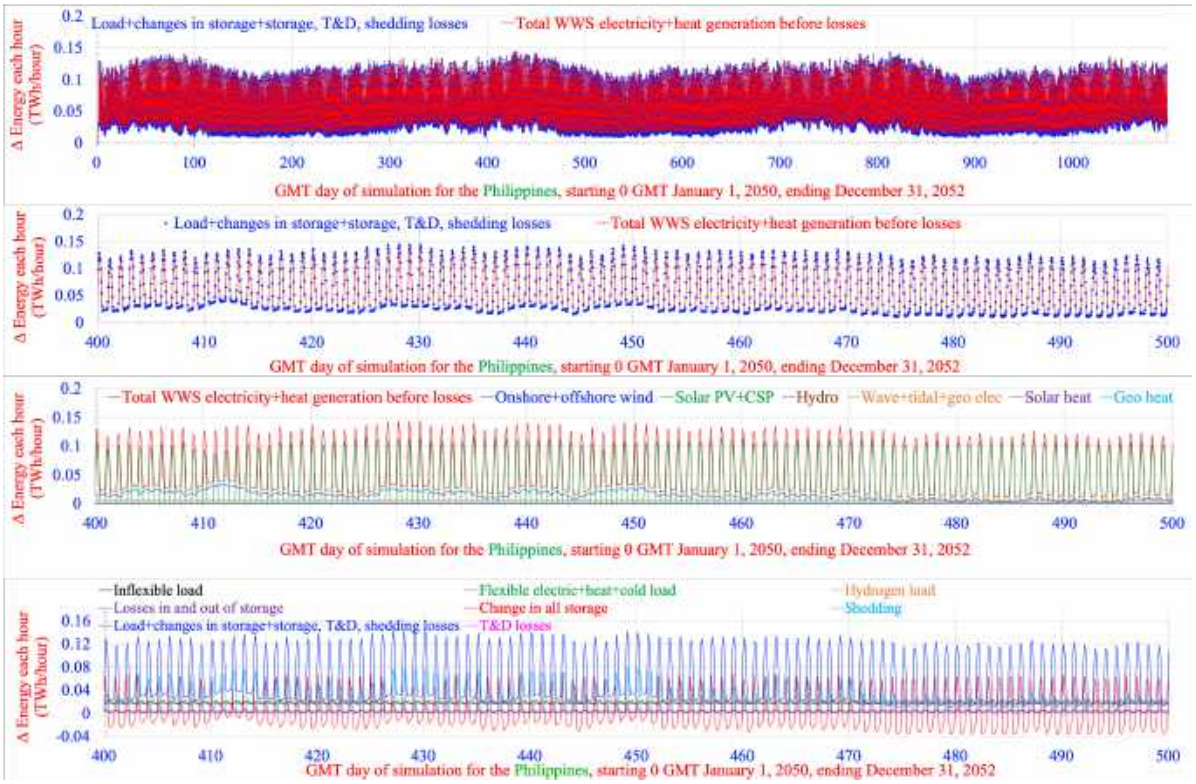

Russia Region

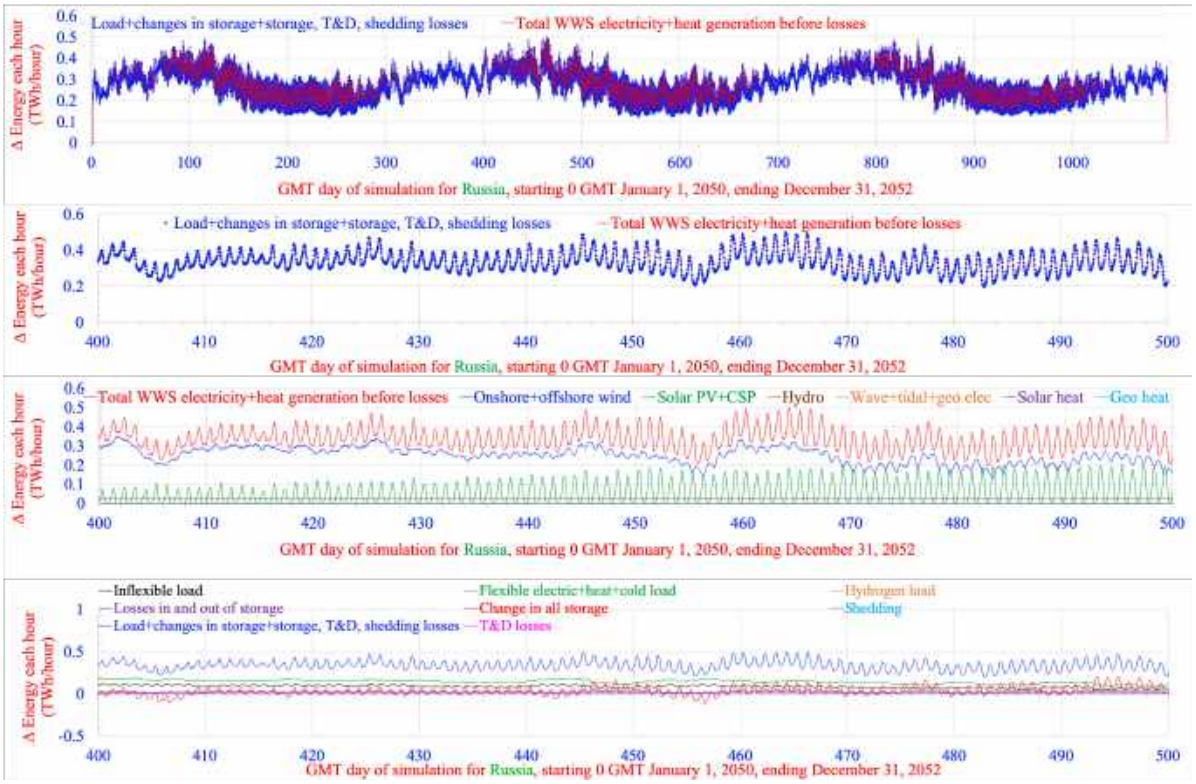

South America

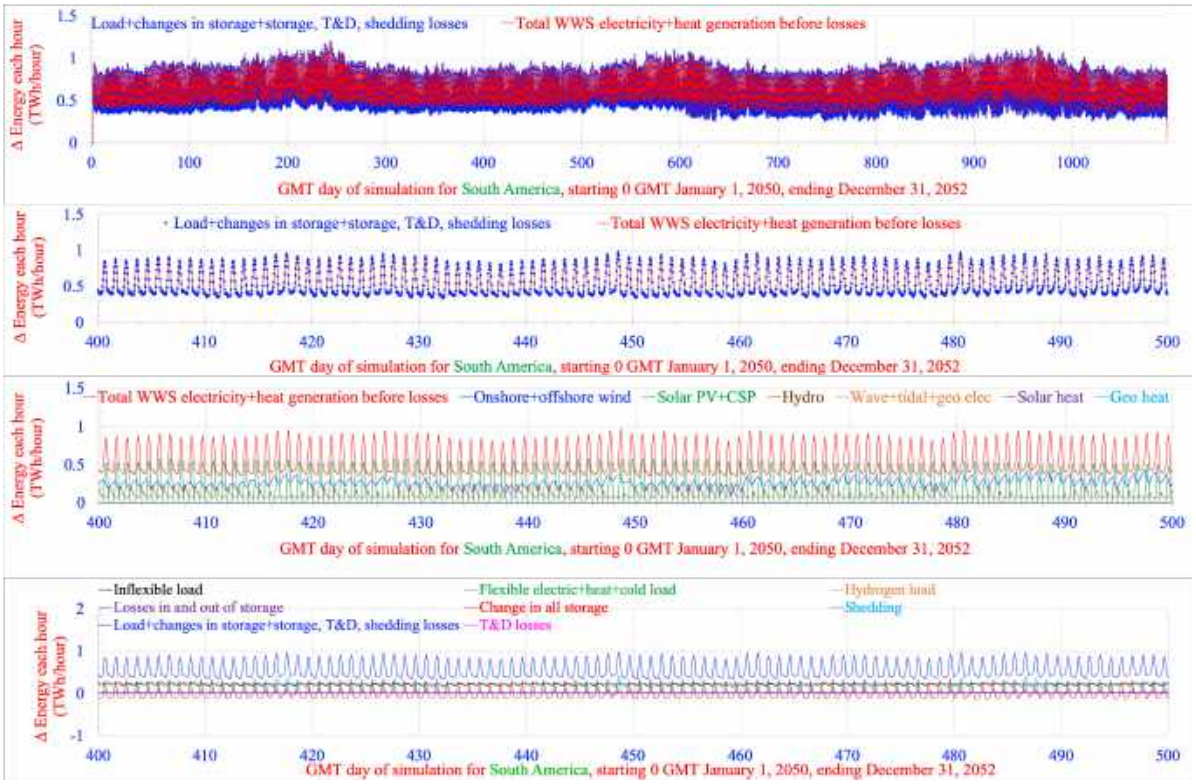

Southeast Asia

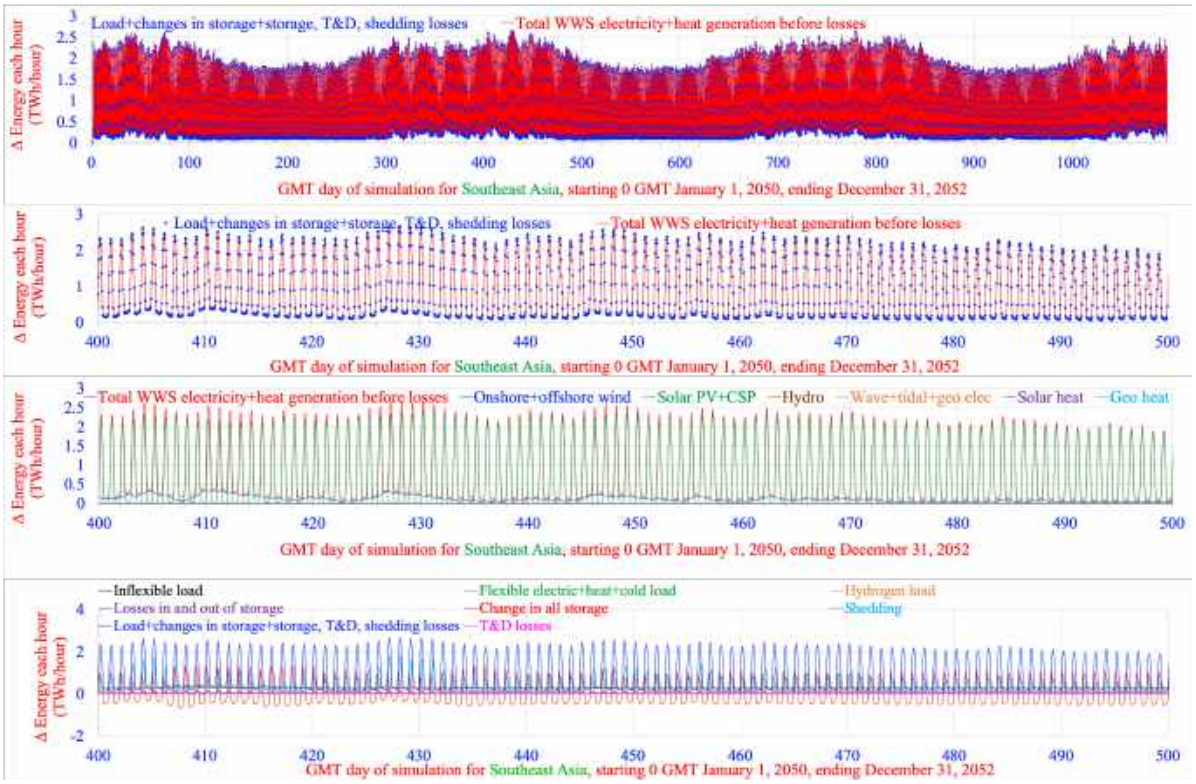

South Korea

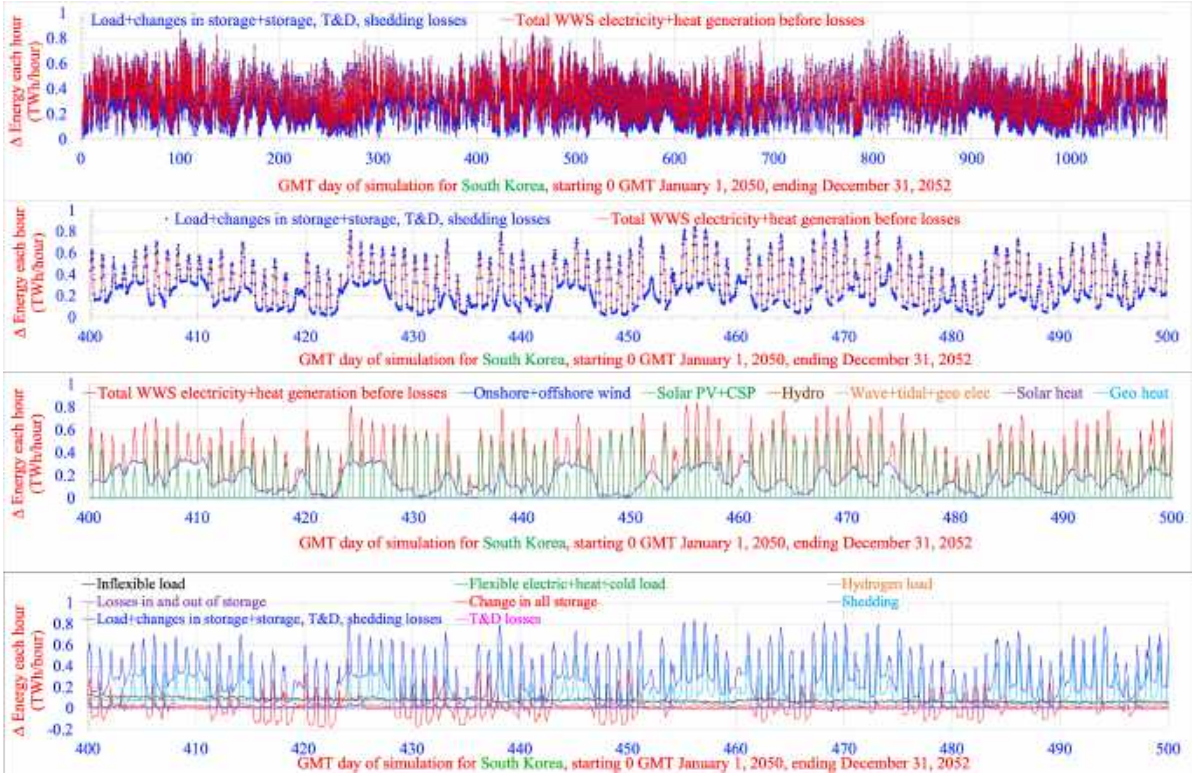
Load+changes in storage+storage, T&D, shedding losses
Total WWS electricity+heat generation before losses
Δ Energy each hour (TWh/hour)
GMT day of simulation for South Korea, starting 0 GMT January 1, 2050, ending December 31, 2052
Load+changes in storage+storage, T&D, shedding losses
Total WWS electricity+heat generation before losses
Δ Energy each hour (TWh/hour)
GMT day of simulation for South Korea, starting 0 GMT January 1, 2050, ending December 31, 2052
Total WWS electricity+heat generation before losses
Onshore+offshore wind
Solar PV+CSP
Hydro
Wave+tidal+geo elec
Solar heat
Geo heat
Δ Energy each hour (TWh/hour)
GMT day of simulation for South Korea, starting 0 GMT January 1, 2050, ending December 31, 2052
Inflexible load
Losses in and out of storage
Load+changes in storage+storage, T&D, shedding losses
Flexible electric+heat+cold load
Change in all storage
T&D losses
Hydrogen load
Shedding
Δ Energy each hour (TWh/hour)
GMT day of simulation for South Korea, starting 0 GMT January 1, 2050, ending December 31, 2052

Taiwan

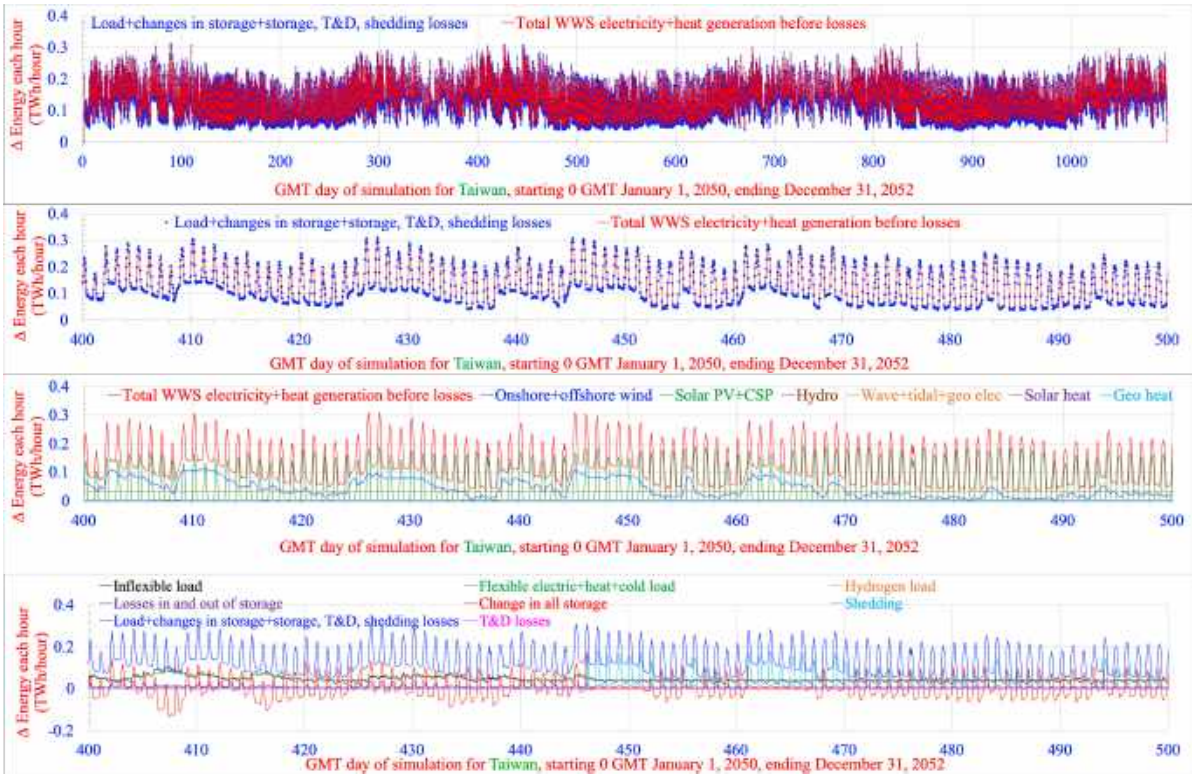
Load+changes in storage+storage, T&D, shedding losses
Total WWS electricity+heat generation before losses
Δ Energy each hour (TWh/hour)
GMT day of simulation for Taiwan, starting 0 GMT January 1, 2050, ending December 31, 2052
Total WWS electricity+heat generation before losses
Onshore+offshore wind
Solar PV+CSP
Hydro
Wave+tidal+geo elec
Solar heat
Geo heat
Inflexible load
Flexible electric+heat+cold load
Hydrogen load
Losses in and out of storage
Change in all storage
Shedding
Load+changes in storage+storage, T&D, shedding losses
T&D losses

United States

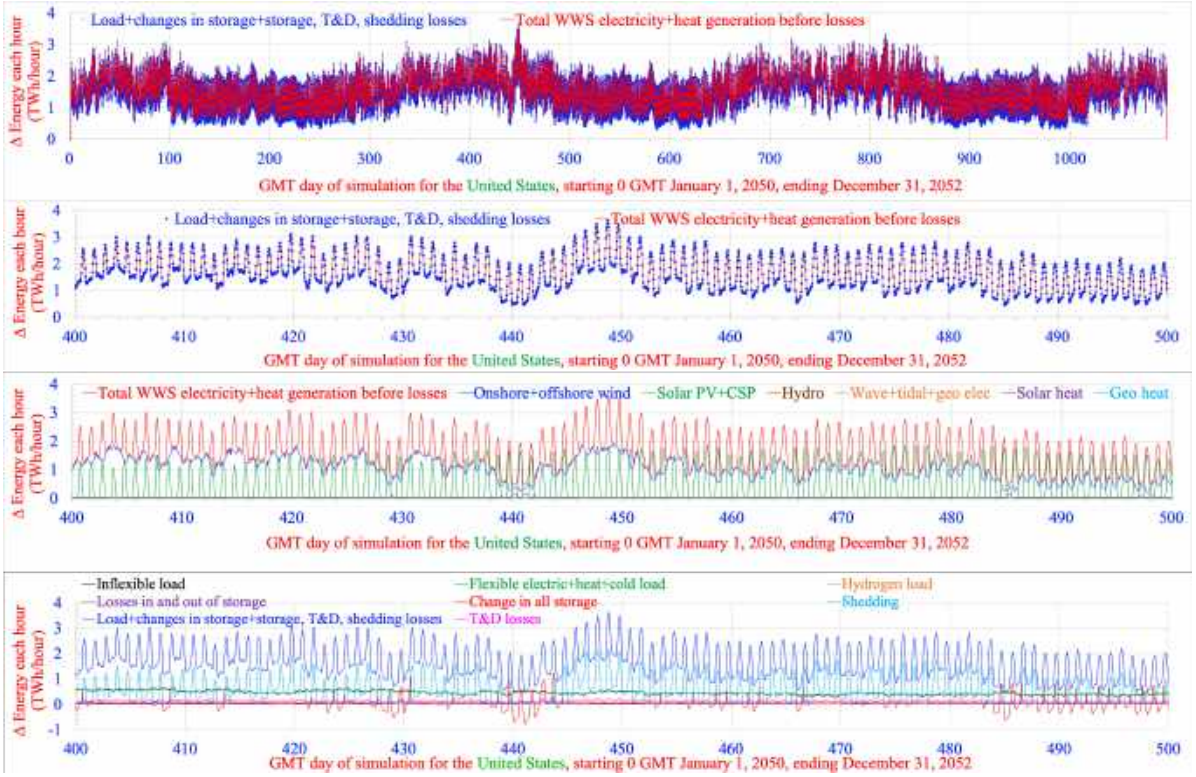

Figure S5. Land footprint and spacing areas (km^2) required beyond existing 2018 installations, to repower 143 countries in each of 24 world regions for all purposes in 2050 with 100% WWS in all energy sectors. Land footprint areas include areas for new utility PV, CSP, solar thermal for heat, geothermal electricity and heat, and hydropower. Spacing areas are new land areas required for onshore wind. Data from Table S26.

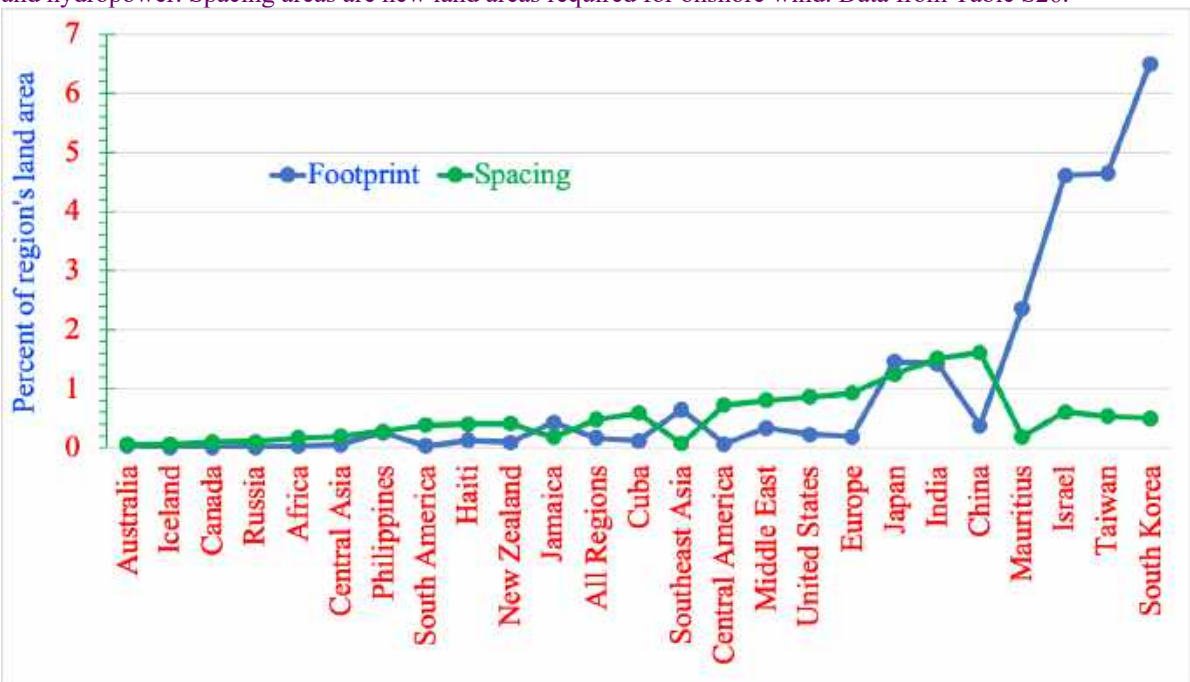

Figure S6. Footprint plus spacing areas (km^2) required beyond existing 2018 installations, to repower 143 countries for all purposes in 2050 with 100% WWS in all energy sectors. For hydropower, the new footprint plus spacing area is zero since no new installations are proposed. For rooftop PV, the circle represents the additional area of 2050 rooftops that needs to be covered (thus does not represent new land).

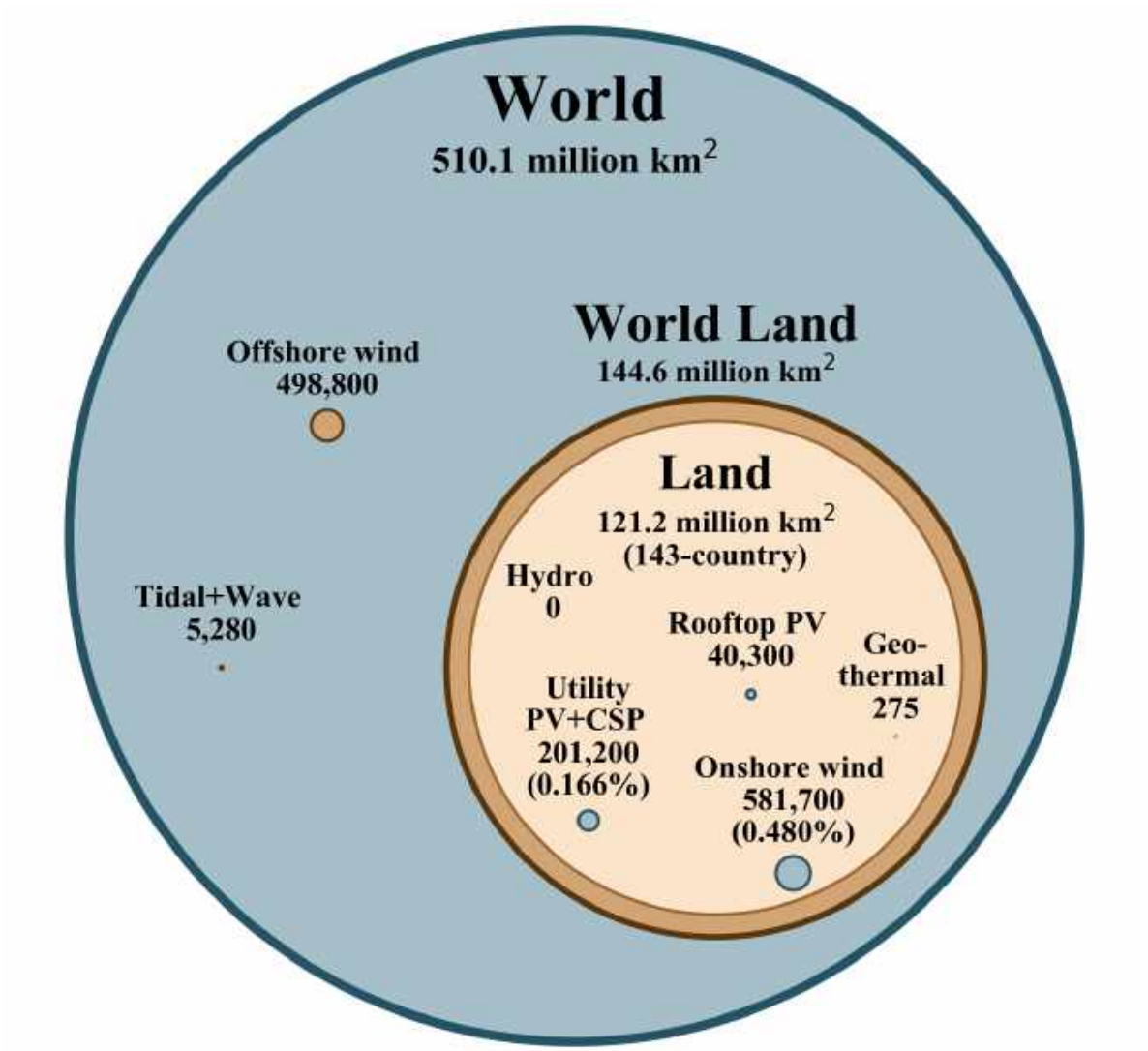

Supplemental References and Notes

1. Jacobson, M.Z., Delucchi, M.A., Cameron, M.A. and Mathiesen, B.V. (2018). Matching demand with supply at low cost among 139 countries within 20 world regions with 100 percent intermittent wind, water, and sunlight (WWS) for all purposes. Renewable Energy *123*, 236-248.

2. IPCC (Intergovernmental Panel on Climate Change) (2018). *Special report: Global warming of 1.5°*. https://www.ipcc.ch/sr15/.

3. World Health Organization (WHO) (2016). Mortality from environmental pollution http://apps.who.int/gho/data/node.sdg.3-9-data?lang=en.

4. Olz, S., Sims R., and Kirchner N. (2007). Contribution of renewables to energy security, International Energy Agency (IEA) information paper. https://web.archive.org/web/20090318231652/http://www.iea.org/textbase/papers/2007/so_contribution.pdf.

5. Jacobson, M.Z., Delucchi, M.A., Bauer, Z.A.F., Goodman, S.C., Chapman, W.E., Cameron, M.A., Alphabetical: Bozonnat, C., Chobadi, L., Clonts, H.A., Enevoldsen, P., Erwin, J.R., Fobi, S.N., Goldstrom, O.K., Hennessy, E.M., Liu, J., Lo, J., Meyer, C.B., Morris, S.B., Moy, K.R., O'Neill, P.L., Petkov, I., Redfern, S., Schucker, R., Sontag, M.A., Wang, J., Weiner, E., and Yachanin, A.S. (2017). 100% clean and renewable wind, water, and sunlight (WWS) all-sector energy roadmaps for 139 countries of the world. Joule *1*, 108-121.

6. Jacobson, M.Z., and Delucchi, M.A. (2009). A path to sustainable energy by 2030. Scientific American *November*.

7. Lund, H., and Mathiesen, B.V. (2009). Energy system analysis of 100% renewable energy systems-The case of Denmark in years 2030 and 2050. Energy *34*, 524-531.

8. Mason, I.G., Page, S.C., and Williamson, A.G. (2010). A 100% renewable energy generation system for New Zealand utilizing hydro, wind, geothermal, and biomass resources. Energy Policy *38*, 3973-3984.

9. Hart, E.K., and Jacobson, M.Z. (2011). A Monte Carlo approach to generator portfolio planning and carbon emissions assessments of systems with large penetrations of variable renewables. Renewable Energy *23*, 2278-2286.

10. Mathiesen, B.V., Lund, H., and Karlsson, K. (2011). 100% renewable energy systems, climate mitigation, and economic growth. Applied Energy *88*, 488-501.

11. Budischak, C., Sewell, D., Thompson, H., Mach, L., Veron, D.E., and Kempton, W. (2013). Cost-minimized combinations of wind power, solar power, and electrochemical storage, powering the grid up to 99.9% of the time. J Power Sources *225*, 60-74.

12. Steinke, F., Wolfrum, P., and Hoffmann, C. (2013). Grid vs. storage in a 100% renewable Europe. Renewable Energy *50*, 826-832.

13. Connolly, D. and Mathiesen, B.V. (2014). Technical and economic analysis of one potential pathway to a 100% renewable energy system. Intl. J. Sustainable Energy Planning & Management *1*, 7-28.

14. Elliston, B., MacGill, I., and Diesendorf, M. (2014). Comparing least cost scenarios for 100% renewable electricity with low emission fossil fuel scenarios in the Australian National Electricity Market. Renew Energy *66*, 196-204.

15. Becker, S., Frew, B.A., Andresen, G.B., Zeyer, T., Schramm, S., Greiner, M., and Jacobson, M.Z. (2014). Features of a fully renewable U.S. electricity system: Optimized mixes of wind and solar PV and transmission grid extensions. Energy *72*, 443-458.

16. Jacobson, M.Z., Delucchi, M.A., Cameron, M.A., and Frew, B.A. (2015). A low-cost solution to the grid reliability problem with 100% penetration of intermittent wind, water, and solar for all purposes. Proc. Nat. Acad. Sci. *112*, 15,060-15,065.

17. Mathiesen, B.V., Lund, H., Connolly, D., Wenzel, H., Ostergaard, P.Z., Moller B., Nielsen, S., Ridjan, I., Karnoe, P., Sperling, K., Hvelplund, F.K. (2015). Smart energy systems for coherent 100% renewable energy and transport solutions. Applied Energy *145*, 139-154.

18. Bogdanov, D., and Breyer, C. (2016). North-east Asian super grid for 100% renewable energy supply: Optimal mix of energy technologies for electricity, gas, and heat supply options. Energy Conversion and Management *112*, 176-190.

19. Connolly, D., Lund, H., Mathiesen, B.V. (2016) Smart energy Europe: The technical and economic impact of one potential 100% renewable energy scenario for the European Union. Renewable and Sustainable Energy Reviews *60*, 1634-1653.

20. Blakers, A., Lu, B., and Socks, M. (2017). 100% renewable electricity in Australia. Energy *133*, 417-482.

21. Zapata, S., Casteneda, M., Jiminez, M., Aristizabel, A.J., Franco, C.J., and Dyner, I. (2018). Long-term effects of 100% renewable generation on the Colombian power market. Sustainable Energy Technologies and Assessments *30*, 183-191.

22. Esteban, M., Portugal-Pereira, J., Mclellan, B.C., Bricker, J., Farzaneh, H., Djalikova, N., Ishihara, K.N., Takagi, H., and Roeber, V. (2018). 100% renewable energy system in Japan: Smoothening and ancillary services. Applied Energy *224*, 698-707.

23. Sadiqa, A., Gulagi, A., and Breyer, C. (2018). Energy transition roadmap towards 100% renewable energy and role of storage technologies for Pakistan by 2050. Energy *147*, 518-533.

24. Liu, H., Andresen, G.B., and Greiner, M. (2018). Cost-optimal design of a simplified highly renewable Chinese network. Energy *147*, 534-546.

25. Aghahosseini, A., Bogdanov, D., Barbosa, L.S.N.S., and Breyer, C. (2019). Analyzing the feasibility of powering the Americas with renewable energy and inter-regional grid interconnections by 2030. Renewable and Sustainable Energy Reviews *105*, 187-205.

26. Bogdanov, D, Farfan, J., Sadovskaia, K., Aghahosseini, A., Child, M., Gulagi, A., Oyewo, A.S., Barbosa, L.S.N.S., and Breyer, C. (2019). Radical transformation pathway towards sustainable electricity via evolutionary steps. Nature Communications *10*, 1077 https://doi.org/10.1038/s41467-019-08855-1.

27. Hansen, K., Breyer, C., and Lund, H. (2019). Status and perspectives on 100% renewable energy systems. Energy *175*, 471-480.

28. Brown, T.W., Bischof-Niemz, T., Blok, K., Breyer, C., Lund, H., and Mathiesen, B.V. (2018). Response to 'Burden of proof: A comprehensive review of the feasibility of 100% renewable electricity systems.' Renewable Sustainable Energy Reviews *92*, 834-847.

29. Diesendorf, M. and Elliston, B. (2018). The feasibility of 100% renewable electricity systems: A response to critics. Renewable and Sustainable Energy Reviews *93*, 318-330.

30. U.S. House of Representatives (2019). H.Res. 109 -- Resolution recognizing the duty of the federal government to create a Green New Deal. https://www.congress.gov/bill/116th-congress/house-resolution/109.

31. Green Party US, Green New Deal – Full Language (2018). https://www.gp.org/gnd_full.

32. World Bank (2017). Agricultural land. https://data.worldbank.org/indicator/AG.LND.AGRI.ZS.

33. Shaner, M.R., Davis, S.J., Lewis, N.S., and Caldeira, K. (2018). Geophysical constraints on the reliability of solar and wind power in the United States. Energy and Environmental Science *11*, 914-925.

34. Sepulveda, N.A., Jenkins, J.D., deSisternes, F.J., and Lester, R.K. (2018). The role of firm low-carbon electricity resources in deep decarbonization of power generation. Joule *2*, 2403-2420.

35. Jacobson, M.Z. (2019). The health and climate impacts of carbon capture and direct air capture, Energy and Environmental Sciences, doi:10.1039/C9EE02709B.

36. Lazard (2019). Lazard's levelized cost of energy analysis – Version 13.0. https://www.lazard.com/perspective/lcoe2019.

37. Hand, M.M., Baldwin, S., DeMeo, E., Reilly, J.M., Mai, T., Arent, D., Porro, G., Meshek, M. and Sandor, D. (2012). Renewable Electricity Futures Study. Volume 1. Exploration of High-Penetration Renewable Electricity Futures (No. NREL/TP-6A20-52409-1). National Renewable Energy Lab.(NREL), Golden, CO (United States).

38. Williams, J.H., Haley, B., Kahrl, F., Moore, J., Jones, A.D., Torn, M.S. and McJeon, H. (2014). Pathways to deep decarbonization in the United States. The U.S. report of the Deep Decarbonization Pathways Project of the Sustainable Development Solutions Network and the Institute for Sustainable Development and International Relations. Nov 25, 2014.

39. MacDonald, A.E., Clack, C.T., Alexander, A., Dunbar, A., Wilczak, J. and Xie, Y. (2016). Future cost-competitive electricity systems and their impact on US CO_2 emissions. Nature Climate Change, *6*, 526-531.

40. REN21 (Renewable Energy Policy Network for the 21st Century) (2019). Renewables 2019 global status report, https://www.ren21.net/gsr-2019/, https://www.ren21.net/gsr-2019/tables/table_06/table_06/.

41. Jacobson, M.Z., Delucchi M.A. et al. (2019). Spreadsheets for 143-country, 24-world region WWS study, http://web.stanford.edu/group/efmh/jacobson/Articles/I/143-countryWWS.xlsx.

42. Jacobson, M.Z. (2001) GATOR-GCMOM: A global through urban scale air pollution and weather forecast model: 1. Model design and treatment of subgrid soil, vegetation, roads, rooftops, water, sea ice, and snow. J. Geophys. Res.: Atmospheres *106*, 5385-5401.

43. Jacobson, M.Z., Kaufmann, Y.J., and Rudich, Y. (2007). Examining feedbacks of aerosols to urban climate with a model that treats 3-D clouds with aerosol inclusions. Journal of Geophysical Research: Atmospheres *112*, D24205.

44. Jacobson, M.Z., and Archer, C.L. (2012). Saturation wind power potential and its implications for wind energy. Proc. Natl. Acad. Sci. *109*, 15,679-15,684.

45. Jacobson, M.Z., and Jadhav, V. (2018). World estimates of PV optimal tilt angles and ratios of sunlight incident upon tilted and tracked PV panels relative to horizontal panels. Solar Energy *169*, 55-66.

46. International Energy Agency (IEA) (2018). World Energy Statistics 2018. OECD Publishing, Paris. https://doi.org/10.1787/world_energy_stats-2018-en.

47. Energy Information Administration (EIA) (2016). U.S. International Energy Outlook 2016. DOE/EIA-0484, 2016. http://www.eia.gov/forecasts/ieo/pdf/0484(2016).pdf.

48. Wilkerson, J.T., Jacobson, M.Z., Malwitz, A., Balasubramanian, S., Wayson, R., Fleming, G., Naiman, A.D. and Lele, S.K. (2010). Analysis of emission data from global commercial aviation: 2004 and 2006. Atmospheric Chemistry and Physics *10*, 6391-6408.

49. Bistak, S., and S.Y. Kim. (2017). AC induction motors vs. permanent magnet synchronous motors. Empowering. http://empoweringpumps.com/ac-induction-motors-versus-permanent-magnet-synchronous-motors-fuji/.

50. Rahman, D., Morgan, A.J., Xu, Y., Gao, R., Yu, W., Hopkins, D.C. and Husain, I. (2016). Design methodology for a planarized high power density EV/HEV traction drive using SiC power modules. In 2016 IEEE Energy Conversion Congress and Exposition (ECCE) pp. 1-7. https://doi.org/10.1109/ECCE.2016.7855018.

51. Jacobson, M.Z., Colella, W.G., and Golden, D.M. (2005). Cleaning the air and improving health with hydrogen fuel cell vehicles. Science *308*, 1901-1905.

52. Fischer, D., and Madani, H. (2017). On heat pumps in smart grids: A review. Renewable and Sustainable Energy Reviews *70*, 342-357.

53. Jacobson, M.Z. (2014). Effects of biomass burning on climate, accounting for heat and moisture fluxes, black and brown carbon, and cloud absorption effects. Journal of Geophysical Research *119*, 8980-9002.

54. Ten Hoeve, J.E., Jacobson, M.Z., and Remer, L. (2012). Comparing results from a physical model with satellite and in situ observations to determine whether biomass burning aerosols over the Amazon brighten or burn off clouds. Journal of Geophysical Research *117*, D08203.

55. Jacobson, M. Z., Lu, R., Turco, R. P., and Toon, O. B. (1996). Development and application of a new air pollution modeling system. Part I: Gas-phase simulations. Atmos. Environ. *30B*, 1939–1963.

56. Jacobson, M. Z. (1997). Development and application of a new air pollution modeling system. Part II: Aerosol module structure and design. Atmos. Environ. *31A*, 131–144.

57. Jacobson, M. Z. (1997). Development and application of a new air pollution modeling system. Part III: Aerosol-phase simulations. Atmos. Environ. *31A*, 587–608.

58. Jacobson, M. Z. (1998). Studying the effects of aerosols on vertical photolysis rate coefficient and temperature profiles over an urban airshed. J. Geophys. Res.,*103*, 10,593-10,604.

59. Jacobson, M. Z. (1999). Isolating nitrated and aromatic aerosols and nitrated aromatic gases as sources of ultraviolet light absorption. J. Geophys. Res. *104*, 3527-3542.

60. Jacobson, M. Z. (1999). Studying The effects of calcium and magnesium on size-distributed nitrate and ammonium with EQUISOLV II. Atmos. Environ. *33*, 3635-3649.

61. Jacobson, M. Z. (1999). Effects of soil moisture on temperatures, winds, and pollutant concentrations in Los Angeles. J. Appl. Meteorol. *38*, 607-616.

62. Jacobson M. Z. (2001). GATOR-GCMM: 2. A study of day- and nighttime ozone layers aloft, ozone in national parks, and weather during the SARMAP Field Campaign. J. Geophys. Res. *106,* 5403-5420.

63. Jacobson, M.Z. (2001). Global direct radiative forcing due to multicomponent anthropogenic and natural aerosols. J. Geophys. Res. *106*, 1551-1568.

64. Jacobson, M. Z. (2002). Control of fossil-fuel particulate black carbon plus organic matter, possibly the most effective method of slowing global warming. J. Geophys. Res. *107*, 4410.

65. Jacobson, M. Z. (2004). The short-term cooling but long-term global warming due to biomass burning. J. Clim. *17*, 2909-2926.

66. Jacobson, M.Z. (2004). The climate response of fossil-fuel and biofuel soot, accounting for soot's feedback to snow and sea ice albedo and emissivity. J. Geophys. Res. *109*, D21201.

67. Jacobson, M.Z. (2005). A refined method of parameterizing absorption coefficients among multiple gases simultaneously from line-by-line data. J. Atmos. Sci. *62*, 506-517.

68. Colella, W.G., Jacobson, M.Z., and Golden, D.M. (2005). Switching to a U.S. hydrogen fuel cell vehicle fleet: The resultant change in emissions, energy use, and global warming gases, J. Power Sources, 150, 150-181.

69. Jacobson, M.Z., and Kaufmann, Y.J. (2006). Wind reduction by aerosol particles. Geophys. Res. Lett. *33*, L24814.

70. Jacobson, M.Z. (2008). The short-term effects of agriculture on air pollution and climate in California. J. Geophys. Res. *113*, D23101.

71. Jacobson, M.Z. (2008). Effects of wind-powered hydrogen fuel cell vehicles on stratospheric ozone and global climate. Geophys. Res. Lett. *35*, L19803.

72. Jacobson, M.Z., and Streets, D.G. (2009). The influence of future anthropogenic emissions on climate, natural emissions, and air quality. J. Geophys. Res. *114*, D08118.

73. Jacobson, M.Z. (2010). The enhancement of local air pollution by urban CO_2 domes. Environ. Sci. Technol. *44*, 2497-2502.

74. Jacobson, M.Z. (2010). Short-term effects of controlling fossil-fuel soot, biofuel soot and gases, and methane on climate, Arctic ice, and air pollution health. J. Geophys. Res. *115*, D14209.

75. Jacobson, M.Z., and Ginnebaugh, D.L. (2010). Global-through-urban nested three-dimensional simulation of air pollution with a 13,600-reaction photochemical mechanism. J. Geophys. Res. *115*, D14304.

76. Jacobson, M.Z., Wilkerson, J.T., Naiman, A.D., and Lele, S.K. (2011). The effects of aircraft on climate and pollution. Part I: Numerical methods for treating the subgrid evolution of discrete size- and composition-resolved contrails from all commercial flights worldwide. J. Comp. Phys. *230*, 5115-5132.

77. Jacobson, M.Z. (2012). Investigating cloud absorption effects: Global absorption properties of black carbon, tar balls, and soil dust in clouds and aerosols. Journal of Geophysical Research *117*, D06205.

78. Whitt, D.B., Wilkerson, J.T., Jacobson, M.Z., Naiman, A.D., and Lele, S.K. (2011). Vertical mixing of commercial aviation emissions from cruise altitude to the surface. Journal of Geophysical Research *116*, D14109.

79. Jacobson, M.Z., and Ten Hoeve, J.E. (2012). Effects of urban surfaces and white roofs on global and regional climate. J. Climate *25*, 1028-1044.

80. Jacobson, M.Z., Archer, C.L., and Kempton, W. (2014). Taming hurricanes with arrays of offshore wind turbines. Nature Climate Change *4*, 195-200.

81. Jacobson, M.Z., Delucchi, M.A., Cameron, M.A., and Mathiesen, B.V. (2018). Matching demand with supply at low cost among 139 countries within 20 world regions with 100% intermittent wind, water, and sunlight (WWS) for all purposes. Renewable Energy *123*, 236-248.

82. Jacobson, M.Z. (2019). Short-term impacts of the Aliso Canyon natural gas blowout on weather, climate, air quality, and health in California and Los Angeles. Environmental Science and Technology *53*, 6081-6093, doi:10.1021/acs.est.9b01495.

83. Zhang, Y., Seigneur, C., Seinfeld, J. H., Jacobson, M. Z., and Binkowski, F. (1999). Simulation of aerosol dynamics: A comparative review of algorithms used in air quality models, Aerosol Sci. Technol., 31, 487-514.

84. Liang, J., and Jacobson, M. Z. (2000). Comparison of a 4000-reaction chemical mechanism with the Carbon Bond IV and an adjusted Carbon Bond IV-EX mechanism using SMVGEAR II. Atmos. Environ. *34*, 3015-3026.

85. Zhang, Y., Seigneur, C., Seinfeld, J. H., Jacobson, M. Z., Clegg, S. L., and Binkowski, F. (2000). A comparative review of inorganic aerosol thermodynamic equilibrium modules: Similarities, differences, and their likely causes. Atmos. Environ. *34*, 117-137.

86. Moya, M., Pandis, S. N., and Jacobson, M. Z. (2002). Is the size distribution of urban aerosols determined by thermodynamic equilibrium? An application to Southern California. Atmos. Environ. *36*, 2349-2365.

87. Barth, M. C., Sillman, S., Hudman, R., Jacobson, M. Z., Kim, C.-H., Monod, A., and Liang, J. (2003). Summary of the cloud chemistry modeling intercomparison: Photochemical box model simulation. J. Geophys. Res. *108*, 4214.

88. Kreidenweis, S. M., Walcek, C., Feingold, G., Gong, W., Jacobson, M. Z., Kim, C.-H., Liu, X., Penner, J. E., Nenes A., and Seinfeld, J. H. (2003). Modification of aerosol mass and size distribution due to aqueous-phase SO_2 oxidation in clouds: Comparisons of several models. J. Geophys. Res. *108*, 4213.

89. Hu, X.-M, Zhang, Y., Jacobson, M.Z., and Chan, C.K. (2008). Coupling and evaluating gas/particle mass transfer treatments for aerosol simulation and forecast. J. Geophys. Res. *113*, D11208.

90. Zhang, Y., McMurry, P.H., Yu, F., and Jacobson, M.Z. (2010). A comparative study of nucleation parameterizations: 1. Examination and evaluation of the formulations. J. Geophys. Res. *115*, D20212.

91. Bahadur, R., Russell, L.M., Jacobson, M.Z., Prather, K.A., Nenes, A., Adams, P.J., and Seinfeld, J.H. (2012). Importance of composition and hygroscopicity of BC particles to the effect of BC mitigation on cloud properties: application to California conditions. J. Geophys. Res. *117*, D09204.

92. Bond, T.C., Doherty, S.J., Fahey, D.W., Forster, P.M., Berntsen, T., Boucher, O., DeAngelo, B.J., Flanner, M.G., Ghan, S., Karcher, B., Koch, D., Kinne, S., Kondo, Y., Quinn, P.K., Sarofim, M.C., Schultz, M.G., Schulz, M., Venkataraman, C., Zhang, H., Zhang, S., Bellouin, N., Guttikunda, S.K., Hopke, P.K., Jacobson, M.Z., Kaiser, J.W., Klimont, Z., Lohmann, U., Schwarz, J.P., Shindell, D., Storelvmo, T., Warren, S.G., and Zender, C.S. (2013). Bounding the role of black carbon in the climate system: A scientific assessment. J. Geophys. Res. *118*, 5380-5552, doi: 10.1002/jgrd.50171.

93. Brasseur, G.P., Gupta, M., Anderson, B.E., Balasubramanian, S., Barrett, S., Duda, D., Fleming, G., Forster, P.M., Fluglestvedt, J., Gettelman, A., Halthore, R.N., Jacob, S.D., Jacobson, M.Z., Khodayari, A., Liou, K.-N., Lund, M.T., Miake-Lye, R.C., Minnis, P., Olsen, S., Penner, J.E., Prinn, R., Schumann, U.,

Selkirk, H.B., Sokolov, A., Unger, N., Wolfe, P., Wong, H.-W., Wuebbles, D.W., Yi, B., Yang, P., Zhou, C. (2016). Impact of aviation on climate: FAA's Aviation Climate Change Research Initiative. Bulletin of the American Meteorological Society, 561-583, doi:10.1175/BAMS-D-13-00089.

94. Olsen, S.C., Brasseur, G.P., Wuebbles, D.J., Barrett, S.R.H., Dang, H., Eastham, S.D., Jacobson, M.Z., Khodayari, A., Selkirk, H., Sokolov, A., Unger, N. (2013). Comparison of model estimates of the effects of aviation emissions on atmospheric ozone and methane. Geophys. Res. Lett. *40*, 6004-6009.

95. Cameron, M.A., Jacobson, M.Z., Barrett, S. R. H., Bian, H., Chen, C.-C., Eastham, S. D., Gettelman, A., Khodayari, A., Liang, Q., Selkirk, H. B., Unger, N., Wuebbles, D. J., and Yue, X. (2017). An inter-comparative study of the effects of aircraft emissions on surface air quality. J. Geophys. Res. Atmos. *122*, 8325-8344, doi:10.1002/2016JD025594.

96. Russell, L.M., Cappa, C.D., Kleeman, M.J., and Jacobson, M.Z. (2018). Characterizing the climate impacts of brown carbon, Final report to the California Air Resources Board Research Division, Project 13-330.

97. Arakawa, A., and Lamb, V.R. (1981). A potential enstrophy and energy conserving scheme for the shallow water equations. Monthly Weather Review 109 18-36.

98. Walcek, C.I., and Aleksic, N.M. (1998). A simple but accurate mass conservative, peak-preserving, mixing ratio bounded advection algorithm with FORTRAN code. Atmospheric Environment *32*, 3863-3880.

99. Mellor, G.L., and Yamada, T. (1982) Development of a turbulence closure model for geophysical fluid problems. Reviews of Geophysics *20*, 851-875.

100. Ketefian, G.S., and Jacobson, M.Z. (2009) A mass, energy, vorticity, and potential enstrophy conserving lateral fluid-land boundary scheme for the shallow water equations. Journal of Computational Physics *228*, 1-32.

101. Jacobson, M.Z. (2002). Analysis of aerosol interactions with numerical techniques for solving coagulation, nucleation, condensation, dissolution, and reversible chemistry among multiple size distributions. Journal of Geophysical Research *107*, 4366.

102. Jacobson, M.Z. (2003). Development of mixed-phase clouds from multiple aerosol size distributions and the effect of the clouds on aerosol removal. Journal of Geophysical Research *108* 4245.

103. Frew, B. A., and Jacobson, M. Z. (2016). Temporal and spatial tradeoffs in power system modeling with assumptions about storage: An application of the POWER model. Energy *117*, 198-213.

104. World Health Organization (WHO) (2017). Global health observatory data, https://www.who.int/gho/phe/outdoor_air_pollution/en.

105. Kirby, B.J. (2004). Frequency regulation basics and trends. ORNL/TM-2004/291, http://www.consultkirby.com/files/TM2004-291_Frequency_Regulation_Basics_and_Trends.pdf.

106. U.S. National Research Council (NRC) (2010). Real prospects for energy efficiency in the United States. National Academies Press, https://www.nap.edu/read/12621/chapter/6#251.

107. European Network of Transmission System Operators for Electricity (ENTSO-E) (2016). European load data, https://www.entsoe.eu/db-query/country-packages/production-consumption-exchange-package.

108. Neocarbon Energy (2016). Future energy system, http://neocarbonenergy.fi/internetofenergy/.

109. Moore, M.A., Boardman, A.E., Vining, A.R., Weimer, D.L., and Greenberg, D.H. (2004). Just give me a number! Practical values for the social discount rate. Journal of Policy Analysis and Management *23*, 789-812.

110. National Center for Environmental Economics (NCEE) (2014). Guidelines for Preparing Economic Analyses. U.S. Environmental Protection Agency.

111. Drupp, M., Freeman, M., Groom, B., and Nesje, F. (2015). Discounting disentangled: an expert survey on the determinants of the long-term social discount rate. The Centre for Climate Change Economics and Policy Working Paper No. 195 and Grantham Research Institute on Climate Change and the Environment Working Paper No. 172.

112. U.S. Office of Management and Budget (OMB) (2003). Circular A-4, Regulatory Analysis. The White House, Washington, D. C., https://www.whitehouse.gov/sites/whitehouse.gov/files/omb/circulars/A4/a-4.pdf.

113. Department of Energy (DOE) (2012). DOE technical targets for hydrogen production from electrolysis. https://energy.gov/eere/fuelcells/doe-technical-targets-hydrogen-production-electrolysis.

114. National Renewable Energy Laboratory (NREL) (2014). Hydrogen station compression, storage, and dispensing technical status and costs. https://www.nrel.gov/docs/fy14osti/58564.pdf.

115. Stetson, N.T. (2012). Hydrogen storage, https://www.hydrogen.energy.gov/pdfs/review12/st_plenary_stetson_2012_o.pdf.

116. World Health Organization (WHO) (2017). Health statistics and information systems, https://www.who.int/healthinfo/global_burden_disease/estimates/en.

117. Global Burden of Disease 2013 Risk Factors Collaborators (GBD) (2015). Global, regional, and national comparative risk assessment of 79 behavioral, environmental and occupational, and metabolic risks or clusters of risks in 188 countries, 1990-2013: a systematic analysis for the Global Burden of Disease Study 2013. Lancet *386*, 2287-2323.

118. Burnett, R. (2018). Global estimates of mortality associated with long-term exposure to outdoor fine particulate matter. Proceedings of the Natural Academy of Sciences *115*, 9592-9597.

119. Van den Bergh, J.C.J.M., and Botzen, W.J.W. (2014). A lower bound the social cost of carbon emissions. Nature Climate Change *4*, 253-258.

120. Moore, F.C., and Diaz, D.B. (2015). Temperature impacts on economic growth warrant stringent mitigation policy. Nature Climate Change *5*, 127-131.

121. Burke, M., Hsiang, S.M., and Miguel, E. (2015). Global non-linear effect of temperature on economic production. Nature *527*, 235-239.

122. National Renewable Energy Laboratory (NREL) (2017). Energy Snapshot: Haiti, https://www.nrel.gov/docs/fy15osti/64121.pdf .

123. National Renewable Energy Laboratory (NREL) (2019). Jobs and Economic Development Impact Models (JEDI), https://www.nrel.gov/analysis/jedi.

124. Erlich, I., and M. Wilch (2010). Frequency control by wind turbines, IEEE PES General Meeting, July 25-29, 2010, doi: 10.1109/PES.2010.5589911, https://ieeexplore.ieee.org/document/5589911.

125. Roselund, C. (2019). Inertia, frequency regulation and the grid, PV Magazine, https://pv-magazine-usa.com/2019/03/01/inertia-frequency-regulation-and-the-grid/.

126. De Stercke, S. (2014). Dynamics of Energy Systems: A Useful Perspective. IIASA Interim Report No. IR-14-013. International Institute for Applied Systems Analysis, IIASA, Laxenburg, Austria.

127. Bloomberg NEF (2019). A behind-the-scenes take on lithium-ion battery prices. https://about.bnef.com/blog/behind-scenes-take-lithium-ion-battery-prices/.

128. European Commission (2019). EDGAR: Fossil CO_2 emissions of all countries, https://edgar.jrc.ec.europa.eu/overview.php?v=booklet2018.

129. Enevoldsen, P., and Jacobson M.Z. Data investigation of installed and output power densities of onshore and offshore wind turbines worldwide, Wind Energy, 2020.

130. Bizee (2019). Custom degree day data, http://www.degreedays.net.